Zwitterionic Ion Chromatography of Common Inorganic Anions Using Stationary Phases Modified with Carboxybetaine-Type Surfactants

By

Colmán Ó Ríordáin,
BSc. (Hons), AMRSC, GradICI

A thesis submitted to Dublin City University in part fulfilment for the degree of

DOCTOR OF PHILOSOPHY

Supervisor: Dr. Brett Paull,
School of Chemical Sciences,
Dublin City University.

May 2006

I hereby certify that this material, which I now submit for assessment on the programme of study leading to the award of Ph.D in Analytical Chemistry is entirely my own work and has not been taken from the work of others save and to the extent that such work has been cited and acknowledged within the text of my work.

Signed: Colman O Riordan (Candidate) ID No.: 98038745

Date: 11/08/06

Acknowledgements

There are a number of people whom I would like to thank for their contributions and assistance during the undertaking of my postgraduate studies

Firstly, I would like to sincerely thank my supervisor, Dr Brett Paull, for all his invaluable advice, suggestions and guidance over the last 4 years I am also grateful for the assistance of Prof Pavel Nesterenko, particularly for synthesising the carboxybetaine-type surfactant used initially for this project

I am also indebted to the numerous members of the Brett Paull research group, both past and present, for their support and camaraderie for the last few years, especially Johnny, Eadaoin, Damian, Leon, Wasim, Marion and Cepta I would also like to express my appreciation for the efforts of the technicians and support staff of the School of Chemical Sciences, particularly Maurice, Mick, Mary and Veronica

Táim an-buioch as ucht an tacaiocht ollmhor agus an cabhair a fuair me i gconai o mo mhuintir uilig, mo thuismitheoiri Noilin agus Eamonn, mo dheartharacha, Domhnall agus Cillian, agus mo dheirfiur, Roisin Caithfidh nach raibh se easca i gconai!

Lastly I would like to express my undying gratitude for all the love, encouragement and support (both emotional and professional) I received from my best friend, and co-worker, Edel Words can't do justice in thanking you for all the times you've been there for me, but suffice to say that I'm forever in your debt, but look forward to repaying that debt in the many years to come

Table of Contents

Abstract

Carboxybetaine-type zwitterionic surfactants were employed to dynamically modify reversed-phase columns (both particle-packed and monolithic in structure), before investigating their use as stationary phases for the determination of common inorganic anions by zwitterionic ion chromatography (ZIC). Both surfactants utilised (namely dodecyldimethylaminoacetic acid and N-dodecyl-N,N-(dimethylammonio)undecanoate (DDMAU)) had a similar structure, with an internal, positively charged ammonium group, and an external, negatively charged carboxylate group, but DDMAU was found to exhibit superior column coating stability, due to its increased hydrophobic character. Both surfactants were found to have a pH dependent effective ion-exchange capacity, with increased eluent pH values resulting in reduced analyte anion retention times, due to increased protonation of the weak acid terminal group of the surfactant molecules. The suitability of these carboxybetaine-modified stationary phases to the determination of nutrient anions in high-ionic strength environmental sample matrices (e.g. seawater samples) has been demonstrated. The ability to apply dual gradient programs (i.e. with a combined eluent pH and flow gradient) provided the opportunity to expedite the elution, and improve the efficiency, of later eluting analyte peaks (i.e. polarisable anions such as iodide and thiocyanate), without sacrificing the resolution and efficiency of earlier eluting anions (e.g. iodate, nitrite etc.). The applicability of DDMAU-modified stationary phases to capillary IC using direct contactless conductivity detection was established, with modified capillary monoliths facilitating the separation of a mixture of 8 anions using flow rates of 1 μL/min and less. Effective column lengths of the DDMAU-modified capillary monolith, and, therefore, analyte retention, could be adjusted through relocation of the contactless conductivity detector utilised.

List of Publications and Presentations

Papers Published:

"Double gradient ion chromatography on a short carboxybetaine coated monolithic anion exchanger".
Brett Paull, Colmán Ó Ríordáin and Pavel N. Nesterenko, *Chem. Commun.* 2 (2005) 215-217.

"Zwitterionic ion chromatography with carboxybetaine surfactant coated particle packed and monolithic type columns".
Colmán Ó Ríordáin, Pavel N. Nesterenko and Brett Paull, *J. Chrom. A.* 170 (2005) 71-78.

"Double gradient ion chromatography using short monolithic columns modified with a long chained zwitterionic carboxybetaine surfactant".
Colmán Ó Ríordáin, Leon Barron, Ekaterina Nesterenko, Pavel N. Nesterenko and Brett Paull, *J. Chrom. A.* 1109 (2006) 111-119.

"Across column detection using monolithic capillary ion chromatography and contactless conductivity detection".
Colmán Ó Ríordáin, Eoin Gillespie, Damien Connolly, Pavel N. Nesterenko and Brett Paull, *submitted to J. Chrom. A* June 2006.

Oral Presentations:

"Zwitterionic Ion Chromatography of Common Inorganic Anions Using Monolithic Columns".
Colmán Ó Ríordáin, Pavel N. Nesterenko and Brett Paull.
18th Annual International Ion Chromatography Symposium
Delta Centre-Ville, Montreal, Canada, 18th-21st of September 2005.

Poster Presentations:

"Application of Zwitterionic Ion Chromatography to High Ionic Strength Samples – Monitoring of Nutrients in Coastal Seawater Samples".
Colmán Ó Ríordáin, Pavel N. Nesterenko and Brett Paull
Analytical Research Forum Incorporating Research and Development 2003
University of Sunderland, U.K. 21st – 23rd of July 2003.

"Zwitterionic Ion Chromatography Using Dynamically Coated Columns and Application to the Monitoring of Nutrients in Coastal Seawater Samples".
Colmán Ó Ríordáin, Danielle Victory, Pavel N. Nesterenko and Brett Paull
16th International Ion Chromatography Symposium
San Diego, CA, USA 21st – 24th of September 2003.

"Zwitterionic Ion Chromatography Using Dynamically Coated Columns and Application to the Monitoring of Nutrients in Coastal Seawater Samples".
Colmán Ó Ríordáin, Danielle Victory, Pavel N. Nesterenko and Brett Paull
1st Annual Symposium for the Irish Research Council for Science, Engineering and Technology (IRCSET)
Royal Hospital Kilmainham, Dublin, Ireland 7th of November 2003.

"Zwitterionic Ion Chromatography Using Dynamically Coated Packed and Monolithic Carboxybetaine Columns and their Application to the Rapid Analysis and Monitoring of Nutrients in Coastal Seawater Samples".
Colmán Ó Ríordáin, Pavel N. Nesterenko and Brett Paull
Analytical Research Forum Incorporating Research and Development 2004
University of Central Lancashire, Preston, U.K. 19th – 21st of July 2004.

"Zwitterionic Ion Chromatography Using Dynamically Coated Packed and Monolithic Carboxybetaine Columns and their Application to the Rapid Analysis and Monitoring of Nutrients in Coastal Seawater Samples".
Colmán Ó Ríordáin, Pavel N. Nesterenko and Brett Paull
7th Asian Conference on Analytical Sciences (Asianalysis VII)
Hong Kong Baptist University, Hong Kong, 28th – 31st of July 2004

"Zwitterionic Ion Chromatography Using Dynamically Coated Packed and Monolithic Carboxybetaine Columns and their Application to the Rapid Analysis and Monitoring of Nutrients in Coastal Seawater Samples".
Colmán Ó Ríordáin, Pavel N. Nesterenko and Brett Paull
3rd Biennial Conference on Analytical Sciences in Ireland
NUI Cork, Cork, Ireland 9th – 10th of September 2004.

"Zwitterionic Ion Chromatography Using Dynamically Coated Packed and Monolithic Carboxybetaine Columns and their Application to the Rapid Analysis and Monitoring of Nutrients in Coastal Seawater Samples".
Colmán Ó Ríordáin, Pavel N. Nesterenko and Brett Paull
17th Annual International Ion Chromatography Symposium
University of Trier, Trier, Germany, 20th – 23rd of September 2004.

"Development of Novel Ion Chromatographic Techniques for Continuous and Simultaneous Monitoring of Anions and Cations in Environmental Samples".
Colmán Ó Ríordáin and Brett Paull
2nd Annual Symposium for the Irish Research Council for Science, Engineering and Technology (IRCSET)
Croke Park, Dublin, Ireland, 2nd of November 2004.

"Zwitterionic Ion Chromatography of Common Inorganic Anions Using Monolithic Columns Coated With DDMAU".
Colmán Ó Ríordáin, Pavel N. Nesterenko and Brett Paull
Analytical Research Forum Incorporating Research and Development 2005
University of Plymouth, Plymouth, U.K., 18th-20th of July 2005.

"Zwitterionic Ion Chromatography of Common Inorganic Anions Using Carboxybetaine-Type Surfactants as Stationary Phases".
Colmán Ó Ríordáin and Brett Paull
3rd Annual Symposium for the Irish Research Council for Science, Engineering and Technology (IRCSET)
Croke Park, Dublin, Ireland, 3rd of November 2005.

List of Figures

Figure 1.11. Chromatograms of an aqueous solution containing (A): 2.0 mM each of Na^+, Mg^{2+}, and Ce^{3+} with Cl^- as the counterion, and (B): 2.0 mM each of Na^+, Mg^{2+}, and Ce^{3+} with NO_3^- as the counterion, using a C_{18} reversed-phase column (250 x 4.0 mm I.D.) modified with Zwittergent 3-14, with pure water as the eluent, and a flow rate of 1.0 mL/min. Detection was by conductivity. Peak Identification: 1: Na^+-Cl^-, 2: Mg^{2+}-$2Cl^-$, 3: Ce^{3+}-$3Cl^-$, a: Na^+-NO_3^-, b: Mg^{2+}-$2NO_3^-$, c: Ce^{3+}-$3NO_3^-$.

Figure 1.12. Chromatograms of an aqueous solution of (a) 10 mM KBr and 10 mM NaSCN (1: Na^+-Br^-, 2: K^+-Br^-, 3: Na^+-SCN^-, 4: K^+-SCN^-), and (b) 10 mM NaSCN and 5 mM $BaCl_2$ (1: Na^+-Cl^-, 2: Ba^{2+}-$2Cl^-$, 3: Na^+-SCN^-, 4: Ba^{2+}-$2SCN^-$). Separation conditions: C_{18} reversed-phase column (250 x 4.6 mm I.D.) modifed with CHAPSO micelles, with pure water as the eluent, a flow rate of 0.7 mL/min, and conductivity detection.

Figure 1.13. Chromatogram of an aqueous sample containing 2 mM NaSCN and 1 mM $CaCl_2$, obtained using a C_{18} reversed-phase column (250 x 4.6 mm I.D.) modified with Zwittergent 3-14 micelles, and pure water as the eluent. Flow rate: 1.0 mL/min. Detection: conductivity. Peak identities: a: Na^+-Cl^-, b: Ca^{2+}-$2Cl^-$, c: Na^+-SCN^-, d: Ca^{2+}-$2SCN^-$.

Figure 1.14. Chromatogram of an aqueous solution containing 1.0 μM each of NaCl and $CaCl_2$, obtained using a C_{18} reversed-phase column (250 x 4.6 mm) modified with Zwittergent 3-14 micelles, an eluent comprised of pure water, and conductivity detection. Flow rate: 1.0 mL/min. Peak identities: (1,1') Na^+ - Cl^- and (2,2') Ca^{2+} - $2Cl^-$.

Figure 1.15. Schematic representation of the change in configuration of adsorbed zwitterionic surfactant molecules (which in this case are DDAPS molecules) upon changing eluent conditions from (a) a salt-free solution, to (b) a salt solution.

Figure 1.16. Schematic survey of the retention mechanism using electrolytic eluents. (a) Establishment of the Donnan membrane, (b) use of a $NaClO_4$ eluent, and (c) use of a $CeCl_3$ eluent.

Figure 1.24. Chromatogram of 18.0 μM each of nitrite, bromide, nitrate, and chlorate in a sample containing 0.482 M chloride and 0.029 M sulphate, using an eluent comprised of 1.0 mM Zwittergent 3-14, in 7.0 mM $Na_2B_4O_7$ / 2.0 mM H_3BO_3, and conductivity detection. Peak identities: (1) - sulphate; (2) - chloride; (3) - nitrite; (4) - bromide; (5) - nitrate; (6) - chlorate.

Figure 1.25. Chromatogram of human saliva obtained using a CHAPS-modifed stationary phase, and a phosphate buffer as the eluent, with detection at 230 nm.

Figure 1.26. Chromatogram of an aqueous solution containing 0.5 μM of various bases, and ribonucleosides, using a Zwittergent 3-14-modified stationary phase, and pure water as the eluent, with UV detection at 210 nm. Analytes: adenine (A), gunanine (G), cytosine (C), thymine (T), and uracil (U); adenosine (rA), guanosine (rG), cytidine (rC), thymidine (dT), and uridine (rU).

Figure 1.27. Chromatograms of anions in radish juice observed using a C_{18} reversed-phase column modified with tetradecyldimethyl(3-sulfopropyl)-ammonium hydroxide (C14SB), with an eluent composed of pure water, a flow rate of 0.7 mL/min, and conductivity detection. (A) - Radish juice upon addition of decoy electrolyte. 1 - unidentified, 2 - Cl^-, 3 - Br^-, 4 - NO_3^-, 5 - NO_3^-. (B) – Radish juice with addition of KI. 1'- unidentified, 2'- K^+-Cl^-, 3'- K^+-Br^-, 4'- K^+-NO_3^-, a – mainly K^+-I^-. (C) – Radish juice upon addition of $MgSO_4$. 2"- Mg^{2+}-$2Cl^-$, 3"- Mg^{2+}-Br^-, 4"- Mg^{2+}-$2NO_3^-$, b – mainly Mg^{2+}-SO_4^{2-}.

Figure 1.28. Determination of inorganic anions in snow using suppressed-ZIC with 10 mM $Na_2B_4O_7$ solution as eluent, using Zwittergent 3-14 as the zwitterionic stationary phase. Peak identities: 1 - sulphate, 2 - chloride, 3 - nitrite, 4 - bromide, and 5 - nitrate.

Figure 1.29. Diagram illustrating indirect conductivity detection (giving a negative analyte peak, as with eluent 1, which has a high limiting equivalent ionic conductance), and direct conductivity detection (displaying a positive analyte peak, as with eluent 2, which has a low limiting equivalent ionic conductance).

Figure 2.7. Chromatogram of a pseudo-seawater sample (consisting of 2.0 ppm nitrate and nitrite, and 50 ppm bromide in a 0.52 M NaCl sample matrix) obtained using a 25 cm carboxybetaine-modified particle-packed C_{18} column, with 150 mM KCl at pH 6.02 (with 0.2 mM dodecyldimethylaminoacetic acid) as the eluent. Flow rate: 0.5 mL/min. Wavelength of detection: 214 nm.

Figure 2.8. Plots of (a) peak area, and (b) peak height, vs. concentration of nitrate and nitrite present in a 0.52 M NaCl pseudo-seawater sample matrix. Data obtained using an eluent composed of 150 mM KCl at pH 6, also containing 0.2 mM dodecyldimethylaminoacetic acid. Flow rate: 0.5 mL/min. Wavelength of detection: 214 nm. Column details: 25 cm carboxybetaine-modified particle-packed C_{18} column.

Figure 2.9. Chromatogram of an undiluted seawater sample, taken at Portmarnock, Co. Dublin, analysed using a 25 cm carboxybetaine-modified particle-packed C_{18} column. Eluent: 150 mM KCl, 0.2 mM dodecyldimethylaminoacetic acid, pH 6. Flow rate: 0.5 mL/min. Wavelength of detection: 214 nm.

Figure 3.1. Comparison of column back pressure across a range of flow rates (0.5-9.0 mL/min) for a monolithic silica column and conventional columns packed with 3.5 μm and 5 μm particles.

Figure 3.2. Comparison of the van Deemter curves obtained using a monolithic silica column, and columns packed with 3.5 μm and 5 μm particles. (■ = 5 μm particle packed column, ● = 3.5 μm particle packed column, ▲= monolithic silica column.)

Figure 3.3. Chromatograms of a 1.0 mM mixture of nitrite, bromide, nitrate and iodide obtained using a 10 cm C_{18} monolith modified with dodecyldimethylaminoacetic acid, and operated at flow rates of 0.5 mL/min (blue trace) and 2.0 mL/min (pink trace). Eluent: 150 mM KCl with 0.2 mM dodecyldimethylaminoacetic acid, at pH 6.0. Wavelength of detection: 214 nm.

Figure 3.4. Effect of eluent KCl concentration upon retention factor (k) for a 10 cm C_{18} monolith modified with dodecyldimethylaminoacetic acid. Other eluent

dodecyldimethylaminoacetic acid, using a constant flow rate of 2.0 mL/min (yellow trace), and under flow gradient conditions (from 2.0 mL/min to 4.9 mL/min) beginning at t = 2.0 min and applied over 1 (blue trace), 2 (red trace) and 3 (green trace) min. Eluent: 10 mM KCl (with 0.2 mM carboxybetaine-type surfactant) at pH 6.0. Wavelength of detection: 214 nm.

Figure 3.11. Chromatograms of a 1.0 mM mixture of nitrite, bromide, nitrate and iodide obtained using a 10 cm C_{18} monolithic column coated with dodecyldimethylaminoacetic acid (pink trace) and with a mixture of dodecyldimethylaminoacetic acid and Zwittergent 3-14 (blue trace). Eluent: 10 mM KCl (with a total zwitterionic surfactant concentration of 0.2 mM [0.1 + 0.1 mM) at pH 6.0. Flow rate: 2.0 mL/min. Wavelength of detection: 214 nm.

Figure 3.12. Chromatograms of (A) 1.0 mM nitrate, bromide, nitrite and iodide, (B) 1.0 mM thiocyanate, and (C) 1.0 mM nitrate, bromide, nitrite, iodide and thiocyanate, all obtained using a 10 cm C_{18} monolith modified with both zwitterionic surfactants, using an eluent composed of 10 mM KCl/0.5 mM $KClO_4$ (in 0.1 mM dodecyldimethylaminoacetic acid/0.1 mM Zwittergent 3-14) at pH 3.0. Flow conditions: (A) + (B), 2.0 mL/min; (C), 2.0 mL/min for 2 min, followed by a linear flow gradient to 4.9 mL/min from 2 to 4 min. Wavelength of detection: 214 nm.

Figure 3.13. Plots of peak area vs. concentration for bromide, nitrate and iodide, prepared in a 0.52 M NaCl sample matrix, obtained using a 10 cm carboxybetaine-modified C_{18} monolithic column, with an eluent composed of 40 mM KCl, with 0.2 mM dodecyldimethylaminoacetic acid, at pH 3.5. Flow rate: 2.0 mL/min. Wavelength of detection: 214 nm.

Figure 3.14. Chromatogram of an undiluted seawater sample taken from Bull Island, Dublin, displaying the separation of bromide and nitrate from the chloride sample constituent, obtained on a 10 cm carboxybetaine-modified C_{18} monolithic column. The inlet chromatogram shows the presence of trace levels of nitrite in the same seawater sample. Eluent: 40 mM KCl, with 0.2 mM dodecyldimethylaminoacetic acid, at pH 3.5. Flow rate: 2.0 mL/min. Wavelength of detection: 214 nm.

combined in series, with an eluent composed of 10 mM citrate buffer at pH 3.1 (also containing 0.2 mM dodecyldimethylaminoacetic acid). Flow rate: 2.0 mL/min. Wavelength of detection: 256 nm.

Figure 3.21. Chromatograms of a 1.0 mM mixture of nitrite, bromide, nitrate, iodide and thiocyanate obtained on a 25 cm carboxybetaine-modified C_{18} particle-packed column, using an eluent comprised of 150 mM KCl/0.2 mM dodecyldimethylaminoacetic acid, and buffered with 10 mM phosphate buffer. Eluent pH conditions: (A) pH gradient from 100% pH 3 at t = 0 min to 100% pH 8 at t = 2.5 min; (B) isocratic conditions with an eluent pH of 6. Flow rate: (A) 1.0 mL/min; (B) 0.5 mL/min. Wavelength of detection: 214 nm.

Figure 3.22. Chromatogram of a 1.0 mM mixture of nitrite, bromide, nitrate, iodide and thiocyanate obtained on a 10 cm carboxybetaine-modified C_{18} monolithic column, and using an eluent of 10 mM KCl with 0.2 mM dodecyldimethylaminoacetic acid (buffered with 10 mM phosphate buffer). Gradient details: pH gradient from 100% pH 6 at t = 0 min to 100% pH 8 at t = 5 min. Flow rate: 2.0 mL/min. Wavelength of detection: 214 nm.

Figure 3.23. Chromatogram of a 1.0 mM mixture of nitrite, bromide, nitrate, iodide and thiocyanate, obtained using a 10 cm C_{18} monolith modified with dodecyldimethylaminoacetic acid, and utilising an eluent composed of 10 mM KCl, with 0.2 mM carboxybetaine-type surfactant, buffered using 10 mM phosphate buffer at the required pH. Gradient conditions: pH gradient of 100% pH 6 to 100% pH 8, and a flow gradient of 1.0 mL/min to 5.0 mL/min, applied over 5 min (from t = 0 min to t = 5 min). Wavelength of detection: 214 nm.

Figure 3.24. Separation of a 0.05 mM mixture of nitrite, bromide and nitrate obtained using a 1.0 cm carboxybetaine-modified C_{18} monolith, with 1 mM KCl in 0.2 mM dodecyldimethylaminoacetic acid at pH 3 as the eluent. Flow rate: 2.0 mL/min. Wavelength of detection: 214 nm.

Figure 3.25. Chromatogram illustrating the separation of a 0.05 mM mixture of nitrate, bromide, nitrite, iodide and thiocyanate achieved using a 1.0 cm

carboxybetaine-modified C_{18} monolithic column, with an eluent composed of 1 mM KCl, with 0.2 mM dodecyldimethylaminoacetic acid, at pH 3. Flow rate: 2.0 mL/min. Wavelength of detection: 214 nm.

Figure 3.26. Effect of eluent flow rate upon peak efficiency for nitrite and nitrate, using a 1.0 cm carboxybetaine-modified C_{18} monolithic column. Eluent: 1 mM KCl, with 0.2 mM dodecyldimethylaminoacetic acid, at pH 3. Wavelength of detection: 214 nm.

Figure 3.27. Effect of eluent flow rate upon peak efficiency for iodide and thiocyanate, using a 1.0 cm carboxybetaine-modified C_{18} monolithic column. Eluent: 1 mM KCl, with 0.2 mM dodecyldimethylaminoacetic acid, at pH 3. Wavelength of detection: 214 nm.

Figure 3.28. Chromatogram illustrating the separation of a 0.05 mM mixture of nitrite, bromide, nitrate, iodide and thiocyanate obtained on a 1.0 cm carboxybetaine-modified C_{18} monolithic column, using an eluent composed of 1 mM KCl, with 0.2 mM dodecyldimethylaminoacetic acid, at pH 3. Flow conditions: 2.0 mL/min constant flow rate for 1 min (from t = 0 min to t = 1 min), followed by a linear flow gradient to 6.0 mL/min over 1 min (from t = 1 min to t = 2 min). Wavelength of detection: 214 nm.

Figure 3.29. Chromatogram illustrating the separation of a mixture of nitrite, bromide, nitrate, iodide and thiocyanate obtained on a 1.0 cm carboxybetaine-modified C_{18} monolithic column, using an eluent composed of 1 mM KCl, with 0.2 mM dodecyldimethylaminoacetic acid, buffered at the required pH using 10 mM phosphate buffer. Dual gradient conditions: From t = 0 min to t = 1 min, eluent pH was 100% pH 3, with a constant flow rate of 2.0 mL/min; pH gradient (to 100% pH 8) and a flow gradient (to 6.0 mL/min) applied over 1 min (from t = 1 min to t = 2 min). Wavelength of detection: 225 nm. Analyte concentration: 0.05 mM (0.25 mM thiocyanate).

Figure 4.7. Chromatogram of a 1.0 mM mixture of iodate, bromate, nitrite, bromide, nitrate, iodide and thiocyanate obtained using a 2.5 cm DDMAU-modified C_{18} monolithic column and an eluent composed of 10 mM phosphate buffer at pH 4.0, with UV detection at 214 nm and a flow rate of 2.0 mL/min.

Figure 4.8. Overlaid chromatograms of a 1.0 mM 7 anion mixture (containing iodate, bromate, nitrite, bromide, nitrate, iodide and thiocyanate) obtained utilising a 2.5 cm DDMAU-modified C_{18} monolithic column, and using initial flow rates of 2.0 mL/min, and a starting 10 mM phosphate buffer eluent pH of 4.0, with the application of a linear dual gradient between 1.5 and 4.5 min. Gradient details: (A) – 100% pH 4.0 to 100% pH 8.0, and 2.0 mL/min to 6.0 mL/min; (B) – 100% pH 4.0 to 100% pH 6.0, and 2.0 mL/min to 6.0 mL/min.

Figure 4.9. Chromatograms obtained using a dual gradient program (100% pH 4 to 100% pH 6, 2.0 mL/min to 4.0 mL/min) over 3 min (from t = 1.5 min to t = 4.5 min) using a 10 mM phosphate buffer eluent (pink trace) and a 1 mM citrate buffer eluent (blue trace). Column: 2.5 cm DDMAU-modified C_{18} monolithic column. Wavelength of detection: 214 nm. Samples injected: Milli-Q water (blue trace), and 1.0 mM iodide and thiocyanate (pink trace).

Figure 4.10. Overlaid chromatograms of a 1.0 mM 7 anion mixture (containing iodate, bromate, nitrite, bromide, nitrate, iodide and thiocyanate) obtained using initial flow rates of 2.0 mL/min, and a starting eluent pH of 4.0, with the application of a linear dual gradient at t = 1.5 min, with the end conditions of the gradient being an eluent pH of 6.0 and a flow rate of 6.0 mL/min. Rate of applied gradient: (A) – 1.5 to 4.5 min; (B) – 1.5 to 2.0 min. Column: 2.5 cm DDMAU-modified C_{18} monolithic column.

Figure 4.11. Schematics of the exterior and the interior of the flow through pH electrode assembly used to measure pH of the column eluate.

Figure 4.12. Column outlet pH values determined during the application of a pH gradient (100% pH 4.06 to 100% pH 6.02 over 1.5 – 4.5 min) using linear (blue

trace), convex (red trace) and concave (yellow trace) gradient profiles. Flow rate: 4.0 mL/min. Column: 2.5 cm DDMAU-modified C_{18} monolithic column.

Figure 4.13. Column outlet pH values determined during the application of a linear pH gradient (100% pH 4.02 to 100% pH 6.04) over 1.5 to 2.5 min (red trace), 1.5 to 3.5 min (blue trace) and 1.5 to 4.5 min (yellow trace). Flow rate: 4.0 mL/min. Column: 2.5 cm DDMAU-modified C_{18} monolithic column.

Figure 4.14. Column outlet pH values determined during the application of a linear pH gradient over 1.5 to 4.5 min. Gradient details: 10mM phosphate buffer eluent pH gradient from 100% pH 3.1 to 100% pH 7.0 (blue trace), and from 100% pH 4.02 to 100% pH 6.04 (red trace). Column: 2.5 cm DDMAU-modified C_{18} monolithic column. Flow rate: 4.0 mL/min.

Figure 4.15. Column outlet pH measured during application of a step gradient (100% pH 4 to 100% pH 6) initialised at t = 0.5 min, at both 2.0 ml/min (red trace) and 4.0 mL/min (blue trace). M = mark indicating point of application of the step gradient; t_{dwell} = dwell time of system. Column: 2.5 cm DDMAU-modified C_{18} monolithic column.

Figure 4.16. Column outlet pH measured during application of a linear pH gradient (100% pH 4 to 100% pH 6) from 1.5 to 4.5 min, using a flow rate of 4.0 mL/min, both with (blue trace) and without the column in place (yellow and red traces). Column: 2.5 cm DDMAU-modified C_{18} monolithic column.

Figure 4.17. Chromatograms illustrating the retention of acetate (dark blue trace), formate (red trace), tungstate (light blue trace) and chlorate (green trace) on a 2.5 cm DDMAU-modified C_{18} monolithic column, employing 10 mM phosphate buffer (at pH 4.07) as eluent and a flow rate of 4.0 mL/min. Wavelength of detection: 214 nm.

Figure 4.18. Chromatograms illustrating the retention of phthalate (orange trace), iodide (dark blue trace), thiocyanate (dark blue trace), 4-hydroxybenzoate (green trace) and chromate (red trace) on a 2.5 cm DDMAU-modified C_{18} monolithic column. Other conditions: As for Fig. 4.17.

Figure 4.19. Chromatogram of a 0.1 mM mixture of iodate, bromate, nitrite, bromide, nitrate, 4-hydroxybenzoate, iodide, thiocyanate and phthalate, obtained using a 2.5 cm DDMAU-modified C_{18} monolithic column, and an eluent comprised of 10 mM phosphate buffer at pH 4.02, and a flow rate of 4.0 mL/min. Wavelength of detection: 214 nm.

Figure 4.20. Chromatogram of a 0.1 mM mixture 9 anions obtained using a 2.5 cm DDMAU-modified C_{18} monolithic column, employing a dual gradient (10 mM phosphate buffer as eluent from 100% pH 4.02 to 100% pH 5.02, and flow rate from 4.0 mL/min to 6.0 mL/min) applied between t = 3.0 and t = 5.0 min. Wavelength of detection: 214 nm. Peak identification: 1 – iodate, 2 – bromate, 3 – nitrite, 4 – bromide, 5 – nitrate, 6 – 4-hydroxybenzoate, 7 – iodide, 8 – system peak, 9 – thiocyanate, and 10 – phthalate.

Figure 4.21. Chromatogram of a 0.1 mM mixture 9 anions obtained using a 2.5 cm DDMAU-modified C_{18} monolithic column, employing a dual gradient (10 mM phosphate buffer as eluent from 100% pH 3.03 to 100% pH 5.02, and flow rate from 4.0 mL/min to 6.0 mL/min) applied between t = 3.0 and t = 5.0 min. Wavelength of detection: 214 nm. Peak identification: 1 – iodate, 2 – nitrite, 3 – bromate, 4 – 4-hydroxybenzoate, 5 – bromide, 6 – nitrate, 7 – iodide, 8 – system peak, 9 – thiocyanate, and 10 – phthalate.

Figure 4.22. Chromatograms of 0.6 mM chloride, 0.2 mM phosphate, 1.0 mM nitrate and 1.0 mM iodide obtained using a 2.5 cm DDMAU-modified C_{18} monolithic column, with an eluent composed of 1.0 mM phthalic acid (at pH 4) and a wavelength of detection of 279 nm. Flow rate: 2.0 mL/min.

Figure 4.23. Chromatograms of 0.1 mM sulphite, 0.1 mM sulphate and 1.0 mM thiocyanate obtained using a 2.5 cm DDMAU-modified C_{18} monolithic column, with an eluent composed of 1.0 mM phthalic acid (at pH 4) and a wavelength of detection of 279 nm. Flow rate: 2.0 mL/min.

Figure 4.24. Chromatograms of 1.0 mM iodide, 0.1 mM sulphite, 0.1 mM sulphate and 1.0 mM thiocyanate obtained using a 2.5 cm DDMAU-modified C_{18} monolithic

Figure 5.3. Photograph illustrating part of the experimental setup of the capillary LC system used.

Figure 5.4. Micrographs, at X 2 magnification, of (a) first capillary monolithic column, from 1.0 to 1.5 cm of total column length (showing non-continuity of stationary phase within capillary walls), and (b) second capillary column utilised from 1.0 to 1.5 cm of total column length (displaying a uniform internal structure).

Figure 5.5. Separation of a 0.5 mM mixture of iodate, nitrite, bromide, nitrate, iodide and sulphate achieved on a DDMAU-modified capillary C_{18} monolithic column, using contactless conductivity detection, and a flow rate of 1.0 μL/min. Eluent: 0.5 mM phthalic acid at pH 4.05. Effective column length: 13.0 cm.

Figure 5.6. Photographs illustrating how placing the contactless conductivity detector further down the length of the capillary column would result in a longer effective column length, with (a) representing an effective column length of approx. 8.5 cm, and (b) representing an effective column length of approx 12.5 cm.

Figure 5.7 (a) and (b). Overlays of chromatograms of a 0.5 mM 8 anion mixture (where 1 represents iodate, 2 - bromate, 3 - nitrite, 4 - bromide, 5 - nitrate, 6 - iodide, 7 – sulphate, and 8 - thiocyanate) obtained using a DDMAU-modified capillary column, with an eluent composed of 0.5 mM phthalic acid at pH 4.05 and a flow rate of 1.0 μL/min., at effective column lengths of 4.5 cm (yellow trace), 8.5 cm (pink trace) and 12.5 cm (blue trace).

Figure 5.8 (a) and (b). Graphs showing the change in retention factor, *k*, as effective column length was increased, for (a) iodate, bromate, nitrite, bromide and nitrate, and for (b) iodide, sulphate and thiosulphate. Eluent: 0.5 mM phthalic acid at pH 4.05. Flow rate: 1.0 μL/min.

Figure 5.9. Photograph of the experimental setup employed to connect the capillary column to an additional piece of open tubular fused silica capillary, across which the conductivity of the eluent would be measured after leaving the column.

Figure 5.10 (a) and (b). Chromatograms of a 0.5 mM 7 anion mixture (plus 2.0 mM thiosulphate) obtained using a DDMAU-modified capillary C_{18} monolithic column, with contactless conductivity detection applied directly across the capillary monolithic column (blue trace), and also across a 100 μm I.D. open tubular capillary connected to the capillary monolith (pink trace). Eluent: 0.5 mM phthalic acid at pH 4.05. Flow rate: 1.0 μL/min. Effective column length: 13 cm. Peak identification: 1 – iodate, 2 – bromate, 3 – nitrite, 4 – bromide, 5 – nitrate, 6 – iodide, 7 – sulphate, and 8 – thiosulphate.

Figure 5.11. Plots of the effect of flow velocity (u) of eluent on the height equal to a theoretical plate (HETP) for nitrate and iodide. Eluent: 0.5 mM phthalic acid at pH 4.05. Effective column length: 8.0 cm. Concentration of standards injected: 0.5 mM.

Figure 5.12. Overlays of chromatograms of a 0.5 mM standard solution of chloride, nitrate and sulphate (blue trace) and an undiluted tap water sample (pink trace) obtained using a DDMAU-modified capillary C_{18} monolithic column, with an eluent composed of 0.5 mM phthalic acid at pH 4.05, and contactless conductivity detection. Flow rate: 1.0 μL/min. Peak identification: 1 – chloride, 2 – nitrate, and 3 – sulphate.

Figure 5.13. Overlays of chromatograms of a tap water sample injected neat (blue trace) and diluted by a factor of 5 (pink and yellow traces) obtained on the DDMAU-modified capillary C_{18} monolithic column with an effective column length of 4.5 cm (blue and pink traces) and 8.5 cm (yellow trace), in conjunction with contactless conductivity detection. Eluent: 0.5 mM phthalic acid at pH 4.05. Flow rate: 1.0 μL/min. Peak identification: 1 – chloride, 2 – nitrate, and 3 – sulphate.

Figure 5.14. An overlay of the chromatograms of a tap water sample obtained pre and post cation-exchange (blue and pink traces respectively) using a DDMAU-modified capillary C_{18} monolithic column with an effective column length of 4.5 cm, with an eluent comprised of 0.5 mM phthalic acid at pH 4.05, and contactless conductivity detection. Flow rate: 1.0 μL/min. Peak identification: 1 – chloride, 2 – nitrate, and 3 – sulphate.

Figure 5.15. Overlays of chromatograms of a tap water sample obtained using a DDMAU-modified capillary C_{18} monolithic column, with an eluent comprised of 0.5 mM phthalic acid at pH 4.05, and contactless conductivity detection, after passing through a cation-exchange cartridge (blue and pink traces) and both a cation-exchange cartridge and a reversed-phase cartridge (yellow trace). Effective column lengths: 4.5 cm (blue trace) and 8.5 cm (pink and yellow traces). Flow rate: 1.0 μL/min. Peak identification: 1 – chloride, 2 – nitrate, and 3 – sulphate.

Figure 5.16. Chromatogram of a 0.5 mM mixture of iodate, bromate, nitrite, bromide, nitrate, iodide, sulphate and thiosulphate (with 2.0 mM thiocyanate and perchlorate) obtained using a DDMAU-modified capillary C_{18} monolithic column, with an eluent composed of 0.5 mM phthalic acid at pH 4.05, and contactless conductivity detection. Flow rate: 0.30 μL/min. Effective column length: 8.0 cm. Peak identification: 1 – iodate, 2 – bromate, 3 – nitrite, 4 – bromide, 5 – nitrate, 6 – iodide, 7 – sulphate, 8 – thiosulphate, 9 – thiocyanate, and 10 – perchlorate.

Figure 5.17. Chromatogram of a mixture of chloride (0.5 mM), chlorite (2.0 mM) and chlorate (0.5mM) obtained using a DDMAU-modified capillary C_{18} monolithic column, with 0.5 mM phthalic acid as eluent, and contactless conductivity detection. Flow rate: 0.30 μL/min. Effective column length: 8.0 cm.

Figure 5.18. Chromatogram of a 0.5 mM mixture of formate, chloride and chloroacetate obtained using a DDMAU-modified capillary C_{18} monolithic column, with 0.5 mM phthalic acid as eluent, and contactless conductivity detection. Flow rate: 0.30 μL/min. Effective column length: 8.0 cm.

Figure 5.19. Chromatogram of a 0.5 mM standard of dithionite obtained using 0.5 mM phthalic acid as eluent, with contactless conductivity detection. Flow rate: 0.30 μL/min. Effective column length: 8.0 cm.

List of Tables

Table 5.2. Comparison of signal-to-noise ratios for 0.5 mM anion standards (except for 2.0 mM thiosulphate) using across-column detection, and detection across an open tubular capillary of 100 μm I.D.

Table 5.3. Peak areas for 0.5 mM anion standards (except for 2.0 mM thiosulphate) using across-column detection, and detection across open tubular fused silica capillaries of 2 different internal diameters (100 μm and 75 μm).

Table 5.4. Retention factors for each anion analysed, using 0.5 mM phthalic acid (pH 4.05) as eluent, with contactless conductivity detection and a flow rate of 0.30 μL/min. Effective column length: 8.0 cm.

List of Abbreviations

A	Adenine
AES	Atomic Emission Spectroscopy
C	Cytosine
C_4D	Capacitively Coupled Contactless Conductometric Detection
CE	Capillary Electrophoresis
CEC	Capillary Electrochromatography
CHAPS	3-[(3-cholamidopropyl)dimethylammonio]-1-propanesulphonate
CHAPSO	3-[(3-cholamidopropyl)dimethylammonio]-2-hydroxy-1-propanesulphonate
CMC	Critical Micelle Concentration
DDAB	Didodecyldimethylammonium bromide
DDAPS	3-(N-dodecyl-N,N-dimethylammonio)propane-1-sulphonate
DDMAU	N-dodecyl-N,N-(dimethylammonio)undecanoate
dT	Thymidine
EDL	Electrical Double Layer
EIC	Electrostatic Ion Chromatography
G	Guanine
HPLC	High Performance Liquid Chromatography
IC	Ion Chromatography
ICP	Inductively Coupled Plasma
I.D.	Internal Diameter
IDA	Iminodiacetic Acid
IIR	Ion-Interaction Reagent
ISE	Ion-Selective Electrodes
LC	Liquid Chromatography
L.O.D.	Limit of Detection
NaTC	Sodium Taurocholate
NaTDC	Sodium Taurodeoxycholate
O.T.	Open Tubular
PAR	4-(pyridylazo)resorcinol
PCR	Post-Column Reaction

PTFE	Poly(tetrafluoroethylene)
rA	Adenosine
rC	Cytidine
RI	Refractive Index
rG	Guanosine
RSD	Relative Standard Deviation
rU	Uridine
T	Thymine
TTA	Tetradecyltrimethylammonium
U	Uracil
UV	Ultraviolet
Vis	Visible
ZIC	Zwitterionic Ion Chromatohgraphy
ZWEDL	Zwitterionic Electrical Double Layer

List of Symbols

A	Contribution to Band Broadening from Eddy Diffusion
A	Cross-Sectional Area of Electrodes in Electrolyte Solution
A^-	Analyte Anion
B	Contribution to Band Broadening from Longitudinal Diffusion
C	Contribution to Band Broadening from Mass Transfer Effects
C	Concentration
C^+	Analyte Cation
F	Flow Rate
G	Conductance
ΔG	Molal Energy
HETP	Height Equivalent to a Theoretical Plate
I	Current
I	Emergent Light Intensity
I_0	Incident Light Intensity
K	Cell Constant
k	Retention Factor
k	Conductivity / Specific Conductance
N	No. of Theoretical Plates
p*I*	Isoelectric Point
R	Resistance
T	Transmittance
t_0	Void Time
t_{dwell}	Dwell Time
t_r	Retention Time
V	Applied Potential
V_r	Retention Volume
V_{dwell}	System Dwell Volume
W	Peak Width
$z_{A,E}$	Charges of the Analyte Ion and Eluent Ion
Λ	Equivalent Conductance
ε	Molar Absorptivity
λ	Limiting Equivalent Ionic Conductance

Chapter 1

Zwitterionic Ion Chromatography

1.1 Background to Ion Chromatography

Chromatography has its origins in the efforts of the Russian botanist M. S. Tswett [1] to separate various plant pigments, such as chlorophylls and xanthophylls, by passing solutions of these pigments through glass columns packed with finely divided calcium carbonate. The principle of ion-exchange had already been recognised in 1850 by the English agricultural chemists J.T. Way and H.S. Thompson [2], while monitoring the power of soils to absorb manure. The combination of chromatographic and ion-exchange techniques, however, was not introduced until much later in the 20th century. Ion chromatography (or IC, as it is most commonly abbreviated) has its foundations in the work of Small, Stevens and Bauman (documented in 1975) [3]. They described a novel ion-exchange chromatographic method for the separation of anionic and cationic species, and their subsequent identification by conductometric detection. The reported method [3] involved the use of a low-capacity ion-exchange stationary phase to accomplish the separation, as well as utilising a second column (called a "stripper" column, and later re-termed a "suppressor") and a conductivity cell as the detection system. This was the beginning of what is labelled "ion chromatography" today, although the term "ion chromatography" itself was coined by the Dionex Corporation, after they had been granted a license by the Dow Chemical Company for further commercial development of the technology [4].

The expansion and development of IC occurred quite rapidly in the following years. By the end of the decade, Gjerde, Fritz and Schmuckler [5,6] had demonstrated that the use of a suppressor was not essential for the conductometric detection of ions in IC. Advances in stationary phase and detection technology facilitated the expansion of the number of species that may be determined using IC, as well as leading to the widespread application of IC techniques in laboratories throughout the world. The term IC now refers to any modern method for the chromatographic separation of ions [7,8].

1.2 Modes of Separation in Ion Chromatography

There are numerous column liquid separation techniques that are applicable for inclusion under the banner of IC. These include: (i) ion-exchange chromatography, (ii) ion-interaction/ion-pair chromatography, (iii) ion-exclusion chromatography, and

(iv) miscellaneous separation techniques (e.g. zwitterionic ion chromatography, and chelation ion chromatography). Each of these can be coupled with one or more detection methods, including conductivity detection, electrochemical detection and spectroscopic detection.

1.2.1 Ion-Exchange Chromatography

Ion-exchange is the equivalent, reversible exchange of ions between two or more ionised species located in different phases, without the formation of new types of chemical bonds [9]. The fundamental principle behind ion-exchange chromatography is based on the dynamic interactions between analyte ions and stationary phases that have oppositely charged groups [10]. The basis of ion-exchange chromatography is similar to that of conventional adsorption chromatography. In adsorption chromatography, a weak interaction is formed between active sites on the stationary phase (usually silanol groups) and molecules nearby, provided a dipole-dipole interaction exists between the active site and the molecules [10]. As the stationary phase sites are permanently surrounded by molecules belonging to the eluent, and as a dipole-dipole interaction exists between the two, the eluent molecules occupy the active sites. Upon sample introduction, adsorption (i.e. the displacement of eluent molecules from the aforementioned active sites) takes place, but only if the interaction between the analyte molecule and the stationary phase is stronger than the interaction between the stationary phase and an eluent molecule. It is the competition between the analyte molecules and eluent molecules that drives elution. For example, if an eluent is classified as being "strong", it will compete more effectively for the active sites than "soft" eluent molecules, thus leading to faster sample elution [10].

In ion-exchange chromatography, the active sites of the stationary phase are ionic groups chemically bound to the surface of the chromatographic stationary phase (examples of which include sulfonic acid, $-SO_3^-H^+$ as cation-exchangers, and quaternary amines, e.g. $-N(CH_3)_3^+OH^-$, as anion-exchangers). The chemically bound ions are referred to as "fixed ions", while the analyte/eluent ions of opposite charge are termed the "counter-ions" [7]. As for analyte molecules in traditional adsorption chromatography (see above), the analyte ions in ion-exchange chromatography compete for places on the stationary phase with ions present in the eluent. These sample ions exchange with the eluent ions, which are called "competing ions".

Retention is again governed by the magnitude of the competition between the analyte ions and the competing ions of like charge in the eluent. These interactions can be represented as follows, where X denotes the ionic sites of the stationary phase, and B denotes the competing ion, and A^- and C^+ represent an analyte anion and cation respectively [10]:

$$A^- + X^+B^- \rightleftharpoons B^- + X^+A^- \qquad \text{(Anion-Exchange)}$$

$$C^+ + X^-B^+ \rightleftharpoons B^+ + X^-C^+ \qquad \text{(Cation-Exchange)}$$

1.2.1.1 Ion-Exchange Selectivity

Selectivity coefficients (which are the equilibrium constants for the ion-exchange process occurring between the analyte ion and the ion-exchange functional group of the stationary phase) provide a means of determining the relative affinities of an ion-exchanger for different ions. The selectivity coefficients for the uptake of cations by strong acid cation-exchangers, and the uptake of anions by strong base anion-exchangers generally adhere to the following general pattern [7]:

Cations: $Ba^{2+} > Pb^{2+} > Ca^{2+} > Cu^{2+} > Mg^{2+} > K^+ > NH_4^+ > Na^+ > H^+ > Li^+$

Anions: $ClO_4^- > SCN^- > I^- > SO_4^{2-} > SO_3^{2-} > NO_3^- > Br^- > NO_2^- > Cl^- > F^- > OH^-$

Selectivity in ion-exchange is generally based on electrostatics (i.e. electroselectivity), which essentially means that the more highly charged an analyte ion, the more strongly it is retained by an ion-exchanger [7]. The size of the solvated analyte ion also has an effect on the observed selectivity in ion-exchange chromatography, with ions having the smallest hydration spheres being retained longer than ions of larger solvated sizes. The solvated size of the analyte ion is of importance, as ions in solution are accompanied by waters of hydration, so that for an ion to leave the eluent to enter the ion-exchange site, it must rearrange and eventually shed its solvation sphere [11]. Therefore, the more effectively an ion sheds its solvation sphere, the closer it associates with the ion-exchange site, resulting in longer retention times. The polarisability of analyte ions also affects selectivity, with ion-exchange selectivity coefficients increasing with the degree of polarisability of the analyte ions, which, for example, is why iodide is more strongly retained than the similarly charged chloride or bromide.

1.2.1.2 Eluent Characteristics

The eluent utilised in ion-exchange chromatography is generally comprised of an aqueous solution of a suitable salt, or mixture of salts. The salt solution may be a buffer, or a separate buffer may be added to the eluent composition. Organic solvents are occasionally added to the eluent used, as the presence of these water-miscible organic solvents reduces the likelihood of column contamination from hydrophobic sample components, through prevention of their binding to the column, which may result in longer retention of analyte ions [12]. However, these organic eluent modifiers may also alter the degree of ionisation of weakly acidic or basic analytes, or change the ion-exchange affinity of hydrophobic ions, and can influence the solvation of the stationary phase functional groups and the analyte ions [13]. Variations in selectivity in ion-exchange chromatography are generally obtained through the use of different stationary phases, as the elution order is chiefly dictated by the interaction between the analyte ion and the ion-exchange functionality of the stationary phase [13]. However, there are certain eluent-related factors that will affect the elution characteristics of analyte ions. The three main properties of the eluent system that have the most significant effect on the retention of analyte ions are [7]:

(1.) *Eluent pH*

Eluent pH can have a drastic effect on the form in which the functional group of the stationary phase exists. The ion-exchange capacity of the stationary phase (i.e. the number of charged groups per unit weight) can vary significantly depending on the pH of the eluent [13], particularly for "weak" anion-exchangers and cation-exchangers.

Eluent pH also exerts an influence on the charges of eluent ions, which is particularly important for anion separations [13]. For example, polyprotic weak acids, which are in widespread use in the ion chromatographic separation of anions, become dissociated with increasing pH, thus increasing the charge on the acid anion, leading to increased eluting power, until complete dissociation of the acid has been reached [13]. The opposite situation occurs for weakly basic eluents, where a decrease in pH results in higher degrees of protonation, thereby causing an increase in the eluting power of the eluent. Similarly, eluent pH also affects the

charges of some analyte ions, principally those which are weak acids or bases, e.g. nitrite, fluoride, phosphate, silicate, cyanide, and carboxylate anions.

The combination of all of the aforementioned effects of eluent pH mean that some buffering capacity may be desirable, as this would maintain a stable pH, thereby resulting in more reproducible retention times.

(2.) Nature of the Competing Ion

The differences between the selectivity coefficients of the competing ion and a particular analyte ion determines the degree to which the analyte ion will be displaced from the stationary phase by the competing ion [4]. Therefore, as different competing ions will have dissimilar selectivity coefficients, adjusting the nature of the competing ion in the eluent will cause analyte ions to elute either more, or less, readily. The factors upon which the selectivity coefficients of eluent ions for certain analyte ions are reliant are the same as those which control the ion-exchange selectivity of the ion-exchange sites of the stationary phase for analyte/eluent ions (see Section 1.2.1.1), namely the size, charge, degree of hydration, and polarisability of the analyte ions [7], and follow the general order stated in Section 1.2.1.1. Electroselectivity exerts the greatest effect on retention of analyte ions, with eluents of greater electrostatic charge having a greater affinity for the available ion-exchange sites of the stationary phase, making them stronger eluents than eluents of lesser charge [7].

(3.) Ionic Strength of the Eluent

The concentration of the eluent can have a very significant effect on the position of the equilibrium point in ion-exchange equilibria, through increasing the amount of competing ions present. Higher concentrations of competing ions in the eluent results in faster elution of analyte ions [4]. This is due to more eluent ions being available to compete with analyte ions to undergo ion-exchange with the functional groups of the stationary phase. This effect becomes more pronounced for multivalent analytes [7]. For example, if the concentration of a monovalent eluent ion is increased, the retention of divalent analytes will decrease twice as rapidly as that of monovalent analytes.

1.2.2 Ion-Interaction/Ion-Pair Chromatography

Under typical reversed-phase HPLC conditions, hydrophilic ionic analytes are very weakly retained. On the other hand, when a lipophilic reagent ion, termed an ion-interaction reagent (IIR), is added to the eluent, ionised species of opposite charge to the IIR can be separated on a reversed-phase column with adequate retention [14]. This mode of chromatography is termed ion-interaction chromatography (IIC, sometimes called ion-pair chromatography). Retention occurs on the basis of the formation of a neutrally charged ion-pair between the analyte ion and the IIR [14]. Examples of IIR include tetraalkylammonium ions for anion separations, and aliphatic sulfonate ions for cation separations.

Comparing the use of a chromatographic system composed of a C_{18} reversed-phase column and an eluent containing a solution of IIR in a mixture of water and one or more organic solvents, to a system utilising an eluent which does not contain any amount of IIR [7], it can be seen that the addition of IIR to the eluent does not significantly alter the retention of neutral analytes, although the retention of analytes having the same charge as the IIR decreases when IIR is added to the eluent composition, while the retention of analytes in possession of the opposite charge to the IIR increases upon addition of IIR to the eluent employed.

The following trends have also been observed when using a C_{18} reversed-phase stationary phase and an eluent comprised of an IIR dissolved in a mixture of water and one or more organic solvents [7]:

- The retention of analytes having an opposite charge to the IIR increased when the concentration of IIR present in the eluent was increased.
- The retention of analytes possessing the opposite charge as that of the IIR increased when the lipophilicity of the IIR was increased.
- Retention of all analytes decreased when the concentration of the organic modifier in the eluent was increased.

Three different mechanisms have been proposed to account for all of the above observations [15]:

1.2.2.1 Ion-Pair Model

In this mechanism, it is proposed [16] that, after sample introduction has occurred, the analyte ion and the IIR form an ion-pair (as in Fig. 1.1). (As previously mentioned, the IIR will act as a counter-ion to the analyte ion, and will have the opposite charge to that of the analyte ion. For the analysis of anions, therefore, the IIR will have a positive charge.)

Figure 1.1. Formation of an ion-pair from an analyte anion and a positively charged ion-interaction reagent (IIR) [7].

This ion-pair will have a net neutral charge, and will partition between the eluent and the stationary phase through typical reversed-phase interactions, competing with the eluent molecules (other than the IIR) for positioning on the active sites of the stationary phase. This concept is illustrated in Fig. 1.2. This means that retention occurs entirely as a result of reactions occurring in the eluent. Neutral analyte molecules are unaffected by the presence of IIR in the eluent, and therefore interact with the stationary phase through conventional reversed-phase interactions.

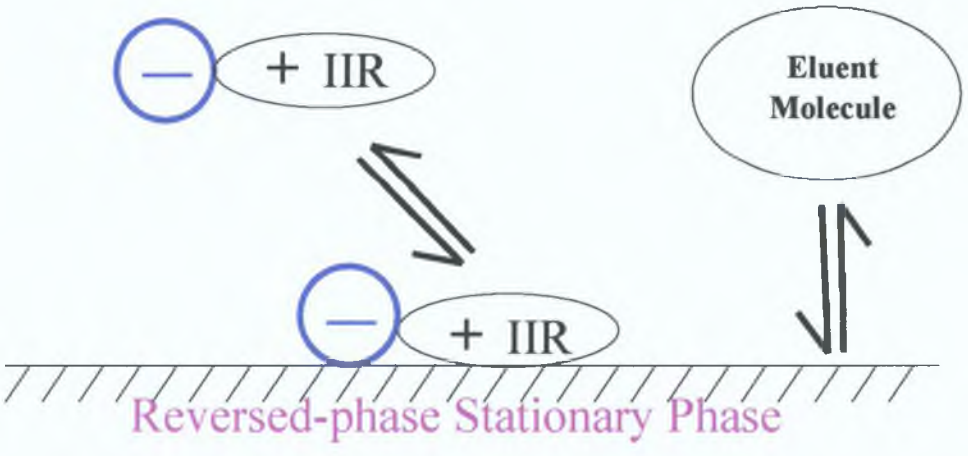

Figure 1.2. Schematic illustration of retention in the ion-pair model, where the retention of analyte anions is shown, and where the IIR is a cation [7].

An increased concentration of IIR (as well as an increase in the lipophilicity of the IIR) will result in increased retention of analytes possessing the opposite charge to the

IIR. Increasing the amount of organic modifier in the eluent will shift the partition equilibrium in the direction of the eluent, thereby lowering retention times.

The ion-pair model does not provide adequate explanation for all observed chromatographic trends, e.g. the ion-pair model requires that neutral ion-pairs formed by various inorganic ions should have varying degrees of lipophilicity in order for separation to occur [7]. These differences are very small for inorganic ions (e.g. Cl^-, Br^-, NO_2^-, NO_3^- etc.), yet these species are easily separated by ion-interaction chromatography.

1.2.2.2 Dynamic Ion-Exchange Model

This model [17] proposes that a dynamic equilibrium exists between the charged IIR located in the eluent and the IIR adsorbed onto the stationary phase by hydrophobic interactions. Adsorption of the IIR imparts an electrostatic charge to the stationary phase, so that the stationary phase now functions as an ion-exchanger. Because these charged active sites are not fixed in position (as in a bonded ion-exchange stationary phase), but are in dynamic equilibrium between the two phases, the column can be considered to be a dynamic ion-exchanger. Introducing an analyte ion with the opposite charge to the IIR results in retention through the usual ion-exchange mechanism. The competing ion for this ion-exchange process can be either the IIR molecules themselves, or an additional ionic species added to the eluent. Analytes with a charge identical to that of the IIR will be repelled by the charged stationary phase, while neutral analytes will be unaffected by the IIR. This mechanism is outlined visually in Fig. 1.3. The percentage of organic solvent in the eluent will affect the amount of IIR molecules which will adsorb onto the stationary phase, with increased percentages of organic solvent resulting in decreased concentrations of IIR on the stationary phase. Altering the lipophilicity of the IIR, or concentration of IIR in the eluent, will change the dynamic ion-exchange capacity of the column, and will result in the effects listed previously in Section 1.2.2. Analytes having a charge identical to that of the IIR are repelled by the charged stationary phase, and therefore exhibit shorter retention times than would be seen if no IIR was present in the eluent, while retention times for neutral analytes are unaffected by the IIR.

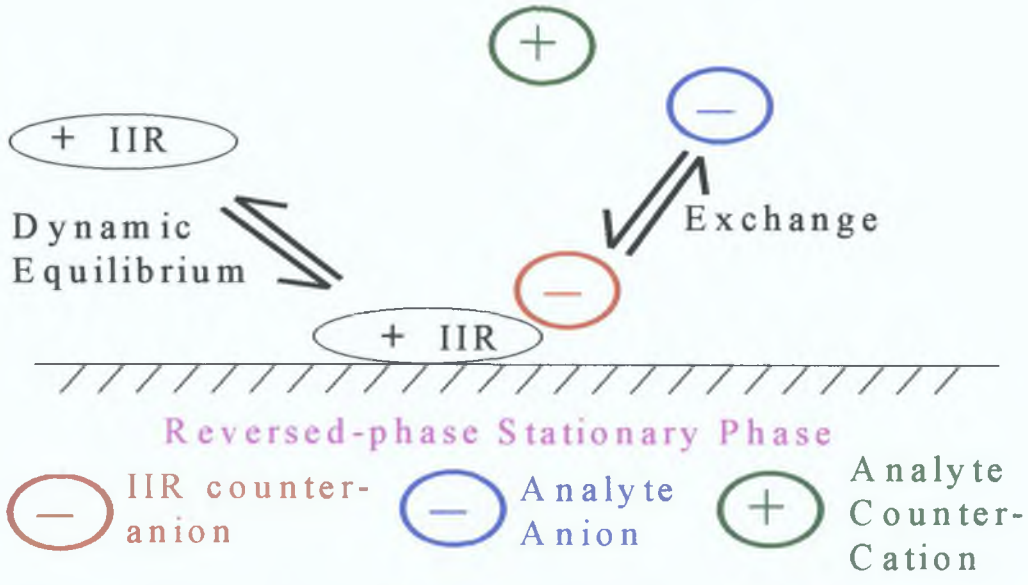

Figure 1.3. Schematic illustration of the dynamic ion-exchange model, for the separation of anionic analytes [7].

1.2.2.3 Ion-Interaction Model

This model [18,19] is generally considered to be a combination of the previous two models, as it displays both the electrostatic effects of the ion-pair model and the adsorptive effects of the dynamic ion-exchange model. This mechanism suggests that the adsorption of the charged IIR ions onto the stationary phase causes the formation of an electrical double layer at the surface of the stationary phase. The adsorbed IIR ions are spaced evenly over the stationary phase, due to repulsive forces from adjacent IIR ions. The adsorbed IIR ions constitute a primary layer of charge, to which the oppositely charged counter-ions present are attracted. The counter-ions themselves comprise a diffuse, secondary layer of charge. The magnitude of the charge in both layers depends on the amount of adsorbed IIR molecules, which, in turn, is dependent on the concentration of the IIR, the lipophilicity of the IIR, and the concentration of organic modifier present in the eluent. This electrical double layer is shown in Fig. 1.4.

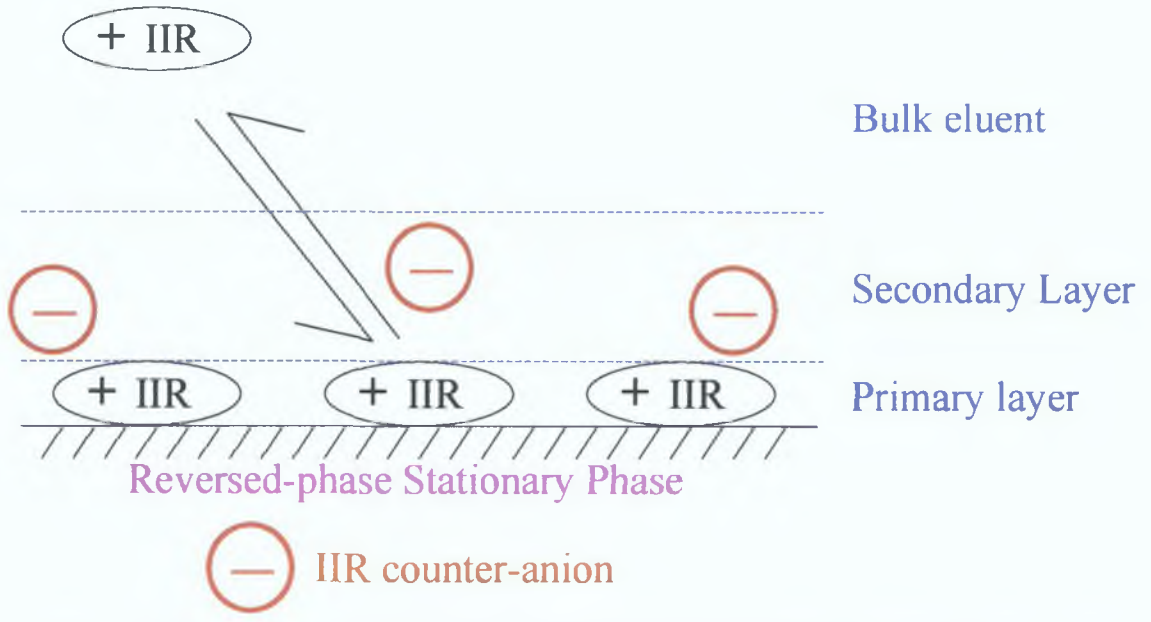

Figure 1.4. Formation of the electrical double layer in the ion-interaction model, using a positively charged IIR and a negatively charged counter-ion [7].

Analyte ions (possessing the opposite charge to the IIR ions) can compete with the IIR counter-ions for a place in the secondary layer of the electrical double layer. Upon entering this layer, these analyte ions are electrostatically attracted by the primary layer, and are therefore retained. However, in order to maintain a charge balance, when these analyte ions enter the primary layer, an oppositely charged IIR ion must accompany them into the primary layer. The overall result is that retention of analyte ions involves a pair of ions (i.e. the analyte ion and the IIR ion), but not necessarily an ion-pair. Fig. 1.5 shows this retention mechanism in further detail. Neutral analytes are able to pass unobstructed through the electrical double layer, meaning that their retention is relatively unaffected by the IIR. Analyte ions possessing the same charge as the IIR will display reduced retention upon addition of an IIR to the eluent, as they will be electrostatically repulsed by the primary layer of the electrical double layer.

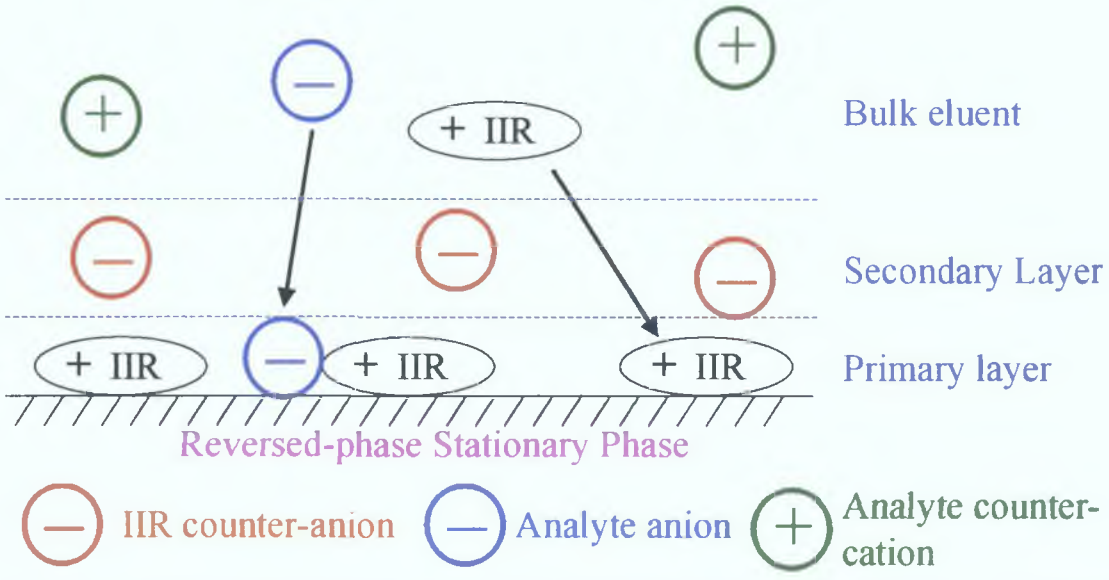

Figure 1.5. Schematic illustration of the ion-interaction model, for the separation of analyte anions [7].

The ion-interaction model has been considered to be most appropriate mechanism for ion-interaction chromatography, as it provides the most consistent agreement with experimental findings [7,19]. This model also explains another potential benefit of ion-interaction chromatography, whereby, unlike conventional ion-exchange chromatography, the separation of non-ionic and ionic or ionisable compounds within a single sample can be achieved, as analyte retention involves its transfer through the electrical double layer, and depends on both electrostatic interactions and adsorptive (i.e. reversed-phase) effects [14].

1.2.3 Ion-Exclusion Chromatography

Ion-exclusion chromatography was introduced in the early 1950's as a means of separating ionic analytes from weakly ionised or neutral analytes [8]. In ion-exclusion chromatography, unlike conventional ion-exchange chromatography, analytes with a partial negative charge (e.g. carboxylic acids) are separated on a cation-exchange resin having anionic functional groups (usually sulfonic acid groups), while analytes possessing a partial positive charge (such as weak bases) are separated on an anion-exchange resin with cationic functional groups (usually quaternary ammonium groups) [20]. Therefore, the characteristic feature of ion-exclusion chromatography is that the charge of the dissociated functional group of the ion-exchange resin is the same as the charge of the analyte(s) of interest (i.e. weakly

ionised analytes). Compounds that can be separated by means of ion-exclusion chromatography include weak organic and inorganic acids, weak organic and inorganic bases, and hydrophilic neutral compounds, e.g. sugars [8].

The chromatographic system can be considered to consist of 3 distinct parts [8]:

(1) A solid resin network, together with its bound ionic functionalities.

(2) Occluded liquid within the pores of the resin beads.

(3) The eluent phase, which flows between the resin beads.

The ion-exchange resin behaves like a semi-permeable membrane, separating the eluent phase from the occluded liquid phase. A schematic representation of how retention occurs in ion-exclusion chromatography is shown in Fig. 1.6. Using Fig. 1.6, the mechanism of separation, using water as an eluent, can be explained as follows: In the case of acidic analytes, e.g. hydrochloric acid and acetic acid, retention will depend on their degree of ionisation [7]. As hydrochloric acid is a strong acid, it will be strongly ionised in solution. The chloride ions formed from the dissociation will be repulsed by the anionic functional groups of the resin, and therefore these ions will not display any retention by the column. However, a weak acid, an example of which is acetic acid, will be only weakly ionised in solution, and will be present mainly as electrically neutral acetic acid molecules in a water eluent (which is commonly employed in ion-exclusion chromatography). This means that acetic acid will exhibit some degree of retention, and will therefore elute later than hydrochloric acid. A similar process occurs for the separation of a weak base (e.g. ammonia) from a strong base (e.g. sodium hydroxide) [7], as in Fig. 1.6 (b). The dissociated sodium ions of the sodium hydroxide molecules are repelled by the cationic functional groups of the resin, and are unretained by the chromatographic system, due to their zero-binding capacity to the resin. Ammonia, however, can penetrate into the pores of the resin, into the occluded liquid phase, due to its low degree of ionisation and resulting low overall charge, thus leading to retention of this compound.

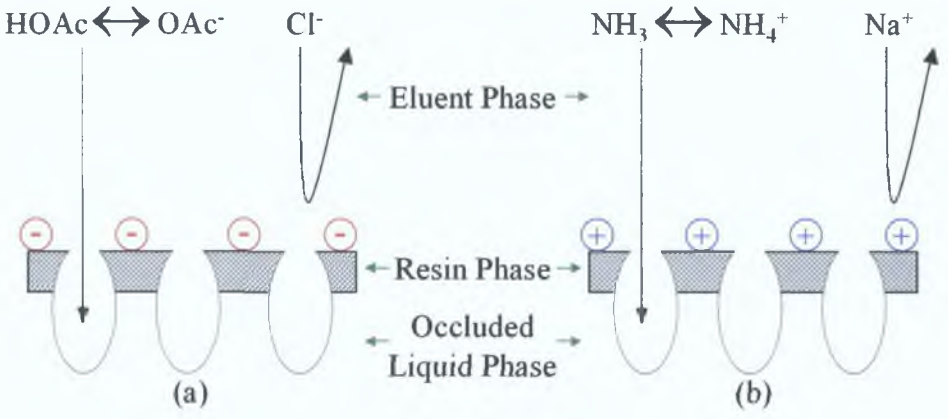

Figure 1.6. Schematic representation of the ion-exclusion chromatography of (a) acidic analytes (e.g. acetic acid, HOAc, and HCl), and (b) basic analytes (e.g. NH_3 and NaOH) [7].

However, the charge of the analyte is not the only factor that has a bearing on retention in ion-exclusion chromatography. There are numerous other factors that can affect retention [7]:

- Molecular size of the analyte.
- Hydrophobic interactions between the analyte and hydrocarbon portion of the stationary phase (which are determined by the nature of the analyte and the amount of organic modifier present in the eluent), as well as hydrogen-bonding interaction between analyte and stationary phase.
- Ion-exchange capacity of the stationary phase.
- Ionic form of the ion-exchange resin.
- Temperature at which the separation is performed.
- Degree of cross-linking of the resin.

The separation of carboxylic acids is the predominant application of ion-exclusion chromatography. Early analyses were carried out using pure water as the eluent, but, at present, the most commonly employed eluents are dilute solutions of strong mineral acids (e.g. sulphuric acid and hydrochloric acid) [8].

1.2.4 Miscellaneous Separation Techniques

1.2.4.1 Chelation Ion Chromatography

Chelation ion chromatography involves the separation of metal ions on a stationary phase which has a suitable ligand immobilised onto the surface. The motivation for the development of this technique came about due to the fact that conventional ion-exchange chromatography does not offer much scope for changing the selectivity (i.e. order of retention) of metal separations [9], which severely limits the versatility of IC methods, particularly in the determination of trace metal concentrations in samples containing massive amounts of other metals. One way of overcoming this obstacle is through the use of a metal chelating ion-exchanger, rather than a simple ion-exchange substrate [9]. Chelating ion-exchangers had been used regularly, but predominantly as a means of preconcentrating transition and rare-earth metals prior to analysis by IC [21], through the elimination of interfering sample matrix components. Chelating ion-exchange (or chelation-exchange for short) stationary phases can be used in IC systems just like ion-exchange columns, but have the advantage (for the analysis of metals) of selective control and insensitivity to changes in ionic strength [9]. In contrast to the sorption mechanism of ion-exchange, where the formation of new types of chemical bonds does not occur, chelation-exchange involves the formation of a coordinate bond between the analyte metal cation and the chelating group of the stationary phase [9]. Therefore, separation by chelation-exchange is controlled by the thermodynamics and kinetics of metal complex formation and dissociation [7]. Slow rates of complex formation/dissociation will lead to chromatograms displaying very broad peaks.

There are numerous chelating ligands available for the formation of chelating stationary phases. This is advantageous, as each one of the broad range of chelating ligands offer unique selectivity. However, the selection of suitable chelating functionality is of utmost importance for efficient separations, as the kinetics of chelation-exchange have been found to be slower than for ion-exchange [7]. These ligands are chemically bound to a support material, which can be silica- or polymer-based. An example of a commercially available chelation-exchanger is Chelex 100, which is a cross-linked polystyrene substrate containing bonded iminodiacetic acid (IDA) groups [7].

When using chelating-exchange, there also exists the option of manipulating analyte retention by varying eluent pH, or by adding a competing ligand to the eluent composition [7]. In general, increased retention of metal cations is observed on increasing the pH of the eluent [9]. This is due to the dissociation of acid groups on the immobilised chelating ligand producing a sharp increase in the conditional stability constants of surface metal complexes. The addition of a complexing or chelating agent to the eluent composition, meanwhile, will result in competition for the analyte cations between the chelating group on the surface of the stationary phase, and the chelating group of the eluent.

Another factor that is taken into account when using chelation-exchangers is the presence of more than one sorption mechanism on the stationary phase [9], as many chelating compounds used in this manner contain weak acid groups, whose conjugate bases form coordinate bonds with the metal cations. At low eluent pH values, these groups can also act as ion-exchange sites.

1.3 Zwitterionic Ion Chromatography (ZIC)

Zwitterionic substances have been used for ion separations since 1981, when Knox and Jurand [22,23] reported the use of a zwitterionic pairing agent, namely 11-aminoundecanoic acid, for the separation of nucleotides and other related species through the formation of ion pairs between the zwitterionic pairing agent and the nucleotide molecules. Since then, amino acids (which are zwitterionic at their respective isoelectric points) have been covalently attached to the surface of silica matrices for the purpose of ion-exchange based separations [24]. As the amino acids can exist in several forms, depending on eluent pH, anion- and cation-exchange properties were both observed using such columns [e.g. 25], while simultaneous determination of anions and cations was possible using a poly(aspartic acid)-functionalised silica column [26], under conditions of optimised eluent pH, with ion-exchange selectivity resulting from a combination of electrostatic attraction and repulsion forces. Work by Yu *et al.* [27,28] on immobilised zwitterionic amino acid-based ligands on silica particles, with the resultant zwiterionic stationary phases used for the separation of a variety of ionic and zwitterionic species, indicated that highly selective quadrupole interactions existed between the bound zwitterionic molecules

and ampholytic organic analytes (such as nucleosides and amino acids), which added a further dimension to selectivity in comparison to simple ion-exchange of analytes possessing a single charge [24].

In 1993 a new form of IC, which employed stationary phases with physically adsorbed zwitterionic surfactant molecules, was introduced [29]. In conventional IC, a stationary phase is used that contains functional groups having either negative charges (thereby acting as cation-exchangers) or positive charges (in the case of anion-exchangers), but not usually both negative and positive charges. In electrostatic ion chromatography (EIC), a term coined by Hu *et al.* in 1993 [29], the stationary phase utilised contains both anionic and cationic functional groups. This means that analyte ions are subjected to both attractive and repulsive forces in their passage through the stationary phase. Zwitterionic surfactant molecules are used to create such positive/negative charged stationary phases, as the positive and negative charges are in close proximity to each other within a single molecule. EIC is also commonly referred to as zwitterionic ion chromatography (ZIC), due to the retention mechanism involved. Different retention models have been proposed for systems using pure water as the eluent, and systems employing electrolytic eluents. Both models will be discussed in detail in Sections 1.3.1, 1.3.4, and 1.3.5.

1.3.1 Fundamental Principles of ZIC

As in all other types of chromatography, the integral concept of IC is that an effective distribution of the analyte (which in the case of IC is an anion or cation) between the stationary phase and the eluent is required for any retention, and therefore separation, to occur [3]. With a stationary phase containing a single functionality (i.e. having either anionic or cationic functional groups), introduction of analyte ions having charges opposite to that of the uni-functional stationary phase means that electrostatic attraction will occur between the charged sites of the stationary phase and the oppositely charged ions of the eluent, leading to the formation of an electrical double layer (EDL), as in the Stern model for an anion-exchanger in Fig. 1.7 below [30,31,32]. To release these electrostatically bound ions back into the bulk solution, and thereby achieve the required effective distribution of the analyte ions between the stationary phase and the eluent, some method of ion-exchange is needed. In other words, the eluent employed must contain a competing ion to replace the analyte ions.

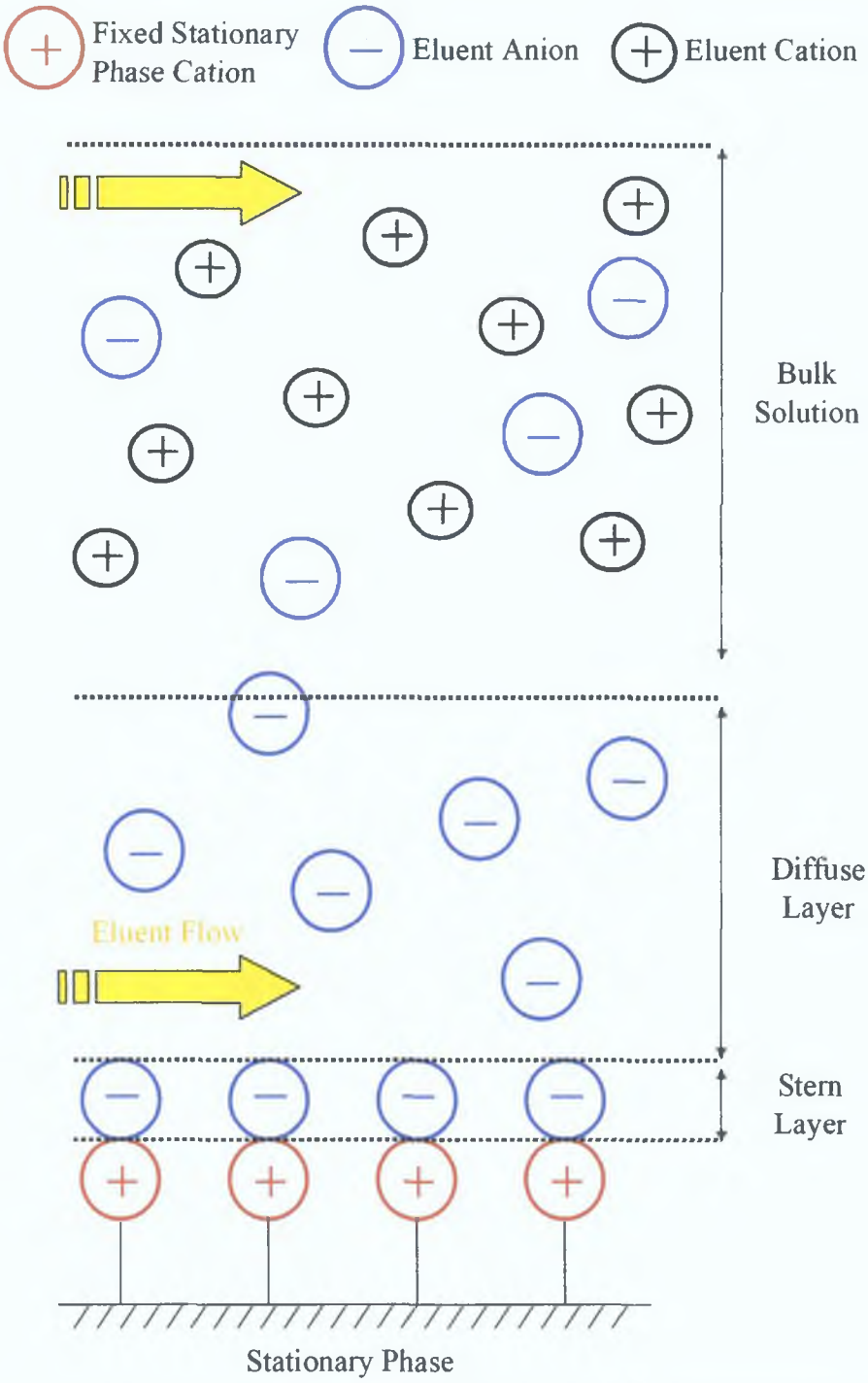

Figure 1.7. Electrical double layer created with a uni-functional stationary phase (which in this case is an anion-exchanger) [30,31,32].

However, when the stationary phase is bi-functional in nature, as in the case of zwitterionic stationary phases, both positive and negative electrostatic fields are produced concurrently, meaning that the EDL contains both anions and cations. This

type of EDL has been named a zwitterionic electrical double layer (ZWEDL) [30]. An illustration of this concept can be seen in Fig. 1.8.

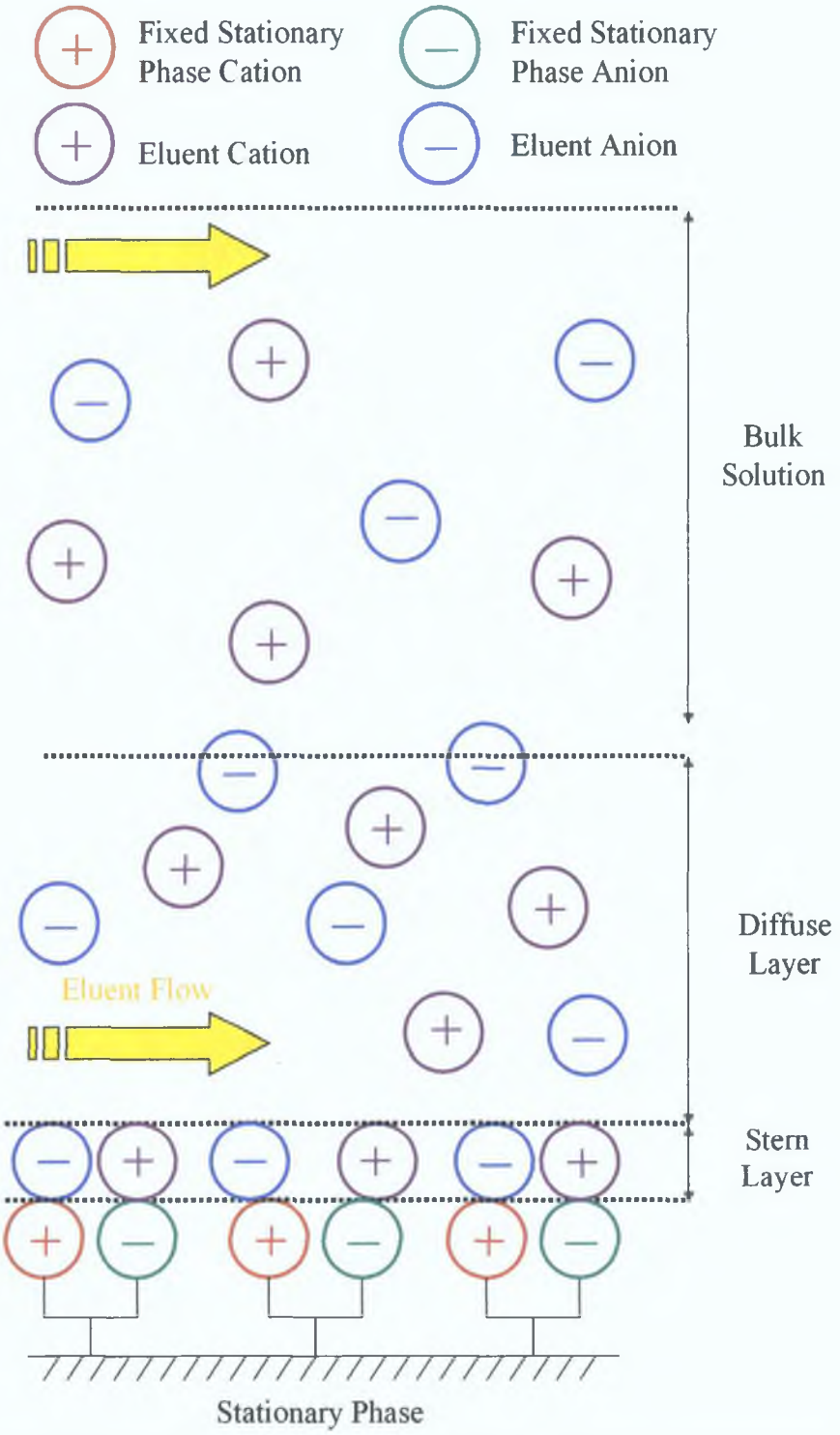

Figure 1.8. Formation of ZWEDL with a zwitterionic stationary phase [30,31,32].

A ZWEDL is considerably different to a conventional EDL, as is evident from Fig. 1.8. The distinctive and unique properties of a ZWEDL are briefly described below:

- Analyte anions and cations are retained simultaneously, because of the electrostatic attraction exhibited by the positive and negative stationary phase functionalities, respectively. In comparison, in the case of a single charge-fixed stationary phase, the EDL created contains either the analyte anions (for a positive charge-fixed stationary phase) or cations (for a negative charge-fixed stationary phase) [30,31,32].
- Analyte ions (anions and cations) are subjected to simultaneous forces of electrostatic attraction and repulsion, due to the positive and negative charges of the zwitterionic stationary phase being located within a single molecule [30,31,32].
- Both of the previous two points indicate that the overall electrostatic affinity between the zwitterionic stationary phase and the analyte ions in the EDL is quite weak, thus rendering the use of a displacing ion in the bulk solution unnecessary [30,31,32]. This implies that pure water alone could be used as an eluent for separations in ZIC.

Analyte anions and cations are retained, and released, in a similar manner. However the separation mechanism is not so simple as to expect the elution of all analyte anions and cations in separated bands. An analyte ion will be retained as explained above, but in order to maintain electroneutrality, an analyte anion will elute in tandem with a cation, as an ion-pairing-like form [29], which, for the sake of simplicity, will be referred to as "ion-pairs", see Fig. 1.9. These forms are not ion-pairs in the conventional sense of the term, as no strong bond exists between both ions. They are merely partners in migration through the chromatographic system, and to the detection cell employed. Therefore, the observed peaks in the subsequent chromatograms are due to the analyte anions, as well as the analyte cations, with which they are associated. This will be discussed further in Section 1.3.4.1.

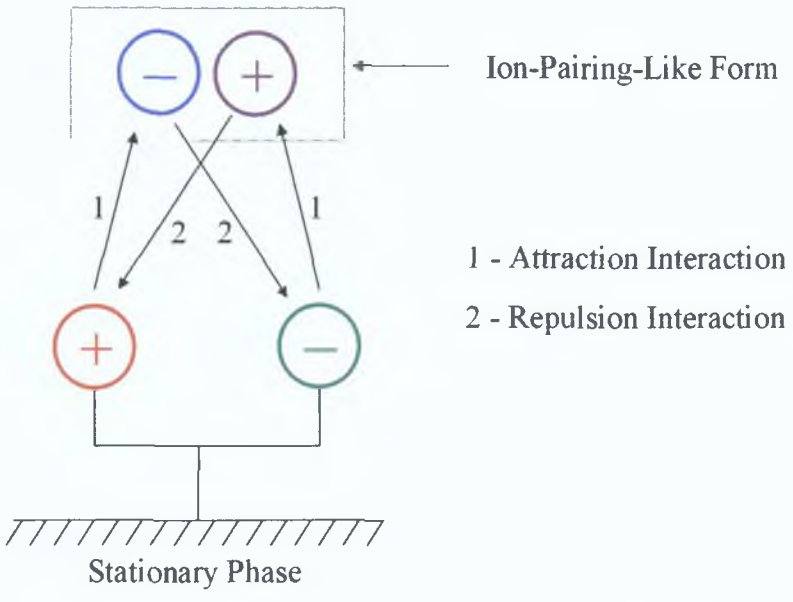

Figure 1.9. Schematic illustrating the simultaneous electrostatic attraction and repulsion interactions between analyte ions and the zwitterionic stationary phase [29].

1.3.2 Preparation of Stationary Phases for ZIC Using Zwitterionic Surfactants

Charged stationary phases suitable for use in ZIC can be prepared by modifying standard C_{18} reversed-phase columns with appropriate zwitterionic surfactants using hydrophobic interactions. Examples of zwitterionic chemicals used in ZIC will be the focus of the following subsection.

1.3.2.1 Nature of Zwitterionic Surfactants Used in ZIC

Molecular structures of some of the most commonly used zwitterionic surfactants in ZIC can be seen in Fig. 1.10 (a-e). Most of the surfactants in Fig. 1.10 are used for the separation of anions. Only one surfactant (N-dodecylphosphocholine) (Fig. 1.10 (e)) is commonly used for the separation of cations. From the structures it can be seen that each surfactant contains an anionic functional group, a cationic functional group, and a hydrophobic region that allows the surfactant to be retained strongly on the C_{18} stationary phase material.

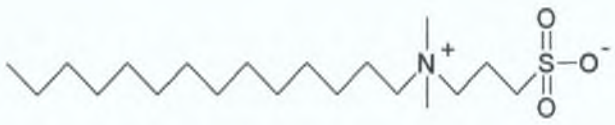

(a) 3-(N,N-dimethylmyristylammonio)propanesulfonate (Zwittergent 3-14) [CMC = 0.1 – 0.4 mM]

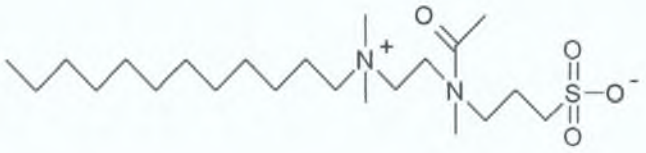

(b) N-[2-acetyl(3-sulfopropyl)aminoethyl]-N,N-dimethyldodecanaminium hydroxide (Ammonium Sulfobetaine – 1) [CMC not available]

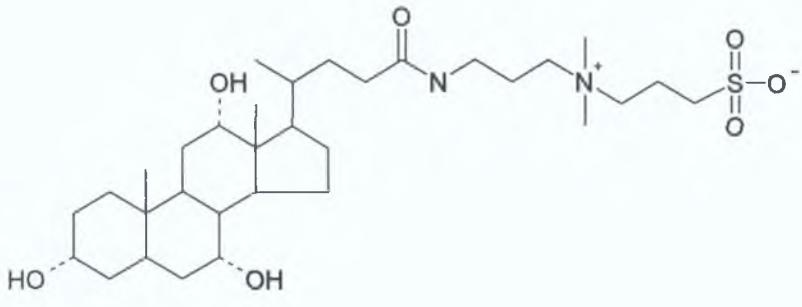

(c) 3-[(3-cholamidopropyl)dimethylammonio]-1-propanesulphonate (CHAPS) [CMC = 6 – 10 mM]

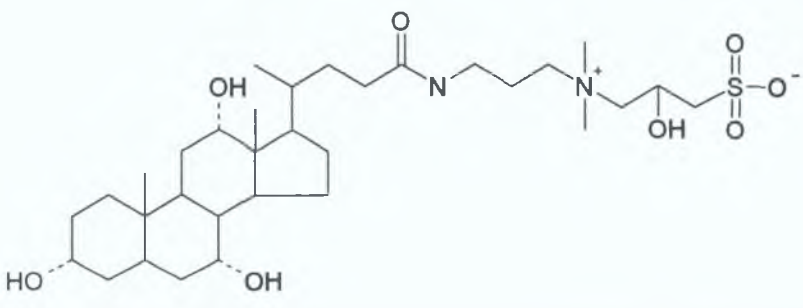

(d) 3-[(cholamidopropyl)dimethylammonio]-2-hydroxy-1-propanesulfonate (CHAPSO) [CMC = 8 mM]

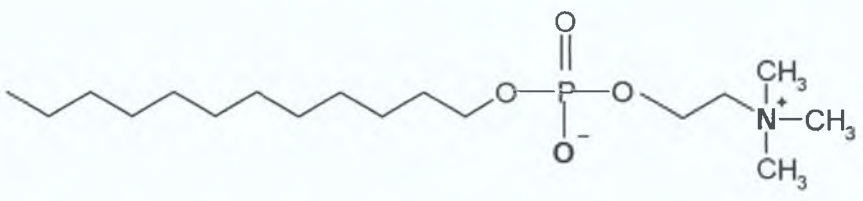

(e) N – Dodecylphosphocholine [CMC = 1.1 mM]

Figure 1.10 (a) – (e). Chemical structures of some zwitterionic surfactants used in ZIC, with their respective values for critical micelle concentration (CMC).

The characteristic of each zwitterionic surfactant that determines whether it is suited to the separation of either anions or cations is the relative position of the positively and negatively charged functional groups. When the negatively charged functional group resides at the outermost end of the molecule, analyte cations within the eluent will form a barrier of cations along the outer edge of the zwitterionic coating (effectively acting as a Donnan membrane). This brings about a weakened negative electrostatic surface potential, and therefore, only analyte anions will be able to penetrate this layer and permeate through to the stationary phase, thus leading to retention and separation of anions, which will form "ion-pairs" with the cations present when being eluted in order to maintain the electroneutrality of the analyte band [29]. The opposite effect occurs when the outer functional group is positively charged.

While most stationary phases for ZIC are created using synthetic zwitterionic surfactants, some naturally occurring biological compounds, which are zwitterionic across a wide pH range, can also be utilised for the same purpose. Phosphatidylcholines (also referred to as lecithins), which are naturally occurring zwitterions found widely in animal tissues as the primary component of biomembranes, have been employed as biomimetic stationary phases for the separation of inorganic anions [33,34]. The interactions between phosphatidylcholines and inorganic anions has been seen to modify the functioning of various membrane-related physiological processes, such as muscle twitch tension, with the strength of the anion-phosphatidylcholine interactions increasing in the order $ClO_4^- > SCN^- > I^- > NO_3^- > Br^- > Cl^- > F^- > SO_4^{2-}$ [35], which suggested that a chromatographic stationary phase based on phosphatidylcholines should show the same selectivity for inorganic anions. The developed stationary phases were shown to be useful for the direct determination of anions having low free energies of hydration (e.g. iodide and thiocyanate) in highly saline solutions, as these analyte anions will have a high propensity to transfer from the eluent to the stationary phase.

1.3.2.2 Column Modification Procedure

In the first paper published on ZIC by Hu *et al.* [29], the chromatographic columns were prepared through dynamic modification, by passing a 30 mM solution of CHAPS, CHAPSO or Zwittergent 3-14 through the C_{18} reversed-phase column at a

flow rate of 0.7 mL/min for 75 minutes, followed by a pure water rinse for at least 40 minutes, to remove any excess surfactant present. Since then, most column modification procedures in ZIC have been based on the above procedure.

Experiments carried out by Umemura *et al.* [36] have shown that the concentration of the surfactant in the column modification solution had no influence on the adsorption of the surfactant to the C_{18} reversed-phase surface. Whether a more concentrated solution was pumped through the column for a short period of time, or a more dilute solution pumped through for a longer time, the amount of zwitterionic surfactant adsorbed was identical, provided the saturation level had been reached.

Major departures from the above modification technique have been documented by Hu *et al.* [37], as well as Umemura *et al.* [38]. One such deviation, termed the "two step modification method" [37], involved the use of a polymer-based column modified initially with CHAPS, and then used as a supporting column for the formation of a zwitterionic stationary phase using Zwittergent 3-14 (or ammonium sulfobetaine-3) using the standard column modification methodology mentioned previously. Another such deviation [38] was concerned with adjusting the amount of surfactant adsorbed by adding various amounts of acetonitrile to the water eluent. The adsorbed surfactant has the effect of suppressing the hydrophobicity of the C_{18} reversed-phase surface, and has been successfully utilised in the separation of nucleosides and their bases. Other experimental results by Hu and Haddad [39] have indicated that zwitterionic stationary phases exhibiting good separation efficiency could be prepared by modifying the stationary phase with low-molecular weight alcohols (such as 1-propanol).

1.3.2.3 Covalently Bonded Stationary Phases for ZIC

Jiang and Irgrum have reported the synthesis of covalently bonded polymer-based [40,41], and silica-based [42], zwitterionic stationary phases for the separation of ionic species. The principal motivation behind their work was that dynamically modified columns usually have inferior stability compared to covalently bonded columns, due to the loss of functional moieties from the dynamically sorbed layer, which is especially problematic in the separation of samples containing biological macromolecules. Jiang and Irgrum [40] utilised a reaction scheme in which

methacrylate polymer beads were activated with epichlorohydrin, followed by the coupling of a (2-dimethylamino)ethanesulfonic acid inner salt to the epoxide groups of the activated polymer beads. The resulting material contained zwitterionic pendant groups (with a terminal negatively charged sulfonate group and an internal positively charged quaternary ammonium group), which retain both the negative and positive charges over a wide pH range (approx. pH 3 – 11), and was applied to the independent and simultaneous separation of inorganic anions and cations using perchlorate eluents.

1.3.3 Use of Pure Water as Eluent in ZIC

Much of the initial research in the area of ZIC focused on the use of pure water as eluent [29,30,31,32]. This is because both anionic and cationic analytes can be retained by the electrostatic attraction exhibited by the opposite charges of the zwitterionic stationary phase, but can also be freed into the eluent without requiring a displacing ion in the eluent composition (as in regular ion-exchange chromatography), due to the repulsive forces resulting from identically-charged ions located nearby within the same molecule.

Having an eluent composed of water alone has many benefits. Firstly, because such IC systems are significantly simpler than those employing complex chemical components, operational costs can be drastically reduced, not just from reduced chemical reagent consumption, but also from the time saved by negating the need for precise eluent preparation and adjusting of such chemical parameters as pH etc. The use of pure water as eluent is also advantageous for the purpose of eluent recycling. Having an eluent comprised of pure water can have a very beneficial impact on sensitivity for trace analysis of ions, as an eluent composed of water alone would have a low background absorbance (for UV detection) and a low background conductance (for conductivity detection).

1.3.4 Trends in ZIC

ZIC displays some unique and complex trends, when compared to conventional ion exchange chromatography. As ZIC is an analytical technique that has only been developed relatively recently, some of the mechanisms involved with observed experimental data are not fully understood. (The bulk of the research carried out to

date in the field of ZIC has focussed primarily on the analysis of anions, and so the majority of the remainder of this Chapter will deal with the separation and detection of anions.)

1.3.4.1 Partitioning Behaviour of Analyte Ions

In early papers on the topic of ZIC using pure water as an eluent, the order of elution for inorganic anions was found to be almost identical to that of traditional ion-exchange chromatography (except for the extremely early elution of sulphate directly before chloride, bromide and iodide, which is due to the hydration energies of the ions, as will be seen later in Section 1.3.5).

However, the above elution order was preserved only when the analyte anions were paired with cations of identical valence values. Injecting sample mixtures containing different salt forms of the same anions could result in differences in the elution order.

Hu and Haraguchi [43] found that the retention time of a single anion in ZIC changes significantly depending on the cation to which it is paired. As can be seen in Fig. 1.11, the retention times for both chloride and nitrate varied considerably, as influenced by the counter-cation to which the anions were paired, with the anion paired to the monovalent cation being less retained than that of the anion paired to the divalent and trivalent cations. Both ICP-AES and UV-absorption detection techniques were utilised to confirm peak identities.

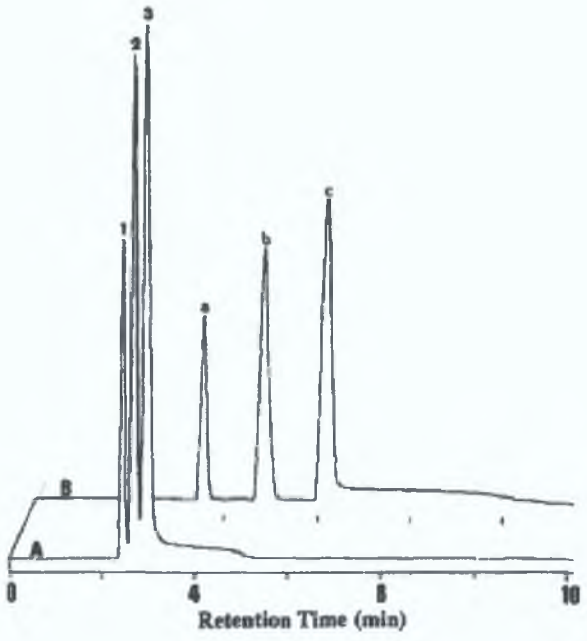

Figure 1.11. Chromatograms of an aqueous solution containing (A): 2.0 mM each of Na^+, Mg^{2+}, and Ce^{3+} with Cl^- as the counterion, and (B): 2.0 mM each of Na^+, Mg^{2+}, and Ce^{3+} with NO_3^- as the counterion, using a C_{18} reversed-phase column (250 x 4.0 mm I.D.) modified with Zwittergent 3-14, with pure water as the eluent, and a flow rate of 1.0 mL/min. Detection was by conductivity. Peak Identification: 1: Na^+-Cl^-, 2: Mg^{2+}-$2Cl^-$, 3: Ce^{3+}-$3Cl^-$, a: Na^+-NO_3^-, b: Mg^{2+}-$2NO_3^-$, c: Ce^{3+}-$3NO_3^-$ [Reproduced from ref. 43].

Further experimental results [44] demonstrated that analyte anions must be paired with cations of differing valencies in order for separation to occur, i.e. if sample thiocyanate is paired with Na^+ and Ba^{2+}, then 2 separate peaks for thiocyanate will occur. However if the only cations available for "ion-pairing" are of equal valency (e.g. Ba^{2+}, Mg^{2+} and Ca^{2+}) then only a single peak for thiocyanate will be visible in the resultant chromatogram. This phenomena is displayed visually in Figs. 1.12 (a.) and (b.), where Fig. 1.12 (a.) has only the monovalent cations Na^+ and K^+, and Fig. 1.12 (b.) displays "ion-pairs" with cations with different valencies, namely Na^+ and Ba^{2+}. As is clear from both chromatograms, Fig. 1.12 (b) displays 4 peaks, compared to the 2 peaks observed in Fig. 1.12 (a). UV absorption and ICP-AES were used once again to confirm peak identities.

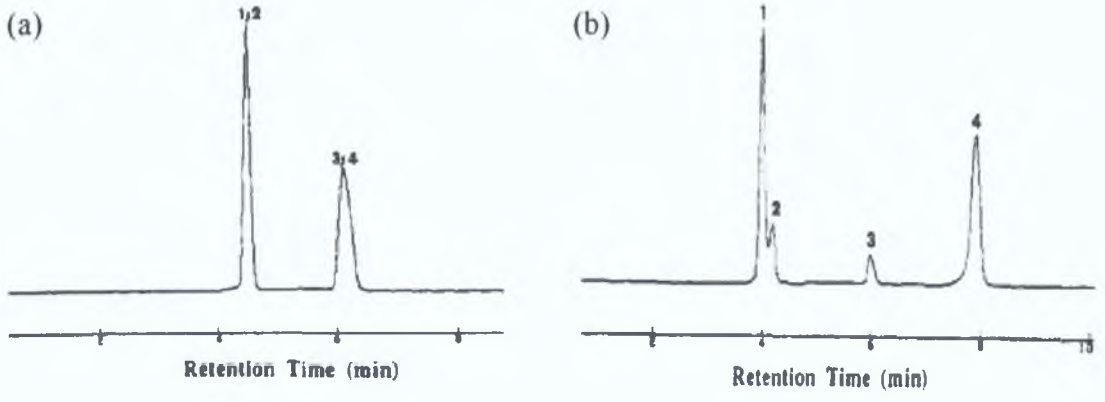

Figure 1.12. Chromatograms of an aqueous solution of (a) 10 mM KBr and 10 mM NaSCN (1: Na^+-Br^-, 2: K^+-Br^-, 3: Na^+-SCN^-, 4: K^+-SCN^-), and (b) 10 mM NaSCN and 5 mM $BaCl_2$ (1: Na^+-Cl^-, 2: Ba^{2+}-$2Cl^-$, 3: Na^+-SCN^-, 4: Ba^{2+}-$2SCN^-$). Separation conditions: C_{18} reversed-phase column (250 x 4.6 mm I.D.) modifed with CHAPSO micelles, with pure water as the eluent, a flow rate of 0.7 mL/min, and conductivity detection [Reproduced from ref. 44].

Therefore, it was concluded that when a mixture of analyte salts is injected in ZIC, "ion-pairs" consisting of all possible combinations of the analyte anions and cations, should be formed. However, it was also discovered [45,46] that the behaviour of ion combinations for the formation of ion-pairs is far more complicated than the previous chromatograms in Figs. 1.11 and 1.12 suggested. For example, Hu *et al.* [45] separated a sample solution containing a mixture of ions (Na^+, Ca^{2+}, Cl^-, Br^-, I^-, SCN^-) using a CHAPS micelle-modified stationary phase. Eight ion-pairs were expected (i.e. both cations paired with all 4 anions), but only six ion-pairs were observed, a fact corroborated by ICP-AES and photodiode array UV-visible detectors. The ion pairs Ca^{2+}-$2Cl^-$ and Na^+-SCN^- were not present.

To explain this observation, the molal energies (ΔG) of the hydrated anion and cation of the ion-pair were investigated. A theory was proposed [45] whereby the ion-pairs that have the highest priority of formation are the ion pairs that contain a cation that has the highest order of molal energy of all the cations present (ΔG_{max}-cation) and an anion of the lowest order of molal energy of all the anions present (ΔG_{min}-anion), or vice versa (i.e. ΔG_{min}-cation + ΔG_{max}-anion).

If we take as an example a sample solution that contains two cationic species (A and C) and two anionic species (B and D) [45], upon separation of this aqueous solution four ion-pairs would be anticipated (namely A-B, A-D, C-B, and C-D). The assumption is made that no chemical interactions occur between the ions in question (i.e. that no energy loss occurs), and that the order of molal energies for the cations is $\Delta G_A > \Delta G_C$, and for the anions is $\Delta G_B > \Delta G_D$. This implies that the formation of the 4 aforementioned ion-pairs is a form of energy redistribution. The least stable ion-pair is A-B ($\Delta G_{max\text{-}cation}$ with $\Delta G_{max\text{-}anion}$), while the combinations of A-D ($\Delta G_{max\text{-}cation}$ with $\Delta G_{min\text{-}anion}$) and C-B ($\Delta G_{min\text{-}cation}$ with $\Delta G_{max\text{-}anion}$) are the medium stable ion-pairs. The C-D ion-pair ($\Delta G_{min\text{-}cation}$ with $\Delta G_{min\text{-}anion}$) is the most stable ion-pair. If the C-D ion-pair is formed to the greatest extent (owing to the fact that it is the most stable), then the least stable ion-pair A-B must also be preferably produced at the same time. Therefore, in order to avoid the formation of the A-B ion-pair, the medium stable ion-pairs (i.e. A-D and C-B) must be produced more than any other combination of ions.

This trend is shown in Fig. 1.13, where a sample containing the cations Na^+ and Ca^{2+} and the anions SCN^- and Cl^- was analysed using a Zwittergent 3-14-modifed C_{18} reversed-phase column [32]. According to Born's equation, the molal energy orders for the cations are $\Delta G_{Na^+} > \Delta G_{Ca^{2+}}$, and for the anions is $\Delta G_{SCN^-} > \Delta G_{Cl^-}$. Therefore, the ion-pairs that have the highest priority of formation are Na^+-Cl^- ($\Delta G_{max\text{-}cation} + \Delta G_{min\text{-}anion}$) and Ca^{2+}-$2SCN^-$ ($\Delta G_{min\text{-}cation} + \Delta G_{max\text{-}anion}$). Hence, the major peaks in the chromatogram in Fig. 1.13 correspond to these two ion-pair species (labelled *a* and *d* respectively). On the other hand, ion-pairs due to Na^+-SCN^- ($\Delta G_{max\text{-}cation} + \Delta G_{max\text{-}anion}$) and Ca^{2+}-$2Cl^-$ ($\Delta G_{min\text{-}cation} + \Delta G_{min\text{-}anion}$) have a significantly lower priority of formation, and thus give rise to minor peaks (labelled *b* and *c* respectively). The size of these minor peaks was subsequently found to be reliant on the ratio of the concentrations of all the analyte ions in the starting sample solution [32].

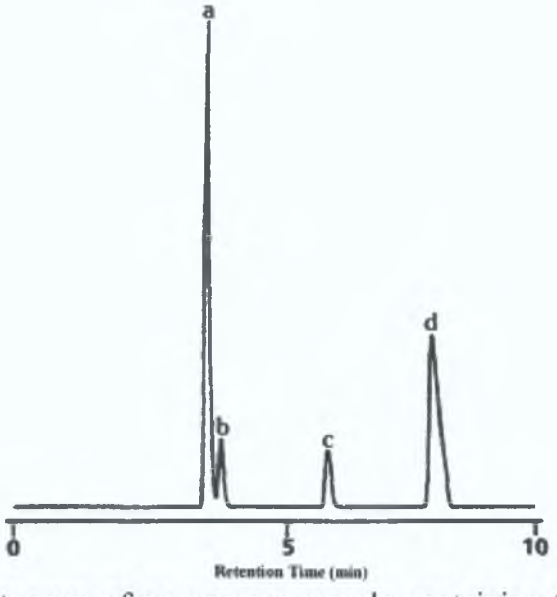

Figure 1.13. Chromatogram of an aqueous sample containing 2 mM NaSCN and 1 mM $CaCl_2$, obtained using a C_{18} reversed-phase column (250 x 4.6 mm I.D.) modified with Zwittergent 3-14 micelles, and pure water as the eluent [Reproduced from ref. 32]. Flow rate: 1.0 mL/min. Detection: conductivity. Peak identities: a: Na^+-Cl^-, b: Ca^{2+}-$2Cl^-$, c: Na^+-SCN^-, d: Ca^{2+}-$2SCN^-$.

1.3.4.2 Methods of Overcoming "Multiple" Distribution of Analyte Ions

There have been a handful of methods employed by researchers in order to simplify the complicated chromatograms obtained using ZIC with pure water as the eluent. The abundance of multiple peaks for identical analytes means that identifying and determining target ions becomes problematic, and over-complicates relatively simple analyses. These techniques are described below:

- Umemura *et al.* [47,48] pre-treated sample solutions, so that all of the analyte anions would elute with common counter cations. A cation-exchange column was used as a preconditioning column before separation, and detection was accomplished by ICP-AES. The use of both Na^+ and Mg^{2+} as the common counter ion was investigated. The use of the divalent cation (Mg^{2+}) resulted in better separations, compared to the monovalent cation (Na^+), but also resulted in longer retention times. Although analyte anions should be rapidly eluted from the cation-exchange column (on the basis of Donnan exclusive theory), adding the cation-exchanger to the chromatographic system still resulted in

extended retention times, which is a disadvantage in the general application of this technique.

- Umemura *et al.* [49] utilised a "decoy electrolyte" in order to control the ion-pair formation of analyte anions with counter cations, leading to the desired conversion of ion-pairs in unknown cation forms to a single, known cation form. The concept of preferential formation of ion-pairs in ZIC has been discussed already in Section 1.3.4.1. The principle of this technique is that if a cation, which has a significantly high priority of formation, is introduced into a sample solution containing different analyte anions, that there will be a greater tendency for the anions to pair with this cation over other cations present in the sample. If this cation is introduced at a high enough concentration, then all subsequent ion-pairs will contain this cation, thereby controlling the ion redistribution. If an anion, which also has a high priority of formation, is also added to the sample, then the sample cations will form ion-pairs with this newly introduced anion. This added salt (i.e. the "introduced" cation and anion) is referred to as the "decoy electrolyte", composed of a "decoy cation" and a "decoy anion" [49].

  It was concluded [49] that suitable decoy electrolytes for the analysis of common anions (e.g. Cl^-, NO_3^-, NO_2^- etc.) were NaI (a monovalent cation combined with an anion that has a significantly longer retention time than the analyte anions) and $MgSO_4$ (a divalent cation combined with an anion that has a shorter retention time than the analyte anions). However, while making use of a decoy electrolyte can successfully control the problem of ion redistribution, it also has several drawbacks. Sample preparation is complicated, while retention times of strongly retained anions (such as iodide) are extended considerably, especially if divalent or trivalent decoy cations are utilised.

1.3.4.3 Trace Analysis in ZIC Using Pure Water as an Eluent

As mentioned previously, the use of pure water as an eluent in IC means that detection can be expected to be very sensitive, because of the fact that the background conductivity is due to deionised water alone, and not an electrolytic eluent. However,

when samples with low concentrations of ions were analysed using zwitterionic stationary phases, it was soon discovered that identical analytes (i.e. identical ion-pairs) displayed separate elution times [30]. An aqueous solution of 1.0 μM NaCl and $CaCl_2$ was separated using ZIC. The resulting chromatogram displayed two main peaks (labelled 1 and 2) and two secondary peaks (labelled 1' and 2') for both the ion pairs Na^+-Cl^- and Ca^{2+}-$2Cl^-$ [30], and can be seen in Fig. 1.14, where split peaks were observed for the same ion-pairs. These secondary peaks had not been observed in previous analyses, where samples had higher concentrations of sample ions. When the concentrations of NaCl and $CaCl_2$ in the sample solutions were lowered to levels below 0.4 μM, the 2 main peaks did not appear in the ensuing chromatograms, while the presence of the two secondary peaks was always noted.

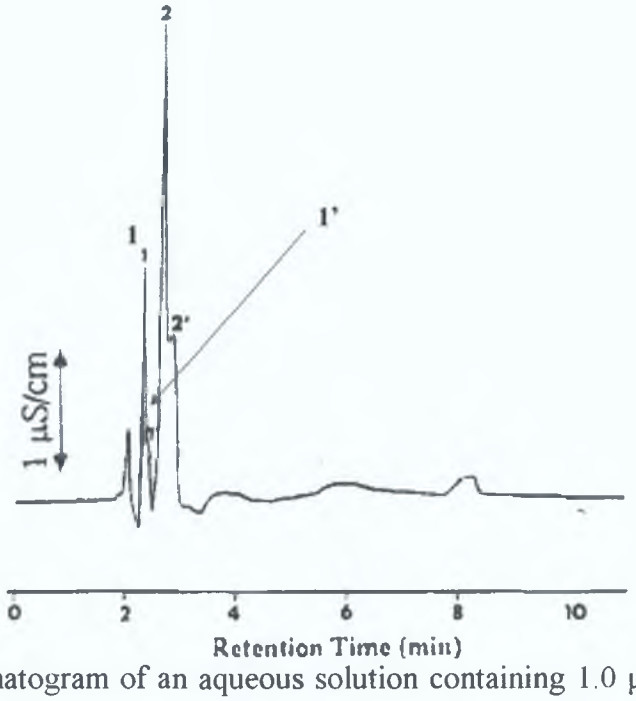

Figure 1.14. Chromatogram of an aqueous solution containing 1.0 μM each of NaCl and $CaCl_2$, obtained using a C_{18} reversed-phase column (250 x 4.6 mm) modified with Zwittergent 3-14 micelles, an eluent comprised of pure water, and conductivity detection [Reproduced from ref. 30]. Flow rate: 1.0 mL/min. Peak identities: (1,1') Na^+ - Cl^- and (2,2') Ca^{2+} - $2Cl^-$.

To explain the occurrence of this main and secondary elution, the Stern model of an electrical double layer (EDL) was used (see Figs. 1.7 and 1.8). It was found that analyte ions eluted from the diffuse layer have a shorter retention time than analyte ions eluted from the Stern layer [30]. In regular IC analyses, there is no observed

difference in elution times for ions eluting from the diffuse layer, and those eluting from the Stern layer. This is because the eluent utilised would contain a significant amount of replacing ions, while in ZIC (using pure water as an eluent) there are very few ions present for replacement purposes (as $[H^+] = [OH^-] = 10^{-7}$ M), thus giving rise to noticeable discrepancies in elution times for the two layers. This difference becomes larger when both the analyte and the stationary phase display hydrophobic properties.

Main and secondary elution almost always occurs in ZIC, but with samples of relatively high analyte concentrations, the diffuse layer peak is so much larger than the peak corresponding to Stern layer elution that the Stern layer peak signal becomes dwarfed by that of the diffuse layer peak, and therefore goes unnoticed. (When ultra-low level ions are analysed however, all analyte ions are eluted from the Stern layer as single sharp peak, and so ultra-trace analysis of anions is one important application of ZIC using pure water as the eluent [32].) In other words, at extremely low sample concentrations, the diffuse layer of the EDL becomes significantly smaller in magnitude, virtually disappearing at ultra-trace levels of analyte ions. This dual elution is a huge disadvantage when it comes to the determination of trace level inorganic anions, as multiple peaks must be taken into account for the same analyte species. One method of overcoming this is through the use of a "sacrifice" species, such as the introduction of a higher concentration of a new species of salt with a longer retention time into the sample solution. For example, Hu *et al.* [30] used 1000 μM CaI_2 as a "sacrifice" species in the separation and detection of 1.0 μM of $CaCl_2$, $CaBr_2$, and $Ca(NO_3)_2$.

1.3.5 Use of Electrolytic Eluents in ZIC

The presence of multiple peaks for single analytes due to ion-redistribution is an obvious drawback of ZIC using an eluent composed of pure water alone (see Section 1.3.4.1). Therefore, it would be of great benefit to be able to overcome this problem, without sacrificing selectivity and sensitivity. Some techniques used initially to try to surmount this problem have already been discussed in Section 1.3.4.1. These methods, however, as mentioned previously, have significant disadvantages of their own. Hu and Haddad [50] developed a method for the separation of common inorganic anions using a conventional C_{18} reversed-phase stationary phase modified

with a zwitterionic surfactant, and an eluent comprised of an aqueous solution containing a small amount of electrolyte. The elution order for sulphate, chloride, nitrite, bromide, nitrate, chlorate, iodide, and thiocyanate was found to be identical to that observed utilising a pure water eluent, but retention times increased for all analytes (sulphate excepted), particularly in the case of the polarisable anions iodide and thiocyanate. Using 10 mM $NaHCO_3$ as the eluent, a single peak was observed for each analyte anion, regardless of the composition (i.e. number of different cations present) of the sample injected. For example, when a sample of nitrate containing sodium and magnesium as the counter-cations was analysed using 10 mM $NaHCO_3$ as the eluent, only one sharp peak (corresponding to the nitrate ion-pairs) was evident in the resulting chromatogram [50], rather than multiple peaks for the ion-pairs formed by the nitrate anion and the various cations present.

1.3.5.1 Mechanism of Separation in ZIC Using Electrolytic Eluents

Okada and Patil [51,52,53] suggested that the introduction of a salt into the eluent phase in ZIC results in changes in the surface morphology of the zwitterionic stationary phase. Taking the sulfobetaine-type zwitterionic surfactant, 3-(N-dodecyl-N.,N-dimethylammonio)propane-1-sulfonate (DDAPS) as a model zwitterionic stationary phase, they proposed that, due to the substantial molecular flexibility of the adsorbed DDAPS molecules, intermolecular (possibly including intramolecular) interactions will take place between adjacent adsorbed molecules through their respective opposite charges, in an eluent environment of pure water [51]. This is shown in Fig. 1.15 (a), where the positive and negative charges of one DDAPS molecule are paired with the negative and positive charges, respectively, of a second, nearby DDAPS molecule. The addition of a salt to the eluent composition significantly weakens this interaction, resulting in a rearrangement of the configuration of the DDAPS molecules (see Fig. 1.15 (b)), thereby providing analyte ions with easier access to the functional groups on the zwitterionic surfactant, which should result in higher degrees of retention of analyte ions. This was supported by other experimental findings [54], which displayed abrupt increases in the k values for 3 test anions upon switching from an eluent comprised of pure water to eluents composed of 1 or 2 mM salt solutions.

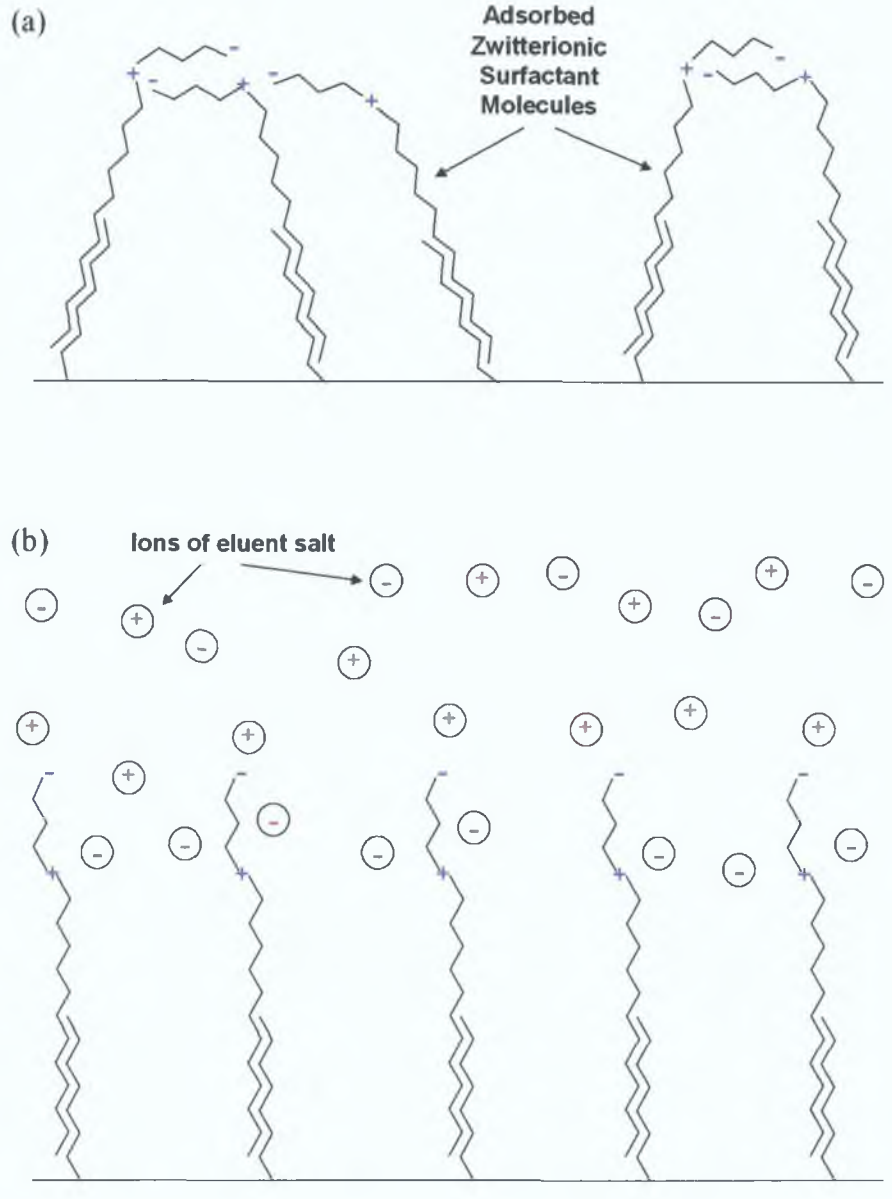

Figure 1.15. Schematic representation of the change in configuration of adsorbed zwitterionic surfactant molecules (which in this case are DDAPS molecules) upon changing eluent conditions from (a) a salt-free solution, to (b) a salt solution [51].

The proposed separation mechanism for a zwitterionic surfactant stationary phase conditioned with an electrolytic eluent [54,55,56] is based on a combination of ion-exclusion effects and chaotropic interactions.

The ion-exclusion effect can be explained as follows, using the zwitterionic surfactant Zwittergent 3-14 (see Fig. 1.10 (a) for structure) as a model stationary phase zwitterion. The terminal sulfonate group of the Zwittergent 3-14 contributes a

negative charge which, as previously mentioned, will electrostatically repel analyte anions. The extent of this negative charge depends on the strength of the interaction between these sulfonate groups and the cations present in the eluent, as well as being reliant on the degree of interaction between the quaternary ammonium groups of the Zwittergent 3-14 molecules and the eluent anions. The surface negative charge will decrease if the eluent cations exhibit strong interaction with the stationary phase. However, the surface negative charge will increase if the eluent anions exhibit strong interaction. The negative charge on the outside of the zwitterionic surfactant is, in other words, a barrier across which analyte anions must travel in order to interact with the positively charged functional group located past the sulfonate group. This electrostatic obstruction can be overcome through the presence of +2 and +3 charged cations in the eluent. This was observed experimentally by Cook *et al.* [54] using chloride and chlorate eluents. In summary, the binding of anions to the positively charged ammonium groups is therefore dependent on the nature of the cations in the eluent.

As mentioned above, chaotropic interactions also play a part in this retention mechanism. Chaotropism refers to the property of certain substances, usually ions, to disrupt the structure of water (leading to an increase in entropy) and thereby promote the solubility of nonpolar substances in polar substances (e.g. water) [57]. Chaotropic anions are large, with a low charge. Examples of chaotropic ions include SCN^- and ClO_4^-. These large, polarisable ions with a diffuse charge do not easily form a well-orientated layer of water molecules at their surface, which tends to disrupt the surrounding water structure [7]. This leads to an increase in free energy, which is the driving force for the binding of these ions with the fixed ions of opposite charge of the stationary phase, thereby favourably diminishing both the disruption to the eluent water structure and the free energy of the system [7]. This binding is referred to as "water-structure induced ion-pairing" [58], and accounts for the very strong retention of anions such as ClO_4^- in conventional IC. Experimental evidence [59,36] has shown that selectivity in ZIC is governed mainly by chaotropic interactions between analyte anions and the positively charged ammonium groups of the zwitterionic surfactant. The more chaotropic the analyte anion (according to the Hofmeister series) the greater the retention of the anion. This effect is visualised in Fig. 1.16.

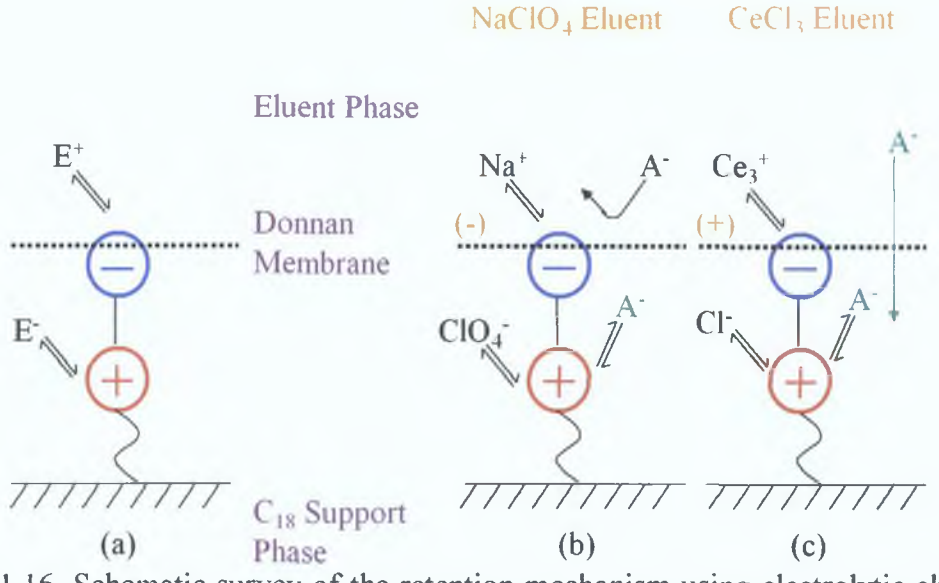

Figure 1.16. Schematic survey of the retention mechanism using electrolytic eluents. (a) Establishment of the Donnan membrane, (b) use of a $NaClO_4$ eluent, and (c) use of a $CeCl_3$ eluent [54].

Fig. 1.16 (a) illustrates the establishment of the Donnan membrane, with the zwitterionic stationary phase in equilibrium with the eluent anions and cations (represented by the symbols E^+ and E^- respectively). When a $NaClO_4$ eluent is used (see Fig. 1.16 (b)), only a weak interaction exists between the Na^+ ion and the negatively charged functional group of the zwitterionic surfactant, while the interaction between ClO_4^- eluent anion and the positively charged functional group is relatively strong, thus giving rise to a relatively strong negatively charged Donnan membrane, which will exert a strong repulsion on analyte anions [54]. Not all analyte anions (represented diagrammatically by the symbol A^-) will be able to penetrate this Donnan membrane, particularly multiply charged anions, such as sulphate. Those anions that are able to cross the membrane will interact chaotropically with the positively charged functional groups of the zwitterionic surfactant, thus leading to retention of anions. When a $CeCl_3$ eluent is utilised (as in Fig. 1.16 (c)), the Ce^{3+} eluent cations interact very strongly with the negatively charged functional group of the stationary phase, while the Cl^- eluent anions exhibit weak interaction with the positively charged functional group. This results in the Donnan membrane becoming slightly positively charged, and so all analyte anions can cross the Donnan membrane relatively freely [54]. This explains why the use of higher valency cation in the eluent

leads to increased retention of analyte anions, e.g. retention of analyte anions was seen to increase upon changing the eluent cation from Na^+ to Ca^{2+} to Ce^{3+} [50], as demonstrated by comparison of the 3 chromatograms in Fig. 1.17. Peak fronting was more pronounced for the iodide peak, due to iodide being retained significantly longer than the other analytes. Again, chaotropic interactions with the positively charged regions of the zwitterionic surfactant are responsible for the retention and separation of these analyte anions.

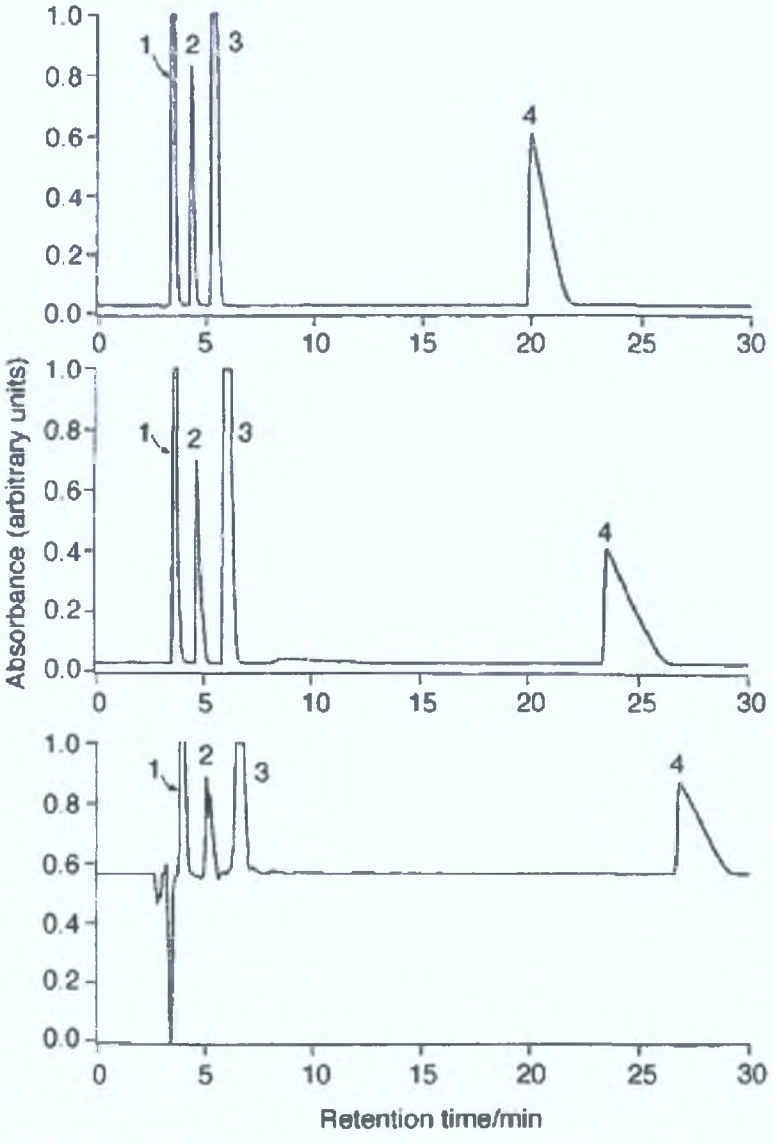

Figure 1.17. Chromatograms of an aqueous solution of 0.1 mM nitrite, bromide, nitrate, and iodide obtained using a CHAPS-modified column, with eluents of 5.0 mM NaCl (upper trace), 5.0 mM $CaCl_2$ (middle trace) and 5.0 mM $CeCl_3$ (lower trace). Flow rate: 1.0 mL/min. Detection: Suppressed conductivity. Peak identification: 1 - nitrite, 2 - bromide, 3 - nitrate and 4 - iodide [Reproduced from ref. 50].

Due to the fact the mechanism discussed here in Section 1.3.5.1 does not rely on electrostatic effects alone, the term "electrostatic ion chromatography" (EIC) does not seem entirely appropriate for this type of IC analysis, and therefore Cook *et al.* [54] suggested that the title "zwitterionic ion chromatography" would be more suitable when referring to this analytical technique in the future.

1.3.5.2 Types of Electrolytic Eluents Employed

There are have been numerous different types of eluents used in ZIC, ranging from traditional IC eluents such as $NaHCO_3$ [50] to less common eluents such as aqueous tetraborate solutions [60]. After comparing $NaHCO_3$ with various carbonate, chloride, sulphate and phosphate salts (i.e. Na_2CO_3, NaCl, $CaCl_2$, $CeCl_3$, Na_2SO_4, Na_3PO_4) as eluent additives for ZIC, Hu and Haddad [50,55] discovered that these electrolytic eluents all resulted in similar analyte selectivity. Cook *et al.* [54] found that for the same eluents, while retention was observed to increase sharply when the eluent composition was changed from pure water to a very low-ionic strength electrolytic solution (< 1-2 mM), further increases in the concentration of the electrolytic eluents resulted in little additional changes in analyte anion retention, with k values for test anions seen to increase by insignificant amounts with each subsequent increase in eluent ionic strength.

Hydroxide solutions ($Ca(OH)_2$ and LiOH) were also evaluated for use in ZIC systems [61], because of the fact that they were expected to show similar selectivity to other electrolyte solutions, and also because they would be well-suited for use in conjunction with suppressed conductivity detection, owing to the ease with which hydroxide ions are converted to water during suppression. However, unlike previous experiments with the aforementioned electrolytic eluents (where increasing the electrolyte concentration of the eluent had very little effect on anion retention), an increase in the concentration of hydroxide present in the eluent resulted in an increase in the retention times of analyte anions. This was attributed to the to very low ion-exchange affinity that the hydroxide ion has for the quaternary ammonium group, which was the positively charged functional group of the Zwittergent 3-14 surfactant molecules used to modify the column in question [61]. This means that the number of hydroxide ions in the anionic region of the electrical double layer (EDL) formed will be significantly smaller than for other electrolytic eluents at similar concentrations.

Also, for the purposes of electroneutrality, the cationic region of the EDL will be less dense than for other electrolytic eluents. Therefore, the binary-EDL for hydroxide eluents is relatively thin, and thus weaker retention of analyte anions will be observed, compared to similar chromatographic systems employing other electrolytic eluents, such as NaCl or $NaHCO_3$. Increasing the concentration of the hydroxide eluent utilised would cause an increase in the thickness of the binary-EDL, thereby leading to increased anion retention. The drawback to the use of hydroxide-based eluents is that the high alkalinity of the hydroxide solutions can cause deterioration of the silica-based reversed-phase column within a relatively short period of time (approx. 3 months) [60].

Jiang and Irgrum [40,41,42] have reported the use of perchlorate eluents for the separation of ionic species using a zwitterionic stationary phase, as perchlorate ions have a higher eluting ability than many other traditional eluent ions in IC. It was found [40,41,42] that increasing the concentration of the perchlorate eluent from 1 mM to 10 mM resulted in a decrease in the retention for analyte anions, as the ClO_4^- eluent anion is very strongly retained by the positively charged group of the zwitterionic stationary phase.

Tetraborate eluents have also been investigated for their use in ZIC systems [60,62]. Tetraborate-based eluents have not found widespread use in IC, despite the low conductance of their suppressed product (i.e. boric acid), as they display weak elution ability for most analyte ions, even those with low ion-exchange selectivity coefficients. The weak retention of the tetraborate ion on the quaternary ammonium group of the zwitterionic surfactant used to modify the stationary phase allowed the formation of a binary-EDL having a thickness determined by the eluent concentration [60], permitting the variation of analyte retention times by changing the eluent concentration, and thus making possible the use of gradient elution in ZIC.

Aqueous acid solutions (e.g. H_2SO_4 and HCl) have also been established as eluent systems for ZIC [63,64,65], as a means of manipulating the separation selectivity of inorganic anions, through the strong interaction between H^+ and the sulphonate groups of the zwitterionic surfactant utilised (namely Zwittergent 3-14). The retention mechanism differs slightly when acidic eluents are used, as the slopes of the resultant

plots of log k versus log [eluent] [63] are significantly more negative than those observed using more traditional eluents, such as $NaClO_4$. The proposed mechanism [63,64] using a sulfobetaine-type zwitterionic stationary phase, involves the absorption of a cationic EDL of H^+ by the negatively charged sulfonate groups, as well as the absorption of an anionic EDL of the eluent counter-anion by the positively charged quaternary ammonium group. However, there exists an equilibrium between the H^+ ions and the sulphonate groups, which can result in the formation of neutral, protonated sulphonic acid groups, if the pH is near to the pK_a of the sulphonic groups of the zwitterions (see Fig. 1.18).

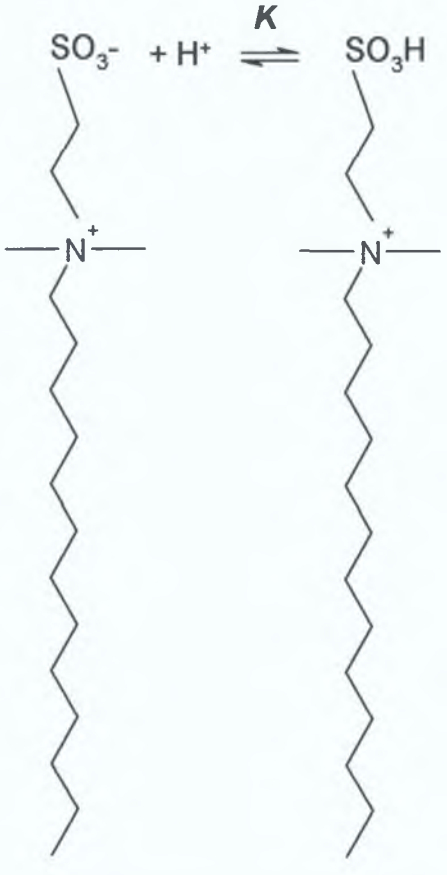

Figure 1.18. Schematic representation of the equilibrium between the zwitterionic and protonated/cationic forms of a sulfobetaine-type stationary phase in the presence of an acidic eluent [63].

When the stationary phase exists in the zwitterionic form (i.e. that displayed on the left hand side of Fig. 1.18) separation of analyte anions will occur through the established ZIC mechanism discussed in previous sections. However, when the stationary phase exists in the protonated form (as seen on the right hand side of Fig.

1.18), separation will occur on the basis of a conventional anion-exchange mechanism. When the two types of stationary phase are in equilibrium both retention mechanisms will contribute to the retention of anions [63].

Macka and Haddad [66] employed an isoelectric ampholytic buffer (namely histidine, at pH 7.7) as an eluent for the separation of inorganic anions and cations on a column modified with zwitterionic surfactants. These buffers are zwitterionic substances in which 2 pK_a values bracketing the isoelectric point (p*I*) are sufficiently close (within 1 pH unit of the p*I*) to provide a certain degree of buffering at the p*I*. Examples of such eluents include amino acids, such as histidine. The motivation for the use of a buffered eluent was that the use of pure water eluents would hinder the application of the technique to the analysis of strongly acidic or alkaline samples, due to a lack of buffering. Macka and Haddad [66] found that as the histidine existed in both an anionic and a cationic form at its p*I*, albeit at very low levels (e.g. only 3% of the histidine molecules are present as anions at the pH value corresponding to the p*I*), these ionic forms could act like counter-ions for the elution of analyte anions and cations in separate bands. The use of histidine as an eluent system also had the additional benefit of possessing a relatively low background conductance, meaning that such an eluent would exhibit high sensitivity for analyte ions using non-suppressed conductivity detection.

1.3.6 ZIC Using a Mixed Cationic-Zwitterionic Surfactant Stationary Phase

The separation of fluoride, phosphate and sulphate by ZIC has proven to be problematic, owing to the small degree of retention these anions exhibit on zwitterionic surfactant-modified stationary phases. As a means of overcoming this challenge, Hu *et al.* [67,68] modified C_{18} reversed-phase columns with a mixture of cationic (e.g. tetradecyltrimethylammonium, TTA) and zwitterionic (Zwittergent 3-14) surfactants. The resulting mixed-bed stationary phases showed that the aforementioned group of anions were more strongly retained on the mixed-bed column, than on the exclusively zwitterionic stationary phase, with clear, baseline separation of all analytes of interest, as can be seen in Fig. 1.19. The 2 types of surfactants were seen to bind analyte anions by independent mechanisms. The zwitterionic surfactant binds ions by an electrostatic mechanism, but the cationic

surfactant binds analyte ions by conventional ion-exchange [68]. By varying the ratio of the concentration of zwitterionic surfactant in the column modification solution to that of the cationic surfactant concentration, retention times could be manipulated, as increasing the mole fraction of the cationic surfactant increased the propensity of the ions to engage in ion-exchange, resulting in longer retention times [67]. This mixed-surfactant modification methodology was applied to the determination of fluoride, sulphate and chloride in tap water samples [68].

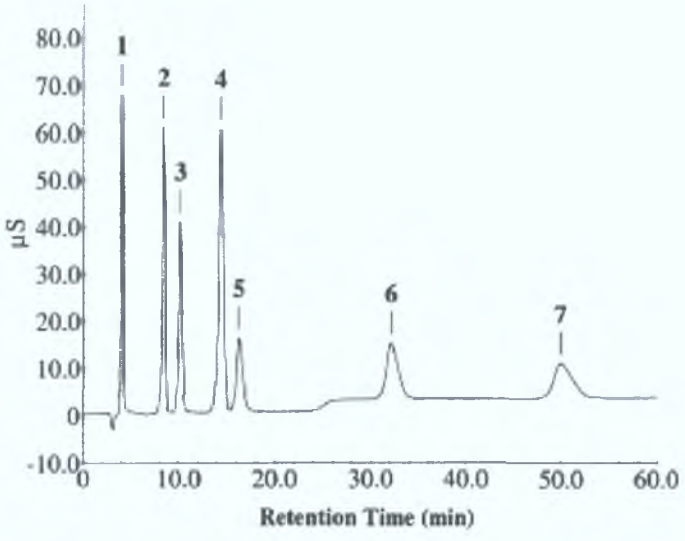

Figure 1.19. Separation of a 0.1 mM mixture of 7 anions obtained using a C_{18} reversed-phase column modified with Zwittergent 3-14 / TTA (in equal amounts, i.e. 10 mM / 10 mM), with 20 mM Na_2CO_3 as the eluent, and suppressed conductivity detection. Peak identification: 1 - fluoride, 2 - phosphate, 3 - chloride, 4 - sulphate, 5 - nitrite, 6 - bromide, and 7 - nitrate [Reproduced from ref. 67].

1.3.7 Separation of Cations Using ZIC

The predominant use for ZIC has been the separation and subsequent analysis of anions, despite the bifunctionality of the stationary phase, and therefore the majority of the proposed separation mechanisms have been based on anion retention data alone. The zwitterionic surfactants used in the analysis of anions using ZIC techniques have generally been of the sulfobetaine-type or the carboxybetaine-type, which usually have an inner positively charged functional group and an outer negatively charged functional group, separated by several methylene groups. It is this positioning of the charged functional groups that accounts for the anion-specific selectivity of these chromatographic systems, as when the anionic functional group is outermost,

only analyte anions are able to distribute effectively into the stationary phase, whereas analyte cations are repelled. For the zwitterionic stationary phase to exhibit selectivity for cations, the terminal functional group of the zwitterionic surfactant molecule must be positively charged, in order to allow the preferential entry of analyte cations into the stationary phase.

Taking an alternative approach, Hu and co-workers [69,70] used phosphocholine-type surfactants (e.g. N-dodecylphosphocholine, and N-hexadecylphosphocholine) to create a zwitterionic stationary phase in which the relative positions of the two charged functional groups were reversed in comparison to sulfobetaine-type surfactants, i.e. having a negative inner charge (from a phosphonate group) and a positive outer charge (from a quaternary ammonium group). An example of the structure of these phosphocholine-type surfactants can be seen in Fig. 1.20. This type of stationary phase was found to have a higher selectivity for cations than sulfobetaine-type surfactants, such as Zwittergent 3-14. The separation of H^+, Ca^{2+}, Mg^{2+} and Ba^{2+} was accomplished using such a system [70]. The observed order of retention was $Ba^{2+} < Mg^{2+} < Ca^{2+} < H^+$, which differs to that of conventional cation-exchange chromatography, thus implying that a retention mechanism other than ion-exchange alone was taking place [70].

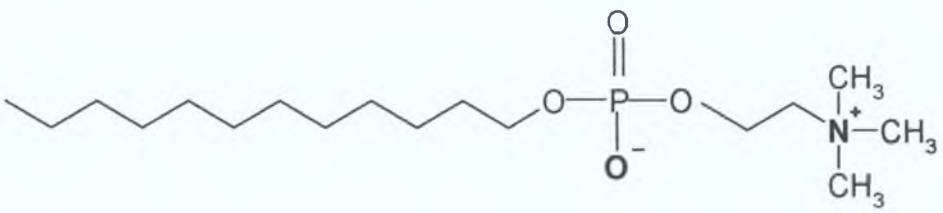

Figure 1.20. Structure of N-dodecylphosphocholine [69].

Cook *et al.* [71] investigated the retention of cations using N-tetradecylphosphocholine to modify the column, and their study found that cations were retained due to the same chaotropic interactions observed with anions on sulfobetaine-type surfactant systems, although cations have a relatively low chaotropic nature, compared to anions [71]. The proposed retention mechanism [71] is based on both ion-exclusion effects, as before, and direct chaotropic interactions with the inner negative charge of the zwitterionic molecules. The build up of a Donnan

membrane at the outer-lying positive charge, which is the cause of the ion-exclusion effects, was proposed to be dependent on the shielding ability of the eluent anion and cation. In other words, the addition of small amounts of electrolytes to the eluent leads to an unfurling of the surface morphology of the stationary phase, which provides sufficient shielding of the charged functional groups to prevent the interaction of adjacent zwitterionic molecules. This increased accessibility of the charges either significantly increases or decreases the retention of analyte ions, depending on the relative affinities of the eluent-anion, eluent-cation, and analyte cation for the available functional groups. These affinities are, once again, determined by the aforementioned Hofmeister series.

The dependence of the ion uptake selectivity of the zwitterionic stationary phase on the polarity of the zwitterionic molecule was supported by zeta potential studies of phosphocholine-type and sulfobetaine-type surfactants [72], where zwitterionic surfactant molecules having a reversed polarity, compared to the commonly employed sulfobetaine-type zwitterionic surfactants for anion separations, displayed different characteristics in ion uptake. For example, the use of an electrolytic solution of Bu_4NCl resulted in a positive potential in the presence of the phosphocholine, but resulted in a negative potential in the presence of the sulfobetaine-type surfactant [72].

Hu and Haraguchi [73] used a C_{18} reversed-phase column modified with zwitterionic bile salt micelles for the simultaneous separation of several inorganic anions and cations. The taurine-conjugated bile salts employed included sodium taurodeoxycholate (NaTDC) and sodium taurocholate (NaTC). The resultant weak/strong-charged stationary phase, with an eluent of aqueous copper (II) sulphate, separated anions and cations on the basis of the formation of "ion-pair-like" forms. An example of the simultaneous separation of anions and cations achieved is shown in Fig. 1.21.

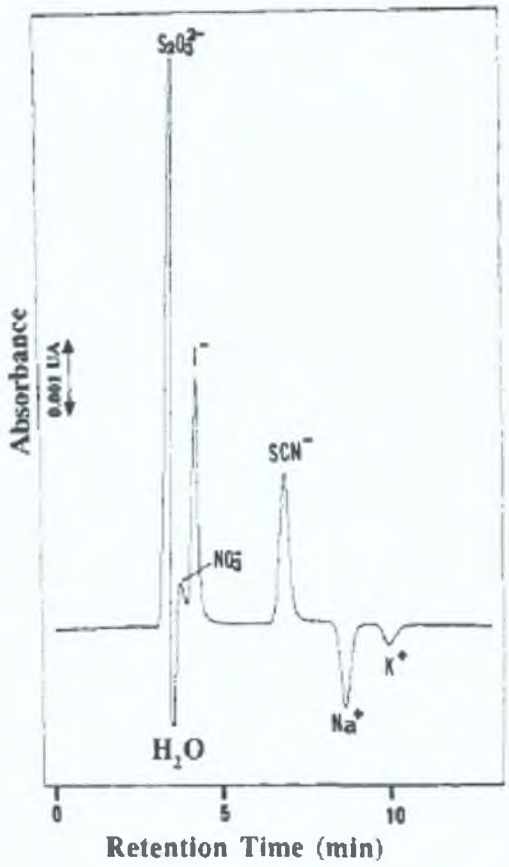

Figure 1.21. Simultaneous separation of several inorganic anions and cations, obtained using a C_{18} reversed-phase column modified with NaTDC, and an eluent composed of 5 mM copper (II) sulphate, with UV detection at 210 nm [Reproduced from ref. 73]. Analytes: 0.5 mM sodium thiosulphate, sodium nitrite, sodium nitrate, potassium iodide, and sodium thiocyanate.

1.3.8 Applications of ZIC

ZIC has many unique attributes that make it particularly suitable to various practical analytical applications. When a pure water eluent is employed in ZIC, there is the potential for extremely low detection limits for conductivity detection, as the background conductance for pure water is very low. Determination of levels of chloride, nitrite, bromide, nitrate, and iodide of 0.1 μM in aqueous samples have been reported in the literature [32].

As discussed in Section 1.3.4.2, elution of analyte ions in ZIC is from both the Stern layer and the diffuse layer [30], which leads to undesirable peak splitting effects. However, when ultra-low level ions (i.e. at sub-ppb levels) are analysed, all analyte ions are eluted from the Stern layer alone, thus giving rise to single, sharp peaks. This

demonstrates the compatibility of ZIC methodologies for the ultra-trace analysis of anions.

The possibility of the simultaneous determination of inorganic cations and anions in ZIC also exists [45], using pure water as the eluent. This method requires the determination of the entire ion-pair combinations formed from all of the analyte anions and cations present in the sample, but the resulting data analysis is quite complex, and is reliant on complete separation of all of the chromatographic peaks, in order to accomplish the recognition of the observed ion-pairs.

1.3.8.1 Analysis of Common Inorganic Anions in Saline Waters

The analysis of samples with a problematic matrix (such as seawater samples) is difficult to achieve using conventional ion-exchange chromatographic techniques. There are a number of reasons for this: Firstly, the large concentration of matrix ions (namely chloride and sulphate) saturate the active sites of the stationary phase, thereby hindering the separation of the target analytes [55]. Secondly, self-elution of the sample band during injection leads to peak broadening, and a subsequent loss of efficiency [55]. Thirdly, the analytes in question are often present at such low levels, that detection problems ensue [55].

Hu *et al.* [74,50] demonstrated that ZIC was highly tolerant towards high ionic strength sample matrices, and so was eminently suitable for seawater analysis, as the aforementioned matrix problems were easily overcome. It was found that the polarisable anions, such as nitrate and iodide, displayed good retention/separation, but that the matrix chloride and sulphate ions showed either very little retention or no retention at all. Hu and Haddad [50] used a ZIC system for the determination of trace level iodide in saline waters, using UV absorbance. A typical chromatogram obtained using this method can be seen in Fig. 1.22.

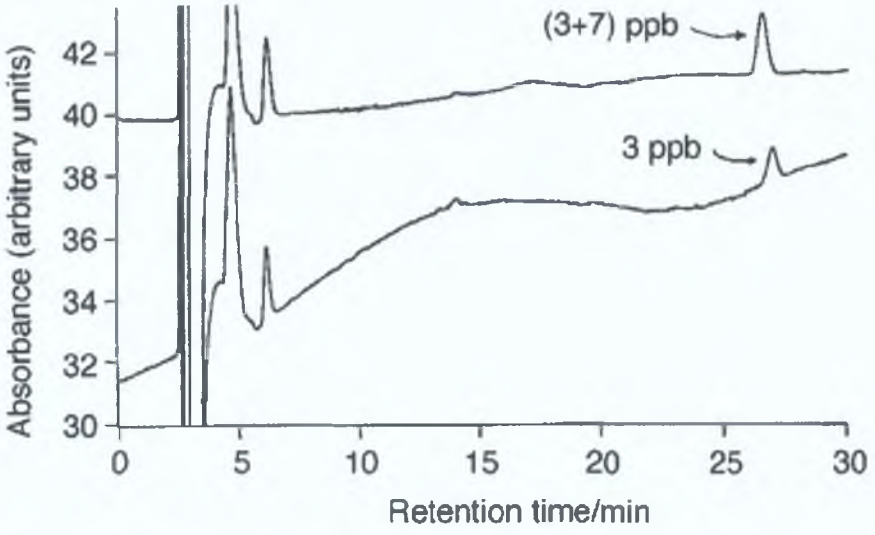

Figure 1.22. Chromatogram showing the determination of trace level iodide in saline (0.6 M NaCl) water, using UV absorbance detection at 210 nm [Reproduced from ref. 50].

Further work in this area [75,55] lead to the development of methods for the determination of bromide, nitrate and iodide in both artificial saline samples (i.e. in a sample matrix of approx. 0.5 M NaCl), and actual seawater samples (see Fig. 1.23). Nitrite, however, in a manner analogous to that of the matrix chloride and sulphate ions, displayed very little affinity for the zwitterionic stationary phase, which resulted in incomplete separation of nitrite from the peak corresponding to the matrix ions. Hu *et al.* [64] adjusted the concentration of acid in their mobile phase in order to change the order of retention from nitrite < bromide < nitrate to bromide < nitrate < nitrite, in order to separate nitrite from the matrix ions, and thus successfully determined the trace concentrations of nitrite in high ionic-strength samples.

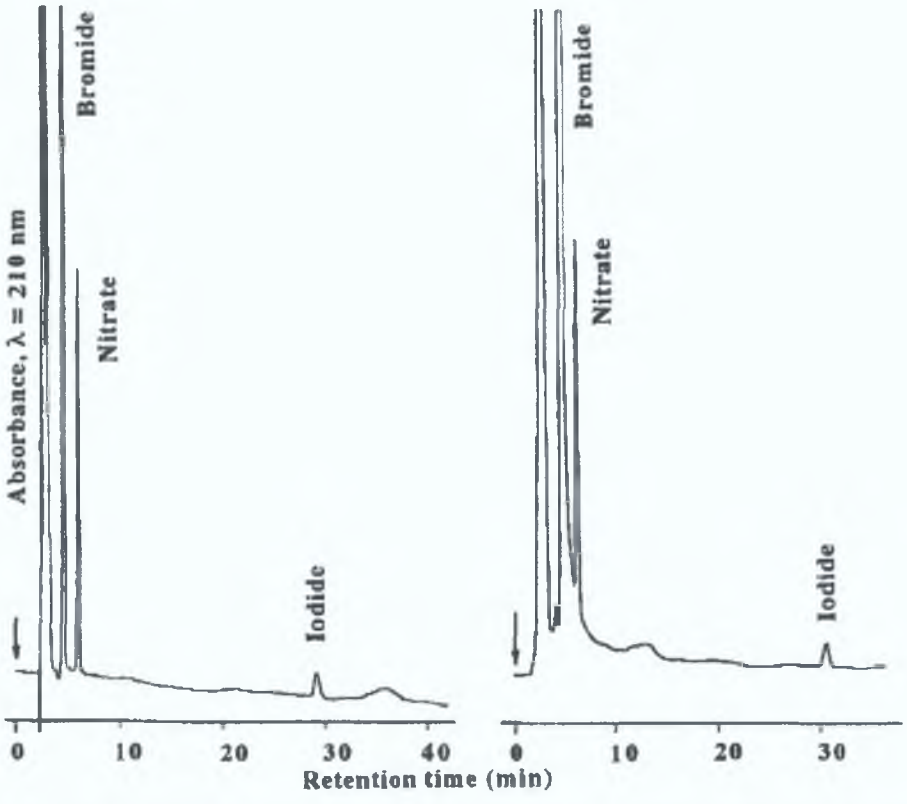

Figure 1.23. Chromatograms of an artificial saline sample (left-hand trace) [comprised of 1000 ppb bromide, 50 ppb nitrate, and 5.0 ppb iodide dissolved in an artificial seawater matrix of approx. 0.52 M NaCl] and an actual seawater sample (right-hand trace) obtained using 20-fold-diluted artificial seawater as the eluent, and a column modified with Zwittergent 3-14 micelles [Reproduced from ref. 55].

Hu *et al.* [76] discovered that applying a perchlorate eluent to a ZIC system resulted in the rapid elution of the iodide ion. This occurred because of the very strong chaotropic interaction between the perchlorate ion and the quaternary ammonium functionality of the zwitterionic surfactant, and the weak interaction between the eluent cation (which was sodium) and the sulfonate group of the zwitterionic molecules. This made it an ideal eluent for the rapid determination of iodide in saltwater samples. Iodide levels in real seawater samples were established within approximately 6 minutes.

Further developments in the field of saline water analysis in ZIC have seen Twohill and Paull [77] document the applicability of a recyclable 2.0 mM Zwittergent 3-14 eluent system for the determination of iodide in solutions of iodised table salt. Other work within this field [62] includes the addition of chlorate to the list of common

inorganic anions analysed for in high ionic strength matrices. The experimentally determined [62] optimum separation of nitrite, bromide, nitrate, and chlorate in an artificial seawater matrix, using an aqueous H_3BO_3-$Na_2B_4O_7$ solution as the eluent, can be seen in Fig. 1.24.

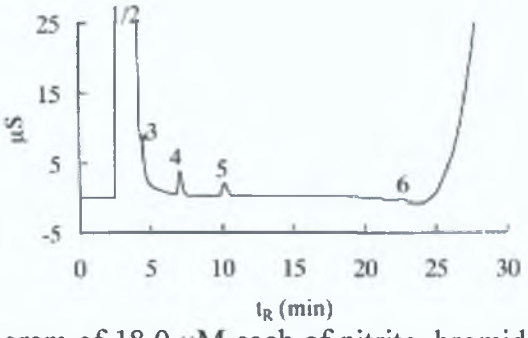

Figure 1.24. Chromatogram of 18.0 μM each of nitrite, bromide, nitrate, and chlorate in a sample containing 0.482 M chloride and 0.029 M sulphate, using an eluent comprised of 1.0 mM Zwittergent 3-14, in 7.0 mM $Na_2B_4O_7$ / 2.0 mM H_3BO_3, and conductivity detection [Reproduced from ref. 62]. Peak identities: (1) - sulphate; (2) - chloride; (3) - nitrite; (4) - bromide; (5) - nitrate; (6) - chlorate.

1.3.8.2 Analysis of Physiological Fluids

Biological samples represent another challenging sample matrix for ion chromatographic analysis. As for seawater samples, the presence of chloride ions in such high concentrations in physiological fluids, in comparison with other anions present, causes some significant difficulties, such as overlapping with peaks corresponding to other analyte ions. The abundance of proteins in many types of biological samples also prove to be detrimental to the quality of the analysis undertaken, as proteins may irreversibly adsorb onto the stationary phase used, thus shortening the lifetime of the separation column [78]. Because of concern regarding these difficulties, most biological samples in IC are subjected to a variety of pretreatment methods, in order to eliminate the chloride ions and/or protein molecules present. However, sample pretreatment is usually time-consuming, and can easily lead to contamination of samples by the reagents involved, thereby producing a significant degree of error in the analytical result [78]. Therefore, taking into account the high tolerance that ZIC systems have for such problematic matrices, ZIC would appear to be a very suitable chromatographic technique for such analyses.

In an early publication regarding ZIC, Hu *et al.* [29] applied a developed ZIC method to the rapid determination of iodide and thiocyanate ions in human saliva samples. Follow-on work undertaken by Hu and Haraguchi [79] showed that the simultaneous determination of 4 inorganic anions (nitrite, nitrate, iodide, and thiocyanate) and organic UV-absorbing compounds (namely α-amylase, which acts as a digestive enzyme in saliva, and tryptophan) in human saliva could be achieved, without any need for complicated sample collection or pretreatment. A representative chromatogram for the analysis of human saliva can be seen in Fig. 1.25.

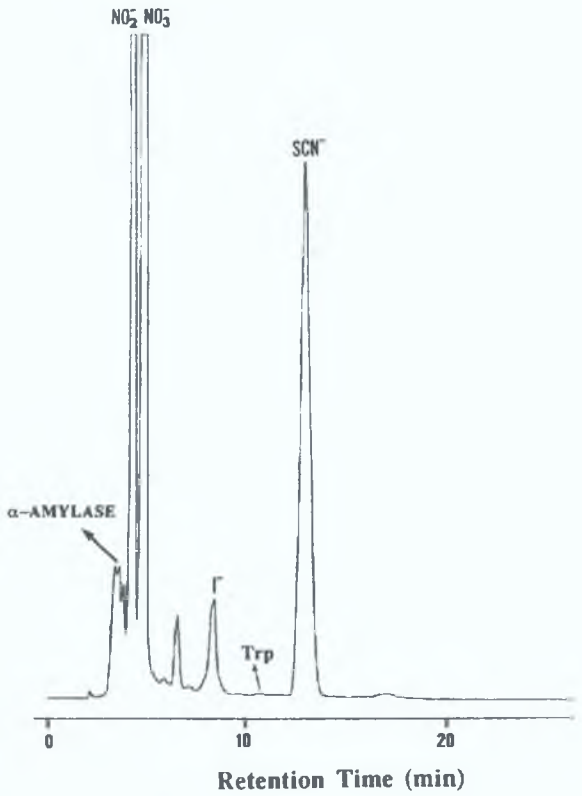

Figure 1.25. Chromatogram of human saliva obtained using a CHAPS-modifed stationary phase, and a phosphate buffer as the eluent, with detection at 230 nm [Reproduced from ref. 79].

Other biological-based fluids analysed using ZIC are human urine and calf serum [78]. For these analyses, the zwitterionic surfactant used to modify the stationary phase was added to the eluent in order to ensure the complete elution of proteins, and therefore maintain column quality. The elution bands for the matrix ions, i.e. sulphate and chloride, were observed as being defined in very narrow zones, and therefore did not mask any other analyte signals. Levels of nitrite, bromide, nitrate, chlorate and

iodide, in both the saliva and serum samples, were quantified, and found to correlate with values obtained using a traditional validated IC method [78].

Umemura *et al.* [80] carried out the determination of several drug compounds (including theophylline and caffeine, which are used in the treatment of asthma and neonatal apnoea, respectively) in human blood serum samples, using a C_{18} reversed-phase column dynamically modified with the zwitterionic surfactant CHAPS. For chromatograms obtained upon injection of untreated serum samples, using an eluent composed of sodium hydrogenphosphate solution, the peaks representing the drugs present in the serum samples were seen to be well resolved from the matrix peak of nearly unretained proteins etc. This is especially useful, as many HPLC methods for therapeutic drug monitoring involve time-consuming sample pretreatments to remove column-fouling proteins [80]. The detection limits for theophylline calculated for the proposed methodology were 60% lower (i.e. 0.2 ppm vs. 0.5 ppm) than those obtained for other HPLC methods which involved no sample pre-treatment [80].

1.3.8.3 Analysis of Nucleosides and Their Bases

Separation of polar organic compounds without the need for ionisation of the analytes is another application of ZIC [32]. When polar organic analytes are passed through a bi-functional zwitterionic stationary phase, hydrophobic interactions between the stationary phase and the analytes are reduced dramatically, mainly as a result of the generation of specific electrostatic fields on the surface of the stationary phase. Mixed-mode separation properties (i.e. a dual mechanism of hydrophobic and electrostatic interactions) have been proposed to explain the observed separations. A practical application of this method has been the separation of nucleosides (and deoxyribonucleosides), and their respective bases [37,38], as can be seen in Fig. 1.26. Nucleosides and their bases are important components of nucleic acids, and were chosen for analysis since they represent typical polar organic compounds [37].

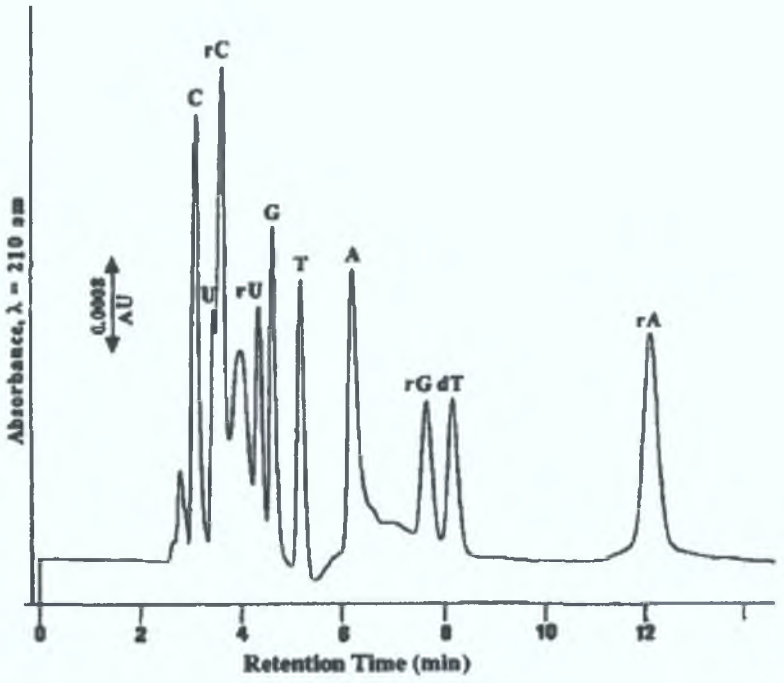

Figure 1.26. Chromatogram of an aqueous solution containing 0.5 μM of various bases, and ribonucleosides, using a Zwittergent 3-14-modified stationary phase, and pure water as the eluent, with UV detection at 210 nm [Reproduced from ref. 37]. Analytes: adenine (A), gunanine (G), cytosine (C), thymine (T), and uracil (U); adenosine (rA), guanosine (rG), cytidine (rC), thymidine (dT), and uridine (rU).

1.3.8.4 Analysis of Vegetable Juices

ZIC was also employed by Umemura *et al.* [49] for the determination of anions in vegetables, making use of decoy electrolytes, as discussed in Section 1.3.4.2. As water was used as the eluent, the analysis of real samples containing several kinds of anions and cations resulted in complicated peak distribution of various ion-pairs, as anions and cations present in the sample solution co-eluted as ion-pairing forms in order to retain charge balance. The radish was used as the vegetable sample. Sample preparation was as follows: Approx. 5 g of radish was washed and cut into pieces, followed by the addition of 15 mL of water. The sample was then homogenised using a mixer, and filtered through a 0.45 μm pore size membrane filter. The resulting filtrate was utilised as the sample solution. The resulting chromatogram of the radish juice can be seen in Fig. 1.27 (A). In order to convert all of the analyte anions present in the radish juice to similar ion-pair forms, 2 types of decoy electrolyte were added to the radish juice sample, namely KI and $MgSO_4$, which converted the ion-pairs to the K^+ and Mg^{2+} forms respectively. The resulting chromatograms of both procedures can

be seen in Fig. 1.27 (B) and (C). Not all anions present were identified, as it was thought that peaks 1 and 1' were the overlapping peaks of anions such as SO_4^{2-}, PO_4^{3-}, F^- etc. Using calibration graphs for KCl, KBr and KNO_3, the levels of Cl^-, Br^- and NO_3^- in the K^+ form were calculated. These experimentally determined values for the concentration of the aforementioned anions in radish juice samples were in agreement with levels determined by conventional IC methodology [49], with the reported values being 98-102% of the values determined by IC.

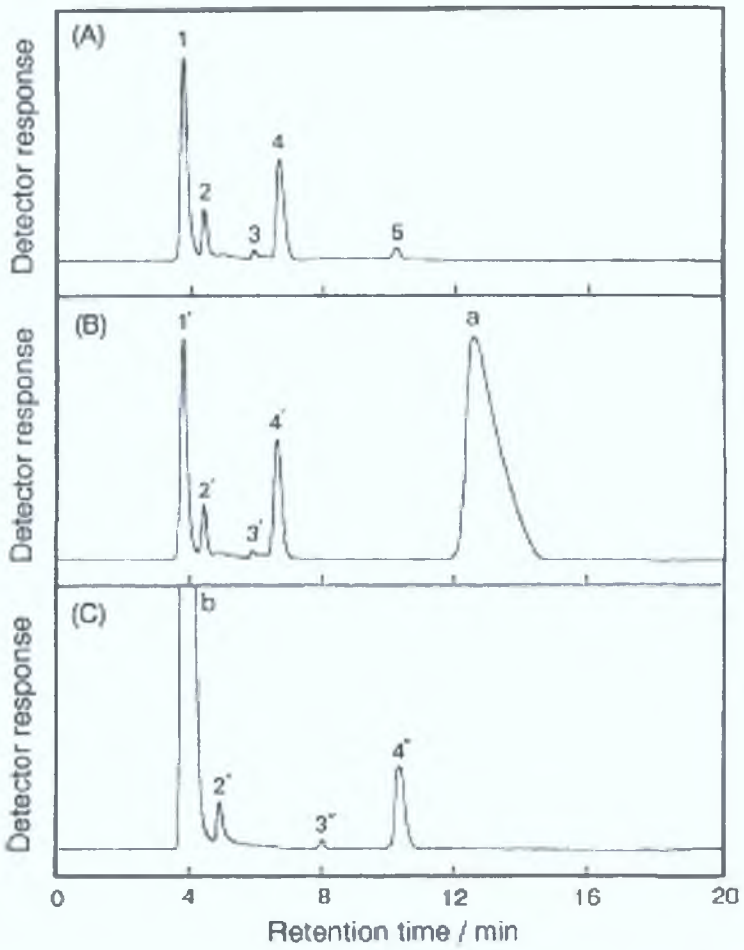

Figure 1.27. Chromatograms of anions in radish juice observed using a C_{18} reversed-phase column modified with tetradecyldimethyl(3-sulfopropyl)-ammonium hydroxide (C14SB), with an eluent composed of pure water, a flow rate of 0.7 mL/min, and conductivity detection [Reproduced from ref. 49]. (A) - Radish juice upon addition of decoy electrolyte. 1 - unidentified, 2 - Cl^-, 3 - Br^-, 4 - NO_3^-, 5 - NO_3^-. (B) – Radish juice with addition of KI. 1'- unidentified, 2'- K^+-Cl^-, 3'- K^+-Br^-, 4'- K^+-NO_3^-, a – mainly K^+-I^-. (C) – Radish juice upon addition of $MgSO_4$. 2"- Mg^{2+}-$2Cl^-$, 3"- Mg^{2+}-Br^-, 4"- Mg^{2+}-$2NO_3^-$, b – mainly Mg^{2+}-SO_4^{2-}.

1.3.8.5 Analysis of Miscellaneous Natural Water Samples

Another possible use for ZIC in environmental analysis is the determination of inorganic anions (e.g. sulphate, chloride, nitrite, bromide and nitrate) in snow and rainwater samples [60], a sample chromatogram of which can be seen in Fig. 1.28. These methods have not been as widely investigated as those for saline solutions, as snow and rainwater sample matrices are not as complex as seawater sample matrices.

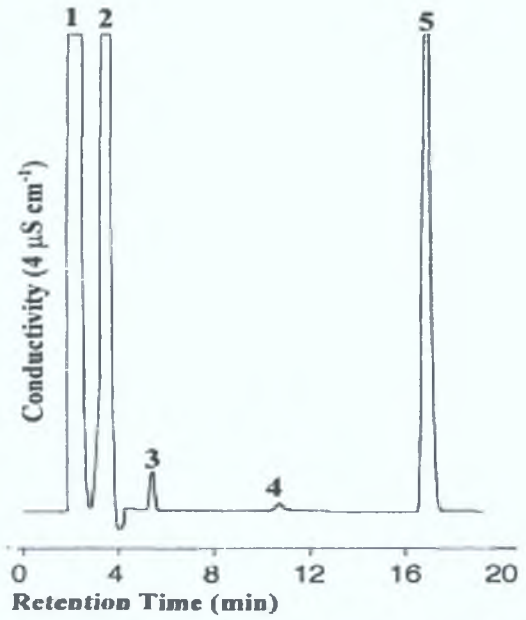

Figure 1.28. Determination of inorganic anions in snow using suppressed-ZIC with 10 mM $Na_2B_4O_7$ solution as eluent, using Zwittergent 3-14 as the zwitterionic stationary phase [Reproduced from ref. 60]. Peak identities: 1 - sulphate, 2 - chloride, 3 - nitrite, 4 - bromide, and 5 - nitrate.

1.4 Detection Methods Employed in Ion Chromatography

While the separation of analyte ions is the central issue in IC, the detection of the separated species is also important. When IC was first introduced in 1975 [3], it was the novel detection approach of suppressed eluent conductivity detection that differentiated this technique from other liquid chromatographic methods [81]. Although conductivity detection remains possibly the most widely employed method of detection for routine work in IC, newer applications meant that the development of other detection techniques, with increased selectivity or the ability to determine analyte structure etc., was necessary.

Detectors can be classified as being either general or selective detectors [8]. A general detector will respond to all, or most, of the ions that pass through the detector cell. A conductometric detector is therefore classified as a general detector, as all ions will conduct electricity to some degree. Spectrophotometric and electrochemical detectors are usually considered to be selective detectors, as they only respond to certain ions, although the use of a post-column reaction of sample ions may turn these techniques into a general-type detector. One factor to take into account when discussing the detection techniques of ionic analytes is the fact that the detection signal observed will depend on the difference between a property of an analyte ion and a property of eluent ions [81].

1.4.1 Conductivity Detection

The underlying principle of conductimetric detection is that a solution of an electrolyte will conduct an electrical current if 2 electrodes are placed into the solution, and a potential applied across the electrodes [7]. The more current conducted by the electrolytic solution, the greater its electrical conductivity. The electrical properties of the solution obey Ohm's Law:

$$V = IR \qquad \text{(Eqn. 1.1)}$$

where V is the applied potential (in volts), I is the current flowing through the solution (in amps), and R is the resistance (in ohms). The resistance of the solution depends on the temperature, and the concentration, and nature, of the ionic species in solution. The conductance, G (unit = Siemens, S), of the solution is equivalent to the reciprocal of the resistance:

$$G = 1 / R \qquad \text{(Eqn. 1.2)}$$

The conductivity, k (units = $S.cm^{-1}$), also referred to as the equivalent conductance, is given by:

$$k = L / AR = LG / A \qquad \text{(Eqn. 1.3)}$$

where A is the cross-sectional area of the electrodes inserted into the electrolyte solution (in cm^2), and L is the distance between the electrodes (in cm). The specific conductance varies with concentration, so therefore another term was introduced that would allow direct comparison between different electrolytes, namely the equivalent conductance, Λ (units = $S.cm^2.equiv^{-1}$). Specific conductance and equivalent conductance are related as follows:

$$\Lambda = 1000\ k / C \qquad \text{(Eqn. 1.4)}$$

where C equals the concentration of the electrolyte (expressed as equivalents per 1000 cm^3). By combining the geometrical dimensions of the cell (i.e. A and L) into a single term, called the cell constant, K (units = cm^{-1}), enables the equation for k (Eqn 1.3) to be rewritten as shown in Eqn 1.6.

$$K = L / A \qquad \text{(Eqn. 1.5)}$$

$$k = G\,K \qquad \text{(Eqn. 1.6)}$$

This means that conductance can now be defined as:

$$G = (\Lambda\ C) / (1000\ K) \qquad \text{(Eqn. 1.7)}$$

However, if G is expressed as μS, rather than S, Eqn. 1.7 becomes:

$$G = (1000\ \Lambda\ C) / K = (\Lambda\ C) / (10^{-3}\ K) \qquad \text{(Eqn. 1.8)}$$

From Eqn. 1.8 it is clear that the conductance of a solution is directly proportional to both the concentration of the electrolyte present and its conductance. However, the conductance of the solution results from a contribution from both the anions and cations present, and so the limiting equivalent ionic conductances, λ (unit = $S.cm^2.equiv^{-1}$), of the individual anions and cations must be taken into account. This leads to a slight adjustment of Eqn. 1.8:

$$G = ((\lambda_+ + \lambda_-)\ C) / (10^{-3}\ K) \qquad \text{(Eqn. 1.9)}$$

where λ_+ and λ_- are the limiting ionic conductances of the cationic and the anionic constituents of the electrolyte respectively. The change in conductance (Δ G), which accompanies elution of the analyte anion can be determined by subtracting the background conductance from the conductance during analyte elution, and can be represented by the following equation (using an anion-exchange system):

$$\Delta G = ((\lambda_{A^-} - \lambda_{E^-}) C_A I_A) / (10^{-3} K) \qquad \text{(Eqn. 1.10)}$$

where λ_{A^-} and λ_{E^-} are the limiting equivalent ionic conductances of the analyte anion and the anionic eluent species respectively, and where C_A equates to the concentration of the analyte anion passing through the detector cell, and I_A represents the degree of ionisation of the analyte anion. The relationship outlined in Eqn. 1.10 indicates that for conductivity detection of IC separations (without eluent conductivity suppression), the signal-to-noise ratio can be maximised by utilising a low-conductivity eluent at a low concentration, and therefore, careful consideration must be given to the eluent composition chosen.

1.4.1.1 Direct vs. Indirect Detection

From looking at Eqn. 1.10, it is evident that sensitive detection can be obtained, provided there is a sizeable difference in the limiting equivalent ionic conductances of the analyte ion and the eluent ions. The difference between these values can be either positive or negative, depending on whether the eluent employed is strongly or weakly conducting. If the limiting equivalent ionic conductance of the eluent used is low, then, upon elution of the analyte ion, and its passing through the detector cell, the conductance will increase (leading to positive peaks), as the analyte ion will have a higher limiting equivalent ionic conductance. This is classified as direct detection [7], as the analyte has a higher value for the measured property compared to the eluent ions. If, on the other hand, the limiting equivalent ionic conductance of the eluent is high, then a decrease in the observed conductance signal (i.e. negative peaks) will follow elution of the analyte ion. This is termed indirect detection, as the analyte has a lower value for the measured property than the eluent ion [7]. This is summarised in Fig. 1.29, where eluent 1 has a higher limiting equivalent ionic conductance compared to the analyte ion (i.e. $\lambda_{E1} > \lambda_A$), resulting in a negative peak through indirect

detection, and eluent 2 has a lower limiting equivalent ionic conductance compared to the analyte ion (i.e. $\lambda_{E2} < \lambda_A$), resulting in a positive peak through direct detection.

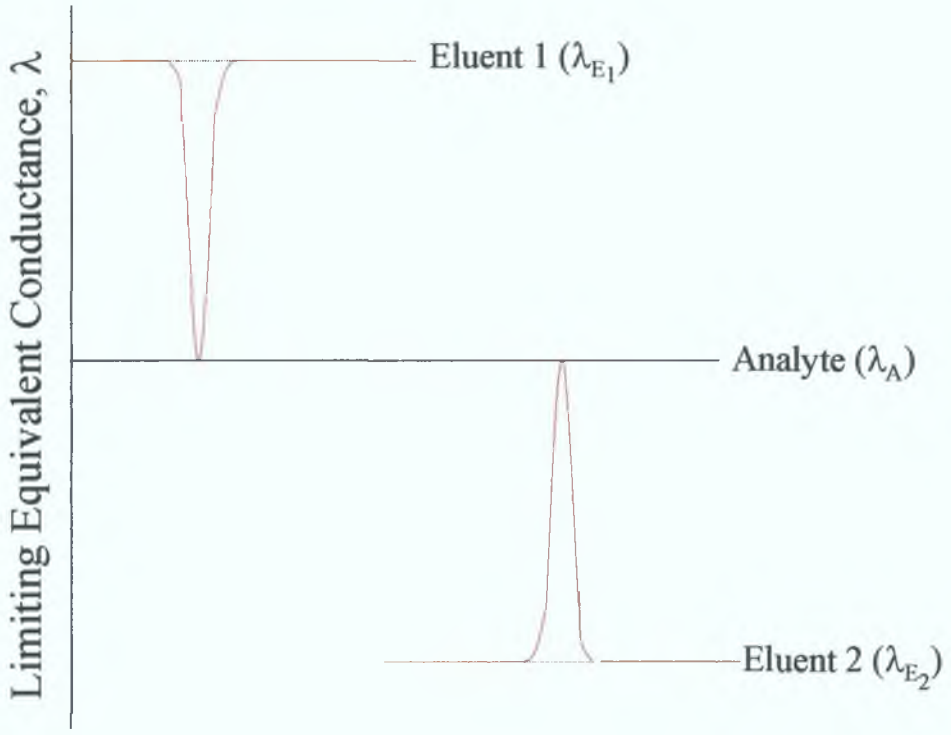

Figure 1.29. Diagram illustrating indirect conductivity detection (giving a negative analyte peak, as with eluent 1, which has a high limiting equivalent ionic conductance), and direct conductivity detection (displaying a positive analyte peak, as with eluent 2, which has a low limiting equivalent ionic conductance) [7].

1.4.1.2 Suppressed Conductivity Detection

Chemical suppression is often used in IC as a means of reducing the background conductance of the eluent, while simultaneously enhancing the conductance of the analyte ion(s). For the pioneering work by Small *et al.* in 1975 [3], a second ion-exchange column, called a "stripper" column, was placed between the column used for separation and the conductivity detector, in order to suppress the eluent conductance. For anion analysis, a basic anion was employed in the eluent, and a H^+-form packed-bed cation-exchange column was used as the "stripper" column. The basic principles of suppressed anion-exchange chromatography can be outlined as follows: The basic, highly conductive eluent (e.g. OH^-) is neutralised by H^+ ions provided by the cation-exchanger of the column [8], forming water molecules, which are much more weakly conductive, in comparison to the OH^- eluent. The analyte salt

passing through the suppressor is converted from the sodium form (Na^+X^-, where X^- is the analyte anion), for example, to a more highly conductive form, containing hydrogen as the counterion (i.e. H^+X^-).

Suppressors evolved over the years, from the original packed-bed design (which caused significant peak broadening, and also needed frequent regeneration) to a membrane suppressor design, to the more recent electrolytic suppressors, introduced by Strong and Dasgupta [82], which use the electrolysis of water to produce the H^+ or OH^- ions required for chemical suppression. In 1992, Dionex launched a commercial electrochemical suppressor called a Self-Regeneration Suppressor [83], which (in the anion-suppression mode) uses electrolytically produced H^+ ions to regenerate the suppressor, allowing for the use of low flow rates for water to the suppressor, as well as negating the need for independent chemical feed. The mechanism for the operation of an Anion Self-Regeneration Suppressor is shown in Fig. 1.30.

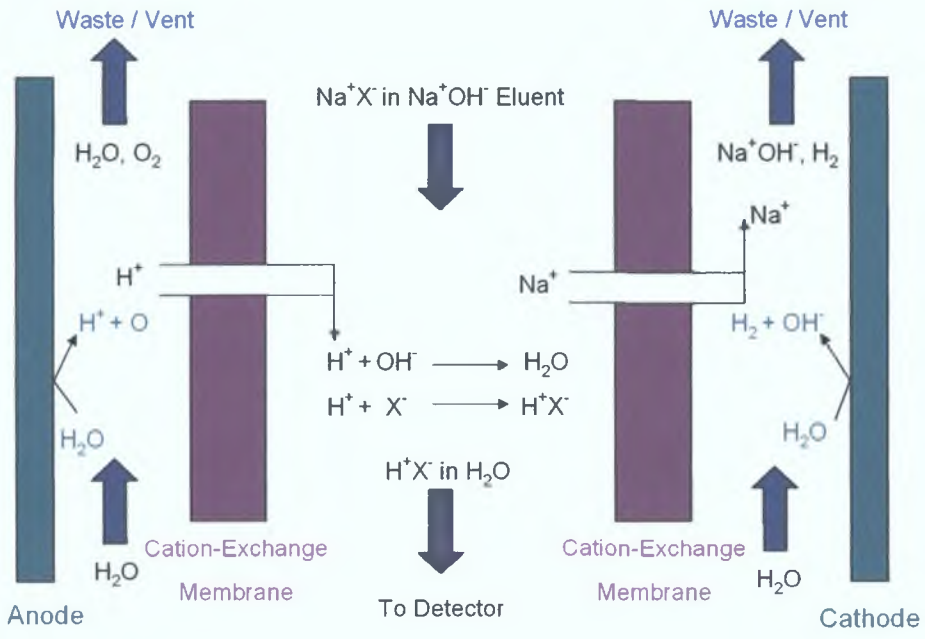

Figure 1.30. Schematic illustrating how an Anion Self-Regenerating Suppressor suppresses eluent conductivity in the analysis of anions [83].

In the Anion Self-Regenerating Suppressor, hydrogen ions generated at the positively charged anode cross the cation-exchange membrane, and neutralise the basic eluent. The sodium counterions of the analyte and eluent are attracted to the negatively

charged cathode, and therefore they permeate the cation-exchange membrane, and form hydroxide compounds, in order to maintain electroneutrality. As for previously used suppressors, the conductance of analyte anions is increased by exchanging their original counterions for the electrolytically generated H^+ ions, thereby creating highly conductive hydride molecules (represented in Fig. 1.30 by H^+X^-). Waste products are vented from both electrodes (water and gaseous oxygen at the anode, and aqueous sodium hydroxide and hydrogen gas at the cathode).

Of course, eluent suppression is not always required in IC, e.g. when using eluents of low conductance, such as, in the case of anion analysis, solutions of aromatic acids.

1.4.1.3 Contactless Conductivity Detection

With the advent of capillary IC, came the need for the development of miniaturised conductivity detectors that would allow detection to occur "across-capillary" (i.e. with the detector placed directly on the capillary column used), thereby forgoing to the requirement for the detector to be in direct contact with the eluent solution. Capacitively coupled contactless conductometric detection (hereafter referred to as C^4D) has been around in some form or another since 1983 [84], but was refined for across-column applications for capillary zone electrophoresis based separations in the late 1990s [85,86]. For on-column C^4D, the detector cell consists of 2 cylindrical electrodes positioned directly on the outer wall of the separation capillary (usually composed of silica) [87]. These electrodes are not in galvanic contact with solution within the capillary. These electrodes are also separated by a small gap, typically 1-2 mm, which defines the length of solution inside the capillary, across which conductivity is measured. The electrodes may be stuck directly onto the capillary wall or may be housed in a moveable detector unit (which has the advantage of being able to be positioned at any location along the length of the capillary column). Such a detector set-up has not seen widespread use in IC, with little mention in the literature outside of capillary electrophoretic applications, outside of a few exceptions [88,89]. C^4D systems also have the advantage of being compact, making them particularly suitable for use in conjunction with portable instrumentation [90]. Multiple C^4D detectors can also be placed on a single capillary column [87], while, as the device works contactlessly, no cleaning or flushing of the detection cell is necessary [85].

1.4.2 Spectroscopic Detection

There are numerous types of spectroscopic detection methods used in IC, the most commonly employed of which is spectrophotometry. Some of the other techniques include refractive index detection and photoluminescence detection.

1.4.2.1 UV-Visible Spectrophotometric Detection

Spectrophotometric detectors have proven to be highly popular for the monitoring of ion-exchange separations. This can be attributed to them being selective, while also allowing selectivity to be adjusted, simply by changing the wavelength monitored by the detector [8]. UV-Vis spectrophotometry is based on the comparison of incident light intensity, I_0, and emergent intensity, I, after passing through the solution of interest [91]. The ratio I/I_o is called the transmittance, T. To obtain the absorbance, A, the ratio I/I_o is logarithmically transformed:

$$A = \log 1/T = \log I_0/I \qquad \text{(Eqn. 1.11)}$$

The relationship between absorbance and concentration of analyte, c, is given by the Lambert-Beer law, which is itself a combination of 2 other laws [91]: (1) Lambert's law states that log I/I_0 is proportional to the pathlength of the detection cell, d (measured in cm), and (2) Beer's law maintains that log I_0/I is proportional to the concentration of analyte, c (units = mol/L). Therefore, the Lambert-Beer law can be stated as follows:

$$A = \varepsilon\, c\, d \qquad \text{(Eqn. 1.12)}$$

where ε is the molar absorptivity of the analyte (units = L / mol.cm). This means that the higher the absorbance, the less light is passing through the detector cell. Eqn. 1.12 shows that A is dimensionless, and so it is typically described in terms of absorbance units, AU [8]. Lambert-Beer's law is only applicable for monochromatic light, as the molar absorptivity is dependent on the wavelength used. Hence, polychromatic light sources decrease the linearity of quantitative analysis, leading to the inclusion of monochromators (usually gratings, in contemporary instruments) in the design of UV-Vis detectors [91].

The difference between the background absorbance of the eluent and the absorbance measured upon analyte elution (Δ A, i.e. the signal) is given by a modification of Eqn. 1.12 described below [91] (assuming the analyte is fully dissociated):

$$\Delta A = (\varepsilon_A - z_A/z_E.\varepsilon_E)\, d\, c_A \qquad \text{(Eqn. 1.13)}$$

where, in the case of anion analysis, ε_A and ε_E are the molar absorptivities of the analyte anion and the eluent anion respectively, and z_A and z_E are the charges on the analyte anion and the eluent anion respectively, and c_A represents the concentration of analyte anions present. Further investigation of Eqn. 1.13 indicates that for the efficient detection of analyte ions, eluent ions should have a low molar absorptivity (at the wavelength in question), while the analyte ions should have a reasonably high molar absorptivity. However, as seen before for conductivity detection in Section 1.4.1.1, indirect detection may be carried out, whereby the magnitude of the analyte and eluent absorptivities would be reversed, resulting in a decrease in the background signal upon elution of analyte ions. This is a useful technique for the determination of analyte ions that do not absorb light in the UV or visible regions of the electromagnetic spectrum, and would therefore be undetectable using direct UV-Vis spectrophotometric detection.

The versatility of UV-Vis spectrophotometric detection can be increased through the use of a post-column reaction (PCR). Detection using PCR involves the chemical reaction of analytes as they elute from the chromatographic column, prior to their passage to the detector [7], in order to enhance the specificity and sensitivity of the detection method. PCR is mostly used in tandem with UV-Vis absorbance detection [81]. An example of this would be the addition of colour-forming reagents to the eluent post-column, e.g. 4-(pyridylazo)resorcinol (PAR) is routinely reacted with transition metal samples through direct mixing in a simple mixing tee-piece, resulting in a colour change from orange to bright red, before detection at 510 nm. However, PCR techniques often contribute substantially to the baseline noise observed during analysis, depending on the pump utilised to deliver the reagent to the mixing coil.

1.4.2.2 Refractive Index Detection

The refractive index (RI) of a medium refers to the ratio of the speed of light in a vacuum relative to the speed of light in the medium under consideration [92]. RI detectors operate on the principle that the addition of a salt (or acid or base) to an aqueous solution will cause a change in the refractive index of the solution [8]. The differences in RI are measured as the analyte ions pass through the detector cell replacing some of the eluent ions, and bringing about a change in the observed RI. The nature of this relative change will determine whether the peak for the analyte ion is positive (direct RI detection) or negative (indirect RI detection). Unfortunately, most of the common IC analytes are not detectable directly by RI measurements [7], but the use of indirect RI detection of common inorganic anions, using eluents composed of aromatic carboxylic acids, for example, has been demonstrated [e.g. 93].

1.4.2.3 Fluorescence Detection

This method of detection measures the change in fluorescence caused by the presence of certain analyte ions. The inherent sensitivity of this technique may be up to 1000 times greater than for UV detection [94]. The mechanism of operation involves the passing of light of a suitable excitation wavelength through the detector cell, followed by the detection (in a right-angled direction) of the higher wavelength radiation emitted [94]. Direct fluorescence detection is highly limited in scope, as most common inorganic ions do not exhibit fluorescence. Sometimes this can be overcome through the addition of derivatising agents to the eluent, e.g. the use of 8-hydroxyquinoline-5-sulphonic acid as an eluent component for the determination of metal ions [95]. With fluorescence detection, care must be taken to ensure that no sample matrix or eluent components that may cause quenching of the fluorescence are present.

1.4.3 Electrochemical Detectors

Electrochemical detectors are sometimes divided into separate groups based on three parameters of electric measurements [8]: Potentiometric detectors (which measure voltage), amperometric detectors (which measure current), and conductometric detectors (which measure resistance). Conductometric detection is usually treated as a distinct detection method [7], and so was discussed separately in Section 1.4.1.

1.4.3.1 Amperometric Detection

Amperometric detection is based on the oxidation or reduction of an analyte at a working electrode at a fixed potential that is high enough to initiate the oxidation or reduction process [81]. The working electrode is placed in a suitable flow-cell, through which the eluent passes. The electric current generated from the electrochemical reaction at the electrode serves as the analytical signal, and is directly proportional to the concentration of the electrochemically active analyte ion [81]. Amperometric detectors are some of the most selective and sensitive detectors used in IC [8]. They are selective, as the potential required to induce electrolysis is different for each ion (provided the analyte is easily oxidisable), while this selectivity can be controlled by manipulating the magnitude of the applied potential and the detector electrode material [8]. In general, amperometric detection is undertaken in the direct mode, i.e. using an electrochemically non-active co-ion in the eluent.

The potential of the working electrode in amperometric detection can also be applied in a pulsed mode, as the electrode surface may suffer from deactivation [96], due to the absorption of organic compounds etc. An example of this is the triple-pulsed mode, where the successive application of a measuring potential, a cleaning potential and a conditioning potential in a repetitive manner leads to a more stable detector response [81].

1.4.3.2 Potentiometric Detection

Potentiometry is the process in which potential changes at an indicator electrode are measured in relation to a reference electrode, under conditions of constant flow (usually zero flow) [96]. The potential of the indicator electrode varies with the concentration of a particular ion (or ions) in the solution. In the case of potentiometric detectors the determination of analyte ions is carried out using ion-selective electrodes (ISEs). This means that the selective determination of analyte ions is achievable even in complex sample matrices. As simple (in both design and operation), easy to miniaturise, and inexpensive as these detectors are, this highly selective approach to detection in IC is not always advantageous, as sometimes it is preferable that the detector display a more general analytical response, so that the detection of a wider range of analytes can be obtained [7]. Therefore, potentiometric detectors are sometimes used in series with more universal detection techniques, or, as has been

reported by Lee *et al.* [97], used as array-type ISEs, where the detection cell contains several different electrodes within a single chip, with each electrode exhibiting separate, distinct selectivities.

1.5 Conclusions

ZIC is a singular IC method with unique separation selectivity for the separation of inorganic anions, and, to a lesser extent, cations. Usually the stationary phases in ZIC are prepared through the modification of C_{18} reversed-phase columns with solutions of zwitterionic surfactants. Both pure water and electrolytic solutions have been successfully employed as eluents for ZIC. It is widely believed that retention occurs through a mixture of electrostatic and chaotropic interactions. Numerous practical applications of ZIC have been shown, for a wide range of samples, giving rise to potentially simpler, less time-consuming methodologies for analyses that have traditionally been regarded as problematic and challenging using standard IC techniques.

References:

1 Fundamentals of Analytical Chemistry, D.A. Skoog, D.M. West, F.J. Holler, 7th edition 1996, published by Saunders College Publishing, Fort Worth, Texas.

2 Ion Exchange Chromatography (Benchmark Papers in Analytical Chemistry, Vol. 1), H.F. Walton, 1976, published by Dowden, Hutchinson and Ross, New York.

3 H. Small, T.S. Stevens, W.C. Bauman, Anal. Chem. 47 (1975) 1803-1809.

4 Ion Chromatography, H. Small, 1st edition 1989, published by Plenum Press, New York.

5 D.T. Gjerde, J.S. Fritz, G. Schmuckler, J. Chrom. 186 (1979) 509-519.

6 J.S. Fritz, D.T. Gjerde, G. Schmuckler, U.S. Patent 4,272,246 (1981).

7 Ion Chromatography: Principles and Applications (J. Chrom. Library Vol. 46), P.R. Haddad and P.E. Jackson, 1st edition 1990, published by Elsevier Science Publishers B.V., Amsterdam.

8 Ion Chromatography, J.S. Fritz and D.T. Gjerde, 3rd edition 2000, published by Wiley-VCH, Weinheim, Germany.

9 P. Jones, P.N. Nesterenko, J. Chrom. A 789 (1997) 413-435.

10 Chromatography and Separation Science, S. Ahuja, 1st edition 2003, published by Academic Press, San Diego, California.

11 C.A. Lucy, J. Chrom. A 1000 (2003) 711-724.

12 P.R. Haddad, M.Y. Croft, Chromatographia 21 (1986) 648-650.

13 C.A. Pohl, J.R. Stillian, P.E. Jackson, J. Chrom. A 789 (1997) 29-41.

14 Encyclopedia of Chromatography, edited by Jack Cazes, 2001 edition, published by Marcel Dekker Inc., New York.

15 M.C. Gennaro, S. Angelino, J. Chrom. A 789 (1997) 181-194.

16 C. Horvath, W. Melander, I. Molnar, P. Molnar, Anal. Chem. 49 (1977) 2295-2305.

17 P.T. Kissinger, Anal. Chem. 49 (1977) 883-883.

18 F.F. Cantwell, S. Puon, Anal. Chem. 51 (1979) 623-632.

19 J. Stahlberg, I. Hagglund, Anal. Chem. 60 (1988) 1958-1964.

20 B.K. Glód, M. Baumann, J. Sep. Sci. 26 (2003) 1547-1553.

21 A. Siriraks, H.M. Kingston, J.M Rivello, Anal. Chem. 62 (1990) 1185-1193.

22 J.H. Knox, J. Jurand, J. Chrom. 203 (1981) 85-92.

23 J.H. Knox, J. Jurand, J. Chrom. 218 (1981) 341-354.

24 P.N. Nesterenko, P.R. Haddad, Anal. Sci. 16 (2000) 565-574.

25 P.N. Nesternko, A.I. Elefterov, D.A. Tarasenko, O.A. Shpigun, J. Chrom. A 706 (1995) 59-68.

26 M.G. Kiseleva, P.A. Kebets, P.N. Nesterenko, Analyst 126 (2001) 2119-2123.

27 L.W. Yu, T.R. Floyd, R.A. Hartwick, J. Chrom. Sci. 24 (1986) 177-182.

28 L.W. Yu, R.A. Hartwick, J. Chrom. Sci. 27 (1989) 176-185.

29 W. Hu, T. Takeuchi, H. Haraguchi, Anal. Chem. 65 (1993) 2204-2208.

30 W. Hu, A. Miyazaki, H. Tao, A. Itoh, T. Umemura, H. Haraguchi, Anal. Chem. 67 (1995) 3713-3716.

31 W. Hu, K. Hasebe, D.M. Reynolds, T. Umemura, S. Kamiya, A. Itoh, H. Haraguchi, J. Liq. Chrom. & Rel. Tech. 20 (1997) 1903-1919.

32 W. Hu, P.R. Haddad, TRAC 17 (1998) 73-79.

33 W. Hu, P.R. Haddad, K. Tanaka, M. Mori, K. Tekura, K. Hasebe, M. Ohno, N. Kamo, J. Chrom. A 997 (2003) 237-242.

34 W. Hu, P.R. Haddad, K. Hasebe, M. Mori, K. Tanaka, M. Ohno, N. Kamo, Biophys. Journal 83 (2002) 3351-3356.

35 R.J. Clarke, C. Lüpfert, Biophys. Journal 76 (1999) 2614-2624.

36 T. Umemura, S. Kamiya, A. Itoh, K. Chiba, H. Haraguchi, Anal. Chim. Acta 349 (1997) 231-238.

37 W. Hu, K. Hasebe, D.M. Reynolds, H. Haraguchi, Anal. Chim. Acta 353 (1997) 143-149.

38 T. Umemura, K. Tsunoda, A. Koide, T. Oshima, N. Watanabe, K, Chiba, H. Haraguchi, Anal. Chim. Acta 419 (2000) 87-92.

39 W. Hu, P.R. Haddad, Anal. Commun. 35 (1998) 49-52.

40 W. Jiang, K. Irgrum, Anal. Chem. 71 (1999) 333-344.

41 W. Jiang, K. Irgrum, Anal. Chem. 73 (2001) 1993-2003.

42 W. Jiang, K. Irgrum, Anal. Chem. 74 (2002) 4682-4687.

43 W. Hu, H. Haraguchi, J. Chrom. A 723 (1996) 251-258.

44 W. Hu, H. Tao, H. Haraguchi, Anal. Chem. 66 (1994) 2514-2520.

45 W. Hu, H. Tao, M. Tominaga, A. Miyazaki, H. Haraguchi, Anal. Chim. Acta 299 (1994) 249-256.

46 T. Umemura, S. Kamiya, R. Kitaguchi, H. Haraguchi, Chemistry Letters 8 (1997)

755-756.

47 T. Umemura, R. Kitaguchi, H. Haraguchi, Anal. Chem. 70 (1998) 936-942.

48 K. Hasebe, T. Sakuraba, W. Hu, J. Liq. Chrom. & Rel. Tech 22 (1999) 561-569.

49 T. Umemura, S. Kamiya, H. Haraguchi, Anal. Chim. Acta 379 (1999) 23-32.

50 W. Hu, P.R. Haddad, Anal. Commun. 35 (1998) 317-320.

51 T. Okada, J.M. Patil, Langmuir 14 (1998) 6241-6248.

52 J.M. Patil, T. Okada, Anal. Commun. 36 (1999) 9-11.

53 T. Masudo, T. Okada, Phys. Chem. Chem. Phys. 1 (1999) 3577-3582.

54 H.A. Cook, W. Hu, J.S. Fritz, P.R. Haddad, Anal. Chem. 73 (2001) 3022-3027.

55 W. Hu, P.R. Haddad, K. Hasebe, K. Tanaka, P. Tong, C. Khoo, Anal. Chem. 71 (1999) 1617-1620.

56 W. Hu, Langmuir, 15 (1999) 7168-7171.

57 Oxford Dictionary of Chemistry, Edited by John Daintith, 5th Edition 2004, published by Oxford University Press, Oxford.

58 J.S. Fritz, J. Chrom. A 1085 (2005) 8-17.

59 K. Iso, T. Okada, Langmuir 16 (2000) 9199-9204.

60 W. Hu, K. Tanaka, P.R. Haddad, K. Hasebe, J. Chrom. A 884 (2000) 161-165.

61 W. Hu, P.R. Haddad, K. Hasebe, K. Tanaka, Anal. Commun. 36 (1999) 309-312.

62 W. Hu, P.R. Haddad, K. Tanaka, S. Sato, M. Mori, Q. Xu, M. Ikedo, S. Tanaka, J. Chrom. A, 1039 (2004) 59-62.

63 W. Hu, P.R. Haddad, K. Tanaka, K. Hasebe, Analyst 125 (2000) 241-244.

64 W. Hu, K. Hasebe, M. Ding, K. Tanaka, Fresenius J. Anal. Chem. 371 (2001) 1109-1112.

65 W. Hu, P.R. Haddad, K. Tanaka, K. Hasebe, Anal. Bioanal. Chem. 375 (2003) 259-263.

66 M. Macka, P.R. Haddad, J. Chrom. A 884 (2000) 287-296.

67 W. Hu, P.R. Haddad, H. Cook, H. Yamamoto, K. Hasebe, K. Tanaka, J.S. Fritz, J. Chrom. A 920 (2001) 95-100.

68 W. Hu, P.R. Haddad, K. Hasebe, H.A. Cook, J.S. Fritz, Fresenius J. Anal. Chem. 367 (2000) 641-644.

69 W. Hu, P.R. Haddad, K. Hasebe, K. Tanaka, Anal. Commun. 36 (1999) 97-100.

70 W. Hu, K. Hasebe, K. Tanaka, J.S. Fritz, J. Chrom. A 956 (2002) 139-145.

71 H.A. Cook, G.W. Dicinoski, P.R. Haddad, J. Chrom. A 997 (2003) 13-20.

72 T. Okada, Anal. Chim. Acta 540 (2005) 139-145.

73 W. Hu, H. Haraguchi, Anal. Chem. 66 (1994) 765-767.

74 W. Hu, S. Cao, M. Tominaga, A. Miyazaki, Anal. Chim. Acta 322 (1996) 43-47.

75 W. Hu, K. Hasebe, K. Tanaka, P.R. Haddad, J. Chrom. A 850 (1999)161-166.

76 W. Hu, P. Yang, K. Hasebe, P.R. Haddad, K. Tanaka, J. Chrom. A 956 (2002) 103-107.

77 E. Twohill, B. Paull, J. Chrom. A 973 (2002) 103-113.

78 W. Hu, K. Tanaka, K. Hasebe, Analyst 125 (2000) 447-451.

79 W. Hu, H. Haraguchi, Anal. Chim. Acta 285 (1994) 335-341.

80 T. Umemura, R. Kitaguchi, K. Inagaki, H. Haraguchi, Analyst 123 (1998) 1767-1770.

81 W.W. Buchberger, TRAC 20 (2001) 296-303.

82 D.L. Strong, P.K. Dasgupta, Anal. Chem. 61 (1989) 939–945.

83 S. Rabian, J. Stillian, V. Barreto, K. Friedman, M. Toofan, J. Chrom. A 640 (1993) 97-109.

84 E. Pungor, F. Pál, K. Tóth, Anal. Chem. 55 (1983) 1728-1731.

85 A.J. Zeeman, E. Schnell, D. Volgger, G.K. Bonn, Anal. Chem. 70 (1998) 563-567.

86 J.A.F. da Silva, C.L. do Lago, Anal. Chem. 70 (1998) 4339-4343.

87 P. Kuban, P.K Dasgupta, J. Sep. Sci. 27 (2004) 1441-1457.

88 E.F. Hilder, A.J. Zeeman, M. Macka, P.R. Haddad, Electrophoresis 22 (2001) 1273-1281.

89 P. Kuban, M.A. Muri, P.C. Hauser, Analyst 129 (2004) 82-86.

90 T. Kappes, B. Galliker, M.A. Schwarz, P.C. Hauser, TRAC 20 (2001) 133-139.

91 B.E. Lendi, V.R. Meyer, LC-GC Europe 18 (2005) 156-163.

92 Physics: Principles With Applications, D.C. Giancoli, 5th edition 1998, published by Prentice-Hall International, London.

93 F.A. Buytenhuys, J. Chrom. 218 (1981) 57-64.

94 Practical High-Performance Liquid Chromatography, V.R. Meyer, 2nd Edition 1994, published by John Wiley & Sons, Chicester, England.

95 P.K. Dasgupta, K. Soroka, R.S. Vithanage, J. Liq. Chrom. & Rel. Tech. 10 (1987) 3287-3319.

96 Principles and Applications of Electrochemistry, D.R. Crow, 4th Edition 1994, published by Blackie Academic and Professional (of Chapman and Hall),

Glasgow.

97 D.K. Lee, H.J. Lee, G.S. Cha, H. Nam, K.-J. Paeng, J. Chrom. A 902 (2000) 337-343.

Chapter 2

Separation of Common Inorganic Anions Using a Carboxybetaine-Modified 25 cm Particle-Packed C_{18} Column

2.1 Introduction

Stationary phases suitable for zwitterionic ion chromatography (ZIC) can be prepared by dynamically modifying standard reversed-phase C_{18} columns using zwitterionic surfactants, as outlined by Hu *et al.* [1]. Within this Chapter, the surfactant used to create the zwitterionic stationary phase was a previously unused carboxybetaine-type surfactant, dodecyldimethylaminoacetic acid, the structure of which can be seen in Fig. 2.1. As illustrated in Fig. 2.1, the surfactant molecule contains an anionic functional group (a weak carboxylic acid terminal group), a cationic functional group (a strong quaternary ammonium group), and a hydrophobic region, which enables it to be strongly retained on the C_{18} stationary phase.

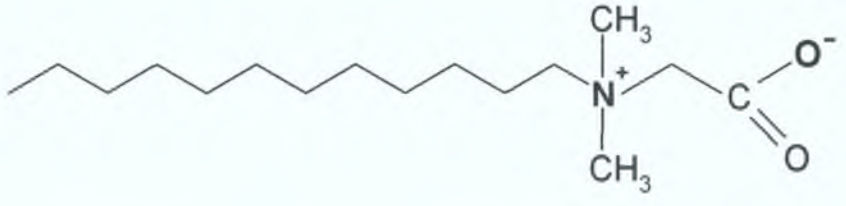

Figure 2.1. Structure of dodecyldimethylaminoacetic acid.

Betaines, and carboxybetaines in particular, are of great importance in the cosmetics (shampoos, facial cleaners etc.) and cleaning products (domestic detergents etc.) industry, principally because of the fact that they exhibit good biodegradability, and because they are far less irritating to the skin and eyes than many other additives [2,3]. Zwitterionic surfactants also improve the foamability, foam stability and rheological behaviour of foams [4] (because of their inherent property of being able to stabilise foams against the anti-foaming action of oil droplets contained in commercial shampoos and hair conditioners [5]), and for this reason are often termed "foam boosters" [4,5]. Alkylbetaines, in particular, are typical additives to conditioning shampoos, due to their softening and antistatic effects on hair [4]. Carboxybetaines have also found widespread industrial application as softening (i.e. conferring antistatic properties) and wetting agents in textile production, and as emulsifiers and dispersants in emulsion polymerisation, paints, photographic emulsions and many other systems [4].

The majority of the published work on ZIC has focussed on the use of zwitterionic surfactants containing both a strong acid group, and a strong basic group

[1,6,7,8,9,10]. The employment of a weak-strong (i.e. weak acidic group, and strong basic functionality) zwitterionic surfactant as a stationary phase material for ZIC has, until recently, received relatively little attention. Hu *et al.* [11] investigated a carboxybetaine-type zwitterionic reagent as a modifier for reversed-phase C_{18} columns, and applied the resulting zwitterionic ion-exchanger to the separation of anions. The zwitterionic surfactant used, namely 3-(heptadecafluorooctylsulfonylamino)-N,N–dimethylpropanammonioethyl-carboxylate ($C_8F_{17}SO_2NHC_3H_6N^+(CH_3)_2$-$C_2H_4$-$COO^-$), contained a quaternary ammonium group and a terminal carboxylate group, separated by 2 methylene groups. No retention of analyte anions was observed using $NaHCO_3$ eluents (at pH 8.47) [11], unlike the results obtained when a similar eluent was used in conjunction with a sulfobetaine-type zwitterionic stationary phase [12]. This was assumed to be due to the strong repulsive effects of the terminal carboxylic acid group at this eluent pH value. Upon switching to the use of dilute acid solutions (e.g. 1.0 mM H_2SO_4) as eluents, the column exhibited very strong retention of the inorganic anions examined [11]. However, this zwitterionic surfactant was not an ideal carboxybetaine for use in ZIC systems, as it contains an additional polar functional sulfonylamido group, which is affected by strong polarisation from the heptadecafluorooctyl radical, which, in turn, could have an effect on the ion-exchange properties of the resulting substrate.

The objective of this Chapter was to investigate whether a carboxybetaine-type surfactant, with a simpler structure than that used by Hu *et al.* [11], could be utilised to produce a dynamically modified zwitterionic ion-exchanger, which would show anion-exchange characteristics under acidic pH conditions, and would enable retention to be lengthened or shortened, as required, through altering eluent pH. It was also envisaged that the application of the developed chromatographic system to the analysis of "real" environmental water samples of high salinity would be possible.

2.2 Experimental

2.2.1 Instrumentation

The chromatographic system used was a Dionex Model DX-100 Chromatograph (Dionex, Sunnyvale, CA, USA), fitted with a 20 µl injection loop, and coupled to a Shimadzu SPD-6AV UV-Vis Spectrophotometric Detector (Kyoto, Japan),

monitoring at 214 nm. The pH of eluents was measured using an Orion Model 420 pH meter (Thermo Orion, Beverly, MA, U.S.A.) with a glass electrode. Processing of chromatograms was carried out using a PeakNet 6.30 chromatography workstation (Dionex, Sunnyvale, CA, U.S.A.).

2.2.2 Reagents

The carboxybetaine-type zwitterionic surfactant used to dynamically modify the stationary phase was dodecyldimethylaminoacetic acid ($C_{12}H_{25}N(CH_3)_2CH_2COOH$), and was synthesised in-house by Prof. Pavel N. Nesterenko according to a procedure by Balykova *et al.* [13], involving the carboxymethylation of dimethyldodecylamine. Dimethyldodecylamine ($CH_3(CH_2)_{11}N(CH_3)_2$) was heated in vacuo at 100° C for 30 min. 10 ml of methanol was added, and the resulting mixture heated to boiling, and then stirred for a further 30 min. An identical number of moles of chloroacetic acid ($ClCH_2COOH$), in 10 ml of methanol, was added dropwise to the mixture of dimethyldecylamine and methanol, yielding dodecyldimethylaminoacetic acid.

All other chemicals used were of analytical reagent grade, and were supplied by Sigma-Aldrich (Tallaght, Dublin, Ireland). All eluents and standard solutions were prepared using deionised water from a Millipore Milli-Q water purification system (Bedford, MA, U.S.A.), and were filtered through a 0.45 μm filter and degassed by sonication. Dilute solutions of NaOH and HCl were used to adjust eluent pH.

2.2.3 Column Preparation

The particle-packed separation column was prepared by dynamically modifying a SUPELCOSIL reversed-phase C_{18} column (250 x 4.6 mm I.D.; 5 μm particle size, obtained from Supelco, Belafonte, PA, U.S.A.) with the carboxybetaine surfactant, by passing 100 mL of a 20 mM aqueous solution of the surfactant through the column at a flow-rate of 1.0 mL/min for a period of greater than 60 minutes. As previously mentioned, the concentration of the zwitterionic surfactant in the column coating solution is of little importance, as the amount of surfactant adsorbed onto the column will be the same, once a certain saturation point has been reached [6]. Following initial modification, the columns were then conditioned with eluents until a steady baseline was achieved.

One of the disadvantages of dynamically modified columns in ZIC is the need for constant regeneration of the zwitterionic stationary phase, as stability will be affected by the loss of functional moieties from the dynamically attached coating. Therefore, in order to stabilise and maintain a constant amount of the carboxybetaine-type surfactant on the surface of the stationary phase, all of the eluents used contained 0.2 mM of the surfactant. This maintained surface coverage, and stopped any potential ion-exchange capacity drop-off due to column bleed. Day-to-day reproducibility was less than 5% RSD of analyte retention times, using eluents incorporating the zwitterionic surfactant.

2.3 Results and Discussion

2.3.1 Effect of Electrolyte Additives to the Eluent

A simple inorganic salt (KCl) was used to evaluate the effect of electrolyte concentration upon anion retention and peak efficiency using the carboxybetaine-functionalised column. The test anions chosen were bromide, iodide, nitrate, and nitrite, as they all exhibit reasonably high absorptivity at a wavelength of 214 nm, while the determination of all of four anions listed is of importance in the analysis of environmental samples, such as seawater samples.

The concentration of KCl in the eluent was varied from 10 to 600 mM KCl, while the concentration of carboxybetaine in the eluent was kept constant, at 0.2 mM. The retention times and peak efficiencies for bromide, iodide, nitrate and nitrite were determined for each concentration of KCl prepared. The effect of the ionic strength of the eluent on anion retention can be seen in Fig. 2.2. The plots of log k vs. log [KCl] on display in Fig. 2.2 were found to be linear, with R^2 values of 0.9867 for nitrite, 0.9845 for bromide, 0.9953 for nitrate and 0.9897 for iodide. As was expected, increasing the amount of KCl present in the eluent, lead to a decrease in the retention observed for all analyte anions, due to increased competition for the ion-exchange sites of the zwitterionic stationary phase. While the observed order of retention (nitrite < bromide < nitrate < iodide) was identical to that of conventional ion-exchange chromatography [14], the slope of each plot (with respective values of –0.6672, -0.6195, -0.6810 and –0.6165 for nitrite, bromide, nitrate and iodide) was significantly less than the expected slope of –1, which is usually the case for a simple ion-exchange

mechanism using a singly charged eluent ion, where the slope of the resulting plot should equal the value calculated from dividing the charge of the analyte anion by the charge of the eluent anion [15], as in eqn. 2.1 below:

$$\log k = \text{Constant} - (z_A / z_E) \log c_E \qquad \text{(Eqn. 2.1)}$$

where z_A and z_E respresent the charges of the analyte ion and eluent ion respectively, and c_E represents the concentration of the eluent counterion.

The proposed reason for the slope of the plots in Fig. 2.2 not being close to –1 in value is that there are 2 effects occurring simultaneously when using electrolytic eluents. Firstly, the addition of small amounts of KCl to the eluent employed results in some increase of ion-exchange capacity of the zwitterionic stationary phase, as this results in the eradication of intra- and inter-molecular salt structures of the carboxybetaine, which exist in low ionic strength eluents between oppositely charged functional groups. Secondly, however, increasing the concentration of the eluent electrolyte brings about the anticipated decrease in retention, in accordance with simple ion-exchange theory, as mentioned previously. The combination of these 2 processes has the overall result of the effect of eluent electrolyte concentration upon analyte anion retention being smaller than that expected for simple ion-exchange. Further study of Fig. 2.2 indicated that the plotted retention data showed a slight deviation in linearity at higher eluent KCl concentrations (> 400 mM KCl), e.g. the slopes of the plots for bromide and iodide begin to become more level above 400 mM KCl. These deviations from linearity suggest that, at these elevated eluent concentrations, there is the possibility that the adsorbed zwitterionic surfactant molecules have reached the point where they are fully opened out, with no intra- or inter-molecular interactions remaining.

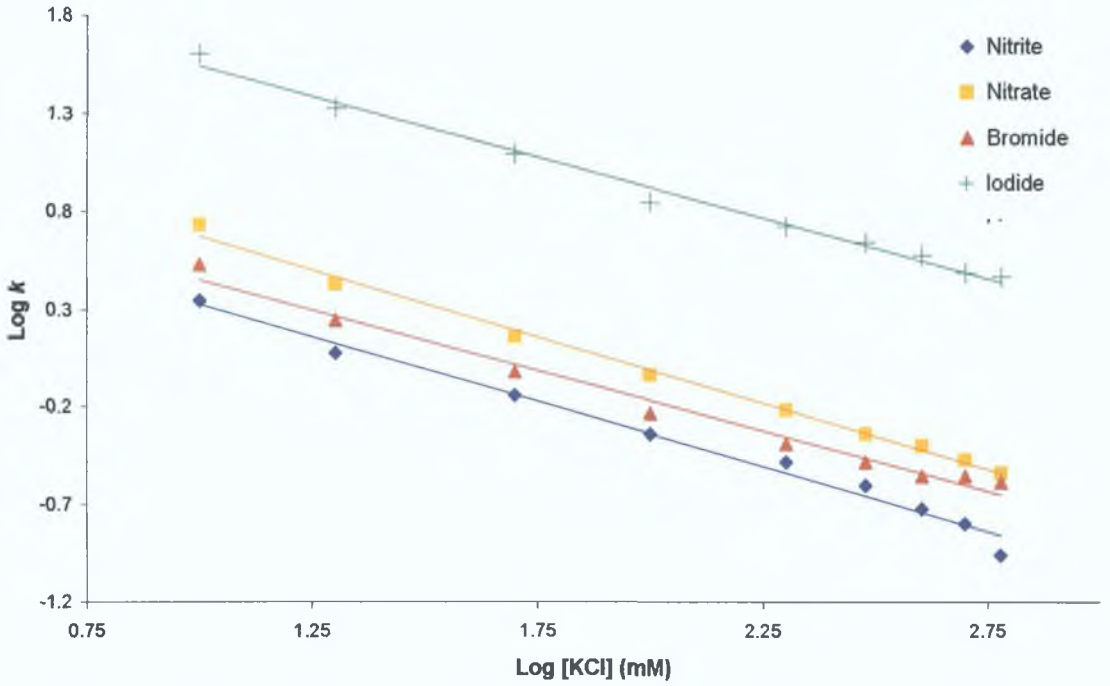

Figure 2.2. Effect of KCl eluent concentration on retention factor (k) for the 25 cm carboxybetaine-modified particle-packed C_{18} column, using a flow rate of 0.5 mL/min, and an injection volume of 20 µl. Direct UV detection was employed at 214 nm. Other eluent conditions: 0.2 mM dodecyldimethylaminoacetic acid. Samples injected: 1.0 mM individual anion standards.

Increasing the KCl concentration of the eluent also had an effect on the observed separation efficiency of the zwitterionic stationary phase. A plot of the number of theoretical plates, N, vs. eluent concentration, as shown in Fig. 2.3, demonstrated how efficiency improved considerably (i.e. displayed higher values for N) between 10 mM and 100 mM KCl, with the variations in peak efficiency becoming less significant at salt concentrations in excess of 100 mM, as the calculated values for N were seen, in general, to level off using ionic strengths of 100 to 600 mM.

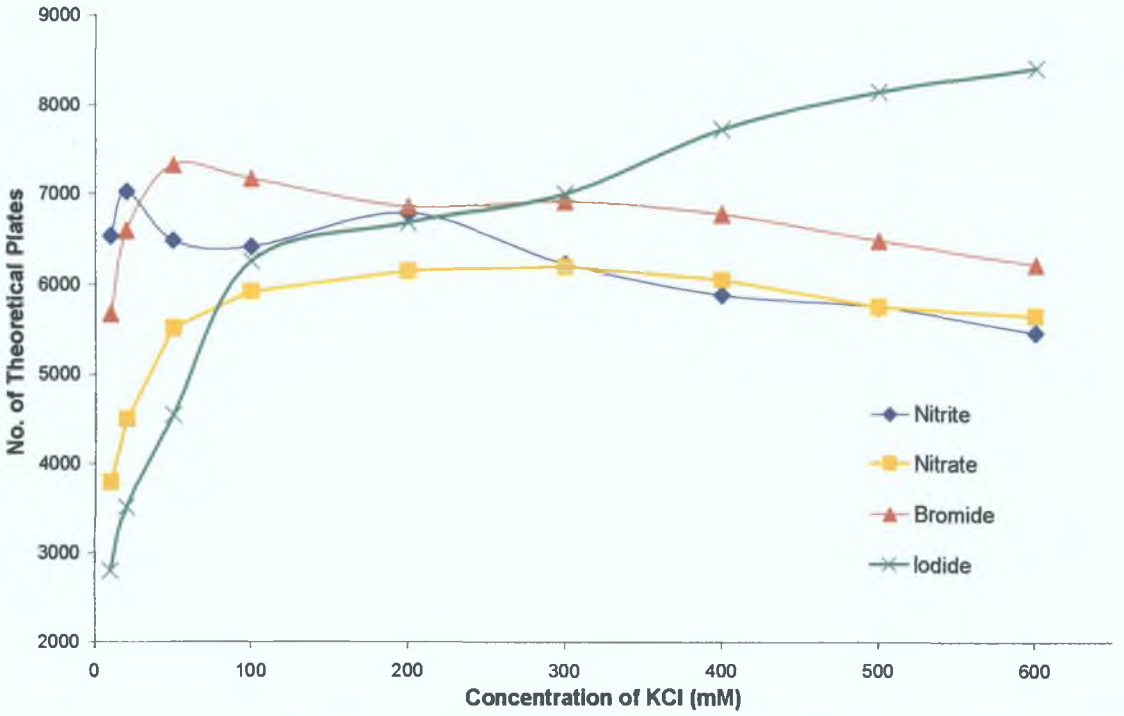

Figure 2.3. Effect of eluent KCl concentration on peak efficiency using a 25 cm carboxybetaine-modified particle-packed C_{18} column, with a flow rate of 0.5 mL/min, and an injection volume of 20 µl. Direct UV detection was employed at 214 nm. Other eluent conditions: 0.2 mM dodecyldimethylaminoacetic acid. Samples injected: 1.0 mM individual anion standards.

The general trend observed in Fig. 2.3 was that higher ionic strength eluents produced more efficient peak shapes, compared to the lower ionic strength eluents. As for the observed effect of eluent ionic strength on retention, the improvements in efficiency that occurred at elevated eluent concentrations can be attributed to structural changes of the carboxybetaine molecules bound to the surface of the C_{18} phase. It is likely that, at low ionic strength, the carboxybetaine molecules arrange themselves as:

(a) Simple intra-molecular salts (although this arrangement will be the least favoured, as the single methylene group connecting the positively charged and the negatively charged functional groups confers the molecule with a degree of inflexibility which would discourage this type of structural arrangement),

(b) Simple inter-molecular salts, or

(c) Micelles.

In practice, however, the carboxybetaine molecules bound to the C_{18} substrate may contain a mixture of all 3 structural assemblies mentioned, which may give rise to

poor ion-exchange kinetics. Increasing the electrolytic concentration of the eluent would eliminate these molecular salt formations of the surfactant molecules, thus resulting in superior ion-exchange kinetics, leading to an increase in the observed peak efficiency. Fig. 2.3 indicates that the eluent KCl concentration at which these salt formations are eradicated is between 50 and 100 mM, as, in general, eluent concentrations greater than this did not result in changes in peak efficiency as significant as those observed at eluent KCl concentrations below 100 mM, resulting in a flatter distribution of data points, compared to the steeper incline of the data points generated below 50-100 mM KCl.

An eluent KCl concentration of between 100 and 200 mM was established as being that most suitable for practical applications, as the use of such an eluent composition resulted in excellent separation of all four inorganic anions tested, without resulting in excessively long run times (e.g. using 100 mM KCl as eluent, with a flow rate of 0.5 mL/min, all four test anions eluted within 7.5 min). The same eluent concentration also provided values for N that were near enough to the highest observed values for nitrite, bromide, and nitrate, but not for iodide, which exhibited optimum peak efficiency at the highest experimental ionic strength of 600 mM.

2.3.2 Effect of Eluent pH

It has already been demonstrated that the strong affinity of the negatively charged carboxylate groups of a carboxybetaine-type zwitterionic surfactant for H^+ ions exerts a major influence on the retention behaviour of anions [11]. This suggests that eluent pH can be utilised to control the degree of protonation of the weak carboxylic group, thus enabling the adjustment of anion retention through eluent conditions. Reducing the number of dissociated carboxylate groups reduces the electrostatic repulsion experienced by analyte anions, thus affording them easier access to the quaternary ammonium site of the zwitterionic surfactant molecule. In other words, lower eluent pH values will result in an increase in the effective anion-exchange capacity. However, for all experiments carried out for this Chapter of work, the dodecyldimethylaminoacetic acid was included as a minor component of the eluent, as well as having been pre-coated onto the stationary phase, in order to facilitate the stabilisation of the zwitterionic coating. This means that any increase in retention caused by decreasing the eluent pH could be partially offset by the increase in the

attraction between the analyte anions and the protonated carboxybetaine present in the eluent. To further investigate this effect, the pH of an eluent comprised of 150 mM KCl, also containing 0.2 mM of the carboxybetaine surfactant, was systematically varied over the pH range 3.5 to 6.5 ($n = 7$), and the retention times of nitrite, bromide, nitrate and iodide determined at each pH value. The results of this pH study can be seen in Fig. 2.4.

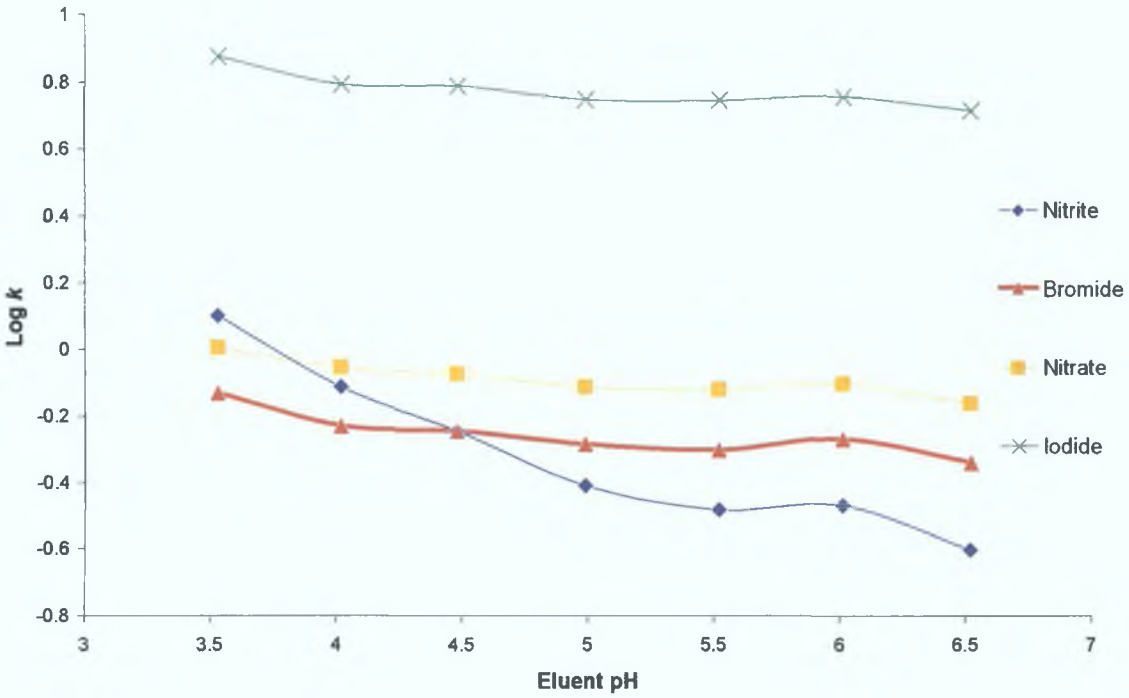

Figure 2.4. Effect of eluent pH upon retention factor (k) for a 25 cm carboxybetaine-modified particle-packed C_{18} column, using an eluent comprised of 150 mM KCl, and containing 0.2 mM dodecyldimethylaminoacetic acid, with a flow rate of 0.5 mL/min, and an injection volume of 20 µl. Direct UV detection was employed at 214 nm. Samples injected: 1.0 mM individual anion standards.

The results outlined in Fig. 2.4 show that the pH of the eluent had a similar effect on bromide, nitrate and iodide, with increased pH causing a subsequent decrease in retention, as anticipated. However, the extent of the effect is considerably less than the effect shown by other investigations into ZIC using a carboxybetaine-type surfactant, where the slopes for log k vs. eluent pH were approx. –0.83 for nitrite, bromide, nitrate, iodide and thiocyanate [11], across a pH range of 5.0 to 5.6, compared to slopes from Fig. 2.4 ranging from –0.0421 to –0.0536 for bromide, nitrate and iodide, with iodide being most affected. The pH study presented here was carried out across a wider range, i.e. from pH 3.5 to pH 6.5. This difference in the pH

effect suggests that the effect of the carboxybetaine being present in the eluent is relatively large, compared to a carboxybetaine-based chromatographic system where the zwitterionic surfactant was only present as a stationary phase coating, as was the case for Hu *et al.* [11].

A further point of interest is the non-linear behaviour of the nitrite ion. As is evident from Fig. 2.4, nitrite had a similar slope to bromide, nitrate and iodide at eluent pH values greater than ~ pH 5 only. At lower pH values nitrite retention increased far more rapidly than for the other test anions, thereby changing the elution order (i.e. from nitrite < bromide < nitrate at pH 6.5, to bromide < nitrate < nitrite at pH 3.5) simply by adjusting the acidic content of the eluent. The reason for this is as follows: For the carboxybetaine-modified column conditioned with an acidic eluent, a binary-EDL (electrical double layer) is formed from the eluent ions (which in this case were chloride and potassium) as well as hydronium ions (H^+). Therefore, one of the factors controlling the elution order of sample anions is the stability of the H^+-anion ion-pair in the binary-EDL. Based on their respective pK_a values, H^+-NO_2^- (pK_a ~ 3.15) is more stable than H^+-Br^- (pK_a ~ -9) and H^+-NO_3^- (pK_a ~ -1.5), and therefore nitrite is retained for longer, compared to bromide and nitrate, at very acidic eluent pH values. Increasing the acid content of the eluent also produces a denser binary-EDL (because of the hydronium ions), which increases the probability of formation of H^+-NO_2^- (i.e. nitrous acid), which also accounts for the longer retention of nitrite [16]. This effect may prove to be quite useful in the determination of nitrite in high ionic strength environmental matrices, such as seawater samples, where nitrite is often incompletely separated from the high concentration of chloride matrix ions. This potential benefit of the change in the order of elution will be investigated further in Chapter 3.

During the study into the effect of eluent pH upon retention, it was also noted that, as with eluent concentration, pH also had quite a significant impact on peak efficiencies (see Fig. 2.5). Peak efficiencies generally increased up to around pH 5 to pH 6, and then decreased sharply when the eluent pH was increased to pH 6.5. The maximum efficiency for all 4 anions was observed using an eluent pH of approx. pH 6, which is above the expected pK_a of the carboxylic acid group, which was anticipated would be between pH 4 and pH 5. The expected reason for this observed trend is that for an adsorbed zwitterion, which contains a weak acid site, the protonation and

deprotonation of that weak acid site would again result in a physical change in the orientation of the absorbed molecule, although the fact that the eluent used in Fig. 2.5 contained 150 mM KCl (which would limit the formation of inner salts) means that the exact cause for this behaviour has not been ascertained. The effect of eluent pH on the non-adsorbed surfactant molecules present in the eluent may also have an impact on analyte peak efficiencies.

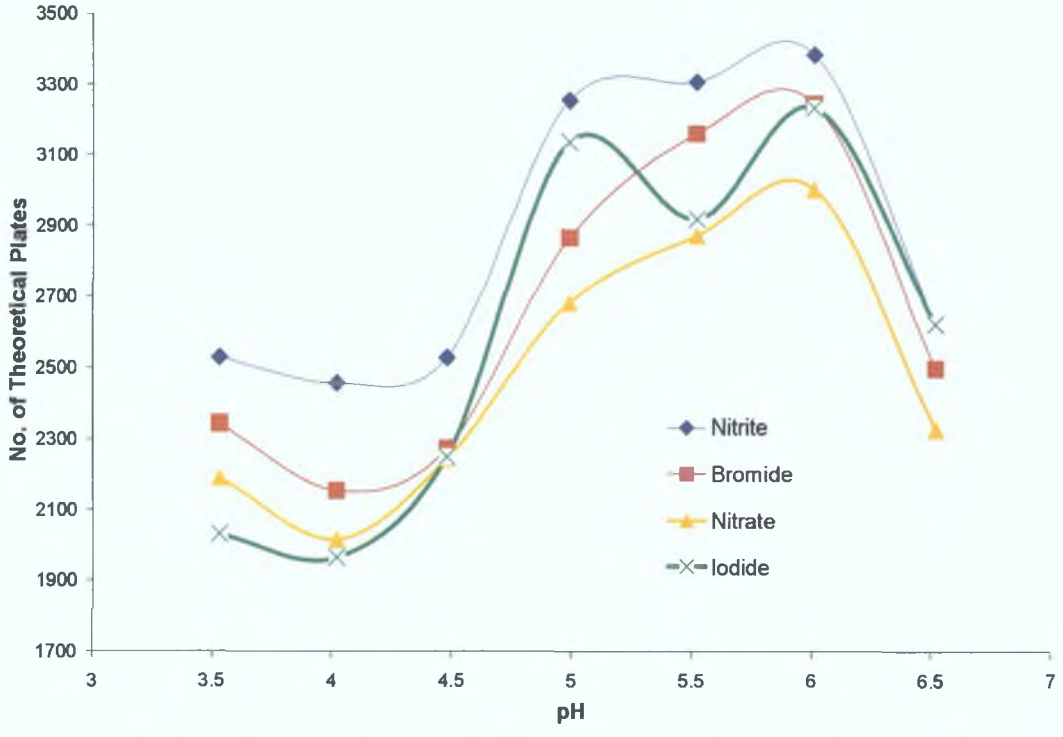

Figure 2.5. Effect of eluent pH upon efficiency for a carboxybetaine-modified 25 cm particle-packed C_{18} column, using an eluent comprised of 150 mM KCl, and containing 0.2 mM dodecyldimethylaminoacetic acid, with a flow rate of 0.5 mL/min, and an injection volume of 20 µl. Direct UV detection was employed at 214 nm. Samples injected: 1.0 mM individual anion standards.

2.3.3 Separation Achieved Under Optimal Conditions

It was concluded from Figs. 2.2 and 2.3 that the presence of 150 mM KCl in the eluent provided the optimum separation and resolution of all 4 anions of interest (nitrite, bromide, nitrate and iodide). The previously detailed pH study suggested that the optimum eluent pH was ~ pH 6, as this resulted in the highest observed number of theoretical plates for all 4 test anions (i.e. N = 3386 for nitrite, 3245 for bromide, 3003 for nitrate, and 3235 for iodide). A sample chromatogram displaying the separation achieved under these optimal conditions can be seen in Fig. 2.6, from which it is clear

that baseline resolution of all analyte anions was achieved, with efficient peak shapes. Resolution of nitrite and bromide was found to be equal to 1.5, while for bromide and nitrate, and nitrate and iodide, resolution was of the order of 2.9 and 22.0 respectively. Values for HETP varied from 74 μm (for nitrite) to 83 μm (for nitrate).

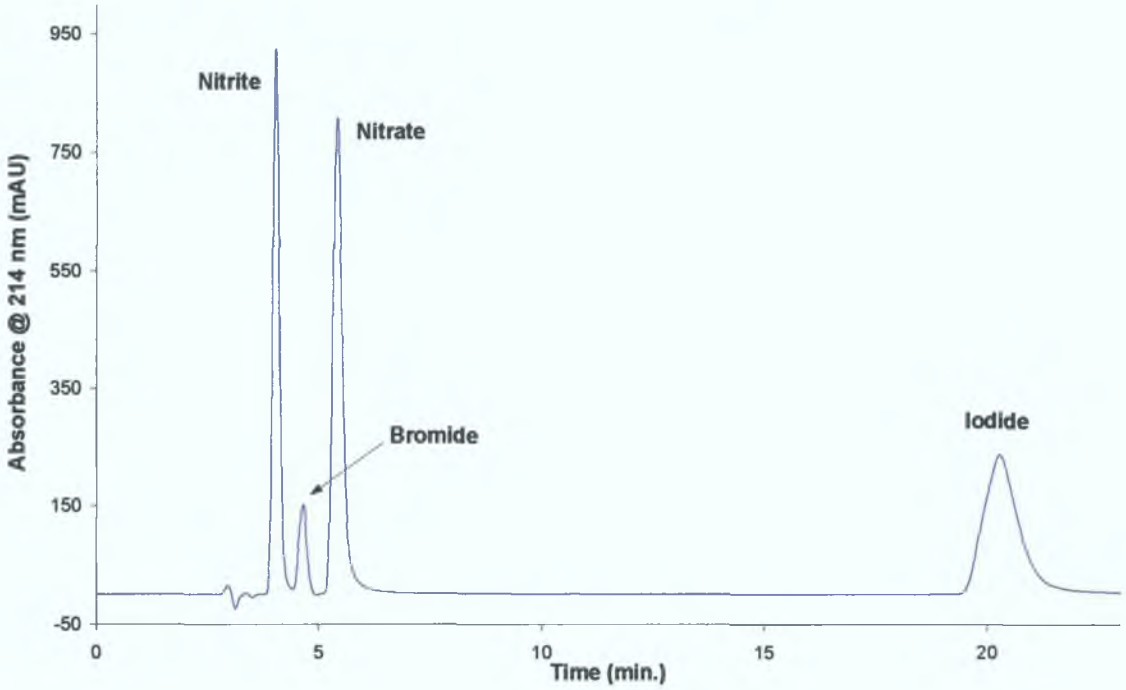

Figure 2.6. Chromatogram illustrating the separation of 1.0 mM mixture of nitrite, bromide, nitrate and iodide obtained using a 25 cm carboxybetaine-modified particle-packed C_{18} column, with an eluent consisting of 150 mM KCl in 0.2 mM dodecyldimethylaminoacetic acid, at pH 6, and a flow rate of 0.5 mL/min. Wavelength of detection: 214 nm.

2.3.4 Application to the Analysis of Nutrients in Seawater Samples

The determination of inorganic anions in seawater is of great importance for a variety of reasons, particularly for environmental purposes. Bromide is the major chemical that reacts with "residual chlorine" in seawater, and so the toxic and kinetic behaviours of chlorine in seawater is assessed and investigated by the determination of bromide levels [17]. Iodide determination in seawater is often undertaken, as iodine is the most abundant biophilic minor element in the oceans [18], playing critical roles in biologically and inorganically mediated oxidation/reduction reactions in the marine environment. Nitrate and nitrite determination in seawater is also of importance for oceanographic studies, as both are biologically active species and

essential nutrients for autotrophic and heterotrophic organisms in marine ecosystems [16].

Ion chromatography is the most effective and convenient method for the separation and determination of ions, especially inorganic anions. However, the elevated concentrations of matrix ions, such as chloride ions, in saltwater samples has many inherent challenges for analytical chemists, e.g. if the ionic strength of an IC sample matrix is too high, the matrix ions swamp the available ion-exchange sites of the stationary phase (in a process known as self-elution), which has a serious effect on separation efficiency [19]. This often necessitates the employment of complicated pretreatment techniques to overcome these difficulties. On-line matrix-eliminating IC [20,21] has also been used for the analysis of nitrite, nitrate and iodide ions in seawater. This is a technique whereby a high ionic strength solution, e.g. artificial seawater, is used as the eluent. For seawater analysis, the stationary phase is equilibrated with matrix ions present in the eluent, before any sample injections are performed. Therefore, the matrix ions present in the sample injected (i.e. high concentrations of chloride ions) display little retention, thus minimising their interference in the determination of other analyte anions. The use of such eluents, however, requires a non-metallic LC system, because of the corrosive effects of high concentrations of chloride etc. The use of such an eluent can also result in peak broadening, and reduced separation efficiency.

Zwitterionic ion chromatography has proven to be highly tolerant towards high ionic strength samples [7,16,17,18,22,23], as detailed in Chapter 1, Section 1.3.8.1. Here, it was intended to develop a method for the analysis of nitrate and nitrite ions in saline samples using the carboxybetaine-modified stationary phase introduced in Sections 2.3.1 and 2.3.2. The first action undertaken was to prepare an artificial seawater sample with a chloride concentration of 0.52 M, which is analogous to the actual chloride concentration of "real" seawater. The concentration of bromide present was 50 ppm, while nitrate and nitrite levels were varied from 0.1 to 10 ppm. These pseudo-seawater samples were then injected directly onto the column and analysed using 150 mM KCl, with 0.2 mM carboxybetaine, at pH 6, as the eluent. The resulting chromatograms, a typical example of which can be seen in Fig. 2.7, showed clear baseline resolution of nitrite, bromide and nitrate, which were well separated from the

chloride matrix signal, although, as is clear from Fig. 2.7, peak efficiency was adversely affected by the elevated ionic strength of the sample matrix, as the values for N for nitrite, bromide and nitrate decreased to 1185, 1147 and 1190, from 3386, 3245 and 3003 (for sample standard solutions prepared in Milli-Q water alone) respectively.

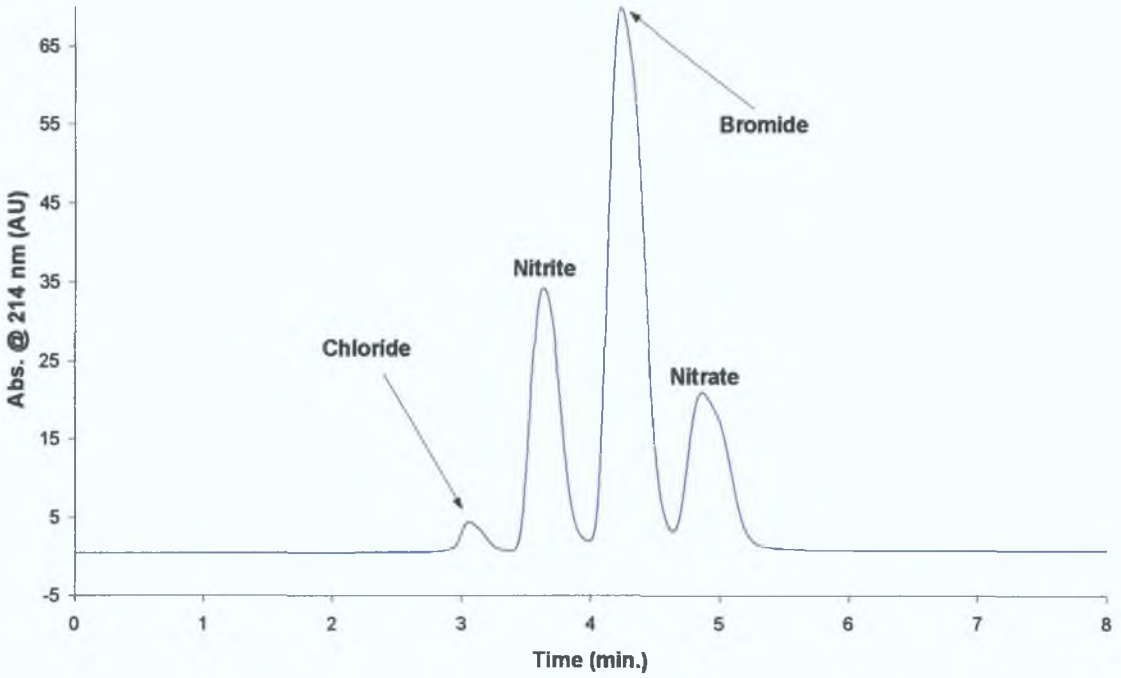

Figure 2.7. Chromatogram of a pseudo-seawater sample (consisting of 2.0 ppm nitrate and nitrite, and 50 ppm bromide in a 0.52 M NaCl sample matrix) obtained using a 25 cm carboxybetaine-modified particle-packed C_{18} column, with 150 mM KCl at pH 6.02 (with 0.2 mM dodecyldimethylaminoacetic acid) as the eluent. Flow rate: 0.5 mL/min. Wavelength of detection: 214 nm.

Linearity plots for nitrate and nitrite, in a 0.52 M NaCl matrix, were constructed, and can be seen in Figs. 2.8 (a) (assembled using peak area values) and (b) (assembled using peak height values). The plots of peak area and peak height vs. nitrate/nitrite concentration were satisfactorily linear, with R^2 values of 0.9964 for both nitrate and nitrite using the peak area method, and R^2 values of 0.9978 and 0.9979 for nitrate and nitrite respectively using the peak height data. The limits of detection for nitrate and nitrite in the artificially prepared seawater matrix were determined to be approx. 11 ppb and 8 ppb respectively.

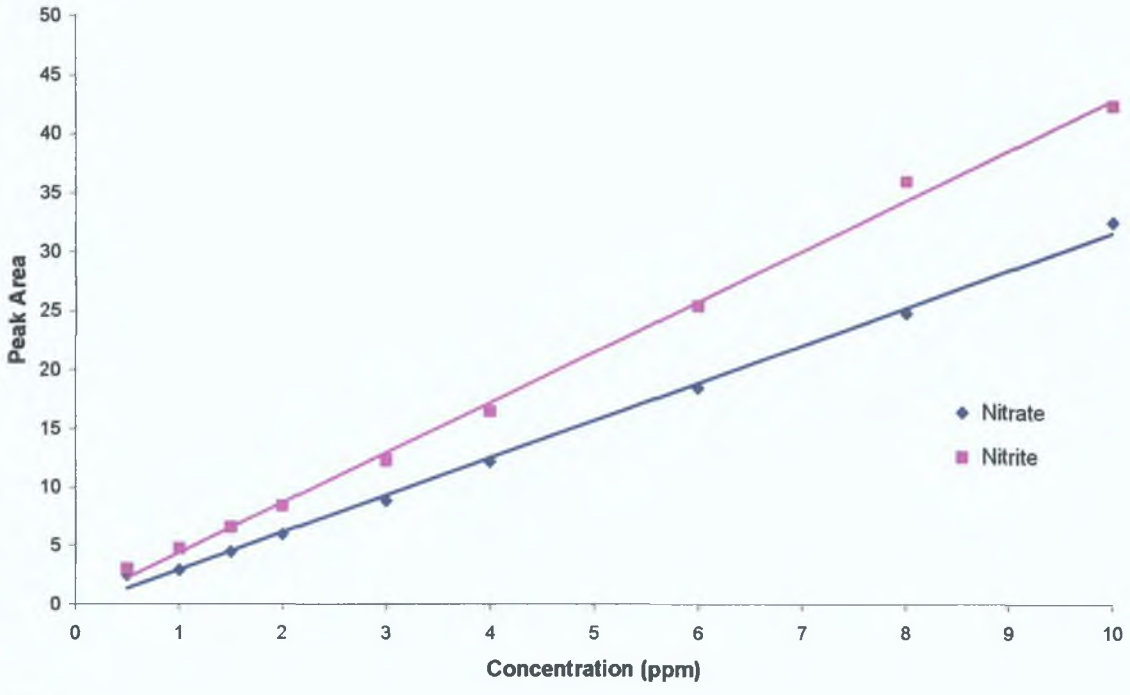

(a)

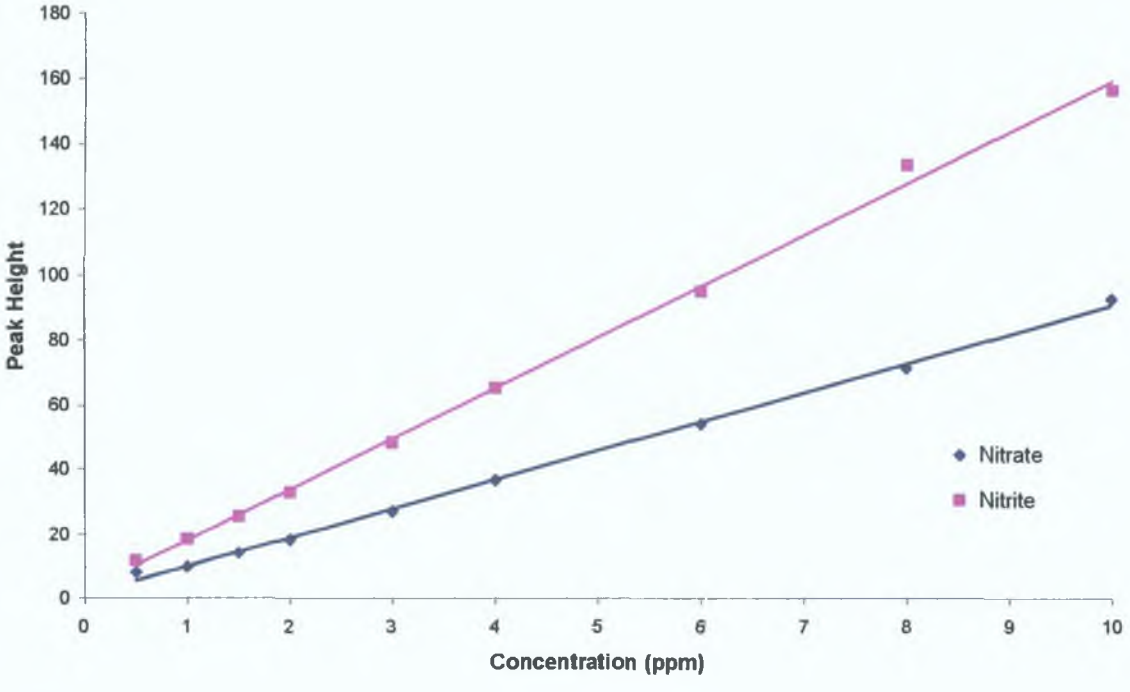

(b)

Figure 2.8. Plots of (a) peak area, and (b) peak height, vs. concentration of nitrate and nitrite present in a 0.52 M NaCl pseudo-seawater sample matrix. Data obtained using an eluent composed of 150 mM KCl at pH 6, also containing 0.2 mM dodecyldimethylaminoacetic acid. Flow rate: 0.5 mL/min. Wavelength of detection: 214 nm. Column details: 25 cm carboxybetaine-modified particle-packed C_{18} column.

Several "real" water samples were then taken from various coastal and estuarine areas in the greater Dublin area. One such seawater sample, taken off the coast of Portmarnock, Co. Dublin, can be seen in Fig. 2.9. Peaks for chloride, bromide, and nitrate, as well as a trace nitrite peak, are clearly visible. It was also observed that peak efficiencies were far superior to those calculated for the pseudo-seawater samples (as in Fig. 2.7), as the calculated values for N for bromide and nitrate for the chromatogram in Fig. 2.9 were (at 6164 and 7564 for bromide and nitrate respectively) far greater than those for the pseudo-seawater sample in Fig. 2.7 (1147 and 1190 respectively). This indicates that carboxybetaine-modified stationary phases are highly tolerant of the saltwater matrix, as separation efficiency remained very high, even for undiluted samples.

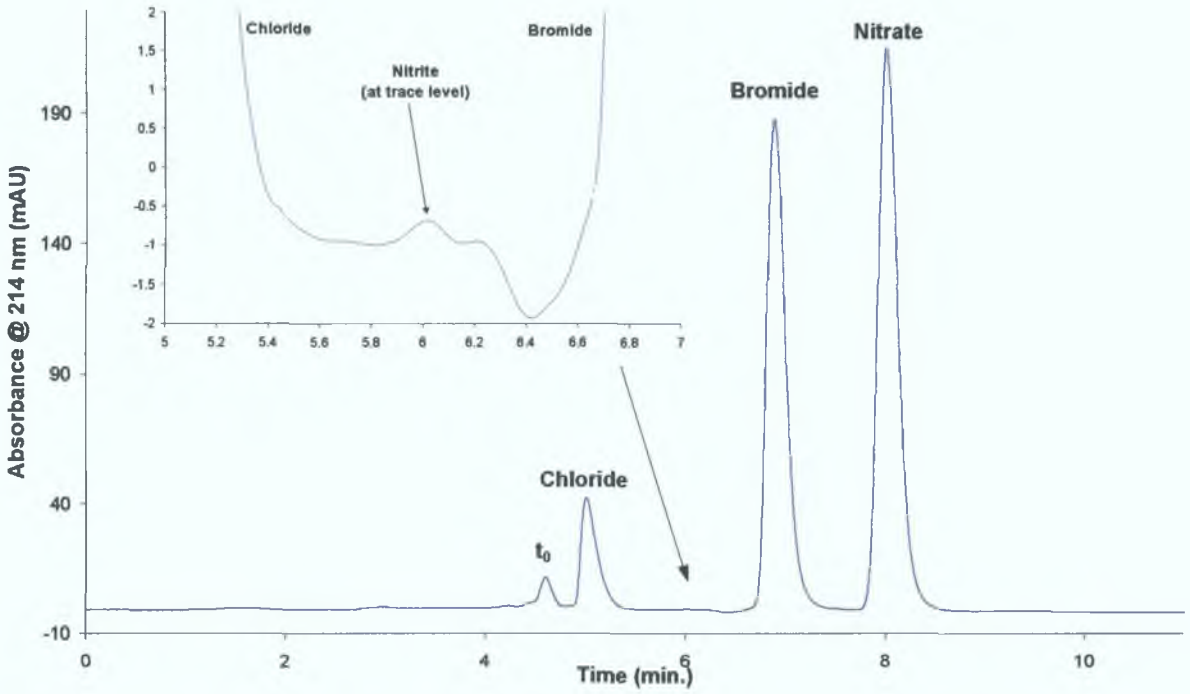

Figure 2.9. Chromatogram of an undiluted seawater sample, taken at Portmarnock, Co. Dublin, analysed using a 25 cm carboxybetaine-modified particle-packed C_{18} column. Eluent: 150 mM KCl, 0.2 mM dodecyldimethylaminoacetic acid, pH 6. Flow rate: 0.5 mL/min. Wavelength of detection: 214 nm.

Analysis of the nitrate content of the coastal and estuarine water samples was carried out using standard addition (n = 5, with nitrate concentrations of 0 – 100 ppm). The R^2 values for the standard addition curves ranged from 0.9934 to 0.9993. For the coastal water sample displayed in Fig. 2.9, the concentration of nitrate present was

found to be 6.51 ppm. The highest observed nitrate concentration was that of an estuarine sample taken on the outskirts of Portmarnock, Co. Dublin, which was found to have 629 ppm of nitrate present, although this concentration of nitrate was beyond the maximum nitrate standard concentration investigated. This was an extremely elevated concentration of nitrate for such a water sample, and may be attributed to the presence of large amounts of human and animal waste matter from temporary settlements further upriver. Another possible source of nitrate pollution is the leaching of nitrates from nearby agricultural lands, although the high nitrate levels may also reflect input from local sewage effluent points.

2.4 Conclusions

Carboxybetaine-modified C_{18} columns have been shown to exhibit unique anion-exchange selectivity, which differs to that seen previously with alternative zwitterionic surfactant-modified stationary phases, such as sulfobetaine-modified columns etc. Ion-exchange capacity and efficiency have been demonstrated to be dependent upon eluent pH and eluent electrolyte concentration, both of which provide new options for the manipulation of analyte retention. The optimal eluent conditions, in terms of resolution, total runtime and peak efficiency, were found to be a KCl concentration of 150 mM, and an eluent pH of 6. The applicability of the carboxybetaine-modified stationary phase to the analysis of saline samples, without any need for pretreatment or dilution of the saltwater matrix, was also illustrated.

References:

1 W. Hu, T. Takeuchi, H. Haraguchi, Anal. Chem. 65 (1993) 2204–2208.

2 P. Wydro, M. Paluch, Journal of Colloid and Interface Science 286 (2005) 387-391.

3 H.I. Leidreiter, B. Grüning, D. Kaseborn, International Journal of Cosmetic Science 19 (1997) 239-253.

4 E.S. Basheva, D. Ganchev, N.D. Denkov, K. Kasuga, N. Satoh, K. Tsujii, Langmuir 16 (2000) 1000-1013.

5 K.D. Danov, S.D. Kralchevska, P.A. Kralchevsky, K.P. Ananthapadmanabhan, A. Lips, Langmuir 20 (2004) 5445-5453.

6 T. Umemura, S. Kamiya, A. Itoh, K. Chiba, H. Haraguchi, Anal. Chim. Acta 349 (1997) 231-238.

7 W. Hu, P.R. Haddad, K. Hasebe, K. Tanaka, P. Tong, C. Khoo, Anal. Chem. 71 (1999) 1617-1620.

8 H.A. Cook, W. Hu, J.S. Fritz, P.R. Haddad, Anal. Chem. 73 (2001) 3022-3027.

9 E. Twohill, B. Paull, J. Chrom. A 973 (2002) 103-113.

10 H.A. Cook, G.W. Dicinoski, P.R. Haddad, J. Chrom. A 997 (2003) 13-20.

11 W. Hu, P.R. Haddad, K. Tanaka, K. Hasebe, Anal. Bioanal. Chem. 375 (2003) 259-263.

12 W. Hu, K. Tanaka, K. Hasebe, Analyst 125 (2000) 447-451.

13 L.A. Balykova, A.F. Sobol, V.E. Limanov, L.M. Vorontsova, E.K. Skvortsova, Khimiko-Farmatsevticheskii Zhurnal 3 (1969) 23-26.

14 Ion Chromatography, J.S. Fritz, D.T. Gjerde, 3rd edition 2000, published by Wiley-VCH, Weinheim, Germany.

15 J. Ståhlberg, Anal. Chem. 66 (1994) 440-449.

16 W. Hu, K. Hasebe, M. Ding, K. Tanaka, Fresenius J. Anal. Chem. 371 (2001) 1109 -1112.

17 W. Hu, S. Cao, M. Tominaga, A. Miyazaki, Anal. Chim. Acta 322 (1996) 43-47.

18 W. Hu, P. Yang, K. Hasebe, P.R. Haddad, K. Tanaka, J, Chrom. A 956 (2002) 103-107.

19 W. Bashir, B. Paull, J. Chrom. A 907 (2001) 191-200.

20 K. Ito, Y. Ariyoshi, F. Tanabiki, H. Sunahara, Anal. Chem. 63 (1991) 273-276.

21 K. Ito, J. Chrom. A 830 (1999) 211-217.

22 W. Hu, P.R. Haddad, Anal. Commun. 35 (1998) 317-320.

23 W. Hu, K. Hasebe, P.R. Haddad, K. Tanaka, J. Chrom. A 850 (1999) 161-166.

Chapter 3

Zwitterionic Ion Chromatography Using Carboxybetaine-Modified Monolithic Columns

3.1 Introduction

Higher column efficiencies in HPLC have been achieved by using smaller particles within chromatographic columns, thereby reducing eddy diffusion and allowing faster mass transfer [1]. However, this approach has been severely limited by the inherent pressure limits of conventional HPLC instrumentation (approximately 350 – 400 kg / cm^2) [2]. A compromise has been necessary between the desired column efficiency and the pressure drop of the column. One possible way of achieving this is to adjust the column length. Another way of overcoming the problem of the high pressure drop associated with the use of small particles is to use a monolithic column instead of a particle-packed column. A *monolithic* stationary phase is the continuous unitary porous structure of an adsorbent material (porous silica or polymer), prepared by in situ polymerisation or consolidation inside the column tubing [3]. In contrast to conventional silica-based chromatographic columns, which are packed with particulate materials, monolithic columns are composed of a single piece of porous silica.

While preparations of organic polymer-based (e.g. polymethacrylate and polyacrylamide) monolithic columns were reported as far back as the late 1960s and early 1970s, silica-based monoliths were not introduced until 1996 [4,5]. The favoured method of synthesis of silica-based monoliths involved the hydrolytic polycondensation of alkoxysilane, accompanied by phase separation in the presence of water-soluble organic polymers [4,6]. The resulting silica gel is then encased in heat-shrinking poly(tetrafluoroethylene) (PTFE) tubing, and compressed with external pressure to eliminate any void spaces between the silica rod and the tube [4,6].

Monolithic silica columns have a structure consisting of 2 interconnected networks of pores, referred to as macropores (or throughpores) and mesopores [7]. The sol-gel process outlined in the previous paragraph allows independent control of the pore size [4]. The network of macropores provides flow paths through and along the length of the column, and also ensures access of analyte molecules to the entire mesopore network [7]. Comparison of monolithic and particle-packed columns revealed that the macropores can be seen as being the equivalent of the interparticle void volume of the packed columns, which means that the macropores are responsible for the high

external porosity of monolithic columns [8]. This high porosity, and the relatively large average size of the macropores, confers a high degree of permeability on the monolithic column [9], while the mesopores provide the specific surface area of the monolithic columns [7,10]. The most commonly employed silica monolithic columns contain macropores with dimensions of approx. 2 μm, and mesopores of around 13 nm in size [8]. The total porosity of these columns is about 85%, which is approx. 15-20% higher than the porosity of a column packed with 5 μm particles [8]. It is generally regarded that 80% of the total porosity of the monolithic columns (with the total porosity being equal to the sum of the external porosity, from the macroporous structure, and the internal porosity, arising from the mesoporous structure) is due to the macropores, while the mesopore network accounts for 10-15% of the total porosity [7]. Therefore, the external porosity of monoliths is almost double that observed in conventional particle packed columns [8]. In fact, Leinweber and Tallarek have stated that silica monoliths have a permeability equivalent to that of a column packed with 11 μm particles [11].

The high external porosity of monolithic columns means that they exhibit very low column back pressure, even when elevated flow rates are utilised [8]. Fig. 3.1 shows the column back pressure at various flow rates, for a monolithic silica column, and for 2 conventional columns packed with different size particles. This graph demonstrates that the monolithic column had the lowest back pressure at each flow rate investigated, and can therefore be routinely operated at higher flow rates than is usually employed with standard particle-packed columns.

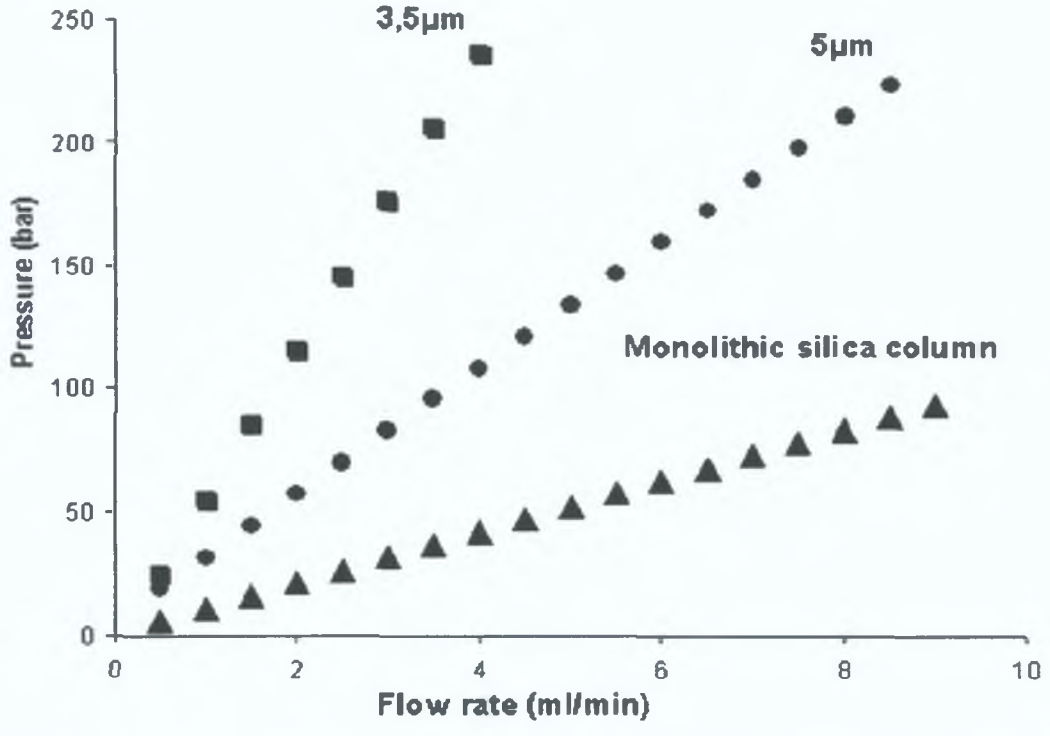

Figure 3.1. Comparison of column back pressure across a range of flow rates (0.5-9.0 mL/min) for a monolithic silica column and conventional columns packed with 3.5 µm and 5 µm particles [Reproduced from ref. 8].

Monoliths also maintain high column efficiencies, even at relatively high linear flow velocities [8]. Fig. 3.2 shows the van Deemter curves for a monolithic silica column, and for conventional particle-packed columns (silica particle size: 3.5 µm and 5 µm). The van Deemter curve for the silica monolith has its lowest point at a theoretical plate height of 8 µm (corresponding roughly to 125,000 N/m), similar to that of the column packed with 3.5 µm particles, while Leinweber and Tallarek found that the performance of monolithic columns is comparable to that of a column packed with 1 µm particles [11]. Even higher column efficiencies could be obtained by connecting several monolithic columns in series, as their inherent high permeability would ensure that the column backpressure would not be a significant deterrent. A further chromatographic property seen with monolithic columns was that retention factors observed using silica monoliths are of the same order of magnitude as for particle packed columns (because the surface area of the mesopores is similar to that of conventional porous particles) [7].

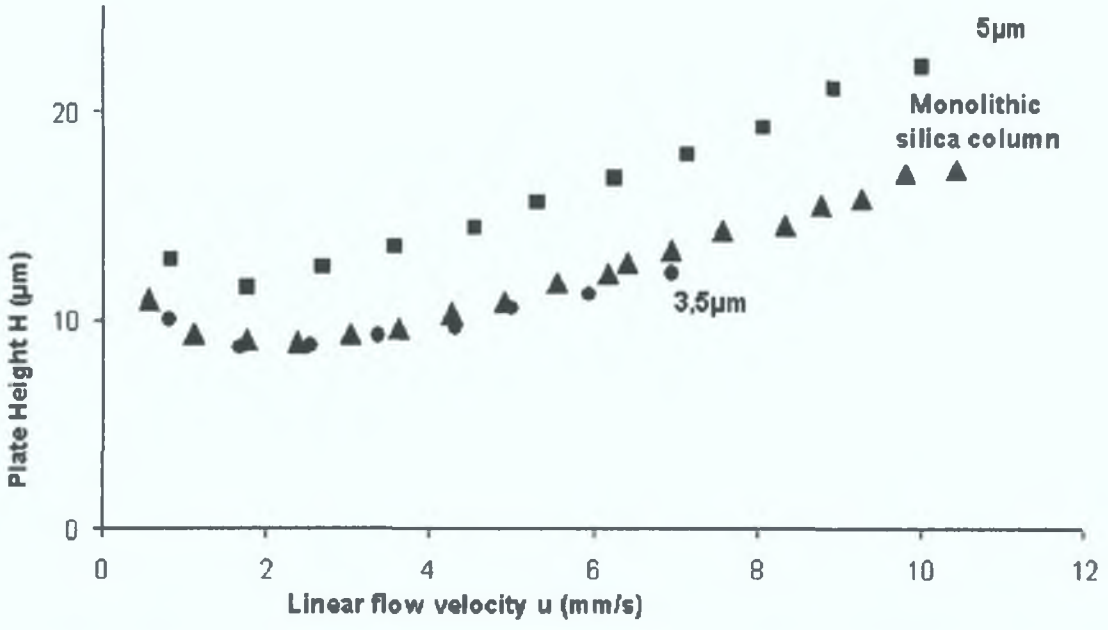

Figure 3.2. Comparison of the van Deemter curves obtained using a monolithic silica column, and columns packed with 3.5 µm and 5 µm particles [Reproduced from ref. 8]. (■ = 5 µm particle packed column, ● = 3.5 µm particle packed column, ▲= monolithic silica column.)

Monolithic columns have been employed by ion chromatographers for the rapid separations of ion mixtures for several years now [12]. Hatsis and Lucy [13] used ion-interaction chromatography on a 5.0 cm silica monolith, with eluent delivery at 16 mL/min. to separate 8 common inorganic anions in less than 15 seconds. Sugrue *et al.* [14] bonded iminodiacetic acid to a 10.0 cm bare silica monolith, and obtained the separation of Mg^{2+} and Ca^{2+} in a 2 M KCl sample matrix within 40 seconds. Hatsis and Lucy [15] reported the separation of a mixture of 7 inorganic anions in approx. 30 seconds, using a 5.0 cm silica monolithic column modified with the ionic surfactant didodecyldimethylammonium bromide (DDAB), utilising a flow rate of 10 mL/min. Xu *et al.* [16] were able to use a 5.0 cm monolithic silica column (modified with lithium dodecylsulphate) for the high-speed determination of acidity, with hydronium ions eluting as a sharp peak prior to elution of other cationic species in less than 1 min, using a flow rate of 1.5 mL/min. Connolly *et al.* [17] also used DDAB to modify a monolithic column (length: 2.5 cm), and found that 8 inorganic anions could be separated in 90 seconds using a moderate flow rate of 4.0 mL/min. Sugrue *et al.* [18] demonstrated the separation of 6 inorganic anions in 105 seconds on a 10.0 cm lysine-bonded bare silica monolith, using a flow rate of 4.9 mL/min.

The aim of the experimental work documented in this Chapter was to use the carboxybetaine-type zwitterionic surfactant dodecyldimethylaminoacetic acid to dynamically modify a silica monolithic column, in order to reduce run times (through the use of higher eluent flow rates) for the separation of common UV-absorbing anions, especially for the well-retained iodide anion. The fact that columns would be monolithic in structure also meant that flow gradient programs could be examined as an additional tool for the decrease of overall times of analysis of analyte anions. It was intended to use these modified monoliths for the rapid analysis of nutrient anions in seawater samples.

3.2 Experimental

3.2.1 Instrumentation

The chromatographic system used was a Dionex Model DX-100 Chromatograph (Dionex, Sunnyvale, CA, USA), fitted with a 20 µl injection loop, and coupled to a Shimadzu SPD-6AV UV-Vis Spectrophotometric Detector (Kyoto, Japan), monitoring at 214 nm. In later work involving flow gradients, an Applied Biosystems 400 Solvent Delivery System (Foster City, CA, U.S.A.) was used to deliver the eluent, while for experiments incorporating pH gradients, a Waters Model 600E Multisolvent Delivery System (Waters, Milford, MA, U.S.A.) was used as the eluent delivery system. The pH of eluents was measured using an Orion Model 420 pH meter (Thermo Orion, Beverly, MA, U.S.A.) with a glass electrode. Processing of chromatograms was carried out using a PeakNet 6.30 chromatography workstation (Dionex, Sunnyvale, CA, U.S.A.).

3.2.2 Reagents

As for Chapter 2, Section 2.2.2.

Phosphate buffer solutions were prepared using monobasic sodium phosphate and dibasic sodium phosphate (Sigma-Aldrich, Tallaght, Dublin, Ireland), and phosphoric acid (85%, Riedel-de Haën, Hanover, Germany) in the appropriate ratios to give the required pH values. Citrate buffer solutions were prepared using citric acid and sodium citrate (both obtained from Sigma-Aldrich, Tallaght, Dublin, Ireland) in the appropriate ratios to give the required eluent pH values.

3.2.3 Column Preparation

The monolithic columns used were Chromolith Performance RP-18e monolithic reversed-phase C_{18} columns (100 mm x 4.6 mm I.D., and 10 mm x 4.6 mm I.D., 2 μm flow through macropores and 13 nm mesopores, obtained from Merck, Darmstadt, Germany). For the initial experiments on the application of pH gradients, the particle-packed column employed was a SUPELCOSIL reversed-phase C_{18} column (250 x 4.6 mm I.D., 5 μm particle size, obtained from Supelco, Belafonte, PA, U.S.A.). The column coating procedure employed was identical to that outlined in Chapter 2, Section 2.2.3. A small amount of the surfactant (0.2 mM) was again added to the eluent composition, as a means of combating column bleed.

3.3. Results and Discussion

3.3.1 Effect of Ionic Strength of Eluent

A 1.0 mM mixture of nitrite, bromide, nitrate, and iodide was analysed using the 10 cm carboxybetaine-coated monolithic column, employing an eluent of the same composition as the previously determined optimum eluent composition for the particulate column (i.e. 150 mM KCl in 0.2 mM carboxybetaine at pH 6). The flow rate utilised was 0.5 mL/min, in order to facilitate direct comparison with the results obtained using the particle-packed column. The resulting chromatogram displayed clear, baseline resolution of all four anions of interest, with retention times of 2.8 min, 3.1 min, 3.4 min, and 10.3 min for nitrite, bromide, nitrate, and iodide respectively, compared to retention times of approximately 4.0 min (for nitrite), 4.7 min (for bromide), 5.5 min (for nitrate), and 20.5 min (for iodide) using the 25 cm particle-packed column at an identical flow rate. This corresponds to reductions of retention times ranging from 30% (for nitrite) to 50% (for iodide). However, as a flow rate of 0.5 mL/min gave rise to negative backpressure values being reported by the eluent delivery system (Dionex Model DX-100), the flow rate was increased to 2.0 mL/min, and the aforementioned sample re-analysed. Employing this higher flow rate resulted in a decrease in the resolution between both nitrite and bromide (down from 1.76 to 1.27) and between bromide and nitrate (decreasing from 1.50 to 1.16), as is evident from Fig. 3.3.

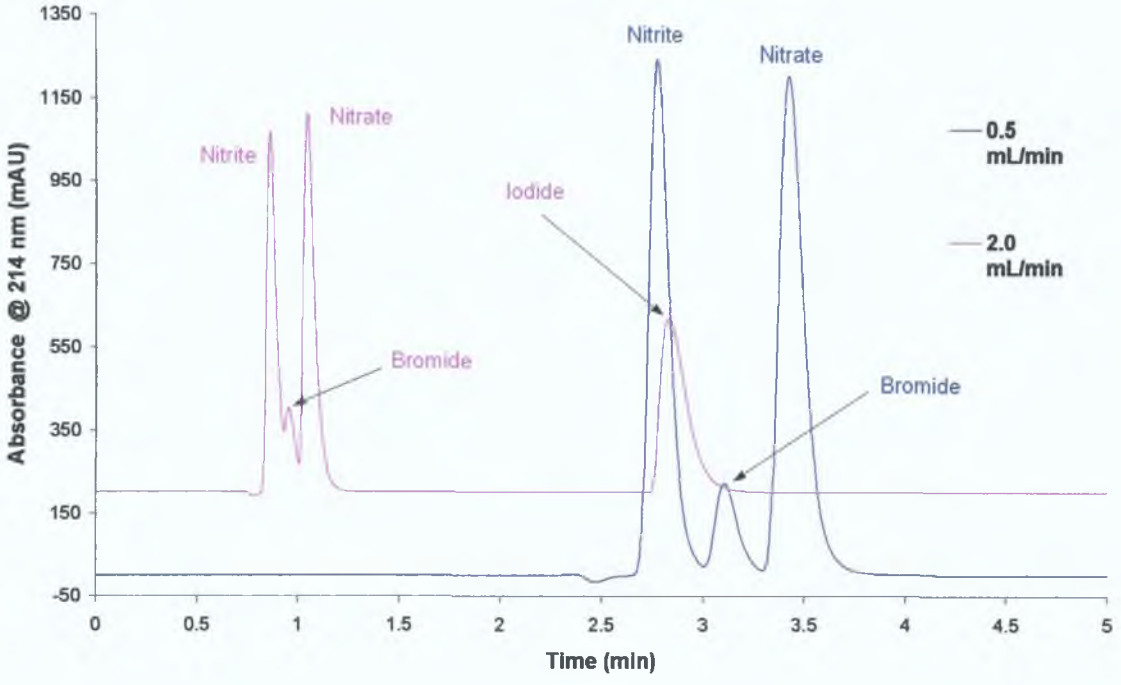

Figure 3.3. Chromatograms of a 1.0 mM mixture of nitrite, bromide, nitrate and iodide obtained using a 10 cm C_{18} monolith modified with dodecyldimethylaminoacetic acid, and operated at flow rates of 0.5 mL/min (blue trace) and 2.0 mL/min (pink trace). Eluent: 150 mM KCl with 0.2 mM dodecyldimethylaminoacetic acid, at pH 6.0. Wavelength of detection: 214 nm.

As an eluent KCl composition of 150 mM did not provide an ideal separation of nitrite, bromide and nitrate, it was thought that decreasing the amount of KCl present in the eluent would facilitate superior resolution of analyte peaks. Therefore, a study into the effect of electrolyte (KCl) concentration of the eluent, over the range 1 to 150 mM, was carried out to assess whether lower concentrations of KCl in the eluent could provide superior separation to 150 mM KCl in the eluent. This investigation was undertaken over a slightly lower concentration range than a similar study carried out using the particle-packed column modified with the same carboxybetaine-type surfactant (see Section 2.3.1) because of the lower ion-exchange capacity of the monolithic stationary phase. A graph showing the effect of eluent KCl concentration upon retention can be seen in Fig. 3.4.

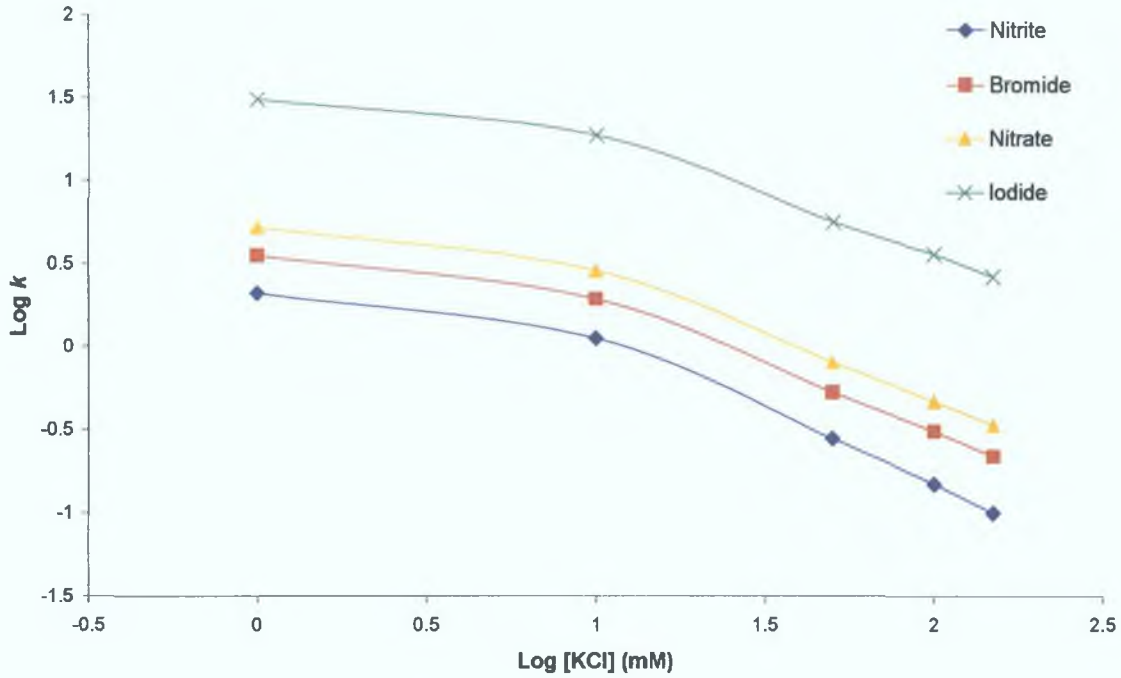

Figure 3.4. Effect of eluent KCl concentration upon retention factor (k) for a 10 cm C_{18} monolith modified with dodecyldimethylaminoacetic acid. Other eluent conditions: 0.2 mM zwitterionic surfactant, pH 6.0. Flow rate: 2.0 mL/min. Samples injected: 1.0 mM individual anion standards.

The results seen in the plots in Fig. 3.4 correlate quite well with those obtained using the particle-packed column for the same eluent preparations (see Section 2.3.1, Fig. 2.2), with R^2 values of 0.9386, 0.9451, 0.9446, and 0.9394, and slopes of –0.5037, -0.5563, -0.5657 and –0.6166, for nitrite, bromide, nitrate and iodide respectively, although, as stated already, this experiment was conducted over a lower concentration range than for the particulate zwitterionic stationary phase. An interesting observation, suggested by Fig. 3.4, is that the previously mentioned counter-acting effect of an increase in retention due to intra- and inter-salt destruction (Section 2.3.1) is more evident, with a clear deviation from linearity below 10 mM KCl. This departure from linearity at lower concentrations was demonstrated by examining the R^2 values obtained when the data points at 1 mM KCl were omitted. These R^2 values improved considerably for all 4 anions (i.e. 0.9994 for nitrite, 0.9999 for bromide, 0.9999 for nitrate, and 0.9992 for iodide).

The effect of eluent electrolyte concentration on peak efficiency is shown in Fig. 3.5. Again, the trends shown by the plots in Fig. 3.5 are very similar to those obtained

using the similarly modified particle-packed column (see Section 2.3.1, Fig 2.3), with increased KCl concentration generally resulting in higher reported values for the number of theoretical plates, N, especially for bromide and iodide.

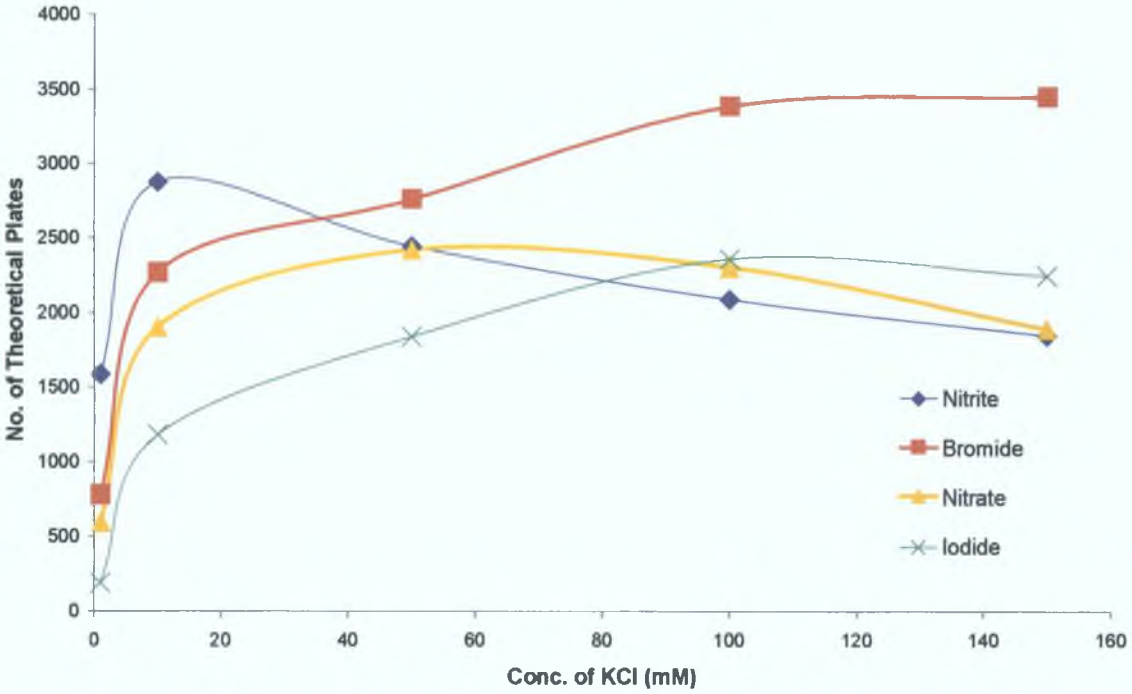

Figure 3.5. Effect of eluent KCl concentration on peak efficiency a 10 cm C_{18} monolith modified with dodecyldimethylaminoacetic acid. Other eluent conditions: 0.2 mM surfactant, pH 6.0. Flow rate: 2.0 mL/min. Samples injected: 1.0 mM individual anion standards.

It was found that the use of an eluent containing 10 mM KCl produced acceptable resolution and peak shapes, without leading to unnecessarily lengthy run times, and that, as with the particle-packed column, the optimum pH for peak efficiency remained pH 6. Overall, the effect of eluent pH on analyte anion retention and peak efficiency was the same as seen in Chapter 2 for the carboxybetaine-modified particle-packed columns. The separation achieved using such an eluent system, and a flow rate of 2.0 mL/min, can be seen in Fig. 3.6. All four anions eluted in less than 6 min (compared to approx. 22 min under optimal eluent conditions using the particle-packed column, as in Section 2.3.3, Fig. 2.6), with clear, baseline separation between all 4 analytes. The optimal eluent KCl concentration for the 10 cm carboxybetaine-modified monolith was considerably smaller than for the similarly modified 25 cm particle-packed column (i.e. 10 mM vs. 100 mM), due to the lower overall column capacity of the shorter column.

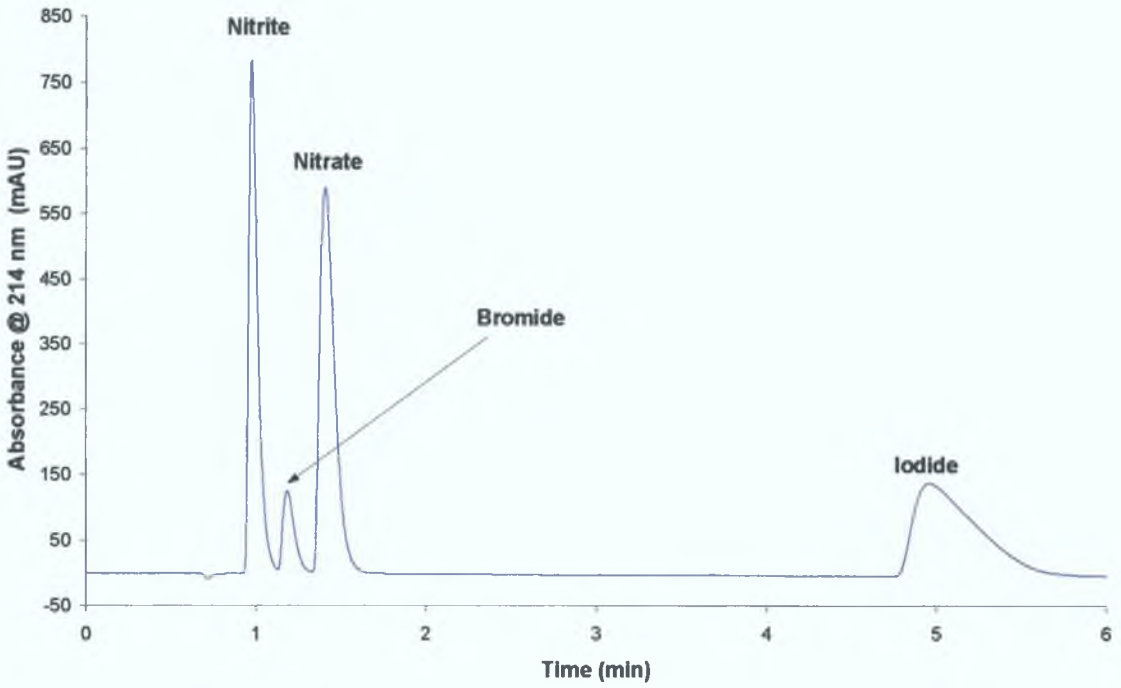

Figure 3.6. Chromatogram displaying the separation of a 1.0 mM mixture of nitrite, bromide, nitrate and iodide on a 10 cm C_{18} monolithic column modified with dodecyldimethylaminoacetic acid. Eluent: 10 mM KCl with 0.2 mM dodecyldimethylaminoacetic acid, at pH 6.0. Flow rate: 2.0 mL/min. Wavelength of detection: 214 nm.

However, the motivation behind the use of a monolithic column in this project was to have the option to employ elevated flow rates, and so reduce retention times significantly. Hence, the same conditions were used to examine the effect of higher flow rates on the observed separation.

3.3.2 Comparison of Flow Rates

It was decided to compare the chromatograms of the anion test mixture obtained at a flow rate of 2.0 mL/min with chromatograms obtained using a series of flow rates ranging from 0.5 mL/min to 4.5 mL/min (as 4.9 mL/min was the maximum flow rate possible using the Applied Biosystems 400 pump). At the highest flow rate of 4.5 mL/min, the backpressure across the monolithic column was only in the region of 90 bar. A 1.0 mM mixture of nitrite, bromide, nitrate and iodide was injected at each flow rate applied. An overlay of some of the resultant chromatograms can be seen in Fig. 3.7.

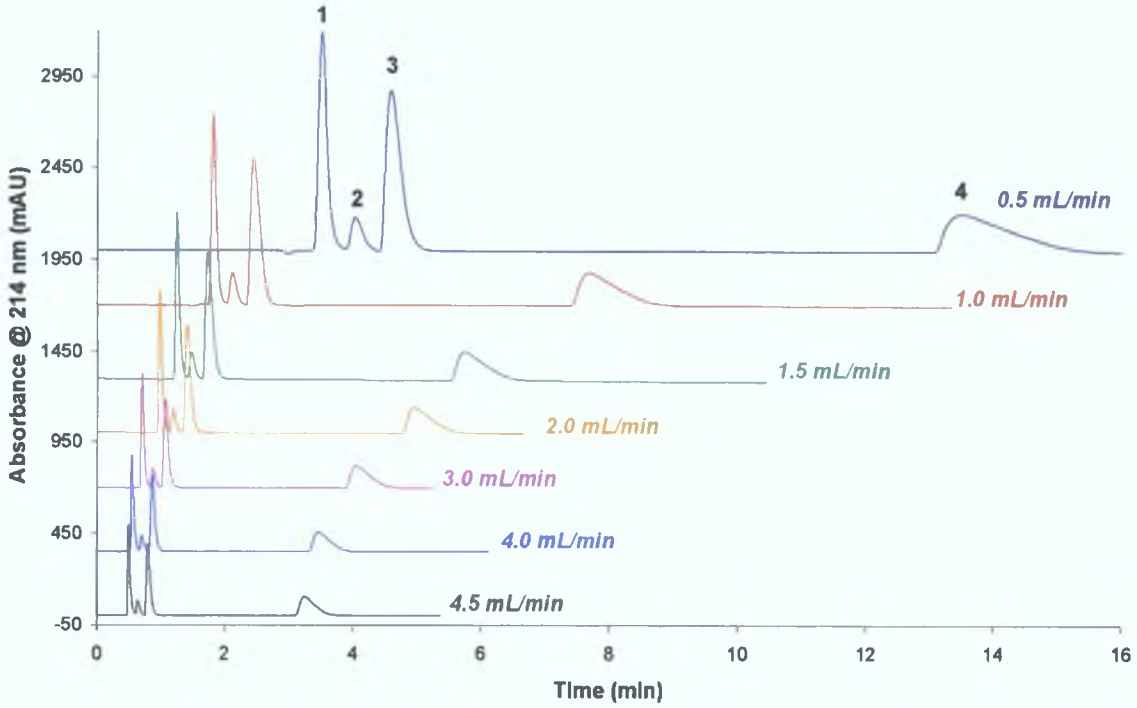

Figure 3.7. Chromatograms showing the separation of nitrite, bromide, nitrate and iodide at eluent flow rates ranging from 0.5 mL/min to 4.5 mL/min, using a 10 cm carboxybetaine-modified C_{18} monolith, and an eluent composed of 10 mM KCl (also containing 0.2 mM of the surfactant) at pH 6.0. Wavelength of detection: 214 nm. Peak identification: 1 – nitrite, 2 – bromide, 3 – nitrate, and 4 – iodide.

As can be seen from the chromatograms overlaid in Fig. 3.7, baseline resolution of nitrite, bromide and nitrate was achieved using all of the flow-rates investigated (0.5 – 4.5 mL/min), with all test anions well removed from the eluent dip. For flow rates above 2.0 mL/min, separation of the 3 aforementioned anions, as well as the later eluting iodide peak, was accomplished in less than 5 minutes. The total run time, utilising a flow rate of 4.5 mL/min, was just under 3.5 min, which is significantly less than the 15 min it took for all anions of interest to elute at 0.5 mL/min, without resulting in a loss of resolution of nitrite, bromide and nitrate. The peaks corresponding to iodide in Fig. 3.7 are suffering from some degree of tailing, possibly due to slower ion-exchange kinetics than the other analyte anions, but increasing the flow rate decreases the magnitude of the tailing, as the shorter retention times at higher flow rates means that less time is available for secondary interactions to occur. Fig. 3.8 illustrates how, in the case of nitrite, bromide and nitrate, peak efficiency tended to decrease (height equivalent of a theoretical plate (HETP) increased) as the flow rate was gradually increased, although, unusually, the decrease in peak

efficiency became less significant at higher flow rates (> 3.5 mL/min). The van Deemter curve for iodide (seen in Fig. 3.8), however, is unusual in shape, as peak efficiency appeared to increase slightly with the use of higher flow rates (as suggested by the iodide peak shapes in Fig. 3.7), for unknown reasons, compared to typical van Deemter curves (e.g. Fig. 3.2), where use of the same high flow rates leads to an increase in HETP for all analytes. Flow rates of 2.0 to 3.0 mL/min appeared to provide the best combination of reasonably fast run times and acceptable peak efficiency values. The efficiency values plotted in Fig. 3.8 are greater than those seen for the carboxybetaine-modified particle-packed columns at comparable flow rates, as mass transfer in monolithic columns is controlled by convection, rather than diffusion, as is the case for particle-packed columns [6]. Convection relies on the flow of eluent to accelerate the mass transfer of analyte molecules, which is in contrast with diffusion, where the concentration gradient is the driving force. The convective flow through the pores of the monolithic stationary phase causes mass transfer resistance to reduce greatly, thereby leading to improved peak efficiency values [6].

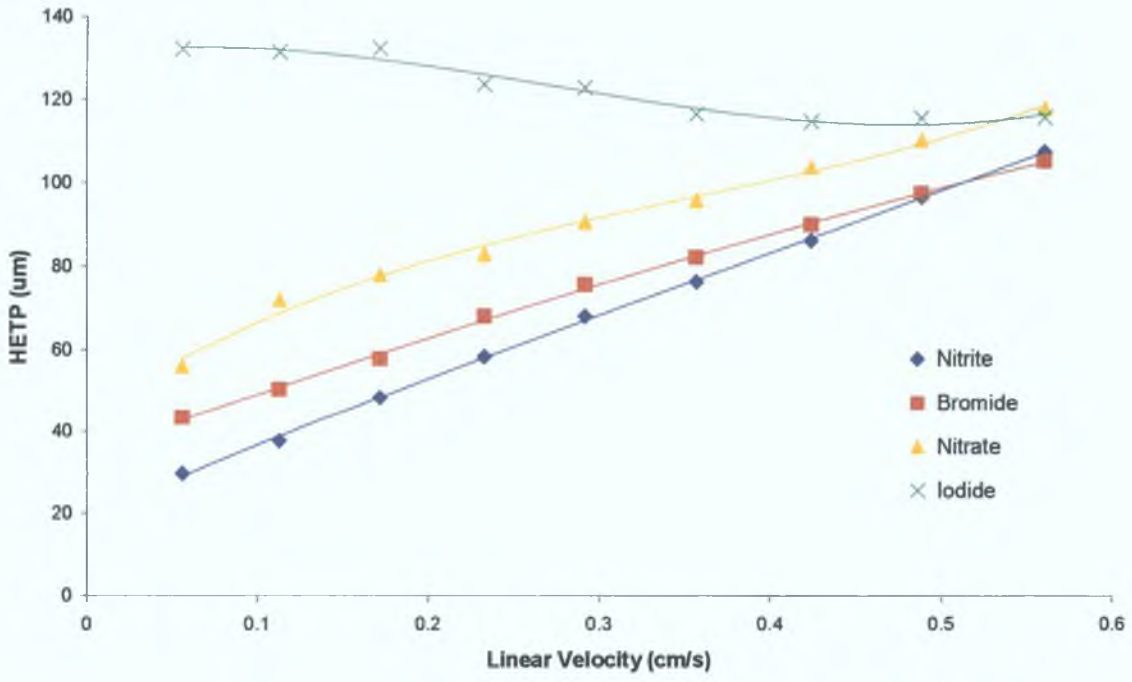

Figure 3.8. Van Deemter curves for nitrite, bromide, nitrate and iodide, obtained using a 10 cm C_{18} monolith modified with dodecyldimethylaminoacetic acid, using an eluent composed of 10 mM KCl (with 0.2 mM dodecyldimethylaminoacetic acid) at pH 6.0.

3.3.3 Use of Flow Gradients

One of the primary goals of modern analytical LC techniques is the resolution of the maximum number of chromatographic peaks within the minimum time [19]. Gradient elution is often used to reduce the time of chromatographic analyses, usually using a gradient involving a change in eluent composition. Flow gradients, however, are of limited use in standard IC, because of the sharp increases in backpressure associated with the use of higher flow rates with conventional particle-packed columns. When flow gradients are employed using particle-packed columns, a temperature gradient is usually required, to reduce eluent viscosity, and therefore bring about a reduction in the pressure generated by the flow gradient [20]. However, porous monolithic columns are not prone to the same sharp pressure increases when higher flow rates are applied, and so are more suitable for such programmed flow gradients [21]. Flow gradient elution on monolithic columns has previously been demonstrated by Cabrera *et al.* [22] using flow rates of 2.0-5.0 mL/min, for the separation of phenols and β-blocking drugs. Within the field of IC, the use of flow gradients to enable faster analyses has not been widely reported. Deguchi *et al.* [23] used a complicated flow gradient program for the analysis of anions and cations, but the flow rates utilised were only low-to-moderate flow rates (from 0.2 mL/min to 1.0 mL/min).

While adequate resolution of all sample components was achieved so far using an isocratic chromatographic system, the distribution of the peaks throughout the chromatogram is less than optimal (i.e. the extended gap between the elution of nitrate and the relatively isolated iodide). Therefore, it was considered advantageous to implement a flow gradient system that would shorten the overall run times, without sacrificing efficiency, or resolution.

A flow rate of 2.0 mL/min was deemed to be suitable for the separation of nitrite, bromide and nitrate, as peak efficiencies were higher than with more elevated flow-rates, but separation of all 3 anions in less than 2 minutes was still possible. However, for the analysis of iodide, the application of a higher flow-rate would be more beneficial, in order to achieve satisfactory peak efficiencies, while also shortening retention time. A 1.0 mM mixture of all 4 anions was injected 5 times. The initial flow rate for all 5 injections was set at 2.0 mL/min. For the first injection the flow was increased from 2.0 mL/min to the maximum flow rate of 4.9 mL/min over a time

frame of just 1 minute. For the second injection this was increased to 2 minutes, and then to 3 minutes for the third, and so on. The five resulting chromatograms can be seen in Fig. 3.9. It should be noted, that in order to calculate values for the number of theoretical plates, N, using the flow gradient programs, it was necessary to take the flow rate of the eluent at different times into account. As a flow gradient-assisted separation can be considered to be a kind of isocratic separation, due to the constant composition of the eluent employed, accurate values for N could be determined by replacing the term of the retention time, t_R, of analyte with a value for the retention volume, V_R, in the equation for measuring N (i.e. $N = 16(t_R^2)/(W^2)$), and measuring peak width, W, as the volume of eluent passed through the column for the corresponding length of time [21].

After examination of the chromatograms shown in Fig. 3.9, it was found that, in the case of nitrite, bromide and nitrate, peak efficiency was at its highest when the maximum flow rate of 4.9 mL/min was not reached until the 5 min mark, with values for N increasing by 170-190% upon going from a 1 min gradient program (from t = 0 min to t = 1 min) to a 5 min gradient program (from t = 0 min to t = 5 min), although these optimum values for N, for nitrite, bromide and nitrate, were only approx. 75% of the values for N reported using a constant flow rate of 2.0 mL/min. However, the objective of the flow gradient was to reduce the retention time for iodide without adversely affecting the previously observed separation and peak efficiency. The overall run time was just under 5.5 min at 2.0 mL/min, compared to less than 3 min when the flow gradient was applied over 1 min at the start of the run, and approx. 4 min when the flow gradient was applied over 5 min from the onset. In the case of the iodide peak, efficiency increased significantly upon application of the flow gradient program, as the highest calculated value for N using a flow gradient was 1339, obtained utilising a flow gradient program over 3 min (from 0 min to 3 min), compared to a value for N of 804 for the iodide peak at a constant flow rate of 2.0 mL/min, which corresponds to an increase of 40%.

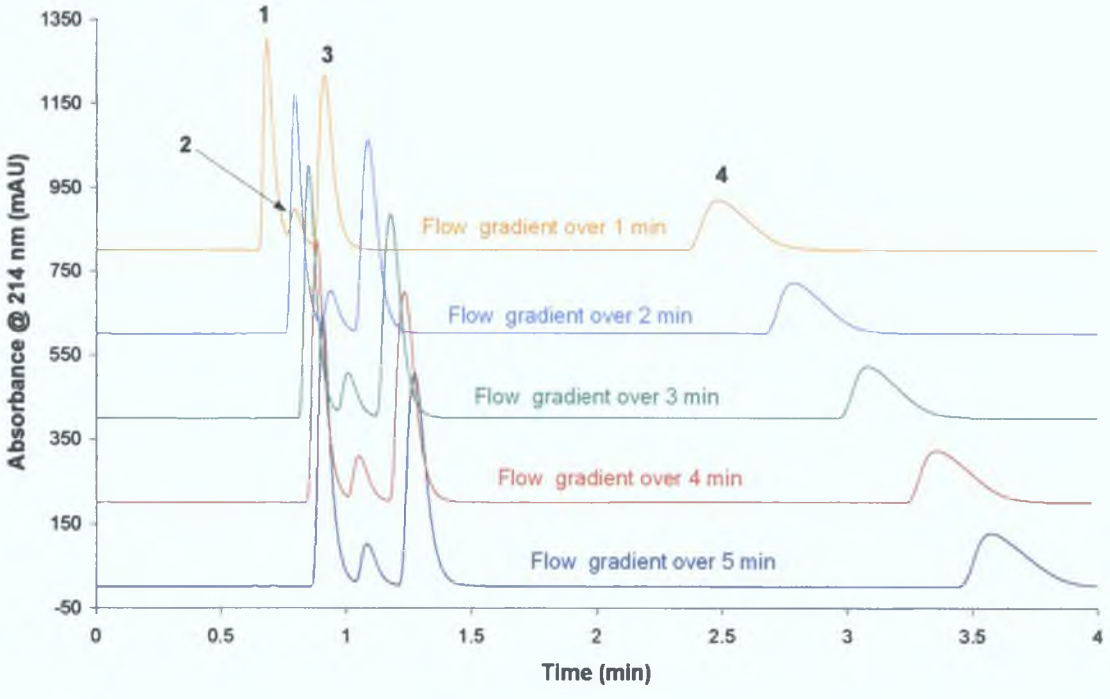

Figure 3.9. Separation of a 1.0 mM mixture of nitrite (1), bromide (2), nitrate (3) and iodide (4), obtained on a 10 cm C_{18} monolithic column modified with dodecyldimethylaminoacetic acid, under flow gradient conditions beginning at 2.0 mL/min and increasing to 4.9 mL/min over 1 (yellow trace), 2 (light blue trace), 3 (green trace), 4 (red trace) and 5 (dark blue trace) min. Eluent: 10 mM KCl (with 0.2 mM carboxybetaine-type surfactant) at pH 6.0. Wavelength of detection: 214 nm.

The next experiment was then to keep the flow rate constant at 2.0 mL/min for 2 minutes (i.e. until after the nitrate had been eluted), and then, at the 2 min mark, to apply a flow gradient up to 4.9 mL/min over 1, 2 and 3 min. Fig. 3.10 demonstrates the effect of these three flow gradient profiles on the separation of the four anions of interest. Upon comparing the chromatograms obtained using a constant flow rate and the steepest flow gradient (i.e. the blue trace in Fig. 3.10), it was observed that the overall run time had decreased by over 1 min. The optimum flow profile for the efficiency of the iodide peak was observed using a flow rate of 2.0 mL/min for 2 min (2 min being adequate time for the elution and acceptable separation of the other 3 anions), and then raising the flow rate up to 4.9 mL/min over 1 min (i.e. from t = 2 to t = 3 min). The difference in the efficiency, and asymmetry of the iodide peak under constant flow conditions, and the steepest flow gradient, can be seen in Table 3.1. From the data contained in Table 3.1, it can be seen that, in addition to the aforementioned lowering of retention time for iodide, the flow gradient caused iodide

peak efficiency to more than double, while also bringing about an improvement in peak shape, by reducing the degree of tailing of the analyte peak.

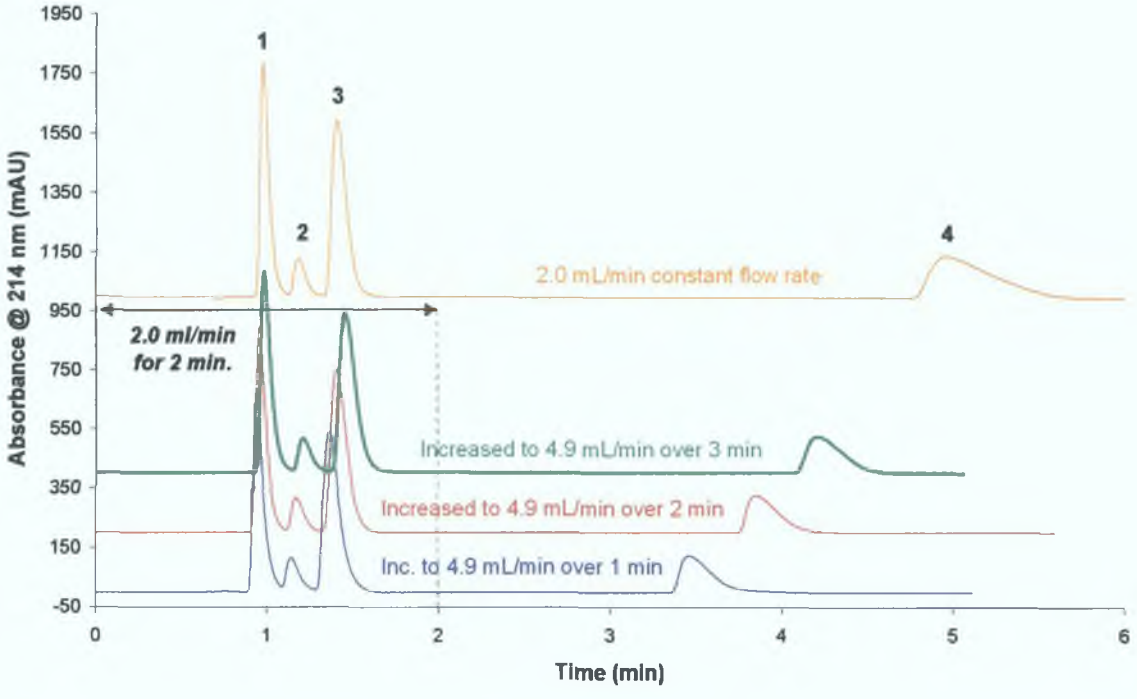

Figure 3.10. Separation of a 1.0 mM mixture of nitrite (1), bromide (2), nitrate (3) and iodide (4), obtained on a 10 cm C_{18} monolithic column modified with dodecyldimethylaminoacetic acid, using a constant flow rate of 2.0 mL/min (yellow trace), and under flow gradient conditions (from 2.0 mL/min to 4.9 mL/min) beginning at t = 2.0 min and applied over 1 (blue trace), 2 (red trace) and 3 (green trace) min. Eluent: 10 mM KCl (with 0.2 mM carboxybetaine-type surfactant) at pH 6.0. Wavelength of detection: 214 nm.

Table 3.1. Effect of flow gradient on iodide peak efficiency and peak shape.

Flow Conditions	Iodide Peak Efficiency, N	Asymmetry
Constant flow rate of 2.0 mL/min	809	2.24
2.0 mL/min for 2 min, ↑ to 4.9 mL/min over 1 min	1659	1.75

Although here the test mixture is quite simple, the results acquired illustrate a particular advantage of the use of monolithic phases combined with flow gradients in the shortening of analysis run times, and possible improvements in peak efficiencies. This was shown to be achievable without the requirement for complex eluent preparation or multiple solutions as in traditional eluent gradient separations.

3.3.4 Use of a Mixed-Bed Stationary Phase

Hu *et al.* [24,25] demonstrated that a stationary phase formed from an adsorbed coating of zwitterionic-cationic mixed micelles (in a 10:1, and 1:1 ratio) could be used for the separation of common inorganic anions. They found that selectivity for some analyte ions was affected by the inclusion of the cationic surfactant (myristyltrimethylammonium) to the zwitterionic (3-(N,N-dimethylmyristylammonium)-propanesulphonate, Zwittergent 3-14) stationary phase. Both types of surfactant appeared to bind analyte ions by independent mechanisms: The zwitterionic surfactant binds ions by a combination of an electrostatic mechanism and chaotropic effects, while the cationic surfactant binds the analyte ions by conventional anion-exchange. However, there has been little mention in the literature of mixed-bed stationary phases in ZIC using only zwitterionic surfactants.

For this experiment a separate C_{18} monolith was coated with a 1:1 mixture of two zwitterionic surfactants, dodecyldimethylaminoacetic acid and the sulfobetaine-type surfactant, Zwittergent 3-14. It was hoped that the use of such a stationary phase might benefit iodide peak shape, or cause iodide to elute earlier. The column modification procedure was the same dynamic modification procedure as before (i.e. passing 100 mL of a 20 mM solution of the carboxybetaine-type surfactant through the column at 0.5 mL/min). The only deviation from this method was the use of a 10 mM dodecyldimethylaminoacetic acid/10 mM Zwittergent 3-14 coating solution. Zwittergent 3-14, unlike the carboxybetaine-type surfactant, contains a strong acid group (i.e. a sulphonate group), compared to the weakly acidic carboxylate group of the carboxybetaine molecule. As for all previous work, all eluents prepared contained a small concentration of both zwitterionic surfactants (0.1 mM of each), to facilitate the regeneration of the stationary phase, and to combat column bleed. The chromatograms obtained under identical chromatographic conditions using the mixed-bed column, and a stationary phase of carboxybetaine-type surfactant alone, can be seen in Fig. 3.11. There appears to be very little difference in retention between the two, except for a slightly extended retention time for the iodide ion.

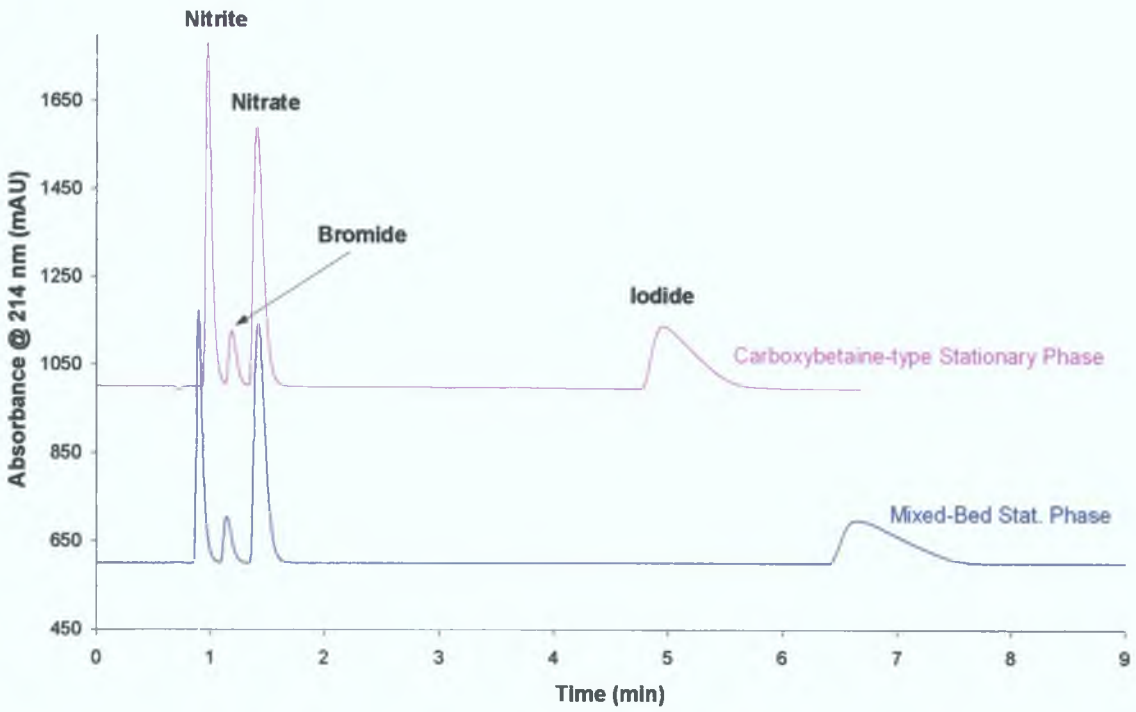

Figure 3.11. Chromatograms of a 1.0 mM mixture of nitrite, bromide, nitrate and iodide obtained using a 10 cm C_{18} monolithic column coated with dodecyldimethylaminoacetic acid (pink trace) and with a mixture of dodecyldimethylaminoacetic acid and Zwittergent 3-14 (blue trace). Eluent: 10 mM KCl (with a total zwitterionic surfactant concentration of 0.2 mM [0.1 + 0.1 mM) at pH 6.0. Flow rate: 2.0 mL/min. Wavelength of detection: 214 nm.

Potassium perchlorate ($KClO_4$) was added to the eluent in a further attempt to shorten retention times, as the perchlorate ion has a higher eluting ability than the chloride ions added to the eluent thus far [26]. The four equivalent oxygens in perchlorate can bond in all directions with quaternary ammonium groups on the zwitterionic stationary phase [27]. This creates a net negative charge on the surface, when the countercation of the negatively charged functional group of the zwitterionic surfactant is not as tightly bound as the perchlorate ion [27], which in turn leads to decreased retention of analyte anions.

An eluent of 10 mM KCl / 2 mM $KClO_4$ (with 0.1 mM dodecyldimethylaminoacetic acid/0.1 mM Zwittergent 3-14) at pH 3 was used in an attempt to separate a 1.0 mM mixture of nitrite, bromide, nitrate and iodide. However, while retention times of all test anions were reduced, inadequate resolution of nitrite, bromide and nitrate was observed. Adjustment of pH (to higher eluent pH values) did not appear to improve

separation. The concentration of perchlorate in the eluent was lowered to 1.0, 0.5 and 0.1 mM. An eluent perchlorate level of 0.5 mM was found to display optimum selectivity for the test mixture.

It was decided at this point to include thiocyanate in the test mixture, to determine whether the rapid analysis of thiocyanate in aqueous samples could be carried out. Determination of thiocyanate is of importance in the health industry, as levels of thiocyanate can be used as a probe as part of health screening programmes for distinguishing between smokers and non-smokers, due to the fact that elevated concentrations of thiocyanate arise from tobacco smoke [28].When the monolithic column was coated with the carboxybetaine-type surfactant alone, retention of thiocyanate was in excess of 100 min.

A chromatogram showing the separation of a 1.0 mM mixture of nitrate, bromide, nitrite, and iodide (labelled chromatogram A), and a separate 1.0 mM thiocyanate standard (labelled chromatogram B) using an eluent consisting of 10 mM KCl/0.5 mM $KClO_4$ in 0.1 mM carboxybetaine/0.1 mM Zwittergent 3-14 at pH 3, and a flow rate of 2.0 mL/min, is shown in Fig. 3.12. The peak corresponding to thiocyanate in the middle trace (chromatogram B) is evidently suffering from extreme peak fronting, and is very broad in comparison to those of nitrate etc. (It would appear that some secondary interaction with some component of the mixed-bed stationary phase is causing the thiocyanate peak to front significantly, as not all peaks in the same chromatogram are afflicted by fronting.) Therefore, a flow gradient was applied to a 1.0 mM mixture of all 5 test anions, whereby the flow rate was maintained at 2.0 mL/min for 1.5 min. (i.e. until after elution of the nitrite peak) before the flow was increased linearly to 4.9 mL/min over 1 min. This can be seen in the upper trace of Fig. 3.12 (labelled chromatogram C), where retention of thiocyanate was reduced to approx. 5.5 min. (from approx. 10 min) with a noticeable improvement in peak appearance and efficiency, although the thiocyanate peak was still not ideally Gaussian in shape. From Fig. 3.12, it can also be seen that the peak corresponding to iodide is significantly sharper, with an improved peak shape, compared to previous chromatograms. This is due to the shorter retention time for iodide using the mixed-bed stationary phase, which, in turn, is due to the retention mechanism involving both

the carboxybetaine-type and sulfobetaine-type zwitterionic surfactants, both of which have differing affinities for iodide, and also for thiocyanate.

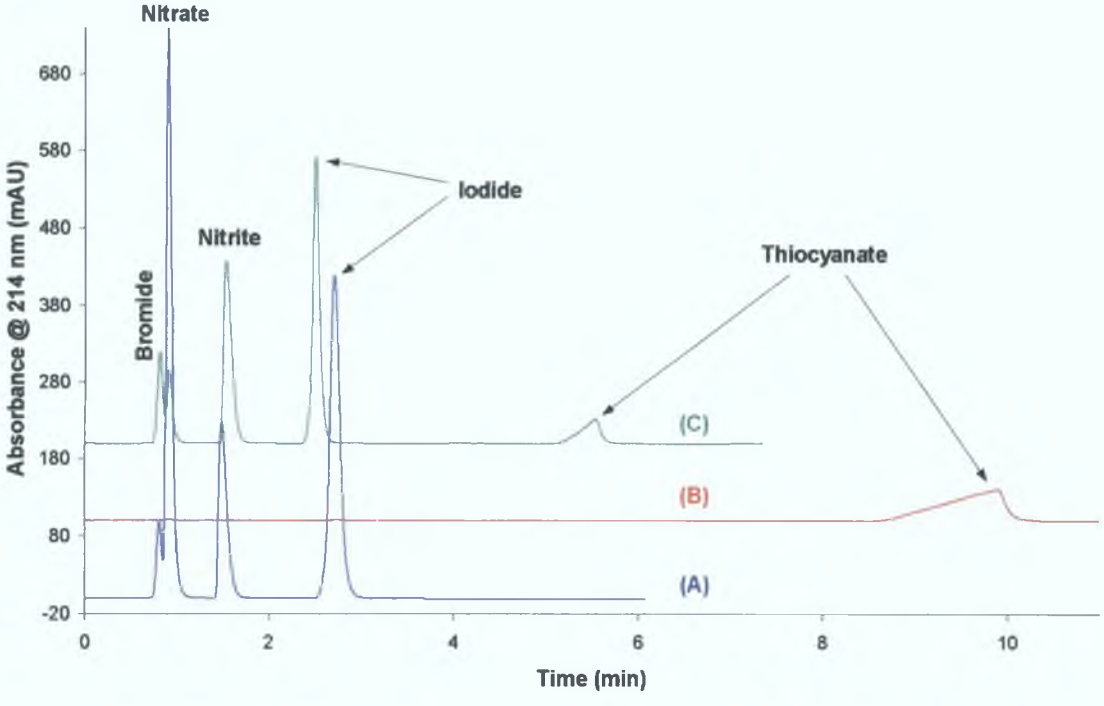

Figure 3.12. Chromatograms of (A) 1.0 mM nitrate, bromide, nitrite and iodide, (B) 1.0 mM thiocyanate, and (C) 1.0 mM nitrate, bromide, nitrite, iodide and thiocyanate, all obtained using a 10 cm C_{18} monolith modified with both zwitterionic surfactants, using an eluent composed of 10 mM KCl/0.5 mM $KClO_4$ (in 0.1 mM dodecyldimethylaminoacetic acid/0.1 mM Zwittergent 3-14) at pH 3.0. Flow conditions: (A) + (B), 2.0 mL/min; (C), 2.0 mL/min for 2 min, followed by a linear flow gradient to 4.9 mL/min from 2 to 4 min. Wavelength of detection: 214 nm.

It was concluded, following the aforementioned experiments using a mixed-bed zwitterionic stationary phase, that such a chromatographic system did not offer any additional benefits when compared to the stationary phase composed of dodecyldimethylaminoacetic acid alone. Therefore, for the remaining work detailed in this Chapter, the monolithic column used was modified with the carboxybetaine-type zwitterionic surfactant alone.

3.3.5 Analysis of Saline Samples

Pseudo-seawater samples were prepared to mimic the high ionic strength matrix of actual seawater, by preparing a solution of 50 ppm bromide, 5 ppm nitrate and 5 ppm

iodide in 0.52 M NaCl. Use of an eluent composed of 10 mM KCl, and including 0.2 mM dodecyldimethylaminoacetic acid, adjusted to pH 6, lead to the dwarfing of the nitrite and bromide analytical signals by the unacceptable level of broadening exhibited by the peak corresponding to the chloride present in the samples analysed. Lowering of the flow rate did not result in an improvement in the separation observed. Therefore, in order to shift retention times favourably, and/or shift the order of elution of the nitrite peak (as seen in Chapter 2), the pH of the 10 mM KCl, with 0.2 mM carboxybetaine-type surfactant, eluent was lowered to pH 3.5. This resulted in an excellent separation of nitrite, bromide and nitrate in less than 5 minutes, without altering the order of elution. However, peak efficiencies were quite poor, and the iodide present in the standard did not elute until relatively late, at 18.87 minutes.

As was previously concluded in Section 3.3.1, increasing the concentration of KCl in the eluent has the effect of shortening retention times significantly. The abovementioned standards prepared in 0.52 M NaCl were re-injected, using eluents containing various concentrations of KCl, ranging from 10 to 40 mM, increasing the ionic strength in 5 mM increments. Use of the 40 mM KCl eluent resulted in a reduction of the retention time for iodide to 6.49 minutes, without losing the acceptable separation of nitrate and bromide.

Calibration curves were assembled using a variety of concentrations, across several orders of magnitude (between 0.5 and 300 ppm; n =5), of bromide, nitrate and iodide in a 0.52 M NaCl sample matrix, with the resulting plots of peak area vs. analyte concentration (which can be seen in Fig. 3.13) giving R^2 values of 0.9976 for bromide, 0.9965 for nitrate and 0.9987 for iodide. (However, in the case of the iodide, concentrations in excess of 50.0 ppm gave rise to poor peak shapes, becoming increasingly irregular in shape as sample concentration was increased.)

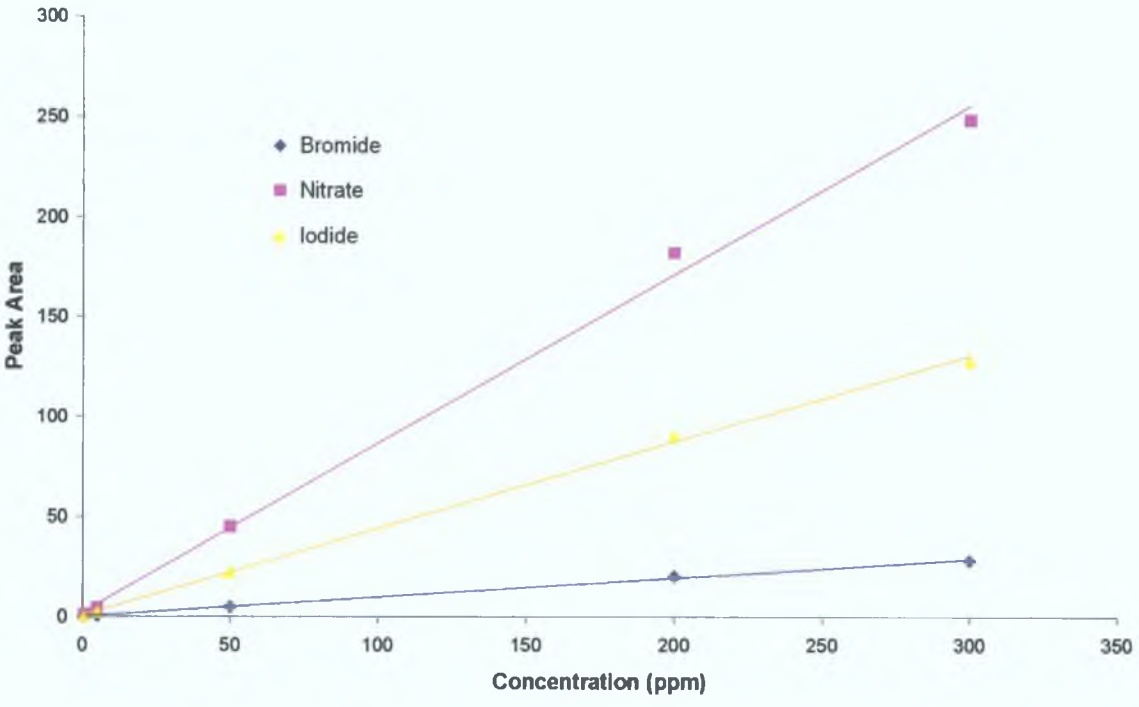

Figure 3.13. Plots of peak area vs. concentration for bromide, nitrate and iodide, prepared in a 0.52 M NaCl sample matrix, obtained using a 10 cm carboxybetaine-modified C_{18} monolithic column, with an eluent composed of 40 mM KCl, with 0.2 mM dodecyldimethylaminoacetic acid, at pH 3.5. Flow rate: 2.0 mL/min. Wavelength of detection: 214 nm.

Real seawater samples were taken from various coastal and estuarine regions surrounding Dublin city, an example of which can be seen in Fig. 3.14. From the standard curves prepared earlier, the concentrations of nitrate and bromide in the seawater samples could be determined, although no iodide was detected in any of these environmental samples. There is the possibility that the amount of iodide in the seawater samples taken was less than 0.1 ppm, which was the lowest detectable concentration of iodide for the standards prepared in the high ionic strength matrix. (Increasing the volume of sample injected from 20 μL to 50 μL, in an attempt to increase the signal for the iodide present in the sample, did not result in a peak for iodide being observed, while nitrate and bromide appeared to overlap when the sample injection volume increased.) The change in elution order, which caused nitrite to elute after bromide and nitrate, enabled the verification of trace nitrite in the seawater samples tested, as illustrated in Fig. 3.14. The brine samples were found to have concentrations of bromide ranging from 4.48 ppm, for an estuarine sample taken in north Co. Dublin, to 80.74 ppm for a water sample taken at a public beach in north

Dublin. Experimentally determined nitrate concentrations varied from a low of 0.5 ppm, for a north Dublin marina sample, to a high of 14.24 ppm, for a relatively polluted Mayne river water sample taken as the river flowed into the estuary near Baldoyle, Co. Dublin. A summary of the calculated nitrate and bromide levels in the saline samples taken can be seen in Table 3.2. (Flow gradient programs were not utilised for this area of work, as the analytes of interest eluted within 2.5 min, with satisfactory peak shapes and efficiencies.)

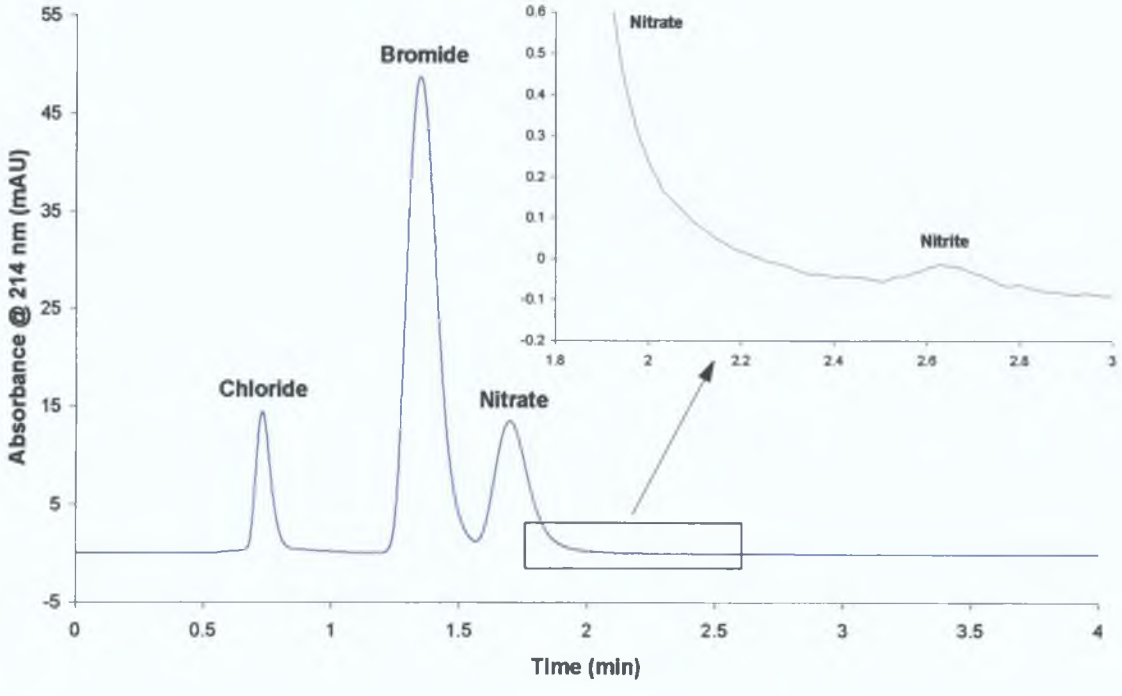

Figure 3.14. Chromatogram of an undiluted seawater sample taken from Bull Island, Dublin, displaying the separation of bromide and nitrate from the chloride sample constituent, obtained on a 10 cm carboxybetaine-modified C_{18} monolithic column. The inlet chromatogram shows the presence of trace levels of nitrite in the same seawater sample. Eluent: 40 mM KCl, with 0.2 mM dodecyldimethylaminoacetic acid, at pH 3.5. Flow rate: 2.0 mL/min. Wavelength of detection: 214 nm.

Table 3.2 Levels of nitrate and bromide determined to be in seawater and estuarine samples taken at various locations around Dublin.

Sample Point	Nitrate Concentration (ppm)	Bromide Concentration (ppm)
Custom House Quay, Liffey River, Dublin City Centre.	0.14	0.61
Poolbeg South (Beach)	7.77	56.68
Poolbeg North (Sea Wall)	1.52	71.88
Bull Island – Clontarf Side of Bull Wall	2.44	70.90
Bull Island – North Side of Bull Wall	2.14	68.78
Sutton Coast	0.50	60.11
Mayne River, Baldoyle	14.24	4.48
Mayne River Estuary, Baldolyle	5.75	47.16
Portmarnock Beach	1.51	80.74
Malahide Marina	2.00	60.24

3.3.6 Separation of Nucleoside Bases

Nucleoside bases (or nucleobases) are one of the components of nucleotides, which, in turn, are the building blocks of nucleic acids. A nucleoside base covalently bound to the 1' carbon of a ribose or a deoxyribose molecule is termed a nucleoside, and when a nucleoside has one or more phosphate groups attached to the 5' carbon it is called a nucleotide [29]. The importance of the analysis of nucleoside bases and related compounds lies in the fact that they are often present in biological sample matrices, due to the catabolism of nucleic acids, enzymatic degradation of tissues and dietary intake [29]. Free nucleosides, and their bases, can readily diffuse out of cells, and so are present mainly in physiological fluids (e.g. serum, plasma, urine etc.). In order to deepen the understanding of metabolic disorders and pathological states, levels of nucleoside bases are regularly undertaken [29].

There are 5 different nucleoside bases, two of which (namely adenine, A, and guanine, G) belong to a double-ringed (a 6-membered pyrimidine ring fused to a 5-membered imidazole ring) class of compounds called purines [30]. The remaining 3 bases, uracil (U), thymine (T) and cytosine (C), are all pyrimidines [30]. The structures for all 5 nucleobases are shown in Fig. 3.15.

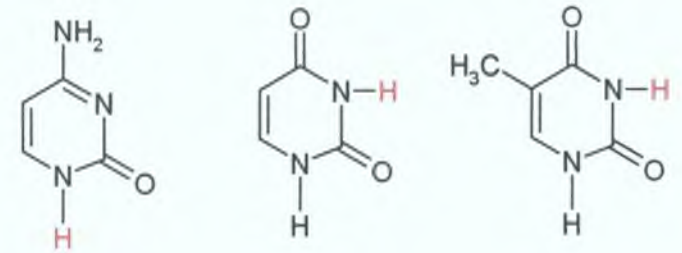

Cystosine (pK_a: 4.56) **Uracil** (pK_a: 10.06) **Thymine** (pK_a: 10.47)

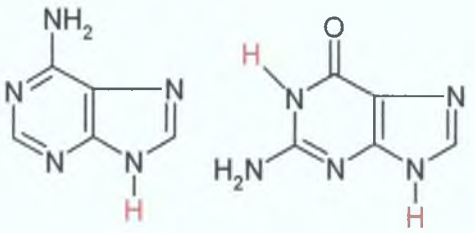

Adenine (pK_a: 3.88) **Guanine** (pK_{a1}: 3.6, pK_{a2}: 10.00)

Figure 3.15. Structure of nucleoside bases (cytosine, uracil, thymine, adenine and guanine), with the ionisable groups of each base highlighted in red [30].

Usually, the separation, and subsequent analysis of nucleoside bases is carried out using ion-exchange chromatography or reversed-phase chromatography [29]. However, when ion-exchange techniques are employed, the analytes had to undergo conversion to ionic species, before being separated by ion-exchange interactions [31]. Hu *et al.* [32] and Umemura *et al.* [33] employed zwitterionic surfactant-modified reversed-phase columns to separate mixtures of nucleosides and their bases using pure water as eluent. They found that while adsorption of the zwitterionic surfactant molecules onto the stationary phase suppressed most of the hydrophobic character of the column, organic analytes of relatively low hydrophobicity (e.g. nucleoside bases) were able to be separated using the modified columns.

As a means of investigating the retention of polar organic analytes on the dodecyldimethylaminoacetic acid stationary phase, nucleoside bases were injected onto the 10 cm carboxybetaine-modified monolithic column, and eluted using an eluent comprised of 10 mM phosphate buffer at pH 3 (also containing 0.2 mM dodecyldimethylaminoacetic acid). While some degree of retention for the nucleoside bases was evident, separation of the 5 bases was not possible, as demonstrated from the chromatograms of 20 μM individual nucleoside base standards seen in Fig. 3.16. An eluent at pH 3 was chosen initially, as this eluent pH was below that of the pK_a values for all 5 analytes of interest, meaning that all of the nucleoside bases would be mainly present in similarly charged forms.

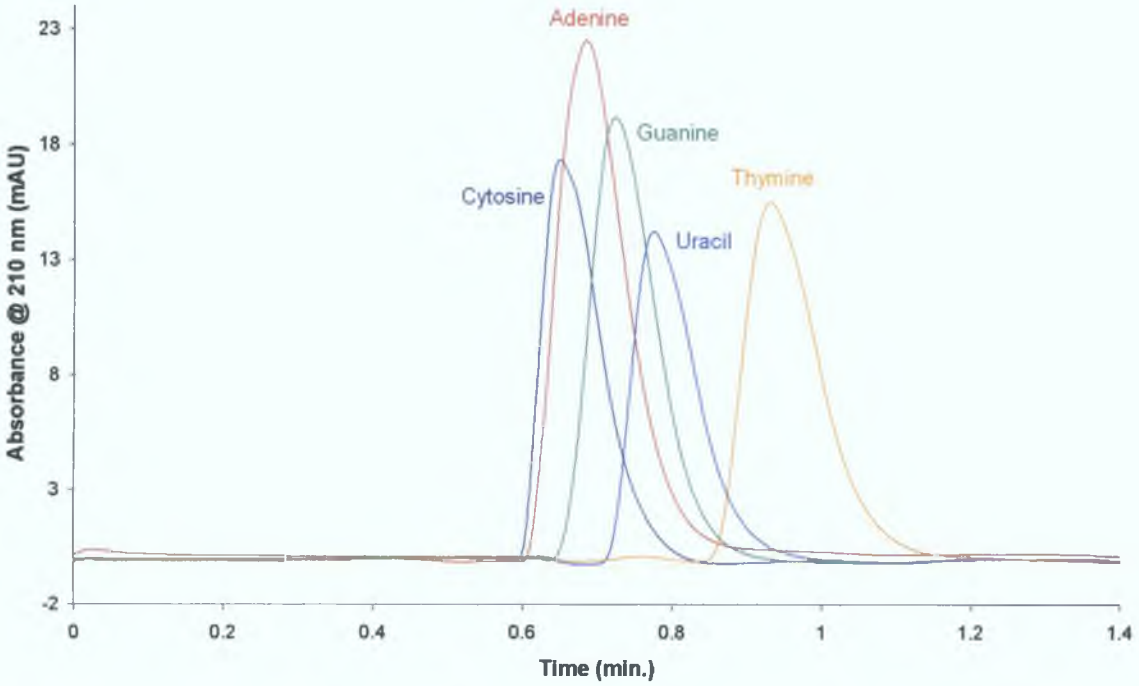

Figure 3.16. Chromatograms of 20 μM standards of cytosine (dark blue trace), adenine (red trace), guanine (green trace), uracil (bright blue trace) and thymine (yellow trace), obtained using a 10 cm carboxybetaine-modified C_{18} monolith, with an eluent composed of 10 mM phosphate buffer at pH 3 (with 0.2 mM dodecyldimethylaminoacetic acid). Flow rate: 2.0 mL/min. Wavelength of detection: 210 nm.

The order of elution of the bases at pH 3 was observed to be: (1) cytosine (C), (2) adenine (A), (3) guanine (G), (4) uracil (U), and (5) thymine (T), although retention was quite minimal, and so the difference in retention times for the bases was small. Aside from the cytosine molecule, retention of the pyrimidine bases (i.e. T and U) is

longer than the retention of the purine bases (i.e. A and G). This order of elution is similar to the order of the nucleoside bases, if placed in order of increasing pK_a, i.e. G (pK_{a1}) < A < C < G (pK_{a2}) < U < T. This is in contrast to the order of elution reported by other researchers using the zwitterionic surfactants Zwittergent 3-14 (C < U < G < A < T) and ammonium sulfobetaine-3 (C < U < G < T < A) [32]. Increasing the eluent pH, from pH 3 to pH 7, caused retention to increase very slightly, and also brought about a change in the elution order of the nucleoside bases, i.e. from C < A < G < U < T at pH 3 to C < U < G < A = T at pH 7, but an improvement in the resulting separation was not effected, as seen from Fig. 3.17. At pH 3 all of the nucleoside bases are present as cationic species, as this is below the pK_a for all 5 analytes, but at pH values greater than pH 4.6 adenine (pK_a = 3.88), guanine (pK_{a1} = 3.6) and cytosine (pK_a = 4.56) exist as anions. This may account for the slight shift in the elution order for adenine, although guanine and cytosine appeared to be unaffected. The remaining two bases (i.e. thymine and uracil) do not take anionic form until a much more basic pH is reached, i.e. > pH 10.

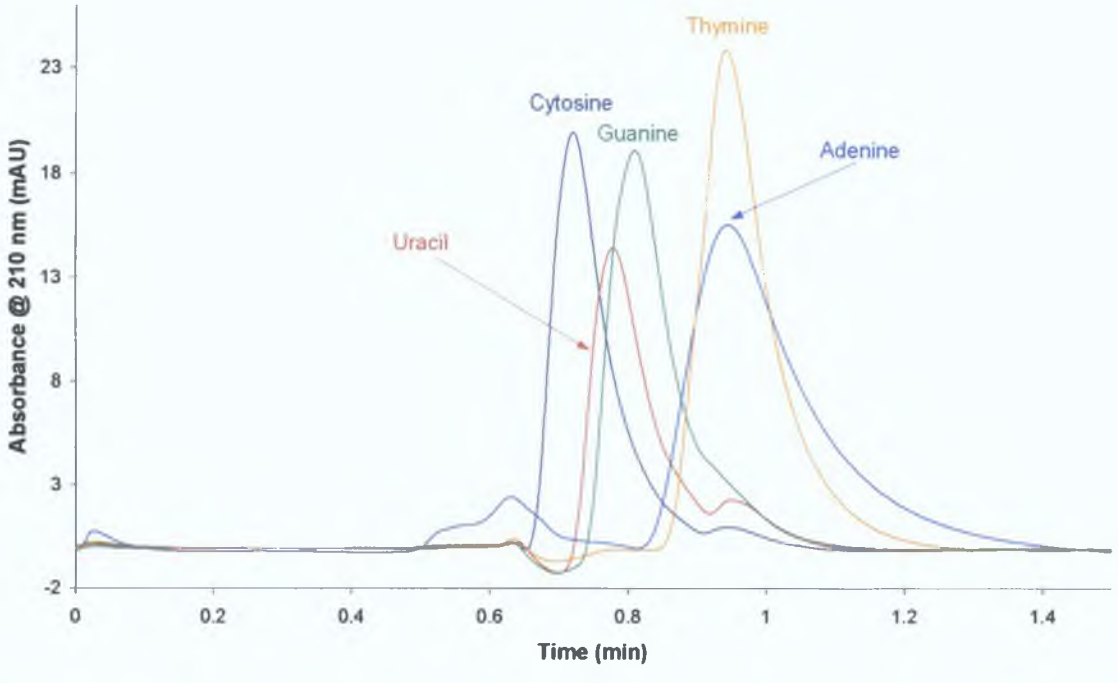

Figure 3.17. Chromatograms of 20 μM standards of cytosine (dark blue trace), uracil (red trace), guanine (green trace), adenine (bright blue trace) and thymine (yellow trace), obtained using a 10 cm carboxybetaine-modified C_{18} monolith, with an eluent composed of 10 mM phosphate buffer at pH 7 (with 0.2 mM dodecyldimethylaminoacetic acid). Flow rate: 2.0 mL/min. Wavelength of detection: 210 nm.

Addition of KCl to the eluent composition, decreasing the buffer concentration of the eluent (from 10 mM to 1 mM phosphate buffer) and increasing the ionic strength of the carboxybetaine-type surfactant present in the eluent system (from 0.2 mM to 0.4 mM), all resulted in negligible differences in retention times. Therefore, in an attempt to lengthen retention times, and so enable baseline separation of the nucleoside bases, 2 identically modified 10 cm carboxybetaine-modified monolithic columns were combined in series, and the bases re-analysed. The resulting chromatograms can be seen in Fig. 3.18. As expected, the use of 2 columns combined in series caused an increase in the retention times observed for all analytes, with the total run time increasing from 1.1 min to approx. 2 min. Resolution of nucleoside bases was improved (except for cytosine and adenine), but remained far from ideal. When a 20 μM mixture of all 5 bases was injected, cytosine and adenine appeared to co-elute, but the remaining sample components were relatively isolated from each other.

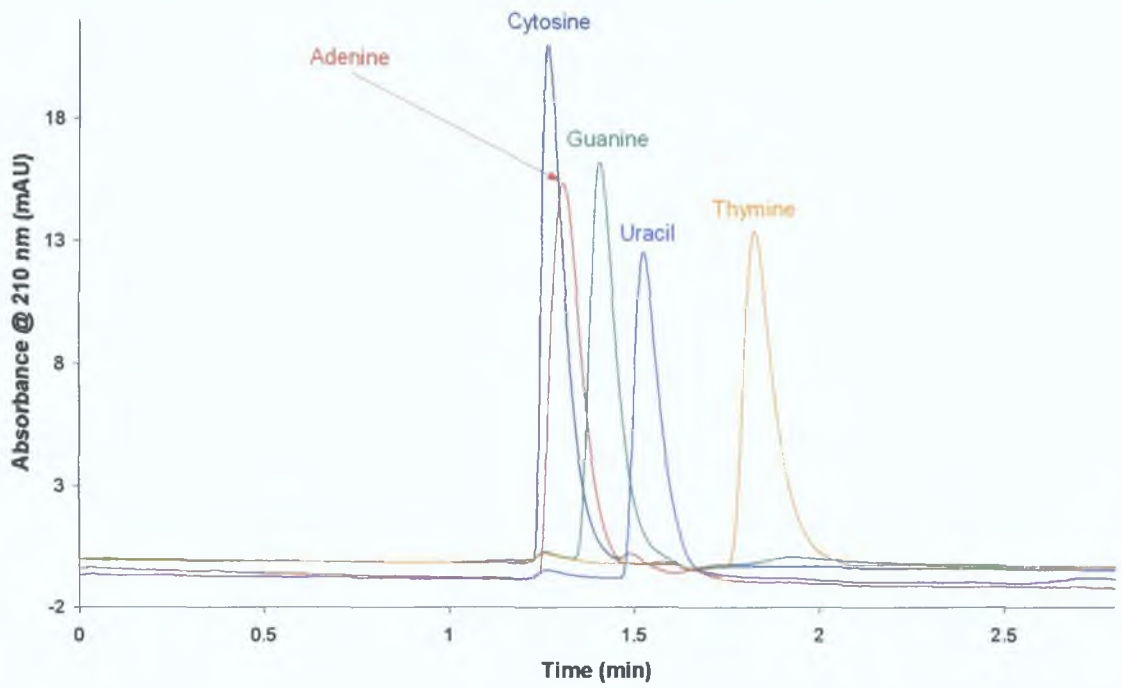

Figure 3.18. Chromatograms of 20 μM standards of cytosine (dark blue trace), adenine (red trace), guanine (green trace), uracil (light blue trace) and thymine (yellow trace), obtained using 2 x 10 cm carboxybetaine-modified C_{18} monoliths combined in series, with an eluent composed of 10 mM phosphate buffer at pH 3 (with 0.2 mM dodecyldimethylaminoacetic acid). Flow rate: 2.0 mL/min. Wavelength of detection: 210 nm.

The effect of eluent pH on retention of uracil, guanine and thymine, using an effective column length of 20 cm, is illustrated in Fig. 3.19. Fig. 3.19 indicates that pH did not have a very significant upon nucleoside base retention, with only slight increase in elution times being apparent. Above pH 3, the guanine peak eluted after uracil, rather than directly before, due to the low pK_a (pH 3.6) of guanine, which would mean that guanine was present predominantly in a deprotonated form at pH 4 and above, and so would be retained longer on the carboxybetaine stationary phase, owing to an increased negative character. Uracil and thymine, on the other hand, have pK_a values of approx 10.06 and 10.47 respectively, and therefore, their negligible increase in retention with increased pH was not as extreme as that observed for guanine.

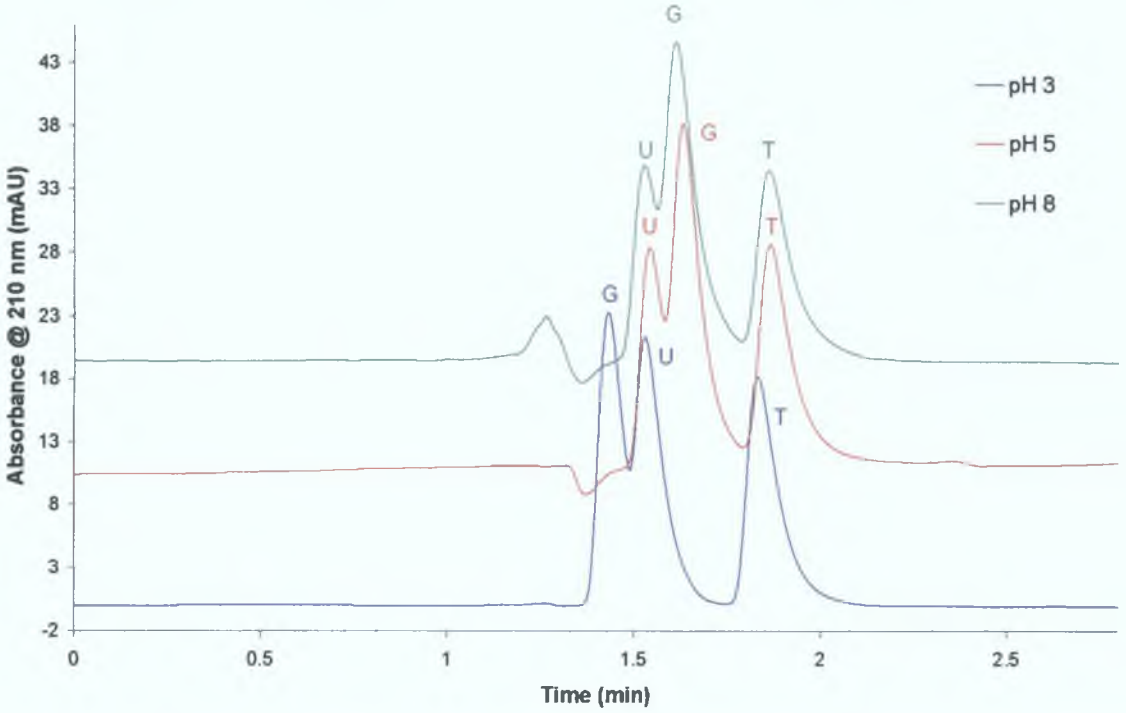

Figure 3.19. Effect of varying eluent pH on retention of uracil (labelled U), guanine (labelled G) and thymine (labelled T), using 2 x 10 cm carboxybetaine-modified C_{18} monolithic columns combined in series. Eluent: 10 mM phosphate buffer (also containing 0.2 mM dodecyldimethylaminoacetic acid) at pH 3 (blue trace), pH 5 (red trace), and pH 6 (green trace). Flow rate: 2.0 mL/min. Wavelength of detection: 210 nm.

The next experiment incorporated the use of a citrate buffer as eluent rather than a phosphate buffer, as was utilised prior to this. The wavelength of detection for this eluent composition was adjusted to 256 nm, to minimise interference from the background absorbance of the citrate eluent. The total run time of the analysis was

essentially the same for both eluent systems, although separation of the early eluting cytosine and adenine peaks improved, while the resolution between guanine and uracil decreased slightly, as can be seen in Fig. 3.20. Upon injection of a 20 μM nucleoside base mixture, all 5 peaks corresponding to each nucleoside base could be identified, although baseline resolution remained unachievable. Previous work by Hu *et al.* [32] and Umemura *et al.* [33] showed significantly longer retention times for the nucleoside bases using sulfobetaine-modified stationary phases, even after taking it into consideration that the flow rate used was quite low (0.7 mL/min) and the eluent employed was pure water. This suggests that the carboxybetaine-type zwitterionic surfactant used in this Chapter reduces the hydrophobic character of the C_{18} stationary phase even further than the sulfobetaine-type zwitterionic surfactants used by the other research groups, as it was thought that "residual" hydrophobic interactions were responsible for nucleoside base retention, with only a small contribution from electrostatic interactions.

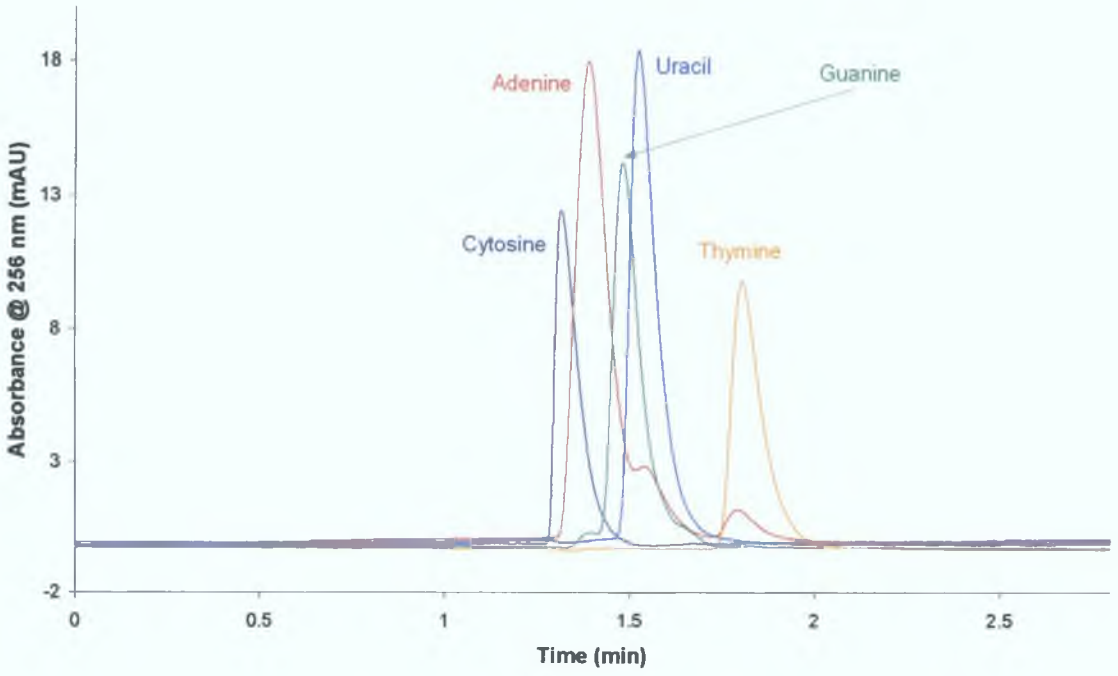

Figure 3.20. Chromatograms of 20 μM standards of cytosine (dark blue trace), adenine (red trace), guanine (green trace), uracil (light blue trace) and thymine (yellow trace), obtained using 2 x 10 cm carboxybetaine-modified C_{18} monoliths combined in series, with an eluent composed of 10 mM citrate buffer at pH 3.1 (also containing 0.2 mM dodecyldimethylaminoacetic acid). Flow rate: 2.0 mL/min. Wavelength of detection: 256 nm.

In summary, from the work undertaken in this Section, it can be concluded that the carboxybetaine-modified column had very little affinity for polar organic analytes, such as nucleoside bases, as they were very weakly retained. Eluent pH had a relatively insignificant effect on analyte retention, but resulted in a slight change in the order of elution. This was thought to be due to protonation or deprotonation of the nucleoside bases, depending on their respective pK_a values.

3.3.7 Combined pH and Flow Gradients

Chromatographers regularly utilise pH gradients as a means of achieving separation within more reasonable time frames [34], and also to reduce peak width and minimise peak tailing through peak compression [35,36]. However, these pH gradients have predominantly been accomplished during the HPLC analysis of organic compounds. Within the field of IC, pH gradients have not seen widespread use. For example, Bruzzoniti *et al.* [37] used a low-range pH gradient (from pH 9.5/9.75 to pH 10/10.5, applied between t = 0 min and t = 10/15 min) in the analysis of inorganic anions and metal ions by suppressed ion chromatography. Another ion-exchange technique that utilises a pH gradient, chromatofocusing [38], is based on the generation of an "internal" pH gradient (i.e. a gradient that is generated within the adsorbent bed of a chromatographic column [34]), through the buffer interaction between a weakly basic, or weakly acidic ion-exchanger and the buffered eluent passed through the column.

From the results obtained thus far using carboxybetaine-modified columns, it is clear that the combination of the structural characteristics of the monolithic column and the dodecyldimethylaminoacetic acid-modified stationary phase presents an opportunity for the use of a combined flow and pH gradient. It has already been shown that an increase of eluent pH will decrease retention significantly (see Chapter 2, Section 2.3.2), which shows that pH can be used to alter retention selectively. Therefore, combining a linear flow gradient with a pH gradient would allow the early eluting peaks (such as nitrite, bromide and nitrate) to elute at a lower pH (which would be close to the optimal pH value for peak efficiency and resolution), while the larger, more polarisable anions (such as iodide and thiocyanate), that have a stronger affinity for the stationary phase, would elute at higher pH values and higher flow rates, which would reduce overall analysis times significantly.

In order to illustrate how extreme an effect an eluent pH gradient would have on analyte anion retention, it was decided to return to the use of the previously employed 25 cm dodecyldimethylaminoacetic acid-modified particle-packed column for the preliminary work in which a pH gradient experiment was conducted. The initial experiment undertaken was to apply a pH gradient from pH 3 to pH 8 for the carboxybetaine-modified particle-packed column, to investigate whether such a method could be used to facilitate the earlier elution of thiocyanate (which was retained for approx. 110 min using a flow rate of 0.5 mL/min and an eluent of pH 3). An early attempt to accomplish the relatively fast elution of thiocyanate by simply adjusting the eluent pH to pH 7 or 8 (where the eluent employed was composed of 150 mM KCl in 0.2 mM carboxybetaine-type surfactant), caused a reduction in the resolution of the early eluting anions (nitrite, bromide and nitrate). Various pH gradient profiles were examined for the particle-packed column at various flow rates (0.5, 1.0 and 2.0 mL/min). Utilising a flow rate of 2.0 mL/min and an eluent pH gradient going from 100% pH 3 to 100% pH 8 in 2.5 minutes, from t = 0 min to t = 2.5 min (using eluents of identical composition and ionic strength, but adjusted to, and buffered at, either pH using 10 mM phosphate buffer at the required pH), resulted in the best separation of all sample components, and the shortest retention time for thiocyanate (approximately 24 min). A sample chromatogram of this specific pH gradient (overlaid, for comparative purposes, with the chromatogram acquired under isocratic conditions with an eluent at pH 6) can be seen as chromatogram (A) in Fig. 3.21. The peak shapes for iodide and thiocyanate improved greatly through the use of the pH gradient, although a system peak was present directly before (but separated from) the iodide peak. For example, the peak width for iodide decreased from 1.16 min under isocratic conditions (pH 6) to 0.36 min after application of the aforementioned pH gradient. The expected change in elution order because of the starting pH (i.e. pH 3) of the pH gradient was also observed, with nitrite now eluting after bromide and nitrate, and not before bromide, as seen with the eluent at pH 6 alone.

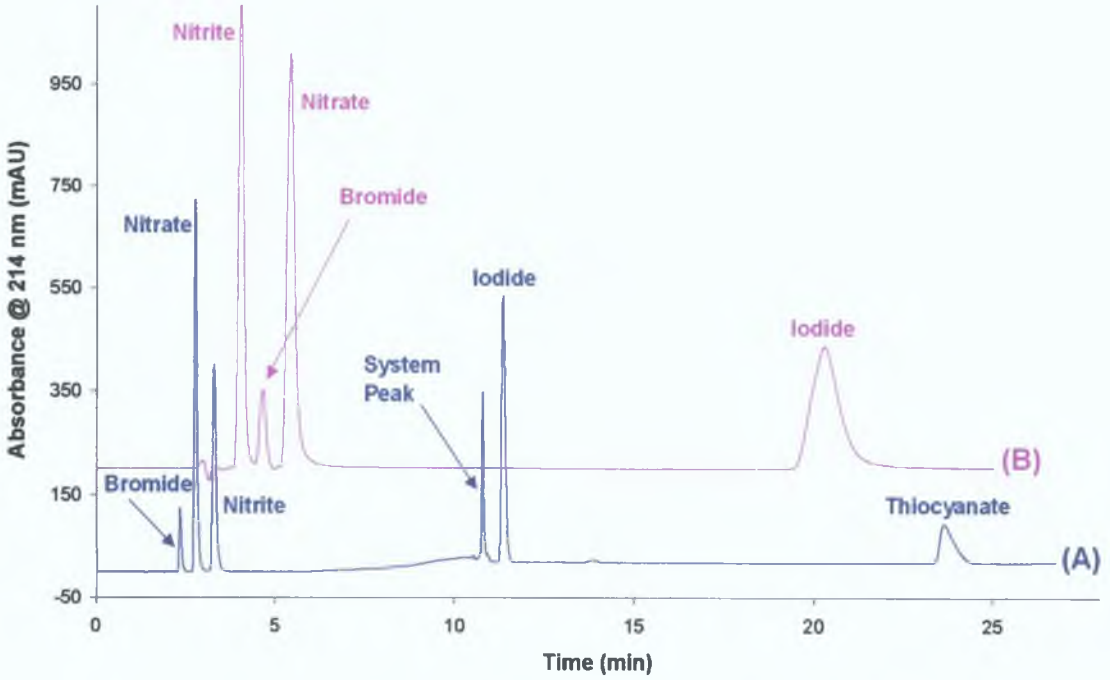

Figure 3.21. Chromatograms of a 1.0 mM mixture of nitrite, bromide, nitrate, iodide and thiocyanate obtained on a 25 cm carboxybetaine-modified C_{18} particle-packed column, using an eluent comprised of 150 mM KCl/0.2 mM dodecyldimethylaminoacetic acid, and buffered with 10 mM phosphate buffer. Eluent pH conditions: (A) pH gradient from 100% pH 3 at t = 0 min to 100% pH 8 at t = 2.5 min; (B) isocratic conditions with an eluent pH of 6. Flow rate: (A) 1.0 mL/min; (B) 0.5 mL/min. Wavelength of detection: 214 nm.

This pH gradient methodology was then applied to the 10 cm carboxybetaine-modified monolithic column. However, the use of a pH gradient from 100% pH 3 to 100% pH 8 (from t = 0 min to t = 5 min) in conjunction with the monolithic column resulted in the co-elution of nitrite, bromide, and nitrate, possibly due to the reduced capacity of the carboxybetaine-modified monolithic column, compared to the particle-packed columns used previously. It was not until the starting pH was increased to pH 6 that these peaks were satisfactorily resolved, although the peak shapes for iodide and thiocyanate remained quite poor (as illustrated in Fig. 3.22).

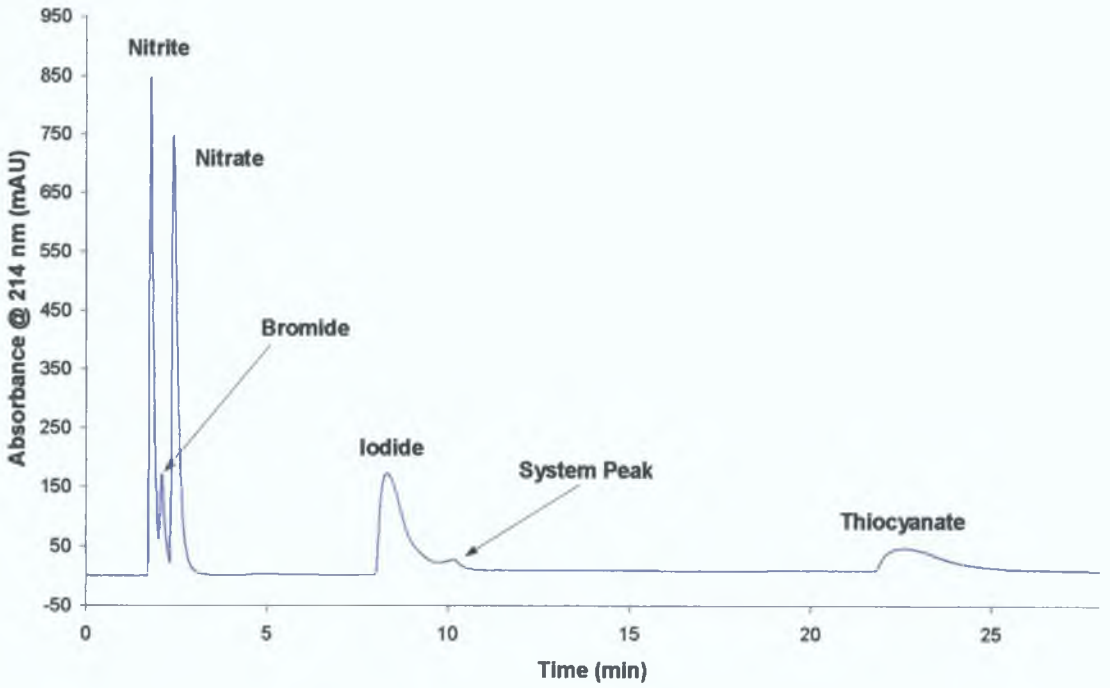

Figure 3.22. Chromatogram of a 1.0 mM mixture of nitrite, bromide, nitrate, iodide and thiocyanate obtained on a 10 cm carboxybetaine-modified C_{18} monolithic column, and using an eluent of 10 mM KCl with 0.2 mM dodecyldimethylaminoacetic acid (buffered with 10 mM phosphate buffer). Gradient details: pH gradient from 100% pH 6 at t = 0 min to 100% pH 8 at t = 5 min. Flow rate: 2.0 mL/min. Wavelength of detection: 214 nm.

The next step was to combine a pH gradient from 100% pH 6 to 100% pH 8, and a flow gradient from 1.0 mL/min to 5.0 mL/min over 5 min. Under these conditions, elution of bromide, nitrate, nitrite, iodide, and thiocyanate was possible in less than 8 minutes (as is evident from Fig. 3.23). Thiocyanate, for example, had a retention time of 7.03 min using the dual gradient method, compared to 22.45 min using a similar pH gradient, at a uniform flow rate of 2.0 mL/min. Once again, an improvement in efficiency for thiocyanate was noted (with N increasing from 1137 at a constant flow rate of 2.0 mL/min to 2210 using the aforementioned dual gradient [i.e. combined pH and flow gradient] method).

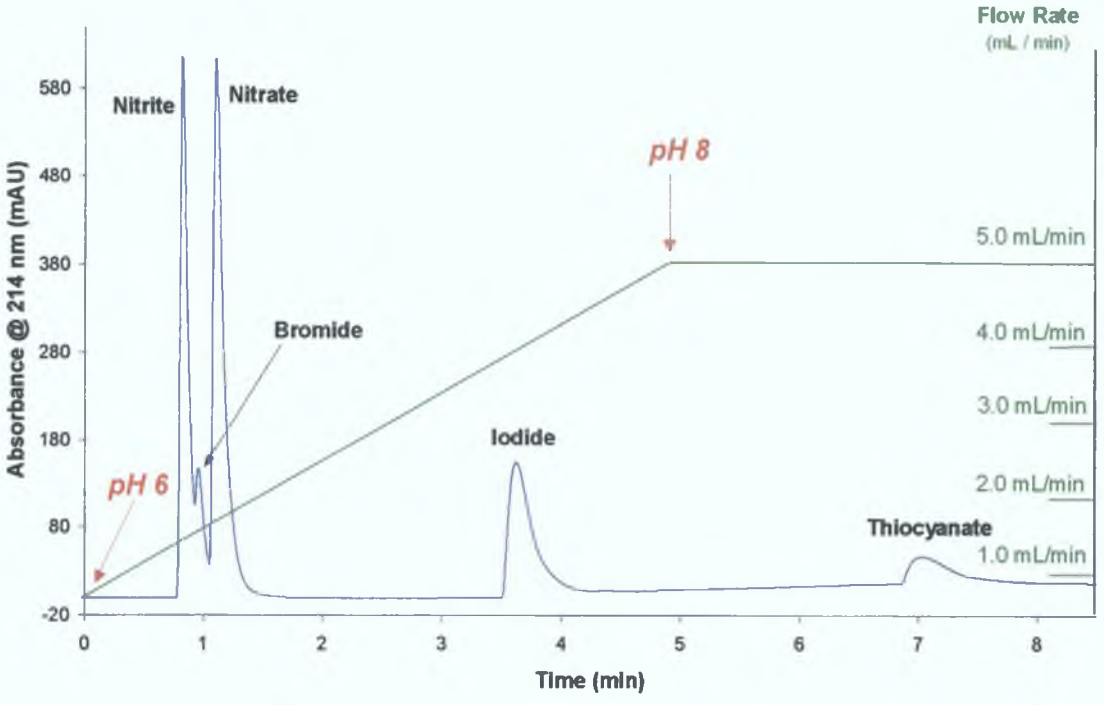

Figure 3.23. Chromatogram of a 1.0 mM mixture of nitrite, bromide, nitrate, iodide and thiocyanate, obtained using a 10 cm C_{18} monolith modified with dodecyldimethylaminoacetic acid, and utilising an eluent composed of 10 mM KCl, with 0.2 mM carboxybetaine-type surfactant, buffered using 10 mM phosphate buffer at the required pH. Gradient conditions: pH gradient of 100% pH 6 to 100% pH 8, and a flow gradient of 1.0 mL/min to 5.0 mL/min, applied over 5 min (from t = 0 min to t = 5 min). Wavelength of detection: 214 nm.

3.3.8 Dual Gradient ZIC on a 1 cm Carboxybetaine-Modified Monolith

The use of a double gradient (pH and flow) technique, such as that used in Section 3.3.7, was examined for an ultra-short carboxybetaine-modified monolithic column. The zwitterionic ion-exchanger was prepared by modifying a 1.0 cm long monolithic column in the same manner as for the 25 cm particle-packed column and the 10 cm monolithic column. Such a short monolithic column has already been shown [39] to have great potential in low-pressure gradient micro-IC for the determination of a number of common inorganic anions.

Upon characterisation, it was found this short carboxybetaine-modified monolithic column resulted in a separation of the anion test mixture (nitrite, bromide, nitrate, iodide and thiocyanate) similar to that observed for the longer carboxybetaine-

modified columns (but with significantly shorter retention times), at identical flow rates under isocratic conditions. This separation is shown here as Figs. 3.24 and 3.25. A lower ionic strength eluent than was previously employed for the 10 cm modified monolith (i.e. 1 mM vs. 10 mM) was used, as the ion-exchange capacity of the 1 cm column was obviously less than that of the longer monolith. Fig. 3.24 illustrates the separation of nitrite, bromide, and nitrate achieved in less than 1 minute, with analyte peaks being well resolved and well removed from the eluent dip at 0.1 min.

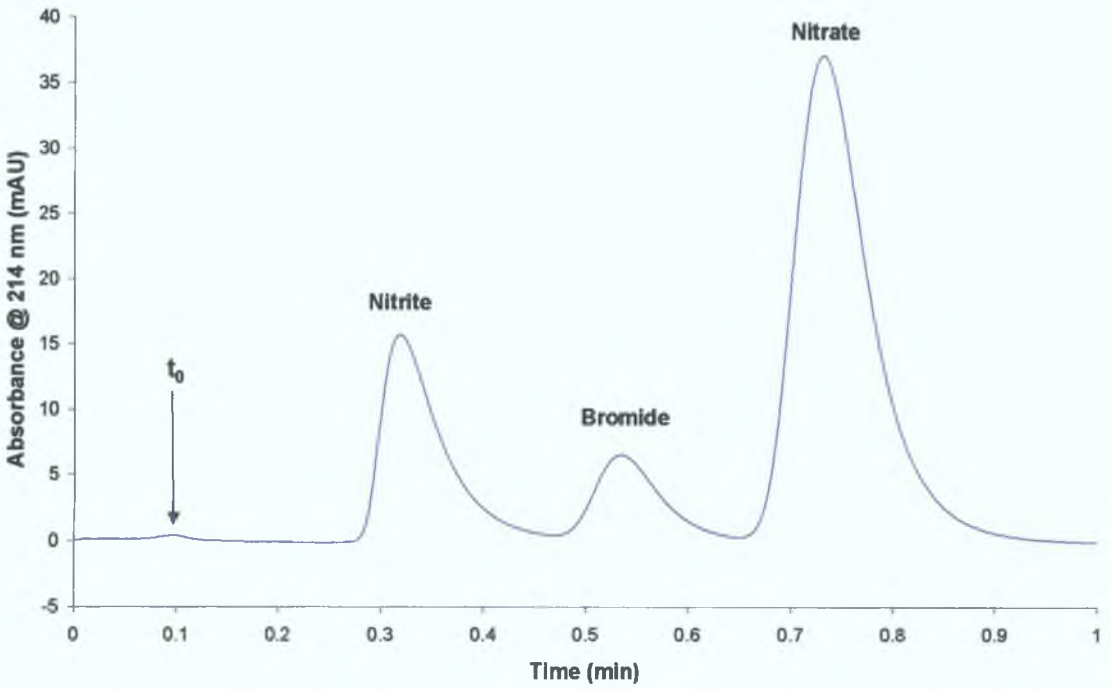

Figure 3.24. Separation of a 0.05 mM mixture of nitrite, bromide and nitrate obtained using a 1.0 cm carboxybetaine-modified C_{18} monolith, with 1 mM KCl in 0.2 mM dodecyldimethylaminoacetic acid at pH 3 as the eluent. Flow rate: 2.0 mL/min. Wavelength of detection: 214 nm.

A notable feature of the separation observed in Fig. 3.24 is the order of elution (i.e. nitrite < bromide < nitrate). This is of interest, as for previous injections using a carboxybetaine-modified stationary phase, the use of an eluent at pH 3 would result in the elution of nitrite after the nitrate peak, because of the low dissociation constant of nitrous acid, HNO_2. It was thought that this could be attributed to the speed of the separation, or the sample having insufficient time to interact with the eluent, as nitrite had eluted fully within 27 seconds. However, when a standard mixture of identical analyte concentration was prepared using the eluent itself as the diluent, there was no

apparent difference between the ensuing chromatogram, and that of the standard mixture prepared in Milli-Q water. Fig. 3.25 shows how the entire sample mixture, including iodide and thiocyanate, could be separated in approx. 17 minutes. The peak efficiencies for this column were found to be very impressive, especially considering the dimensions of the column involved. The peaks corresponding to iodide and thiocyanate were seen to have values for N of 896 and 972 respectively (with these values resulting in values for N/m in the region of 90,000-100,000 for both anions).

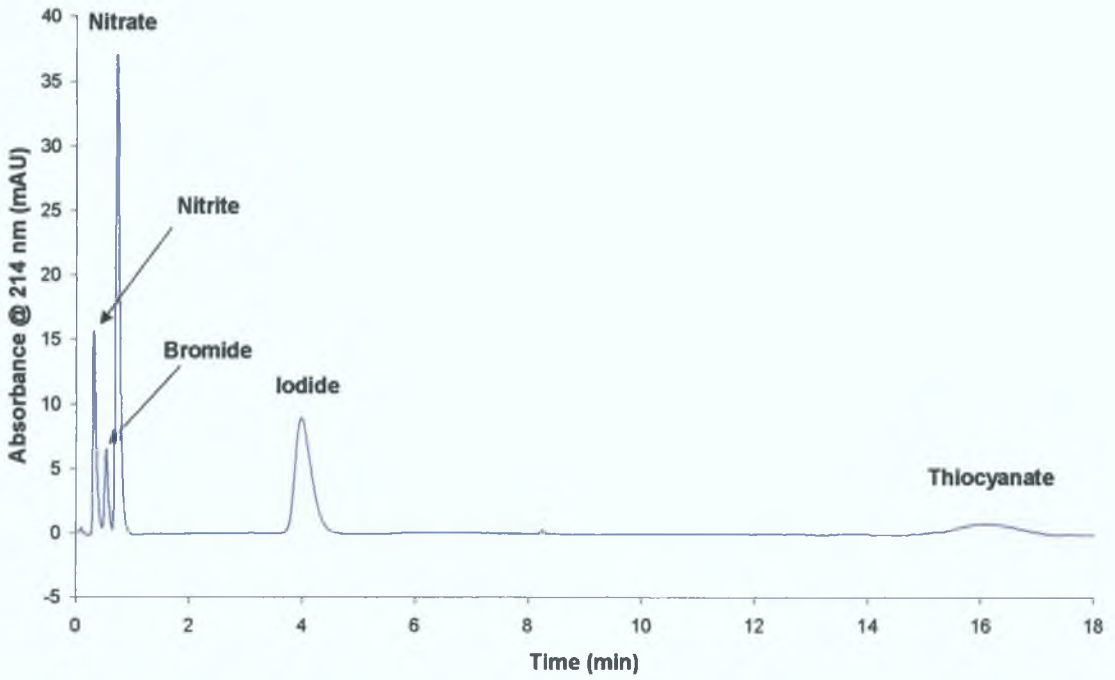

Figure 3.25. Chromatogram illustrating the separation of a 0.05 mM mixture of nitrate, bromide, nitrite, iodide and thiocyanate achieved using a 1.0 cm carboxybetaine-modified C_{18} monolithic column, with an eluent composed of 1 mM KCl, with 0.2 mM dodecyldimethylaminoacetic acid, at pH 3. Flow rate: 2.0 mL/min. Wavelength of detection: 214 nm.

While the separation on display in Fig. 3.25 is relatively rapid, when compared to previous analyses, the chromatogram is far from optimal, due to the large gap (approx. 12 minutes) between the elution of iodide and the elution of thiocyanate, which accounts for around 70% of the total run time. Simply increasing the flow rate drastically, in an attempt to overcome this problem, would mean that the favourable separation of the weakly retained trio of nitrite, bromide, and nitrate would be lost, or at the very least, severely compromised.

An investigation into the effect of flow rate on peak efficiency was carried out using 4 test anions (nitrite, nitrate, iodide, and thiocyanate), and is summarised in Fig. 3.26 (for nitrite and nitrate) and Fig. 3.27 (for iodide and thiocyanate). The values for linear flow velocity plotted in Figs. 3.26 and 3.27 correspond to flow rates of 2.0, 3.0, 4.0, 5.0 and 6.0 mL/min. It was found that for the early eluting species (namely nitrite and nitrate), increasing flow rate caused a continuous decrease in efficiency (i.e. increased HETP, and decreased N), while for the latest eluting species (namely thiocyanate) the optimum flow rate in terms of peak efficiency was between 4 and 5 mL/min. Iodide displayed a decrease in efficiency with the use of elevated flow rates, but this decrease was not as dramatic as that observed for nitrite and nitrate. The reason for these contrasting behaviours was probably due to the extremely short interaction time between the early eluting species and the stationary phase. For example, when a flow rate of 6.0 mL/min. was used, nitrite eluted after a mere 6 seconds.

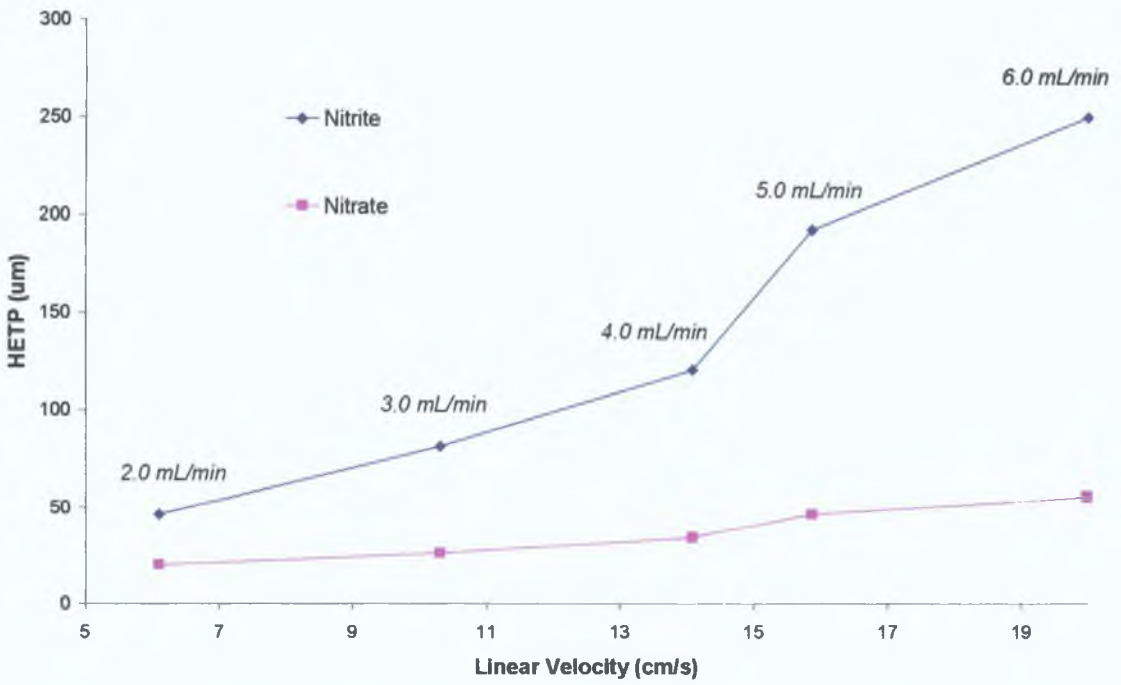

Figure 3.26. Effect of eluent flow rate upon peak efficiency for nitrite and nitrate, using a 1.0 cm carboxybetaine-modified C_{18} monolithic column. Eluent: 1 mM KCl, with 0.2 mM dodecyldimethylaminoacetic acid, at pH 3. Wavelength of detection: 214 nm.

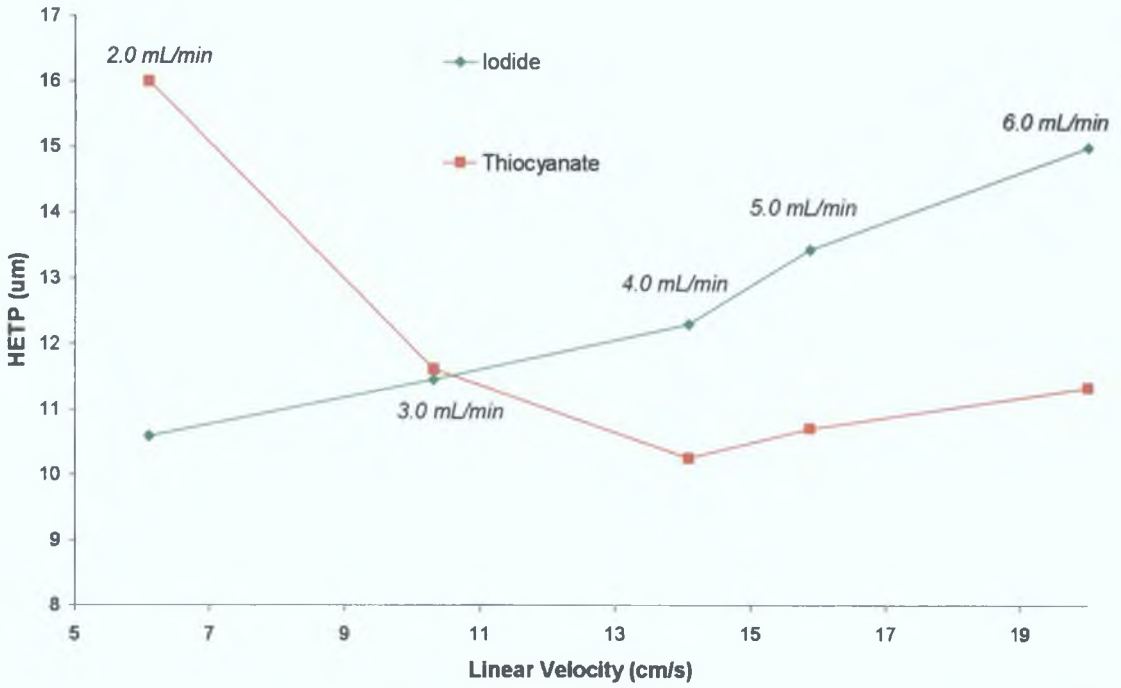

Figure 3.27. Effect of eluent flow rate upon peak efficiency for iodide and thiocyanate, using a 1.0 cm carboxybetaine-modified C_{18} monolithic column. Eluent: 1 mM KCl, with 0.2 mM dodecyldimethylaminoacetic acid, at pH 3. Wavelength of detection: 214 nm.

Taking the results in Figs. 3.26 and 3.27 into account, and in an attempt to lower retention times as much as possible, a flow gradient program was developed. It was hoped that this would maintain the resolution and efficiency of the early eluting species, while causing iodide and thiocyanate to elute earlier, giving a more efficient peak for the thiocyanate peak at least. The optimum flow gradient profile was determined to be a constant flow rate of 2.0 mL/min for 1 min. and then a linear flow gradient to 6.0 mL/min over 1 min (as shown in Fig. 3.28). Under these conditions, the separation of all five test anions was achieved in less than 7 min (which is approx. 10 min faster than the overall run time using a constant flow rate of 2.0 mL/min), with peak efficiency for thiocyanate, for example, increasing from 599 (for the thiocyanate peak observed under iscocratic conditions in Fig. 3.25) to 865 (after taking flow gradient into account).

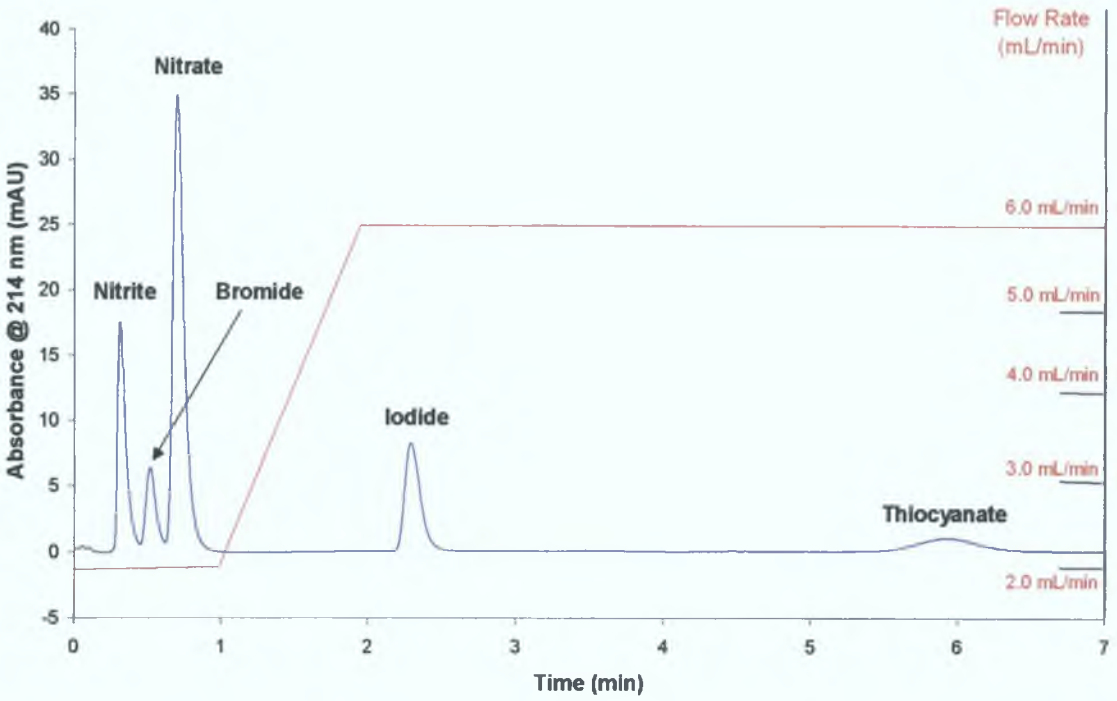

Figure 3.28. Chromatogram illustrating the separation of a 0.05 mM mixture of nitrite, bromide, nitrate, iodide and thiocyanate obtained on a 1.0 cm carboxybetaine-modified C_{18} monolithic column, using an eluent composed of 1 mM KCl, with 0.2 mM dodecyldimethylaminoacetic acid, at pH 3. Flow conditions: 2.0 mL/min constant flow rate for 1 min (from t = 0 min to t = 1 min), followed by a linear flow gradient to 6.0 mL/min over 1 min (from t = 1 min to t = 2 min). Wavelength of detection: 214 nm.

Section 3.3.7 introduced the concept of a dual gradient technique whereby both flow rate and eluent pH were increased over a short period of time, during the chromatographic run. The separation of a 0.05 mM mixture of nitrite, bromide, nitrate and iodide and 0.25 mM thiocyanate was achieved using a combination of pH and flow gradient, applied over 1 min, from t = 1 min to t = 2 min. However, using the normal detector wavelength of 214 nm lead to a rise in the baseline as the thiocyanate eluted, which lead to the formation of a very broad, intrusive system peak alongside the thiocyanate peak. The presence of this system peak was due to the release and subsequent elution of eluent and buffer ions, which had been retained by the carboxybetaine stationary phase, due to the decrease in column capacity brought about by the increased eluent pH conditions mid-run. Increasing the wavelength of detection to 225 nm lead to a sharper, more efficient peak for thiocyanate, but as

expected, no peak appeared representing bromide, as bromide (unlike nitrate etc.) does not absorb at this particular wavelength. The separation achieved using the aforementioned dual gradient profile and a wavelength of detection of 225 nm can be seen in Fig. 3.29. It can be seen that separation of all sample components could be achieved in little over 3 minutes, without sacrificing the separation of the earlier eluting peaks. If the starting eluent pH and flow rate conditions had been maintained, and a dual gradient not applied to the system, it would have taken approx. 17 min for all analyte anions to elute (see Fig. 3.25), which equates to a decrease of over 80%. Fig. 3.29 also shows how the application of the dual gradient resulted in a considerable improvement in the peak shape and peak width for iodide and thiocyanate, compared to previously obtained chromatograms.

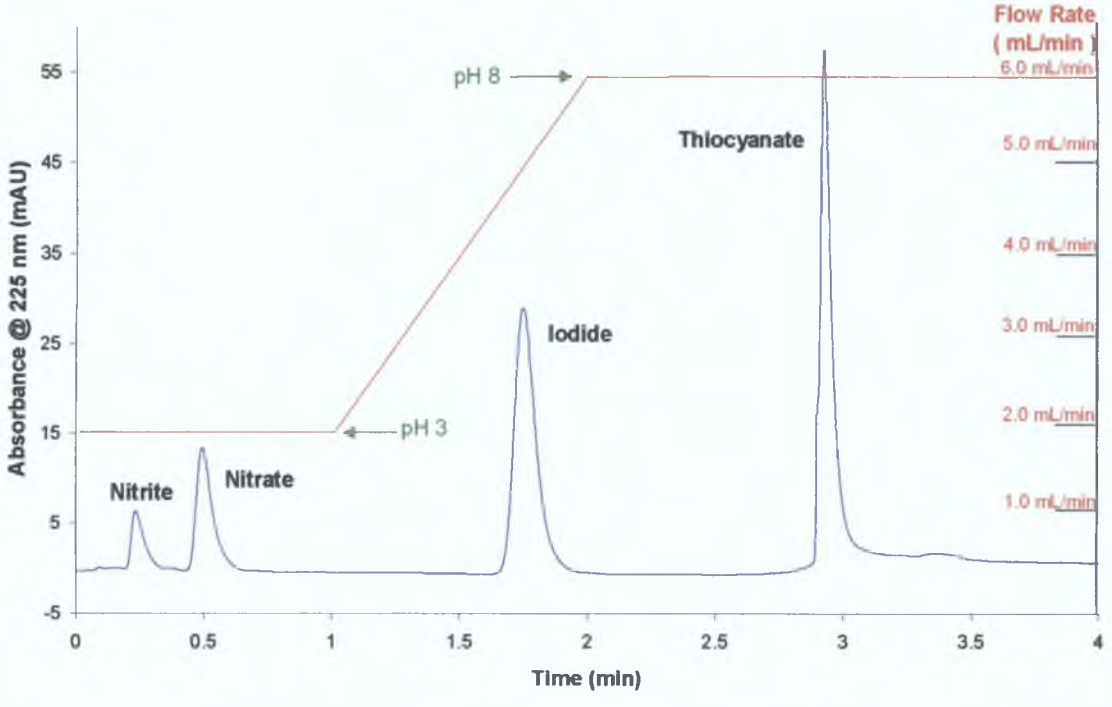

Figure 3.29. Chromatogram illustrating the separation of a mixture of nitrite, bromide, nitrate, iodide and thiocyanate obtained on a 1.0 cm carboxybetaine-modified C_{18} monolithic column, using an eluent composed of 1 mM KCl, with 0.2 mM dodecyldimethylaminoacetic acid, buffered at the required pH using 10 mM phosphate buffer. Dual gradient conditions: From t = 0 min to t = 1 min, eluent pH was 100% pH 3, with a constant flow rate of 2.0 mL/min; pH gradient (to 100% pH 8) and a flow gradient (to 6.0 mL/min) applied over 1 min (from t = 1 min to t = 2 min). Wavelength of detection: 225 nm. Analyte concentration: 0.05 mM (0.25 mM thiocyanate).

The robustness of the 1.0 cm carboxybetaine-modified silica monolith was then scrutinised by injecting the same standard (0.05 mM nitrite, nitrate and iodide) 50 times in sequence, and looking at the effect this had on the resulting retention times. An overlay of injections #1, #10, #20, #30, #40 and #50 is shown in Fig. 3.30. As Fig. 3.30 clearly demonstrates, the column coating is reasonably robust. Retention times for nitrite and nitrate did not fluctuate as the number of injections performed increased (with std. deviations of less than 2% for their retention times). Comparison of injection numbers 1 and 50 indicate that the iodide peak shifted downwards slightly, but not significantly so (as standard deviation of retention times for iodide was approximately 3.2%).

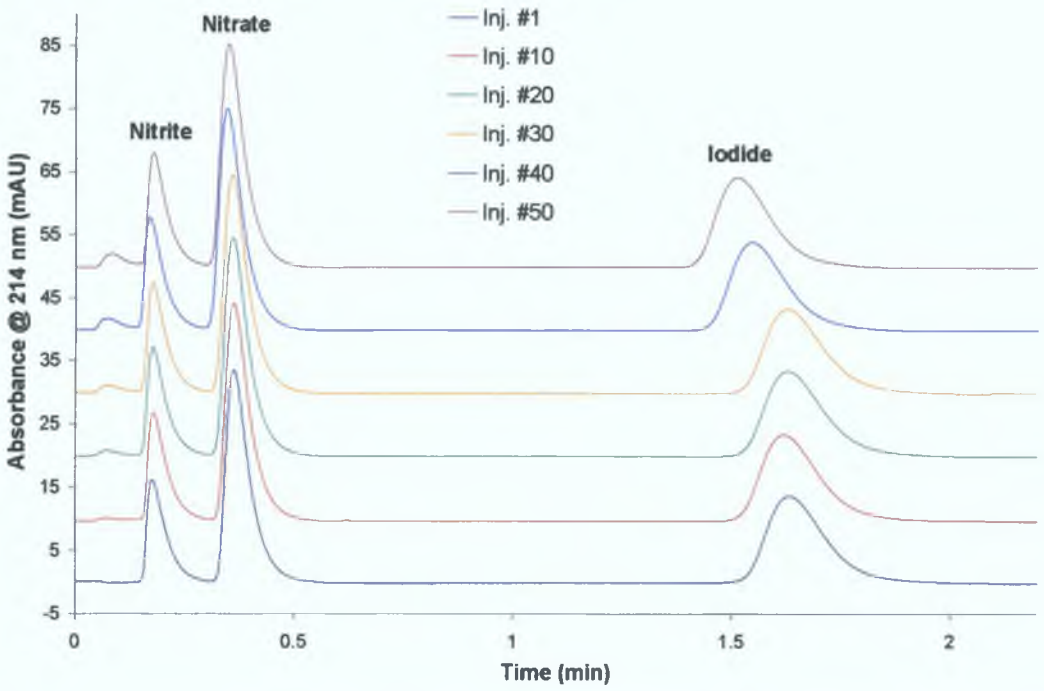

Figure 3.30. An overlay of sequential repeat injections #1, #10, #20, #30, #40 and #50, obtained using a 1.0 cm carboxybetaine-modified C_{18} monolith, using an eluent comprised of 1 mM KCl, with 0.2 mM dodecyldimethylaminoacetic acid, at pH 3. Flow rate: 3.0 mL/min. Wavelength of detection: 214 nm.

3.4 Conclusions

The use of C_{18} monolithic columns in zwitterionic ion chromatography has been shown to be of great potential in the truncation of analyte anion retention times. Carboxybetaine-modified monoliths were also found to have excellent prospects as a means of improving peak efficiencies of later eluting, large polarisable anions, such as

thiocyanate and iodide, through the use of elevated flow rates, and combined pH and flow gradients, which enable the stationary phase to act as an adjustable-capacity anion-exchanger, with increased eluent pH values causing capacity to decrease, thereby shortening runtimes significantly. The analytical methodology introduced in this Chapter has been seen to be applicable to the detection of nitrate and bromide in high ionic-strength samples, such as coastal and estuarine water samples, although the retention, and subsequent separation, of polar organic analytes (e.g. nucleoside bases) was less successful. It has been demonstrated that high efficiency, rapid ion chromatographic separations can be achieved using ultra-short (1.0 cm) monolithic anion-exchangers, which are compatible with flow gradient and double gradient (pH + flow) separations.

References:

1 N. Ishizuka, H. Kobayashi, H. Minokuchi, K. Nakanishi, K. Hirao, K. Hosoya, T. Ikegami, N. Tanaka, J. Chrom. A 960 (2002) 85-96.

2 N. Tanaka, H. Kobayashi, N. Ishizuka, H. Minakuchi, K. Nakanishi, K. Hosoya, T. Ikegami, J. Chrom. A 965 (2002) 35-49.

3 I. Gusev, X. Huang, C. Horváth, J. Chrom. A 855 (1999) 273-290.

4 H. Minakuchi, K. Nakanishi, N. Soga, N. Ishizuka, N. Tanaka, Anal. Chem. 68 (1996) 3498-3501.

5 S.M. Fields, Anal. Chem. 68 (1996) 2709-2712.

6 H. Zou, X. Huang, M. Ye, Q. Luo, J. Chrom. A 954 (2002) 5-32.

7 M. Al-Bokari, D. Cherrak, G. Guiochon, J. Chrom. A 975 (2002) 275-284.

8 K. Cabrera, J. Sep. Sci. 27 (2004) 843-852.

9 M. Kele, G. Guiochon, J. Chrom. A 960 (2002) 19-49.

10 N. Ishizuka, H. Minakuchi, K. Nakanishi, K. Hirao, N. Tanaka, Coll. Surf. A 187-188 (2001) 273-279.

11 F.C. Leinweber, U. Tallarek, J. Chrom. A 1006 (2003) 207-228.

12 B. Paull, P.N. Nesterenko, TRAC 24 (2005) 295-303.

13 P. Hatsis, C.A. Lucy, Analyst 127 (2002) 451-454.

14 E. Sugrue, P. Nesterenko, B. Paull, Analyst 128 (2003) 417-420.

15 P. Hatsis, C.A. Lucy, Anal. Chem. 75 (2003) 995-1001.

16 Q. Xu, K. Tanaka, M. Mori, M. Helaleh, W. Hu, K. Hasebe, H. Toada, J. Chrom. A 997 (2003) 183-190.

17 D. Connolly, D. Victory, B. Paull, J. Sep. Sci. 27 (2004) 912-920.

18 E. Sugrue, P.N. Nesterenko, B. Paull, J. Chrom. A 1075 (2005) 167-175.

19 P.N. Nesterenko, M.A. Rybalko, Journal of Analytical Chemistry 60 (2005) 349-354.

20 F. Houdiere, P.W.J. Fowler, N.M. Djordjevic, Anal. Chem. 69 (1997) 2589-2593.

21 P.N. Nesterenko, M.A. Rybalko, Mendeleev Commun. 14 (2004) 121-122.

22 K. Cabrera, D. Lubda, H.M. Eggenweiler, H. Minakuchi, K. Nakanishi, J. High Res. Chrom. 23 (2000) 93-99.

23 K. Deguchi, K. Kohda, M. Ito, J. Chrom. A 845 (1999) 165-170.

24 W. Hu, P.R. Haddad, K. Hasebe, H.A. Cook, J.S. Fritz, Fresenius J. Anal. Chem. 367 (2000) 641-644.

25 W. Hu, P.R. Haddad, H. Cook, H. Yamamoto, K. Hasebe, K. Tanaka, J.S. Fritz, J. Chrom. A 920 (2001) 95-100.

26 Ion Chromatography: Principles and Applications (J. Chrom. Library Vol. 46), P.R. Haddad and P.E. Jackson, 1st edition 1990, published by Elsevier Science Publishers B.V., Amsterdam.

27 H.A. Cook, W. Hu, J.S. Fritz, P.R. Haddad, Anal. Chem. 73 (2001) 3022-3027.

28 Z. Glatz, S. Nováková, H. Sterbová, J. Chrom. A 916(2001) 273-277.

29 Chromatography: Fundamentals and Applications of Chromatography and Related Differential Migration Methods, Part B: Applications, E. Heftmann, 5th edition 1992, Published by Elsevier Science Publishers B.V., Amsterdam.

30 Biochemistry, G. Zubay, 4th edition 1998, Published by Wm. C. Brown, Dubuque, IA, U.S.A.

31 C. Horvath, S.R. Lipsky, Anal. Chem. 41 (1969) 1227-1234.

32 W. Hu, K. Hasebe, D.M. Reynolds, H. Haraguchi, Anal. Chim. Acta 353 (1997) 143-149.

33 T. Umemura, K. Tsunoda, A. Koide, T. Oshima, N. Watanabe, K. Chiba, H. Haraguchi, Anal. Chim. Acta 419 (2000) 87-92.

34 A.V. Ivanov, P.N. Nesterenko, Journal of Analytical Chemistry 54 (1999) 494-510.

35 R. Kaliszan, P. Wiczling, M.J Markuszewski, Anal. Chem. 76 (2004) 749-760.

36 R. Kaliszan, P. Wiczling, Anal. Bioanal. Chem. 382 (2005) 718-727.

37 M.C. Bruzzoniti, E. Mentasti, C. Sarzanini, Anal. Chim. Acta 382 (1999) 291-299.

38 Y. Liu, D.J. Anderson, J. Chrom. A 762 (1997) 207-217.

39 D. Victory, P. Nesterenko, B. Paull, Analyst 129 (2004) 700-701.

Chapter 4

Separation of Common Inorganic Anions and Nucleoside Bases Using Monolithic Columns Modified with N-dodecyl-N,N-(dimethylammonio)undecanoate

4.1 Introduction

In Chapters 2 and 3 the zwitterionic reagent used to modify C_{18} chromatographic columns was the alkyl carboxybetaine-type surfactant dodecyldimethylaminoacetic acid. However, a drawback to the use of this surfactant was the poor stability of the column coating, which necessitated the inclusion of small amounts of the surfactant in the eluent, in order to combat column bleed and therefore stabilise column ion-exchange capacity. Therefore, in a bid to create a semi-permanent stationary phase for ZIC, a new surfactant was chosen, which would exhibit higher coating stability than the previously used surfactant, thus negating any requirement for inclusion within the eluent. The surfactant chosen was N-dodecyl-N,N-(dimethylammonio)undecanoate (DDMAU), the structure of which is outlined in Fig. 4.1 below:

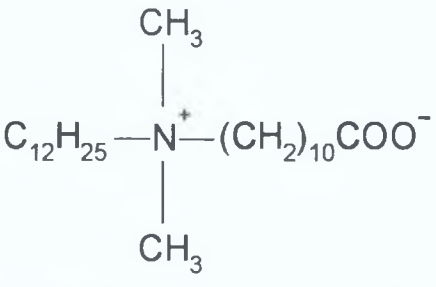

Figure 4.1. Structure of N-dodecyl-N,N-(dimethylammonio)undecanoate (DDMAU).

DDMAU has a similar structure to the previously employed dodecyldimethylaminoacetic acid, as they are both in possession of a similar C_{12} hydrophobic tail and a strong internal anion-exchange site (i.e. an ammonium group). However, they differ in the length of their methylene interchange arms, with DDMAU containing a C_{10} chain linking the anion-exchange site with a terminal carboxylic acid, while dodecyldimethylaminoacetic acid possesses only one methylene group in the same position. This additional C_9 chain has the effect of improving its coating stability on a reversed-phase column, although this particular zwitterionic surfactant has not previously been investigated for this purpose. It has been shown [1] that increasing the number of inter-charge methylene groups in carboxybetaine-type surfactants increases the total hydrophobicity of the zwitterionic molecule, which tends to lower the critical micelle concentration (cmc), as well as causing the charge separation in the zwitterionic head group to grow, thereby increasing the strength of the repulsive dipole-dipole interaction between headgroups at the interface.

Most of the references made to DDMAU in the available literature have involved the utilisation of DDMAU in the extraction of mycoplasma membrane protein antigens [2,3,4]. Mycoplasmas are pathogenic bacteria, the envelope of which is composed of only a plasma membrane [2]. Surfactants such as DDMAU play a prominent role in research into biological membranes, as they are necessary for the solubilisation of amphiphilic proteins, i.e. those proteins that are embedded within the lipid bilayer or attached to the bilayer by an acyl or a lipoyl moiety [2]. The usefulness of such zwitterionic surfactants stems from the fact that, like the major constituent of biological membranes, the phospholipid molecule, they contain a hydrophilic head and a hydrophobic tail [3]. They are able to compete with the lipids in a bilayer, while being more hydrophilic than the lipids, thus enabling the solubility of surfactant-protein complexes in aqueous solutions [4].

The objective for this Chapter of work was to use DDMAU to form a zwitterionic stationary phase for ion chromatographic separations of common UV-absorbing anions, without the need to add any amount of the surfactant itself to the eluent, or to regenerate the stationary phase coating at any stage.

4.2 Experimental

4.2.1 Instrumentation

The chromatographic system used was a Waters Model 600E Multisolvent Delivery System (Waters, Milford, MA, U.S.A.), fitted with a 20 µl injection loop, and coupled to a Shimadzu SPD-6AV UV-Vis Spectrophotometric Detector (Kyoto, Japan), monitoring at 214 nm. The pH of eluents was measured using an Orion Model 420 pH meter (Thermo Orion, Beverly, MA, U.S.A.) with a glass electrode, whilst the column outlet pH was monitored using a flow through pH electrode assembly (Sensorex, Garden Grove, CA, U.S.A.). Processing of chromatograms was carried out using a PeakNet 6.30 chromatography workstation (Dionex, Sunnyvale, CA, U.S.A.).

4.2.2 Reagents

The zwitterionic surfactant used to dynamically modify the stationary phase was N-dodecyl-N,N-(dimethylammonio)undecanoate (DDMAU) (Calbiochem, La Jolla, CA, U.S.A.). All other chemicals used were of analytical reagent grade, and were supplied

by Sigma-Aldrich (Tallaght, Dublin, Ireland). All eluents and standard solutions were prepared using deionised water from a Millipore Milli-Q water purification system (Bedford, MA, U.S.A.), and were filtered through a 0.45 μm filter and degassed by sonication. Dilute solutions of NaOH and HCl were used to adjust the pH of the eluents. For phosphate buffered eluents, the phosphate buffer solutions were prepared using monobasic, and dibasic, sodium phosphate (Sigma-Aldrich) and phosphoric acid (85%, Riedel-de Haën, Hanover, Germany), in the appropriate ratios to give the required eluent pH values. Citrate buffer eluents were prepared using the appropriate combinations of citric acid and sodium citrate (both from Sigma-Aldrich) to give the required eluent pH values.

4.2.3 Column Preparation

The silica-based monolithic separation columns used were Chromolith monolithic reversed-phase C_{18} columns (100 mm x 4.4 mm I.D., and 25 mm x 4.6 mm I.D., obtained from Merck (Darmstadt, Germany)). The columns were dynamically modified with the zwitterionic surfactant, by passing 100 mL of a 20 mM aqueous solution of DDMAU through the column at a flow-rate of 0.7 mL/min for a period of greater than 60 minutes. Following initial modification, the columns were then rinsed with Milli-Q water for approx. 45 minutes at a flow rate of 1.0 mL/min. Following this, the columns were conditioned with eluent until a steady baseline was achieved.

Monitoring of the column eluate absorbance during the modification procedure outlined above, allowed the ion-exchange capacity of the column to be calculated by means of the breakthrough method. It was found that for the 2.5 cm column, a coating of 157 μmol DDMAU was obtained.

4.3 Results and Discussion

4.3.1 Selectivity for Common Inorganic Anions

Initial experiments using the 10 cm DDMAU-modified C_{18} monolith utilised a simple eluent composed of 10 mM KCl, without the presence of any additional buffer or DDMAU. Retention times of several UV-absorbing anions (namely iodate, bromate, nitrite, bromide, nitrate, iodide and thiocyanate) were determined using this eluent composition. However, after carrying out consecutive injections using the freshly

modified column, it was found that retention times for all 7 test anions were increasing over time. This is not usually the case with dynamically modified columns, where initial column bleed while conditioning often causes a decrease in the observed retention times. An overlay of 4 repeat injections of a 1.0 mM mixture of the 7 aforementioned test anions, showing the steady increase in retention times for the analyte anions, can be seen in Fig. 4.2. This trend is particularly evident for the anions that were retained the longest, i.e. iodide and thiocyanate. In the case of iodide, retention time increased from approx. 6.0 minutes to approx. 9.0 minutes for identical sample solutions injected for the first and fourth time. For thiocyanate, retention time increased from approx. 24 minutes to approx. 34 minutes.

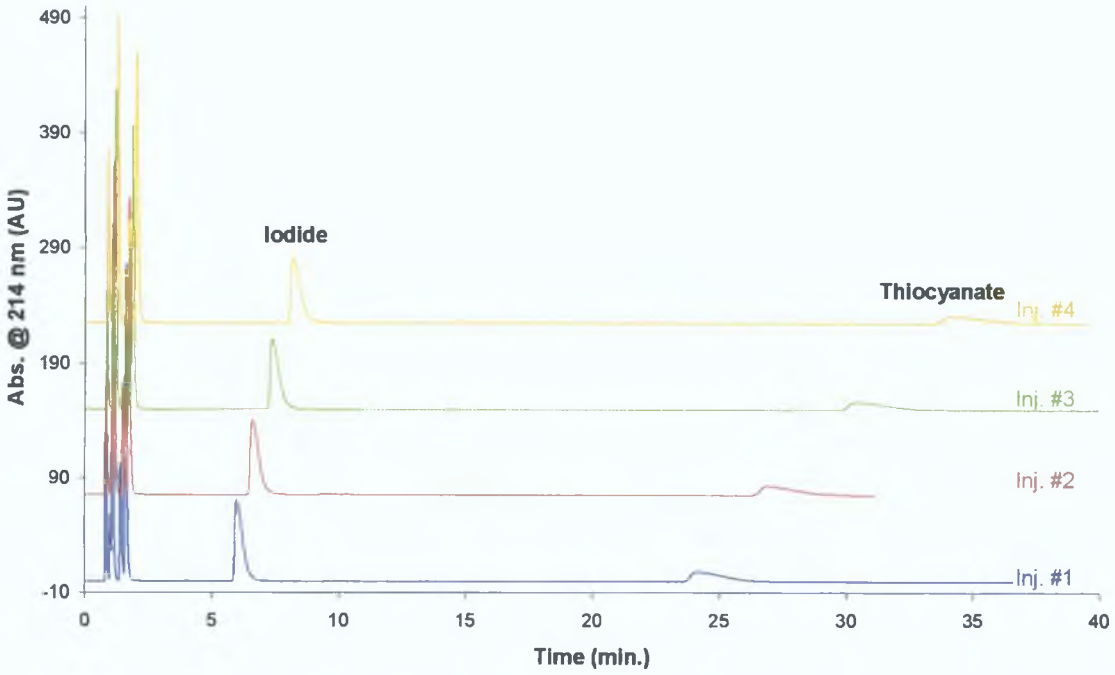

Figure 4.2. Overlays of 4 chromatograms of a 1.0 mM 7 anion mixture (iodate, bromate, nitrite, bromide, nitrate, iodide and thiocyanate) obtained in sequence on a 10 cm DDMAU-modified C_{18} monolithic column using an eluent comprised of 10 mM KCl, and UV detection at 214 nm. Flow rate: 2.0 mL/min.

At first, the effect outlined in Fig. 4.2 was thought to be due to a gradual change in the structural arrangement of the adsorbed surfactant. However, upon measuring of the eluent pH pre- and post-column it was established that this effect was predominantly due to significant column buffering, as the pH of the solution pre-column (pH 5.55) and post-column (pH 6.58) differed by 1 pH unit.

As a means of addressing the problem of unstable retention times, buffered eluents were used for subsequent experiments. An eluent containing 10 mM phosphate buffer (at pH 6.01) was prepared, and the same 1.0 mM mixture of iodate, bromate, nitrite, bromide, nitrate, iodide and thiocyanate was repeatedly injected. An example of one such separation achieved can be seen in Fig. 4.3. The previously observed continuous increase in retention of analyte anions was no longer apparent. Over 15 repeat injections, the % R.S.D. of the retention times for thiocyanate, for example, was 1.1 %. This would indicate that employing a buffered eluent system had the desired effect of overcoming the column buffering effects.

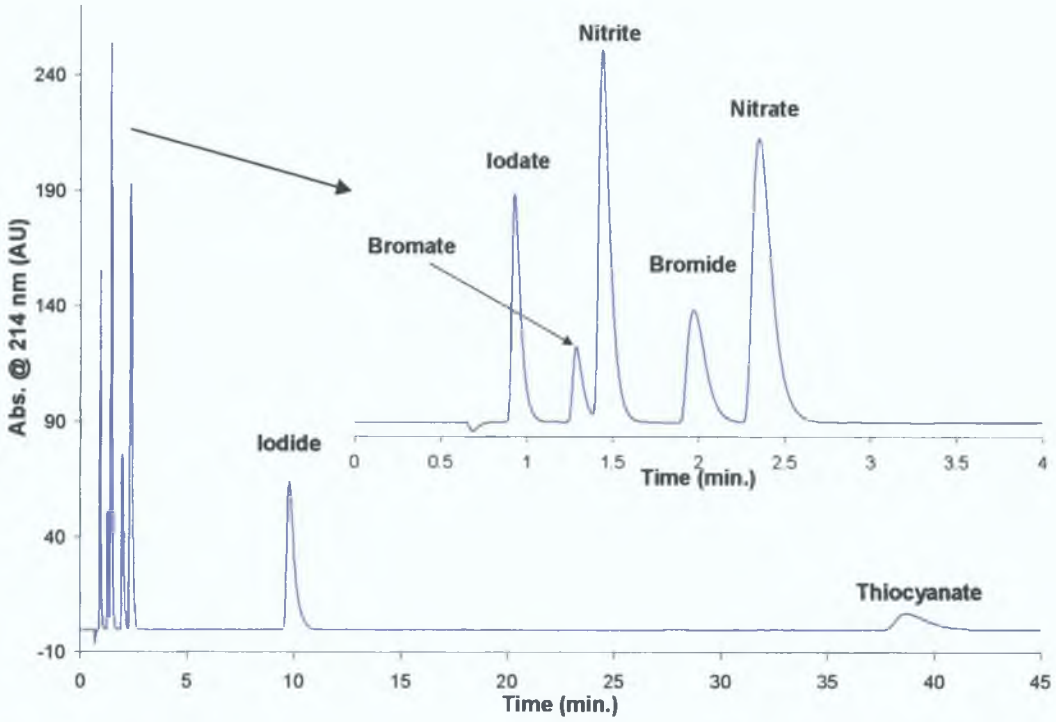

Figure 4.3. Chromatogram of a 1.0 mM mixture of iodate, bromate, nitrite, bromide, nitrate, iodide and thiocyanate obtained using a 10 cm DDMAU-modified C_{18} monolith, with 10 mM phosphate buffer at pH 6.01 as eluent, with UV detection at 214 nm. Flow rate: 2.0 mL/min.

4.3.2 Effect of pH on Anion Retention

4.3.2.1 pH Study using 10 cm Monolithic Column

A series of phosphate buffered eluents covering the pH range from 3.0 to 8.0 was prepared, and individual sample standards of iodate, bromate, nitrite, bromide, nitrate, iodide and thiocyanate injected at each pH value. The resulting chromatograms showed large decreases in anion retention between pH 3.0 and pH 6.0, while at pH

values greater than 6.5, only iodide and thiocyanate displayed a significant degree of retention. At the most acidic eluent pH values, some of the analyte anions exhibited very strong interaction with the DDMAU stationary phase. Taking thiocyanate as an example, it was found that at pH 3.0 thiocyanate was retained in excess of 240 minutes, compared to a mere 5 minutes at the highest pH investigated of pH 8.0. The peak shape for thiocyanate also improved considerably as eluent pH was increased. Even the earliest eluting anion, namely iodate, experienced a significant decrease in retention time as the eluent pH was increased from pH 3 to pH 8, i.e. from approx. 4.2 minutes to approx. 0.7 minutes. This reduction in retention times is shown in Fig. 4.4, which overlays the chromatograms obtained using eluents of pH 3.0 and 6.0, demonstrating that the run time for the early eluting group of anions (i.e. iodate, bromate, nitrite, bromide and nitrate) could be reduced from just under 40 minutes to approx. 2.0 minutes simply by increasing the eluent pH by 3 pH units. However, resolution of these same 5 anions was less than satisfactory at pH values in excess of pH 6.5.

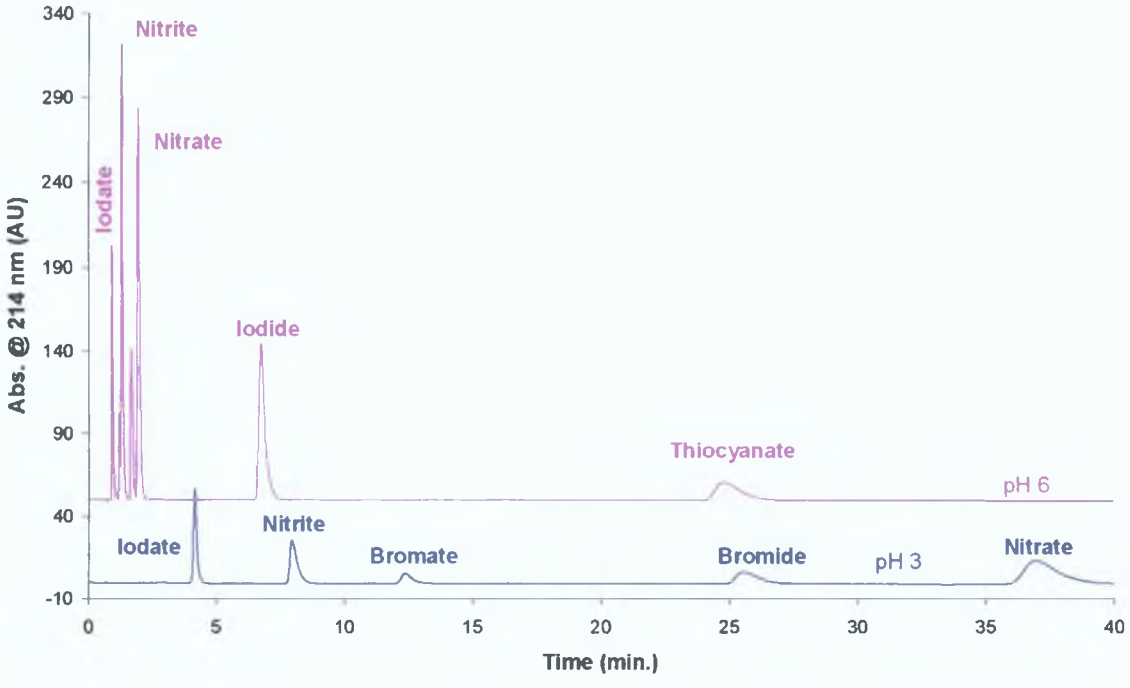

Figure 4.4. An overlay of chromatograms of a 1.0 mM mixture of iodate, bromate, nitrite, bromide, nitrate, iodide and thiocyanate obtained using a 10 cm DDMAU-modified C_{18} monolithic column, and an eluent composed of 10 mM sodium phosphate buffer at pH 3.0 (lower, blue trace) and pH 6.0 (upper, pink trace), with a wavelength of detection of 214 nm. Flow rate: 2.0 mL/min.

The pH data outlined above reflects the anticipated shielding effect of the dissociated terminal carboxylate groups on the DDMAU molecules, i.e. at acidic pHs the carboxylate groups located at the end of the DDMAU molecules remain associated, bringing about a reduction in the electrostatic repulsion experienced by analyte anions, thus affording the anions easier access to the internal ammonium sites of the DDMAU molecules, as outlined in Fig. 4.5. This results in the anions being retained for a longer period of time. The opposite occurs at more basic eluent pH values, where the terminal carboxylate groups dissociate, thus creating a negatively charged barrier, the movement across which is made more difficult for analyte anions because of the electrostatic repulsion witnessed by the anions due to the presence of the terminal negative charge. The magnitude of the observed pH effect is much greater than that seen in Chapter 3 using C_{18} monoliths modified with dodecyldimethylaminoacetic acid. As the primary difference between both carboxybetaine-type surfactants is the distance between the two charged sites, it was concluded that the shielding effect of the terminal carboxylic acid group is amplified as the distance between the charges is increased, which is as expected.

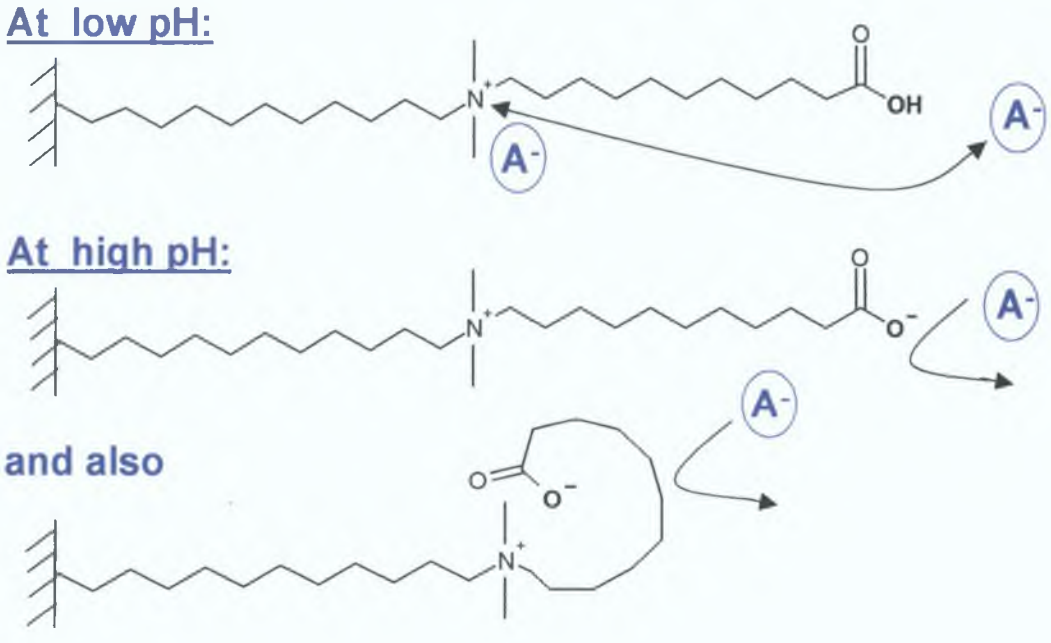

Figure 4.5. Schematic illustrating the shielding effect of the dissociated carboxylate groups of the DDMAU molecule, with decreased pH reducing the electrostatic repulsion experienced by analyte anions. (A^- represents an analyte anion.)

The exact relationship between anion retention and pH can be seen in Fig. 4.6, which shows plots of log k (retention factor) vs. eluent pH, with R^2 values for the logarithmic plots ranging from 0.9901 (for thiocyanate) to 0.9969 (for iodide), except in the case of iodate and nitrite, which had R^2 values of 0.9589 and 0.9785 respectively. This graph indicates a non-linear relationship between retention and pH, with an apparent sigmoidal curved response for most of the analyte anions. Performing first derivative analysis on the retention data suggested that the pI of the DDMAU stationary phase was approx. pH 6, with an expected pK_a value of pH 4.5 – 5.0. The slightly anomalous behaviour of nitrite under acidic conditions, which, at pH values below pH 4, sees the order of retention shift from 1 – iodate, 2 – bromate, and 3 – nitrite, to 1 – iodate, 2 – nitrite and 3 – bromate, is due to the formation of nitrous acid (pK_a = 3.15).

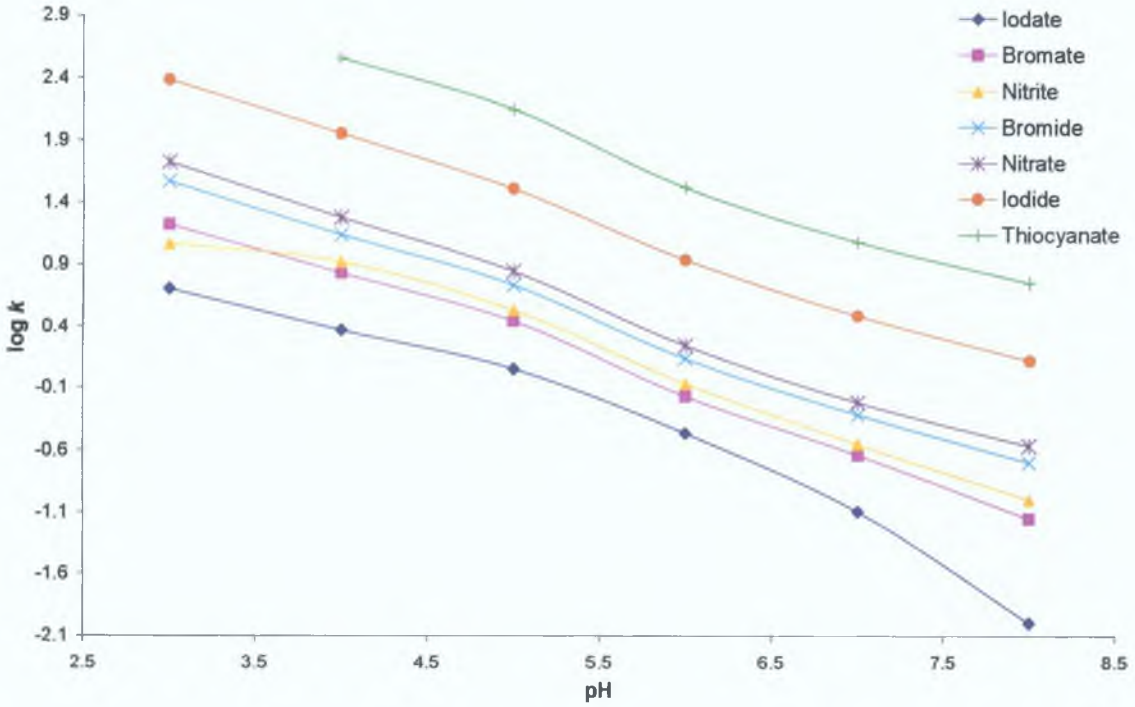

Figure 4.6. Plots of log k vs. eluent pH using a 10 cm DDMAU-modified C_{18} monolithic column, using data obtained with an eluent composed of 10 mM phosphate buffer, and a flow rate of 2.0 mL/min.

4.3.2.2 Separations Using 2.5 cm Monolithic Column

As was determined from the pH study conducted using the 10 cm DDMAU-modified C_{18} monolith, the more polarisable anions (namely iodide and thiocyanate) were retained for excessive amounts of time, even at relatively acidic eluent conditions. For example, the lowest eluent pH that enabled the satisfactory resolution of the early

eluting group of analyte anions (i.e. from iodate to nitrate) was pH 6. However, at this eluent pH iodide and thiocyanate did not elute until approx. 8.0 min and 25.0 min respectively. This suggested that a shorter monolithic column, also modified with DDMAU, could be used to determine all of the 7 test analyte anions within a shorter time frame. The shorter monolith also had the added advantage of lower column backpressures.

Therefore, a short 2.5 cm C_{18} monolith was modified with DDMAU in the same manner as for the 10 cm monolith, and evaluated for column selectivity and efficiency. As for the 10 cm column, retention decreased rapidly with increased pH, with thiocyanate eluting at approx. 170 minutes at pH 3, but eluting in less than 1 minute at pH 8. It was also observed that, because of the reduced ion-exchange capacity of the shorter monolith, optimal resolution of all seven anions of interest was achievable using a more acidic eluent than was previously used with the modified 10 cm C_{18} monolithic column, i.e. using an eluent pH of 4.0 rather than pH 6.0. The resulting chromatogram obtained using an eluent at pH 4.0 (with an overall runtime of just under 60 minutes) can be seen in Fig. 4.7. As can be seen from Fig. 4.7, iodide and thiocyanate were still excessively retained relative to the other test anions. Peak shapes and resolution of component peaks were more than satisfactory, as they were comparable to those seen in chromatograms obtained using the longer 10 cm monolith.

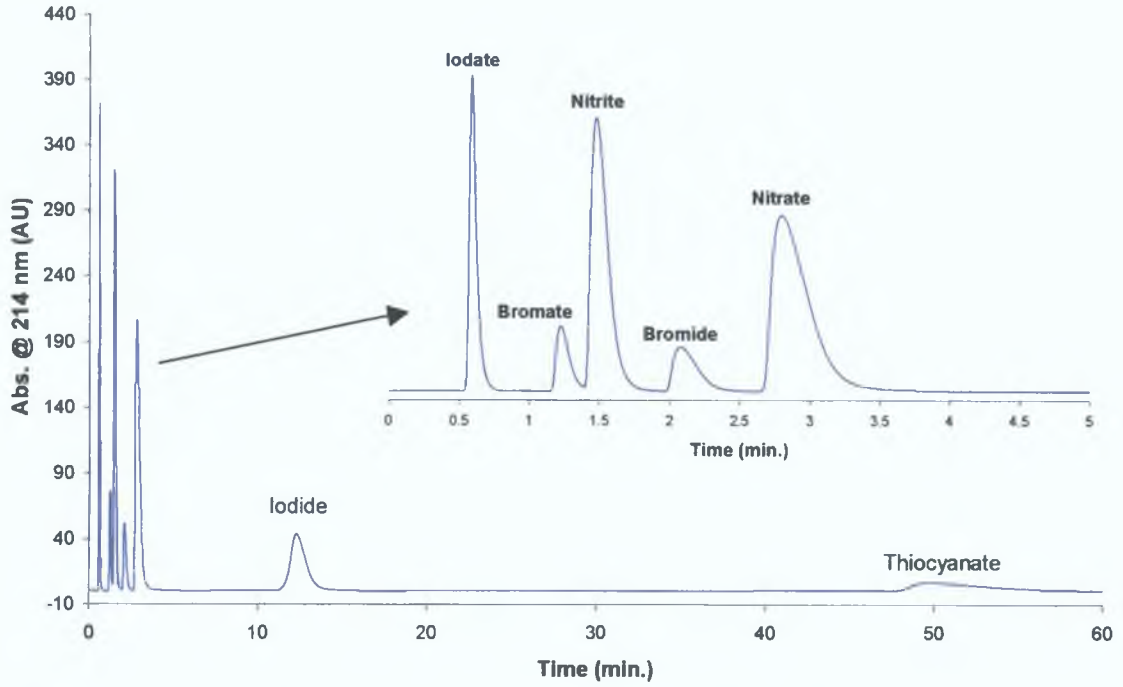

Figure 4.7. Chromatogram of a 1.0 mM mixture of iodate, bromate, nitrite, bromide, nitrate, iodide and thiocyanate obtained using a 2.5 cm DDMAU-modified C_{18} monolithic column and an eluent composed of 10 mM phosphate buffer at pH 4.0, with UV detection at 214 nm and a flow rate of 2.0 mL/min.

Comparison of the peak efficiencies calculated for injections made under identical chromatographic conditions (eluent: 10 mM phosphate buffer at pH 4.0; flow rate: 2.0 mL/min) illustrate how efficiency decreased by approx. 31% upon switching to the shorter DDMAU coated monolith, i.e. from an average peak efficiency of 41,721 N/m using the 10 cm monolith, to an average peak efficiency of 28,771 N/m using the 2.5 cm monolith. The individual calculated peak efficiency values are assembled in Table 4.1. Although the shorter column resulted in slightly less efficient peaks than those obtained using the longer column, baseline resolution was still readily achieved. In fact, despite the observed loss in efficiency upon shortening column length, the calculated peak efficiency values were nevertheless greater than, or comparable to, previous anion separations in ZIC, e.g. using a particle-packed column modified using the zwitterionic surfactant Zwittergent 3-14, Twohill and Paull reported values for N for nitrite and nitrate which corresponded to around 14,400 N/m and 16,200 N/m respectively [5].

Table 4.1. Comparison of efficiency values calculated for al 7 analyte anions using C_{18} monolithic columns of different lengths (10 and 2.5 cm) modified with DDMAU, employing an eluent composed of 10 mM phosphate buffer at pH 4.0.

Analyte Anion	*Efficiency Using 10 cm Monolith (N/m)*	*Efficiency Using 2.5 cm Monolith (N/m)*
Iodate	44,910	29,360
Bromate	54,290	31,240
Nitrite	53,920	27,920
Bromide	27,810	31,000
Nitrate	39,650	23,400
Iodide	49,270	30,520
Thiocyanate	22,200	27,960

4.3.3 Application of Combined pH and Flow Gradients

It was evident from the data presented in Fig. 4.7 that in order to obtain complete resolution of all 7 anions of the test mixture within a reasonable time frame, a gradient approach was required that would incorporate the significant effect of pH on anion retention. The fact that the column used was monolithic in nature also meant that the 2.5 cm DDMAU-modified C_{18} monolithic column would be suitable for use in conjunction with flow gradients (as seen for dodecyldimethylaminoacetic acid-modified columns in Chapter 3), owing to the high flow through porosity of the monolithic skeleton, which results in relatively low backpressures at elevated eluent flow rates.

The motivation behind the employment of a dual gradient, encompassing an eluent pH gradient, as well as an eluent flow rate gradient, can be summarised as follows:

- As seen in Section 3.3.2 in the previous Chapter, the effects of flow rate upon peak efficiency are not necessarily uniform for early and late eluting anions, and therefore the use of elevated flow rates outside the context of a gradient program would compromise the separation/resolution of the early eluting anions (i.e. iodate, bromate, nitrite, bromide and nitrate). Therefore, the application of a flow gradient from lower to higher flow rates mid-run would

maintain the efficiency and resolution of the aforementioned early eluting anions, while allowing the quicker elution of the later eluting anions (namely iodide and thiocyanate).

- It has already been discussed in Section 4.3.2 how an increase in eluent pH brought about a sizeable reduction in retention times. However, with the 2.5 cm monolithic column, the use of eluent pH values above pH 4 or 5 resulted in co-elution of the 5 early eluting anions. Therefore, increasing eluent pH mid-run would preserve the optimal resolution of the less retained analytes, while also shortening the retention times observed for iodide and thiocyanate.

- Therefore, combining both gradient approaches (i.e. eluent pH and flow rate) within a single dual gradient program would facilitate the baseline separation of the early eluting anions, while also greatly reducing the retention of iodide and thiocyanate.

The initial gradient conditions investigated utilised 2 phosphate buffer eluents of equal overall concentration (10 mM), one of which was at pH 4.0, and the other at pH 8.0. A linear gradient was programmed to switch from 100% pH 4.0 to 100 % pH 8.0 over 3 minutes (between t = 1.5 min and t = 4.5 min), while also simultaneously increasing flow rate in a linear fashion from 2.0 mL/min to 6.0 mL/min over the same time period. The resulting chromatogram can be seen as trace (A) in Fig. 4.8. As would be expected, this dual gradient did indeed result in a significantly reduced overall runtime, because of the earlier elution of the peaks corresponding to iodide and thiocyanate. Under isocratic conditions, and using an eluent pH of 4.0, the overall runtime was just under 60 min. However, upon application of the combined pH and flow gradient, the overall runtime for all 7 test anions was reduced to less than 5 minutes, a reduction of approx. 91.5%. This was achieved, as hoped, without hindering the resolution of the early eluting anions, while also bringing about a visible improvement in peak shape for thiocyanate.

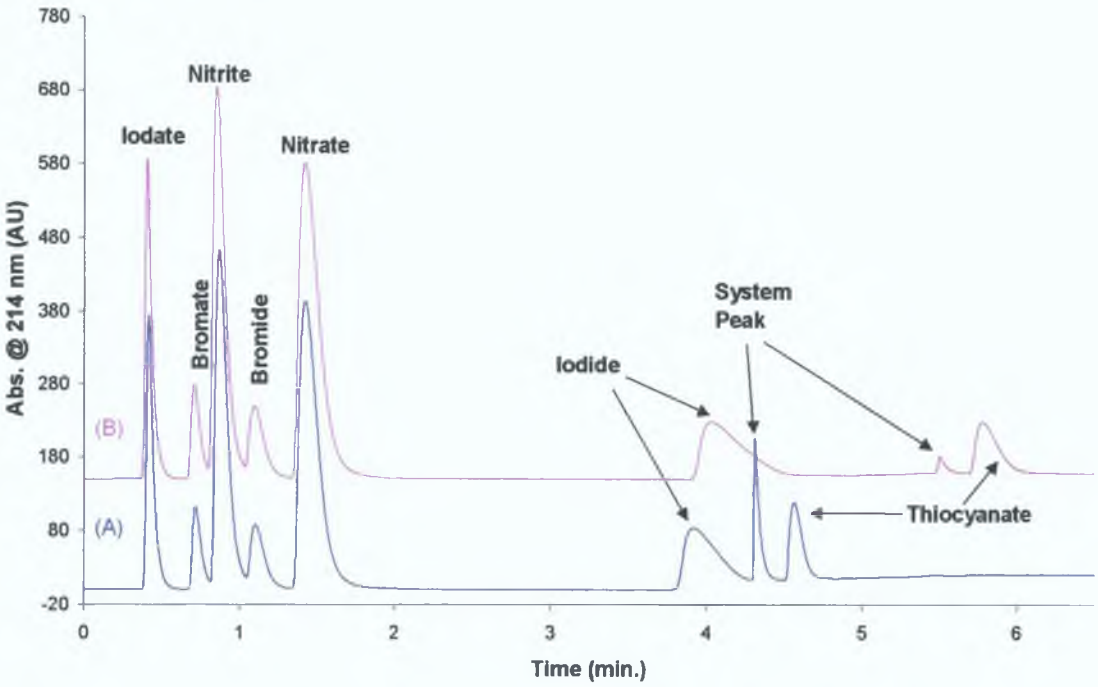

Figure 4.8. Overlaid chromatograms of a 1.0 mM 7 anion mixture (containing iodate, bromate, nitrite, bromide, nitrate, iodide and thiocyanate) obtained utilising a 2.5 cm DDMAU-modified C_{18} monolithic column, and using initial flow rates of 2.0 mL/min, and a starting 10 mM phosphate buffer eluent pH of 4.0, with the application of a linear dual gradient between 1.5 and 4.5 min. Gradient details: (A) – 100% pH 4.0 to 100% pH 8.0, and 2.0 mL/min to 6.0 mL/min; (B) – 100% pH 4.0 to 100% pH 6.0, and 2.0 mL/min to 6.0 mL/min.

However, as is apparent from trace (A) in Fig. 4.8, the applied dual gradient resulted in the presence of a large, sharp and intrusive system peak situated directly between the peaks corresponding to iodide and thiocyanate. Blank injections of Milli-Q water alone also resulted in an identical system peak being present. This implies that the cause of the observed system peak was a change in column ion-exchange capacity with the change in eluent pH. For example, as the eluent pH is increased, the related dissociation of the carboxylic groups of the DDMAU molecules creates a negatively charged barrier that will subject analyte anions to increased electrostatic repulsive effects, thereby reducing the effective anion-exchange capacity of the column. This decrease in ion-exchange capacity causes retained anions to be released from the stationary phase, many of which will be eluent anions, i.e. phosphate ions. The elution of these suddenly released ions will result in a disturbance in the baseline of the ensuing chromatogram. The magnitude of this system peak is related to the

absorbance of the eluent anions. This was confirmed through the substitution of the phosphate buffered eluents for other eluent systems, e.g. a citrate eluent. 1 mM citrate buffers were prepared at pH 4 and pH 6. (10 mM citrate buffers had a background absorbance that was off the scale of the detector using 214 as the wavelength of detection.) A blank sample, containing Milli-Q water alone was injected using the citrate eluent system, and subjected to a dual gradient program, with eluent pH increasing from 100% pH 4 to 100 % pH 6, and flow rate increasing from 2.0 mL/min to 6.0 mL/min. An overlay of the resulting chromatogram, illustrating the magnitude of the system peak, with a chromatogram obtained under identical gradient conditions utilising phosphate eluents can be seen in Fig. 4.9. It is obvious from these overlaid chromatograms that the dimensions of the system peak increased by several orders of magnitude, as citrate ions absorb more strongly at 214 nm than the phosphate eluent ions.

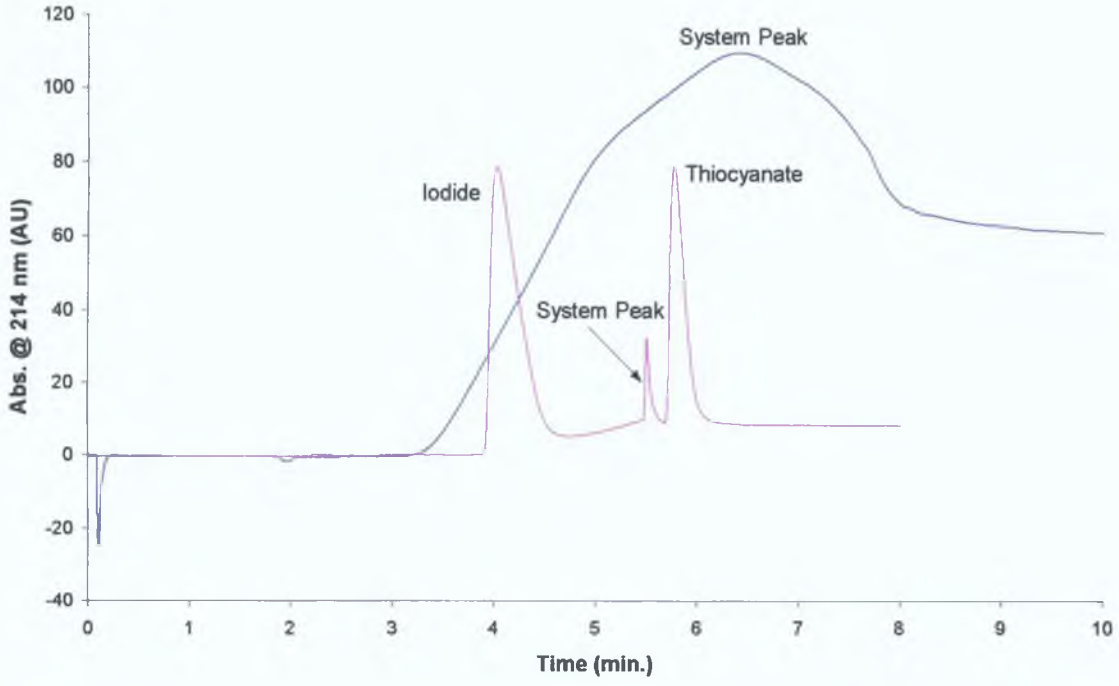

Figure 4.9. Chromatograms obtained using a dual gradient program (100% pH 4 to 100% pH 6, 2.0 mL/min to 4.0 mL/min) over 3 min (from t = 1.5 min to t = 4.5 min) using a 10 mM phosphate buffer eluent (pink trace) and a 1 mM citrate buffer eluent (blue trace). Column: 2.5 cm DDMAU-modified C_{18} monolithic column. Wavelength of detection: 214 nm. Samples injected: Milli-Q water (blue trace), and 1.0 mM iodide and thiocyanate (pink trace).

In an attempt to reduce the dimensions and possible interference of the system peak associated with the programmed dual gradient utilised with phosphate buffers as eluents, it was decided to reduce the end pH conditions of the pH gradient, i.e. the final pH of the gradient was lowered from pH 8.0 to pH 6.0. The resulting chromatogram can be seen as trace (B) in Fig. 4.8, in which it can be seen that reducing the end pH of the gradient resulted in the system peak eluting approx. 1.3 minutes later, and being considerably smaller in stature. The overall runtime was also increased by more than 1 minute. In an effort to regain the sub-5 minute runtime witnessed using the gradient applied in Fig. 4.8 (A), without subjecting the system to further disturbance, it was decided to increase the rate of the applied dual gradient. The start and end conditions remained the same, i.e. from 100% pH 4.0 to 100 % pH 6.0, and from 2.0 mL/min to 6.0 mL/min, but the gradient was applied over a shorter time period than before, i.e. over 0.5 min (from t = 1.5 min to t = 2.0 min) rather than 3 min (from t = 1.5 min to t = 4.5 min). The subsequent chromatogram is labelled as trace (B) in Fig. 4.9. This resulted in the desired decrease in the overall runtime to below 5 min, while also resulting in a system peak of almost identical proportions as for the chromatogram obtained when the gradient was applied across 3 min, as visualised by comparing traces (A) and (B) in Fig. 4.10.

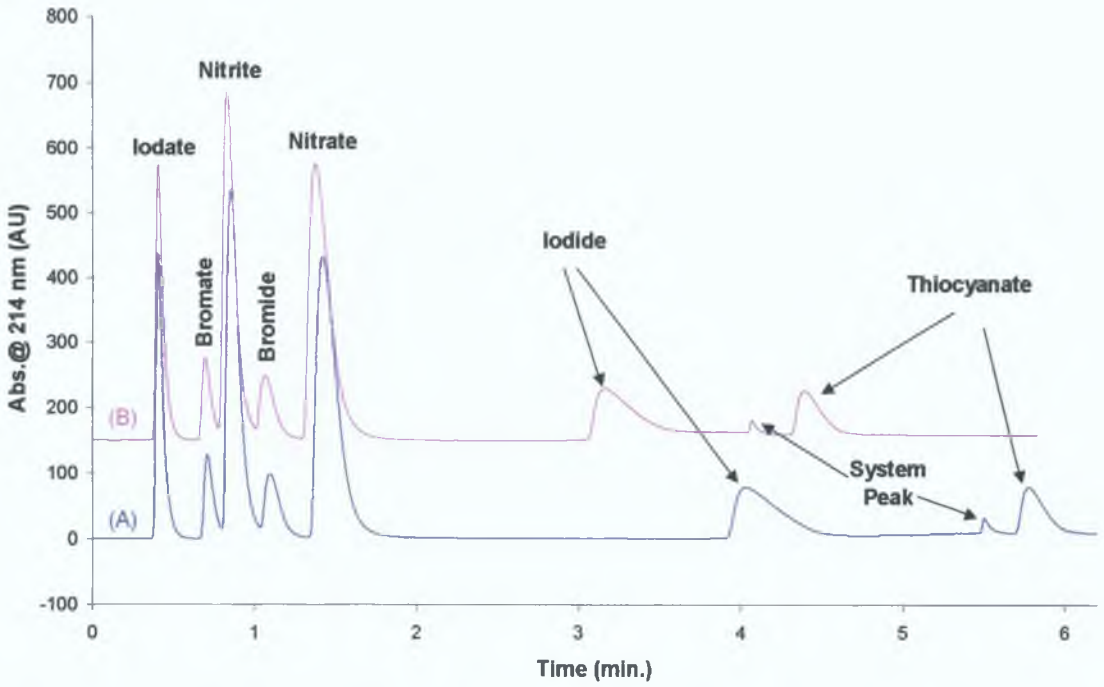

Figure 4.10. Overlaid chromatograms of a 1.0 mM 7 anion mixture (containing iodate, bromate, nitrite, bromide, nitrate, iodide and thiocyanate) obtained using initial flow rates of 2.0 mL/min, and a starting eluent pH of 4.0, with the application of a linear dual gradient at t = 1.5 min, with the end conditions of the gradient being an eluent pH of 6.0 and a flow rate of 6.0 mL/min. Rate of applied gradient: (A) – 1.5 to 4.5 min; (B) – 1.5 to 2.0 min. Column: 2.5 cm DDMAU-modified C_{18} monolithic column.

4.3.3.1 Analytical Performance of Dual Gradient Separation

(1) Reproducibility:

Multiple injections (n = 6) of a 1.0 mM mixture of iodate, bromate, nitrite, bromide, nitrate, iodide and thiocyanate were made, employing a combined eluent pH (100% 10mM phosphate buffer at pH 4.0 to 100% 10 mM phosphate buffer at pH 6.0) and flow (2.0 mL/min to 6.0 mL/min) gradient from 1.5 to 4.5 min. In between each successive injection, the chromatographic system was re-equilibrated with the initial eluent conditions for 20 min at a flow rate of 2.0 mL/min. The resultant data regarding retention time reproducibility is shown in Table 4.2. As is clear from this set of data, the % RSD for all seven analyte anions was below 4%, with the two anions most affected by the applied dual gradient, i.e. iodide and thiocyanate, displaying particularly impressive reproducibility, with % RSD values of 0.7% and 0.1% respectively.

Table 4.2. Mean, standard deviation and % RSD values of retention times of all 7 analyte anions (n = 6), using a combined eluent pH and flow gradient from 1.5 to 4.5 min.

Analyte Anion	*Mean Ret. Time (min)*	*Std. Dev. Of Ret. Time (min)*	*% RSD*
Iodate	0.53	0.017	3.2
Bromate	0.96	0.037	3.8
Nitrite	1.09	0.038	3.5
Bromide	1.52	0.047	3.1
Nitrate	1.95	0.036	1.9
Iodide	4.54	0.034	0.7
Thiocyanate	5.53	0.008	0.1

(2) Limits of Detection:

To determine the limits of detection (L.O.D.) for iodide and thiocyanate upon application of the same dual gradient used previously for the investigation of reproducibility, a 0.02 mM mixture of both analytes was injected, as was a sample blank (100% Milli-Q water), which was also subjected to the same gradient conditions. The heights of the analyte peaks and the distance between the upper and lower amplitudes of the baseline noise for the blank injections were compared, and the results for L.O.D. calculated using: L.O.D. = 3 x baseline noise. (In the case of iodate, bromate, nitrite, bromide and nitrate a 0.005 mM standard solution was used for the determination of their respective L.O.D. values.) The results of these calculations are summarised within Table 4.3.

Table 4.3. Limits of detection for analyte anions, employing a dual gradient applied between 1.5 min and 4.5 min of the chromatographic run time, using UV absorbance detection at 214 nm. Gradient details: 10 mM phosphate buffer as eluent, from 100% pH 4.0 to 100% pH 6.0, and 2.0 mL/min to 6.0 mL/min flow rate.

Analyte Anion	*L.O.D. (μM)*	*L.O.D. (ppm)*
Iodate	0.72	0.13
Bromate	5.10	0.65
Nitrite	0.97	0.04
Bromide	1.85	0.15
Nitrate	0.97	0.06
Iodide	6.66	0.83
Thiocyanate	3.84	0.22

(3) Linearity:

A range of low concentration standards (5 various concentrations between 0.005 mM and 1.0 mM) of the 7 anion test mixture were prepared, and analysed in triplicate, again using a dual gradient program (2.0 mL/min to 6.0 mL/min, and 10 mM phosphate buffer as eluent from 100% pH 4.0 to 100% pH 6.0) applied between 1.5 and 4.5 min of the chromatographic run time. Table 4.4 contains the R^2 values for the linear trendlines obtained for all 7 analyte anions. As Table 4.4 demonstrates, the observed trendlines were highly linear, as the lowest R^2 value was 0.9989 (for iodide), with the mean R^2 value being equal to 0.9993.

Table 4.4. Linearity data for all 7 analyte anions obtained using dual gradient program. Dual gradient details: Same as for Table 4.3.

Conc. Injected (mM)	*Iodate Peak Area*	*Bromate Peak Area*	*Nitrite Peak Area*	*Bromide Peak Area*	*Nitrate Peak Area*	*Iodide Peak Area*	*Thiocyanate Peak Area*
0.005	0.1202	0.0259	0.1587	0.0345	0.2507	0.0464	0.4358
0.01	0.2304	0.0550	0.3159	0.0768	0.4541	0.0851	0.7563
0.02	0.4759	0.1154	0.6798	0.1970	1.1338	0.2035	0.8266
0.1	2.9230	0.6417	4.7869	1.2704	6.2387	1.1771	1.9194
1.0	22.8666	4.9983	41.7237	10.3507	51.8039	8.8884	11.8667
R^2	*0.9992*	*0.9992*	*0.9997*	*0.9994*	*0.9996*	*0.9989*	*0.9991*

4.3.4 Monitoring of pH of Column Eluate

To investigate both the pH dependent ion-exchange capacity behaviour of the DDMAU-modified C_{18} monolithic column, and the origins of the system peak observed during application of pH gradients, the rate of change of the pH of the column eluate was monitored during the application of a pH gradient, such as those outlined in Section 4.3.3. This was accomplished through the use of a flow through pH detector cell (seen in Fig. 4.11) connected to the column outlet, before column eluate was vented to waste.

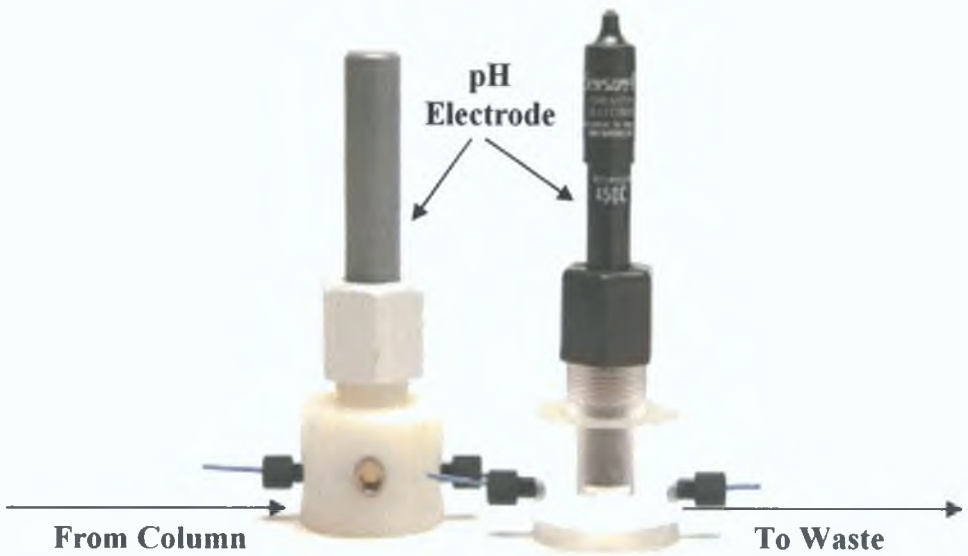

Figure 4.11. Schematics of the exterior and the interior of the flow through pH electrode assembly used to measure pH of the column eluate [6].

Using 10 different pre-programmed gradient profiles, ranging from convex to linear to concave, the pH of the column eluate in each case was monitored over the runtime of the injections in question, utilising a constant flow rate of 4.0 mL/min. The resulting plots of pH vs. time for the linear gradient profile, the most extreme convex gradient profile and the most extreme concave gradient profile can be seen in Fig. 4.12. The results obtained showed that the DDMAU-modified column exhibited a considerable buffering capacity, as can be seen from the shape of the pH response. Initially, as the column eluate response showed signs of a variation in pH, the change in eluate pH was gently sloped, with pH increasing slowly by approx. 0.2 pH units, before the change in pH suddenly became more rapid until the end pH value of approx. pH 6 was reached. The reason for this observed pH profile is that the column maintains the

starting pH conditions until the buffering capacity of the column (owing to the presence of the weak acid group) is consumed. This is then followed by a more rapid increase in eluate pH, the timing of which corresponds approximately to the observed system peak seen in the corresponding chromatogram.

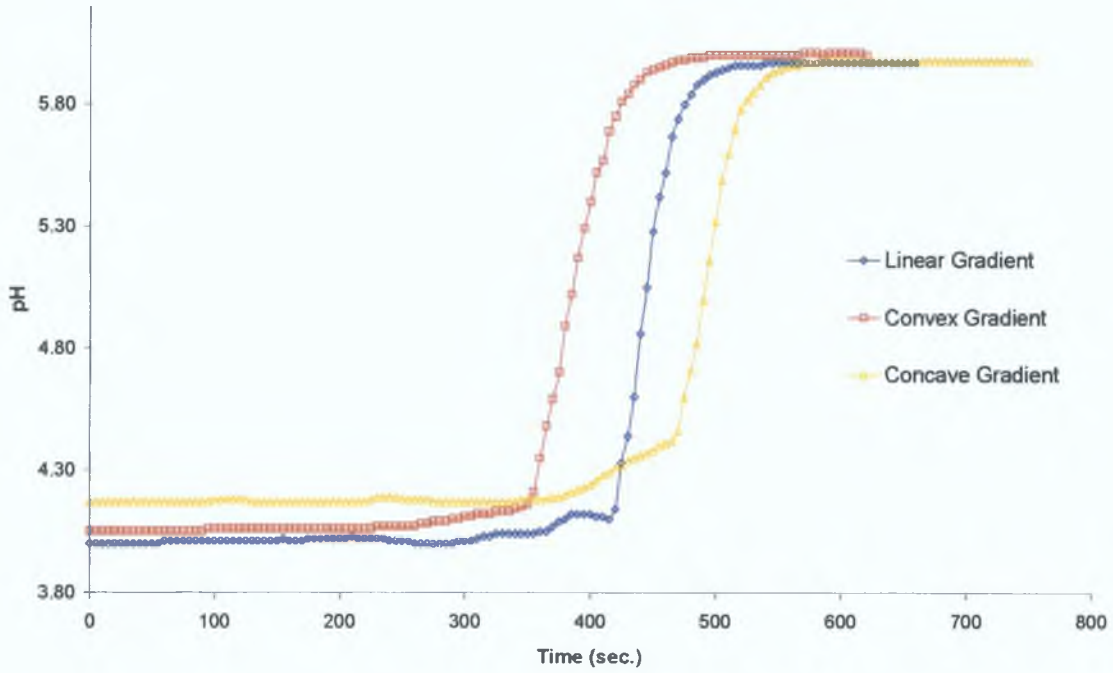

Figure 4.12. Column outlet pH values determined during the application of a pH gradient (100% pH 4.06 to 100% pH 6.02 over 1.5 – 4.5 min) using linear (blue trace), convex (red trace) and concave (yellow trace) gradient profiles. Flow rate: 4.0 mL/min. Column: 2.5 cm DDMAU-modified C_{18} monolithic column.

Adjusting the slope of the gradient (i.e. applying identical pH gradient conditions across smaller timeframes; 1 and 2 min compared to the previously employed 3 min gradient program) had very little effect on the pH profile of the column eluate, as is clear from Fig. 4.13. The shape of eluate pH response remained virtually identical, but the onset of the rapid increase in pH was delayed slightly. It was noted that as the end pH condition of the gradient was reached earlier, the buffering capacity of the column was saturated at an earlier stage, e.g. approx. 100 seconds earlier for the 1 min gradient when compared to the 3 min gradient program. Changing the time span of the pH gradient applied did not cause the system peak to alter significantly, but merely to appear approx. 1 – 1.5 min earlier in the subsequent chromatogram.

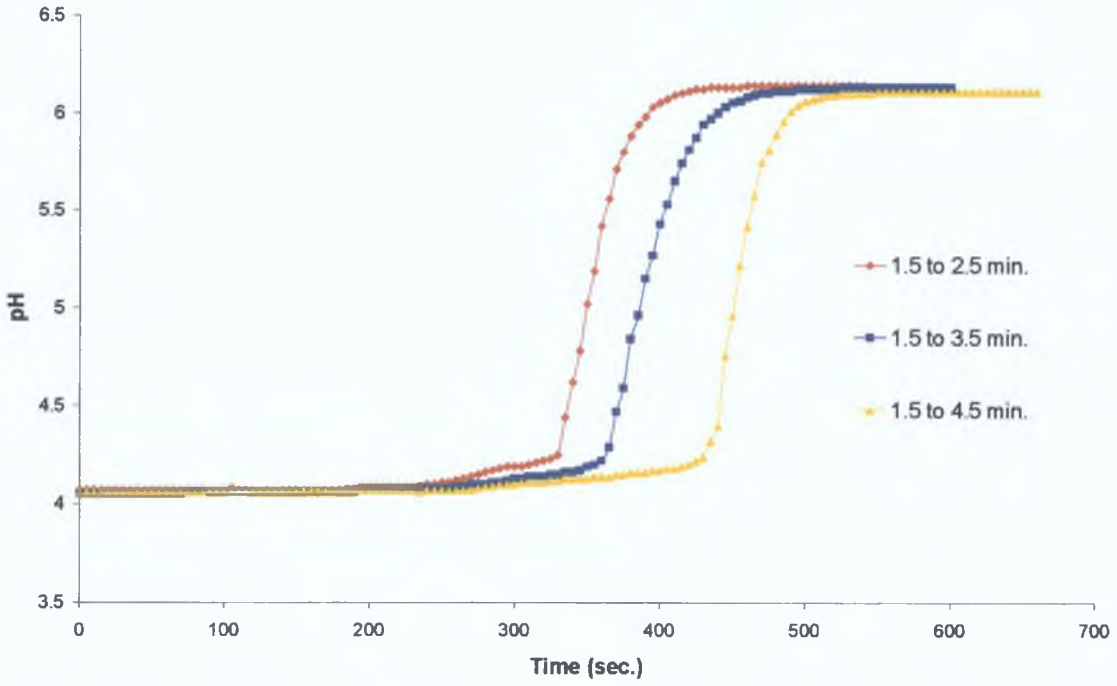

Figure 4.13. Column outlet pH values determined during the application of a linear pH gradient (100% pH 4.02 to 100% pH 6.04) over 1.5 to 2.5 min (red trace), 1.5 to 3.5 min (blue trace) and 1.5 to 4.5 min (yellow trace). Flow rate: 4.0 mL/min. Column: 2.5 cm DDMAU-modified C_{18} monolithic column.

To investigate whether adjusting the start and end pH conditions of the pH gradient would have a significant effect on the profile of column eluate pH, sodium phosphate eluents at pH 3.1 and pH 7.0 were used in place of the eluents at pH 4.0 and pH 6.0. A linear gradient was employed, which would begin at t = 1.5 min and end at t = 4.5 min, as used for the blue trace in Fig. 4.12 and the yellow trace in Fig. 4.13. Typical results for the monitoring of the eluate pH for such a pH gradient are displayed as the blue trace in Fig. 4.14. This plot indicates that the general outline of the pH curve obtained remained the same, when compared to the data obtained using the previous eluent pH values, but that the scale of the response was greater (due to a larger difference between the start and end pH values, i.e. around 4 pH units vs. 2 pH units) and more perceptible and pronounced in appearance. The rapid increase in eluent pH following consumption of column buffering capacity, familiar from previous eluent pH profiles, was also observed to occur sooner using the eluents at pH 3 and pH 7 than when the eluents at pH 4 and pH 6 were utilised, but the monitored pH was seen to level off almost simultaneously.

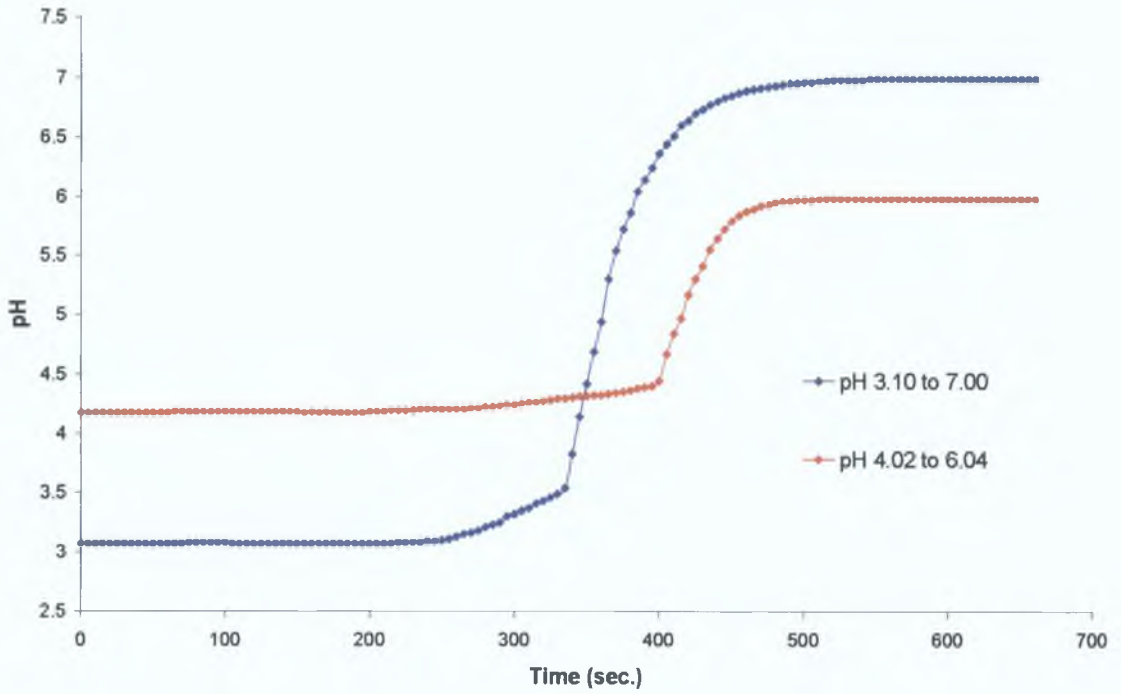

Figure 4.14. Column outlet pH values determined during the application of a linear pH gradient over 1.5 to 4.5 min. Gradient details: 10mM phosphate buffer eluent pH gradient from 100% pH 3.1 to 100% pH 7.0 (blue trace), and from 100% pH 4.02 to 100% pH 6.04 (red trace). Column: 2.5 cm DDMAU-modified C_{18} monolithic column. Flow rate: 4.0 mL/min.

4.3.4.1 Determination Of Effective Column Capacity

As a means of distinguishing between column buffering, from which effective column ion-exchange capacity could be calculated, and system dwell volume (V_{dwell}), a modified version of an experiment referred to in recent literature by Hendriks *et al.* [7] was undertaken. The column in the chromatographic set-up was replaced with a union, leaving the sample injector connected directly to the UV detector through an eluent pH probe. A step gradient (i.e. switching to end conditions of gradient program immediately) was run, starting at 0.5 min, going from initial low eluent pH conditions (pH 4) to an eluent of higher pH (pH 6), at a single uniform flow rate. The experiment was carried out in duplicate, at 2 different flow rates, 2.0 mL/min and 4.0 mL/min. The pH of the column eluate was monitored as the step gradient was applied, and the resulting graphs of pH vs. time can be seen in Fig. 4.15.

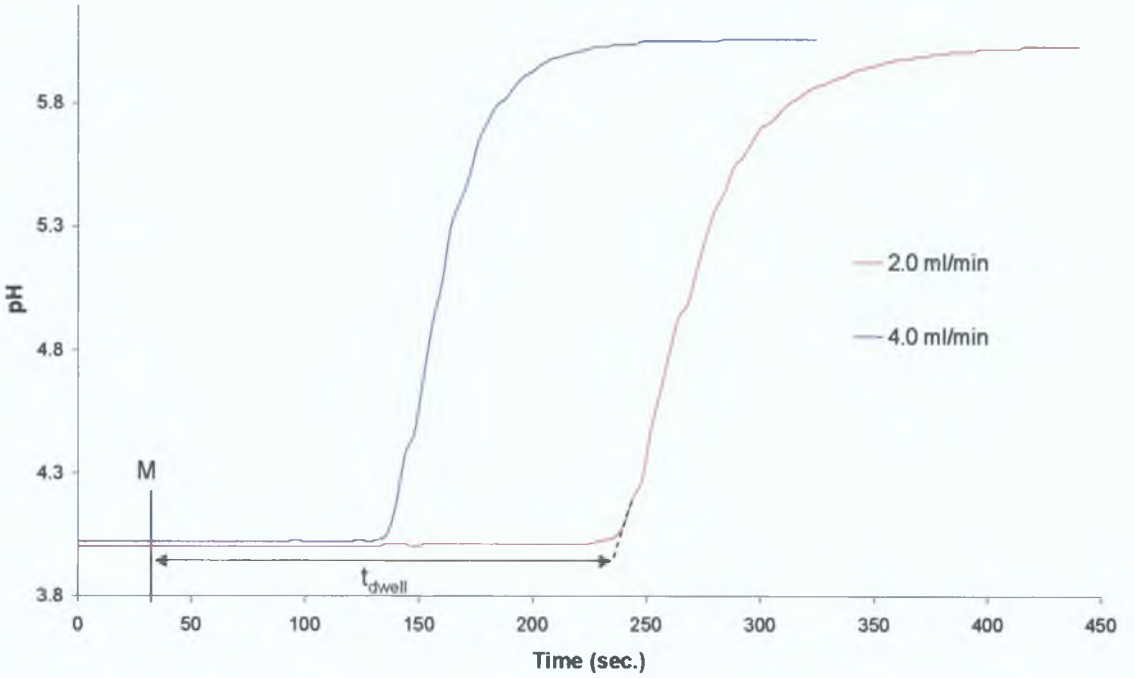

Figure 4.15. Column outlet pH measured during application of a step gradient (100% pH 4 to 100% pH 6) initialised at t = 0.5 min, at both 2.0 ml/min (red trace) and 4.0 mL/min (blue trace). M = mark indicating point of application of the step gradient; t_{dwell} = dwell time of system. Column: 2.5 cm DDMAU-modified C_{18} monolithic column.

The dwell time, t_{dwell}, is the time from the point of inception of the eluent step gradient to the tangent that extends through the inflection point of the curved area of the pH plot, as shown in Fig. 4.14. The dwell volume, V_{dwell}, can be calculated by multiplying the dwell time by the eluent flow rate, F:

$$V_{dwell} = t_{dwell}F \qquad \text{(Eqn. 4.1)}$$

Using this equation the calculated values for V_{dwell} were found to be 7.00 mL (at the 2.0 mL/min flow rate) and 7.06 mL (at the 4.0 mL/min flow rate), giving an average V_{dwell} of 7.03 mL.

Repeating this experiment with the column attached allowed confirmation and calculation of the buffering capacity of the column, and thus its effective anion-exchange capacity. A comparison of the column eluate pH using a pH gradient between 1.5 and 4.5 min, both with the column in place, and with a union substituting

for the column, can be seen in Fig. 4.16. Taking the concentration of the phosphate buffer eluent (10 mM) and the flow rate of 4.0 mL/min into account, the effective ion-exchange capacity of the modified monolith was determined to be 112 μmol of DDMAU, which is below the experimentally determined value of 157 μmol of DDMAU calculated for the column coating. This was anticipated, as not all the DDMAU molecules bound to the reversed-phase substrate will be available to participate in the anion-exchange process.

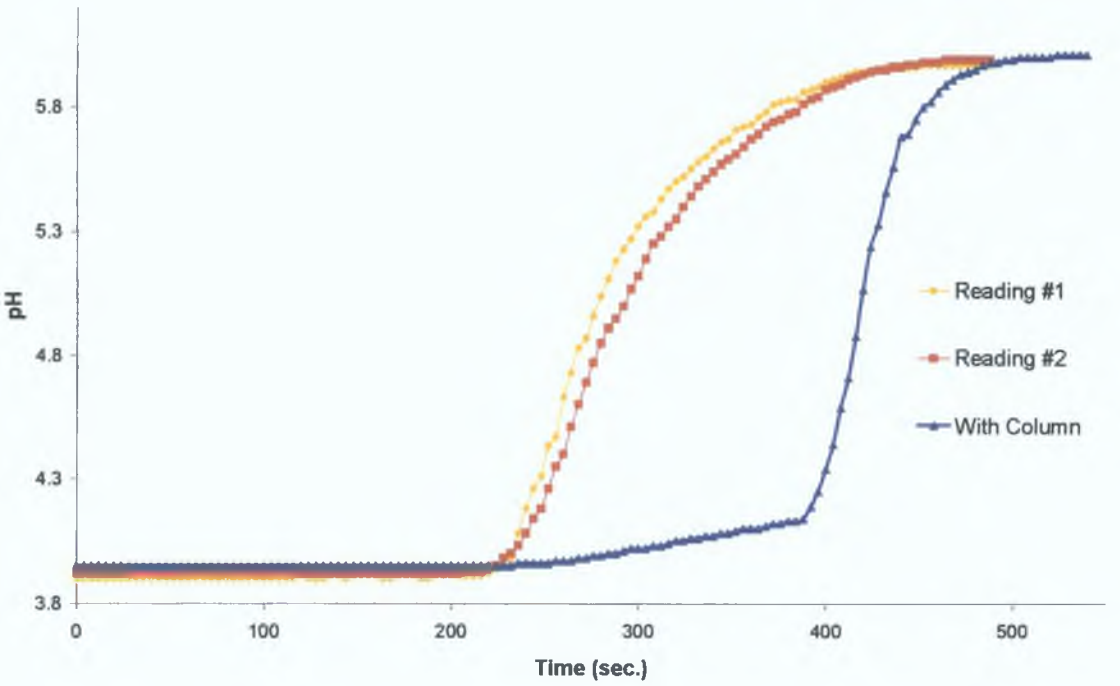

Figure 4.16. Column outlet pH measured during application of a linear pH gradient (100% pH 4 to 100% pH 6) from 1.5 to 4.5 min, using a flow rate of 4.0 mL/min, both with (blue trace) and without the column in place (yellow and red traces). Column: 2.5 cm DDMAU-modified C_{18} monolithic column.

The point of inflection of the pH curve obtained when the column was attached to the chromatographic system (see blue trace of Fig. 4.16), corresponded, in time, to the appearance of the small system peak within the chromatogram, after taking the duration of the system dwell time into consideration.

4.3.5 Anion Selectivity Study

The selectivity of the DDMAU-modified C_{18} monolith for other UV absorbing anions was investigated. Utilising a 10 mM phosphate buffer (at pH 4.07) as the eluent, and a 4.0 mL/min flow rate, several UV absorbing anionic species were injected (at the 1.0 mM level), and detected at a wavelength of 214 nm. (Citrate was also injected, but, after 60 min, was undetected across injections of various concentrations.) The results are summarised in Table 4.5.

Table 4.5 Retention data for 1.0 mM standard solutions of all anionic species injected, using a 2.5 cm DDMAU-modified C_{18} monolithic column, with 10 mM phosphate buffer (at pH 4.07) as eluent, and a flow rate of 4.0 mL/min. Wavelength of detection: 214 nm.

Analyte Anion	Ret. Time (min)	Ret. Factor, *k*	Peak Area
Acetate	0.189	0.57	0.11
Iodate	0.257	1.14	11.73
Formate	0.343	1.86	0.09
Bromate	0.506	3.21	3.06
Nitrite	0.599	3.99	19.32
Bromide	0.843	6.02	4.36
Nitrate	1.097	8.14	35.58
Tungstate	1.156	8.63	0.07
Chlorate	1.853	14.44	0.60
4-Hydroxybenzoate	2.134	16.78	43.87
Iodide	4.502	36.52	36.18
Chromate	5.059	41.16	3.20
Thiocyanate	17.33	143.44	13.06
Phthalate	40.130	333.42	56.22

Some sample chromatograms of the additional anions investigated can be seen in Fig. 4.17 (acetate, formate, tungstate and chlorate) and in Fig. 4.18 (4-hydroxybenzoate, chromate and phthalate). The concentration of each standard injected was 1.0 mM. Injection of phthalate (see Fig. 4.18) resulted in a large, broad peak at approx. 42 min, which is almost 25 min longer than the retention time for thiocyanate.

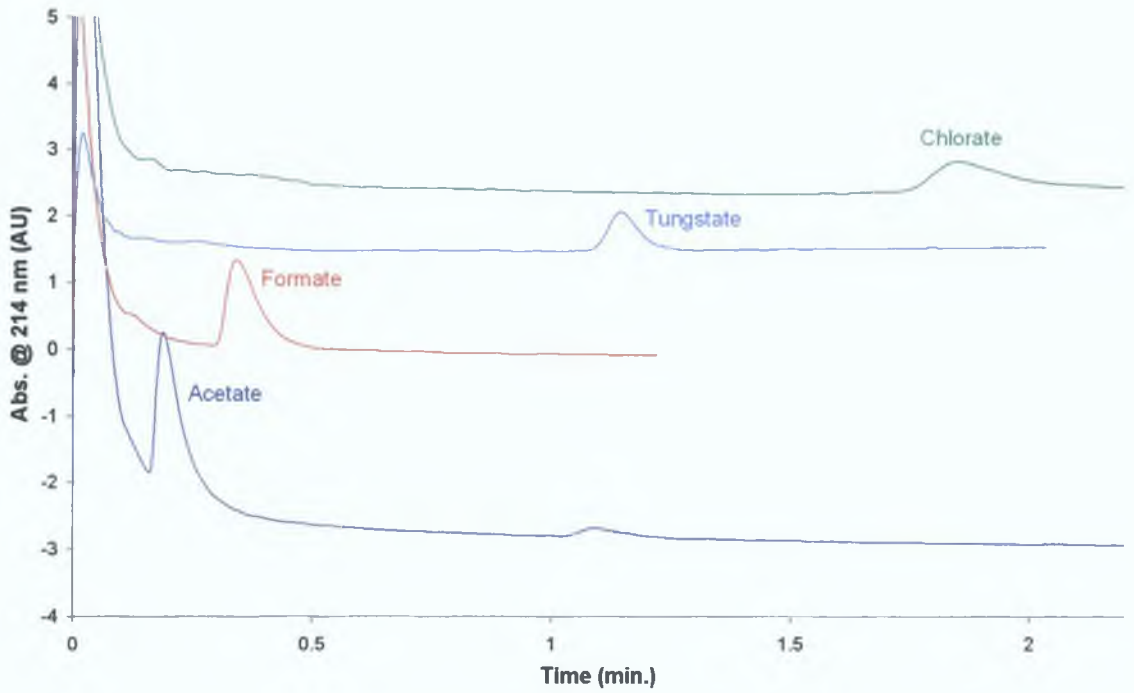

Figure 4.17. Chromatograms illustrating the retention of acetate (dark blue trace), formate (red trace), tungstate (light blue trace) and chlorate (green trace) on a 2.5 cm DDMAU-modified C_{18} monolithic column, employing 10 mM phosphate buffer (at pH 4.07) as eluent and a flow rate of 4.0 mL/min. Wavelength of detection: 214 nm.

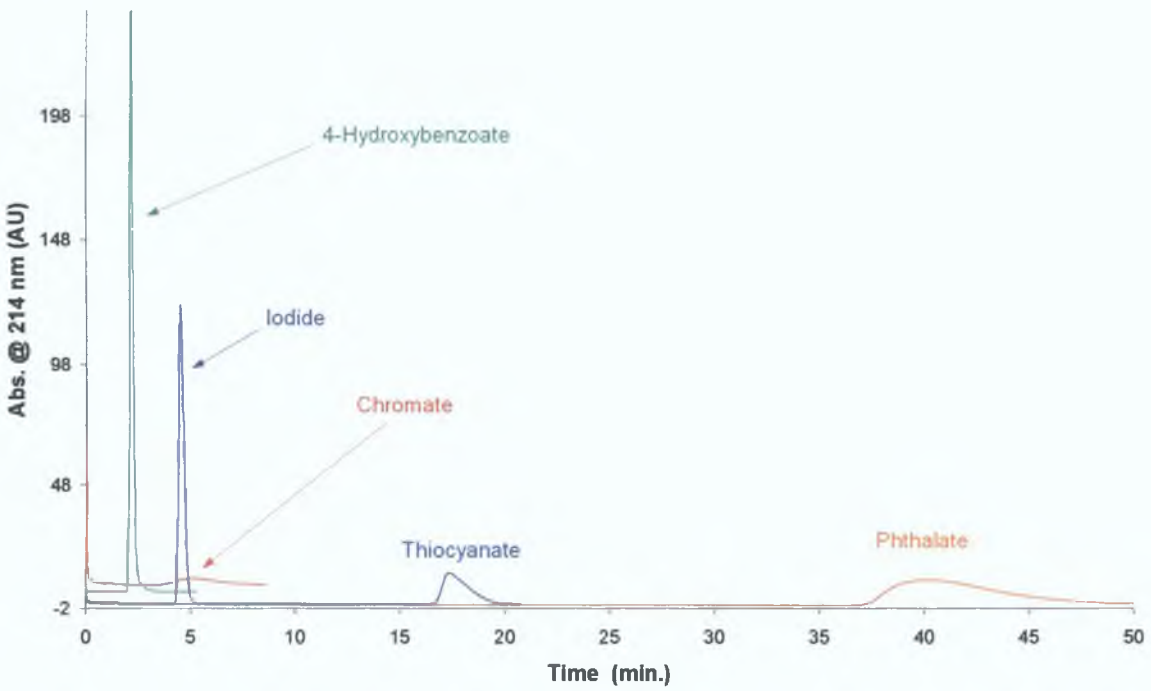

Figure 4.18. Chromatograms illustrating the retention of phthalate (orange trace), iodide (dark blue trace), thiocyanate (dark blue trace), 4-hydroxybenzoate (green trace) and chromate (red trace) on a 2.5 cm DDMAU-modified C_{18} monolithic column. Other conditions: As for Fig. 4.17.

4.3.5.1 Separation of a Mixture of 9 Analyte Anions

A new test mixture incorporating the findings of Section 4.3.5 was prepared. A mixture of iodate, bromate, nitrite, bromide, nitrate, 4-hydroxybenzoate, iodide, thiocyanate and phthalate (all at 0.1 mM) was injected, using 10 mM sodium phosphate at pH 4.02, and analysed at 214 nm. The resulting chromatogram can be seen in Fig. 4.19.

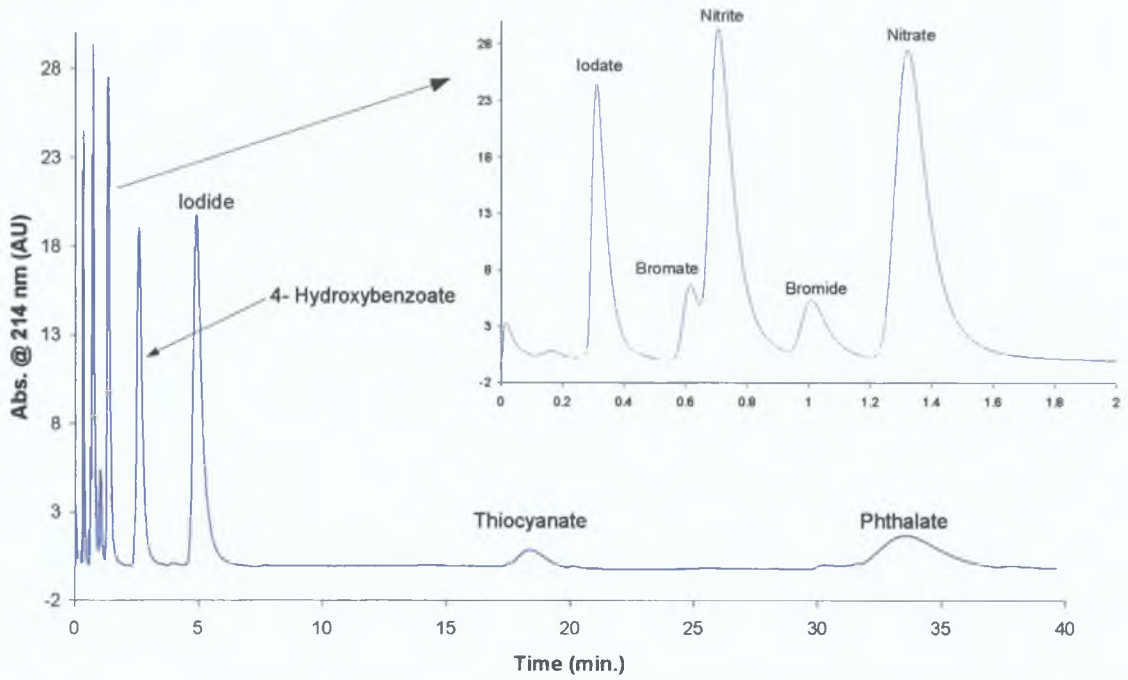

Figure 4.19. Chromatogram of a 0.1 mM mixture of iodate, bromate, nitrite, bromide, nitrate, 4-hydroxybenzoate, iodide, thiocyanate and phthalate, obtained using a 2.5 cm DDMAU-modified C_{18} monolithic column, and an eluent comprised of 10 mM phosphate buffer at pH 4.02, and a flow rate of 4.0 mL/min. Wavelength of detection: 214 nm.

Upon application of a dual gradient program (100% pH 4.02 to 100% pH 7.00, and 4.0 to 6.0 mL/min) from t = 3.0 min to t = 5.0 min, the overall runtime was reduced to less than 7 min, but the peaks for thiocyanate and phthalate, and the system peak resulting from the pH gradient all co-eluted. This indicated that retention of phthalate had reduced from almost 35 min to less than 7 min. Adjusting the timing of the pH gradient, by applying the pH gradient across 7 min (i.e. from t = 3.0 min to t = 10.0 min) rather than 2 min (i.e. from t = 3.0 min to t = 5.0 min) did nothing to aid separation of the 3 peaks in question. Use of a flow gradient alone (over 2 min,

starting at t = 2.0 min), with an eluent pH of 4.02, did not reduce the overall analysis time by a significant degree (28 min vs. 35 min).

Using an eluent of 10 mM phosphate buffer at pH 6.04, the retention of phthalate, relative to the other test anions, was examined, under isocratic conditions. It was found that at this pH, phthalate eluted at approx. 0.8 min, which was faster than thiocyanate (1.8 min) and just after the appearance of the iodide peak (0.55 min). Increasing the eluent pH to pH 7.00 resulted in the phthalate peak eluting prior to iodide (at approx. 0.2 min), and directly on top of the peaks for bromide and nitrate. This shows that the effect of increasing eluent pH causing decreased retention is much more pronounced for phthalate than, for example, nitrate or thiocyanate. The reason for this is due to phthalate having a pK_a of 5.41. This means that at eluent pH values greater than pH 5.41, the phthalate molecule would deprotonate, and would therefore increase its effective charge from -1 to -2. However, as the terminal carboxylate group of the DDMAU molecules of the stationary phase would also be dissociated at these pH levels, the phthalate ions would experience a larger degree of repulsion from the negatively charged functional groups of the DDMAU molecule than before, relative to the majority of the other analyte anions. This would manifest itself in reduced retention times being observed for phthalate, with these reductions in retention times being more significant for phthalate than for other anions such as iodide.

Therefore, in order to prevent phthalate from co-eluting with thiocyanate or the system peak etc., the end pH condition of the pH gradient was reduced from 7.00 to 5.02, with the remaining gradient conditions remaining the same as before. The ensuing chromatogram of a 0.1 mM 9 anion mixture is displayed as Fig. 4.20. It is evident from this chromatogram that separation of thiocyanate and phthalate was now achieved. However, the system peak resulting from the pH gradient appeared as a shoulder on the front of the thiocyanate peak. The overall runtime was less than 12 min, which is almost a third of the total runtime required under isocratic conditions (approx. 35 min).

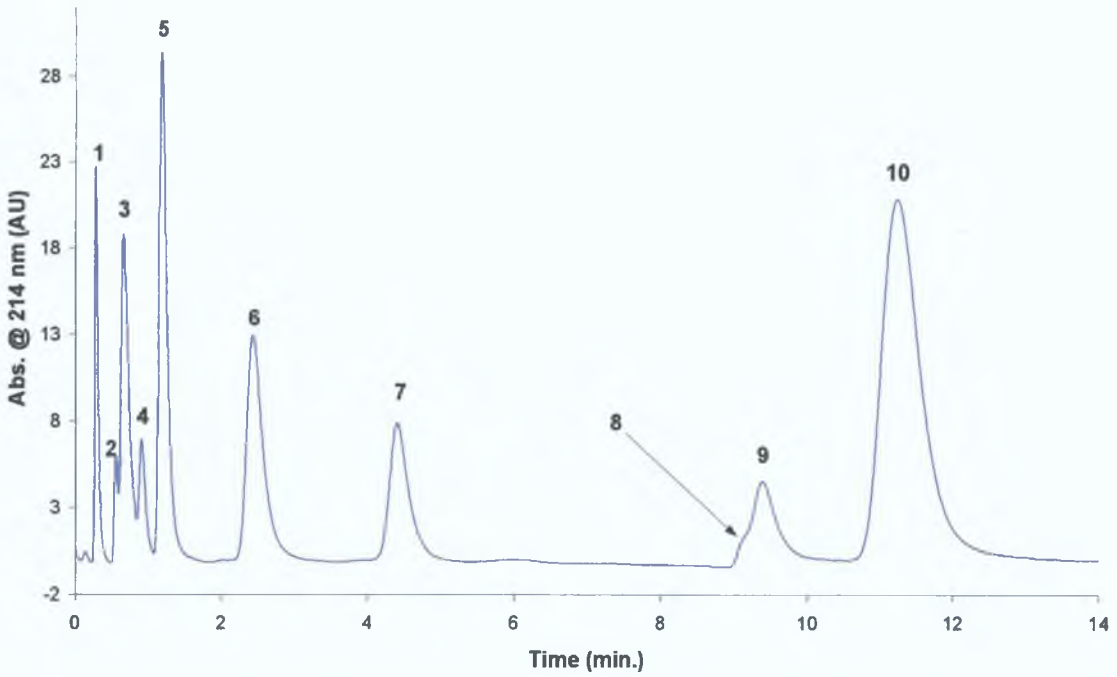

Figure 4.20. Chromatogram of a 0.1 mM mixture 9 anions obtained using a 2.5 cm DDMAU-modified C_{18} monolithic column, employing a dual gradient (10 mM phosphate buffer as eluent from 100% pH 4.02 to 100% pH 5.02, and flow rate from 4.0 mL/min to 6.0 mL/min) applied between t = 3.0 and t = 5.0 min. Wavelength of detection: 214 nm. Peak identification: 1 – iodate, 2 – bromate, 3 – nitrite, 4 – bromide, 5 – nitrate, 6 – 4-hydroxybenzoate, 7 – iodide, 8 – system peak, 9 – thiocyanate, and 10 – phthalate.

Gradient conditions were then altered slightly, in an attempt to minimise interference for the thiocyanate peak from the system peak. The starting pH of the gradient was lowered from 4.02 to 3.03. The resulting chromatogram can be seen in Fig 4.21, from which it is clear that the thiocyanate peak and the system peak were still far from satisfactorily resolved, although the overall runtime increased by approx 2 min to less than 14 min. The order of retention was seen to change yet again, with 4-hydroxybenzoate now eluting between bromate and bromide, instead of directly before iodide. In a manner analogous to the case of phthalate discussed earlier, this change in elution order was as a direct result of the eluent pH being lower than the pK_a for 4-hydroxybenzoate (pK_a = 4.48). The early-eluting group of anions (namely iodate, bromate, nitrite, bromide and nitrate) were better resolved in Fig. 4.21 than in Fig. 4.20, as the starting pH of the gradient was slightly lower (i.e. pH 3.03 vs. pH

4.02), resulting in slightly longer retention times for the aforementioned group of analyte anions.

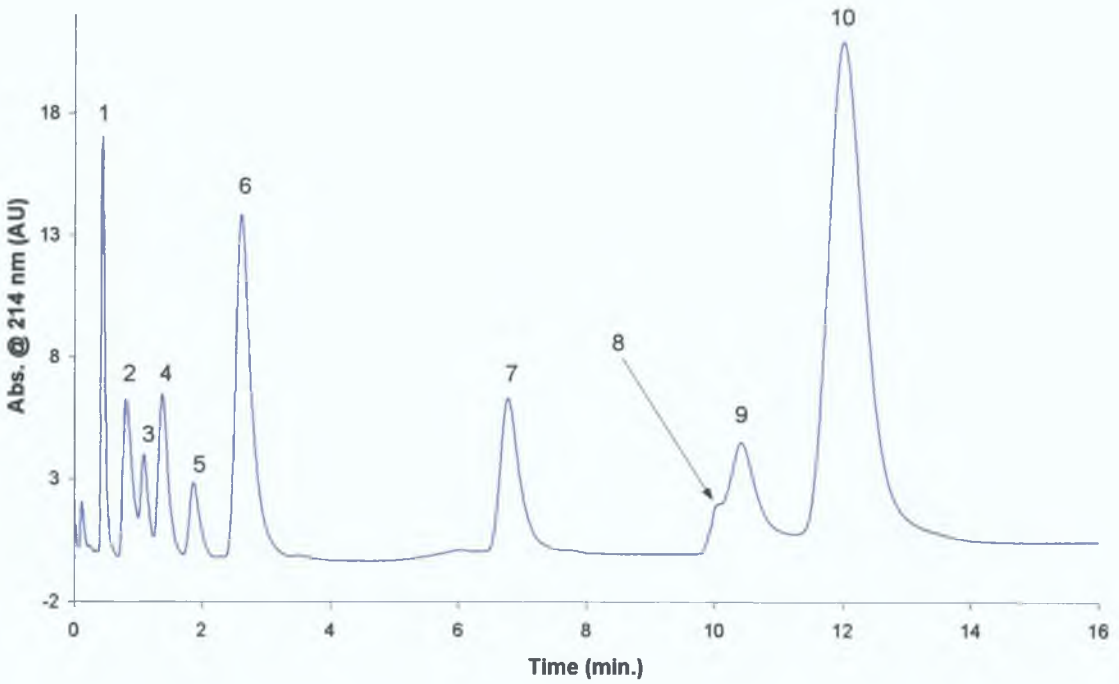

Figure 4.21. Chromatogram of a 0.1 mM mixture 9 anions obtained using a 2.5 cm DDMAU-modified C_{18} monolithic column, employing a dual gradient (10 mM phosphate buffer as eluent from 100% pH 3.03 to 100% pH 5.02, and flow rate from 4.0 mL/min to 6.0 mL/min) applied between t = 3.0 and t = 5.0 min. Wavelength of detection: 214 nm. Peak identification: 1 – iodate, 2 – nitrite, 3 – bromate, 4 – 4-hydroxybenzoate, 5 – bromide, 6 – nitrate, 7 – iodide, 8 – system peak, 9 – thiocyanate, and 10 – phthalate.

Bringing the onset of the application of the dual gradient forward to t = 2.0 min (from t = 3.0 min), and shortening the timeframe of the combined gradient from 2.0 min to 1.0 min, had no positive effect on the separation of the system peak and the thiocyanate peak. Changing the wavelength of detection to 220 nm and 217 nm (from 214 nm), as performed for a dual gradient application in Chapter 3, did not lead to a reduction in size of the system peak, but yielded a sizeable decrease in the observed signal for bromide.

Sections 4.3.5 and 4.3.5.1 have shown that while a number of additional anions are retained on the DDMAU-modified monolith, complete separation of all analyte anions investigated for this selectivity study was not possible, due to significant

overlapping of neighbouring peaks, e.g. acetate and formate. Some other anionic species injected resulted in peaks of such small magnitude that they were barely detected above the baseline, e.g. chromate. A mixture of 9 analyte anions could be separated satisfactorily, namely iodate, bromate, nitrite, nitrate, 4-hydroxybenzoate, iodide, thiocyanate and phthalate. Under isocratic conditions this separation took approx. 35 min, but application of a dual gradient program facilitated the elution of the same sample mixture in less than 14 min.

4.3.6 Indirect Detection Using a Phthalate Eluent

As it was not required to add DDMAU to the eluents employed using DDMAU-modified C_{18} monolithic columns, it was thought that indirect detection using a pththalate eluent would enable the separation and analysis of additional non-UV absorbing, or weakly UV absorbing, anionic species, such as chloride, fluoride, phosphate, sulphite and sulphate. Indirect spectrophotometric detection is widely used in ion chromatographic analysis, and is based on the use of eluent ions of greater absorptivity than target analyte ions, leading to decreased absorbance accompanying the elution of these analyte anions [8]. Phthalate eluents are commonly used for the indirect spectrophotometric detection of anions [8].

An eluent comprised of 2.0 mM phthalic acid (pH 4.00) was prepared, and used to analyse individual standards of a variety of common inorganic anions, namely fluoride, chloride, sulphate, sulphite, iodide and thiocyanate, using a wavelength of detection of 279 nm. However, the DDMAU-modified column displayed negligible retention of sulphate and sulphite, and no apparent retention of fluoride and chloride. Iodide and thiocyanate produced negative peaks at approx. 0.7 min and 1.8 min respectively. The use of a phthalate eluent at a lower ionic strength (i.e. 1.0 mM vs. 2.0 mM) resulted in a considerable increase in retention times, as seen from the sample chromatograms overlaid in Figs. 4.22 and 4.23. Thiocyanate, for example, eluted at 4.6 min, compared to approx. 1.8 min using an eluent ionic strength of 2.0 mM. Chloride, sulphite and sulphate all displayed clear negative peaks removed from the injection peak at 0.2 min. Injection of fluoride, however, did not result in any detectable analyte signal, while sulphite and sulphate were seen to have overlapping retention times (of approx. 2 min). Phosphate eluted at a retention time that was virtually identical to the retention time for chloride (at 0.47-0.50 min).

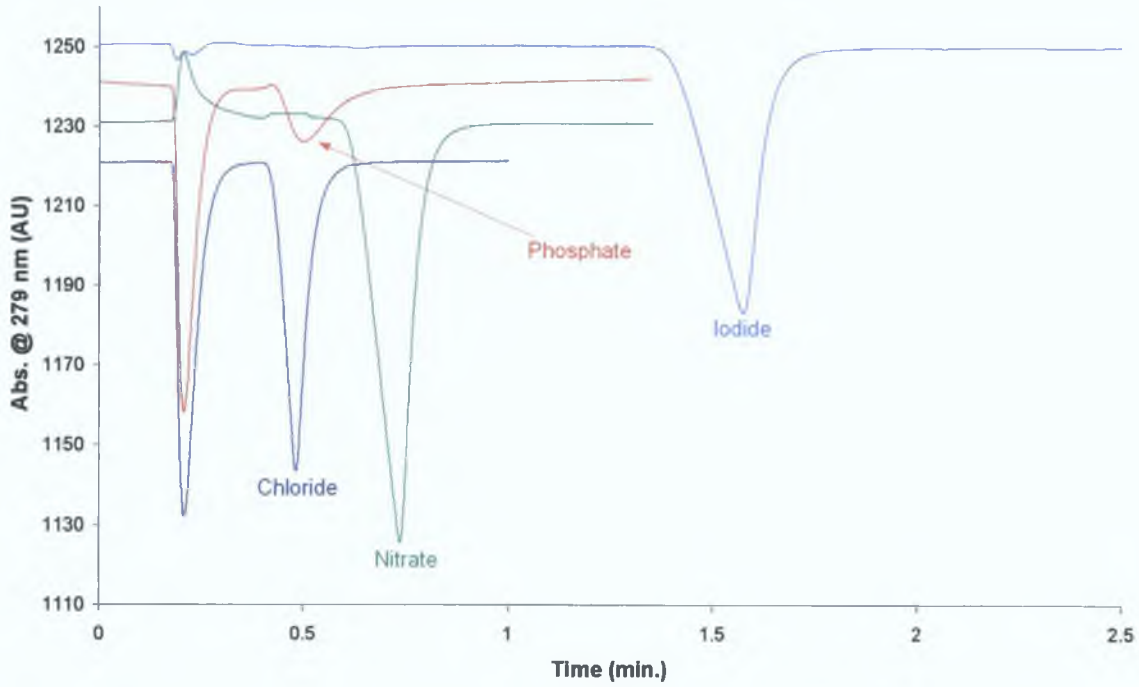

Figure 4.22. Chromatograms of 0.6 mM chloride, 0.2 mM phosphate, 1.0 mM nitrate and 1.0 mM iodide obtained using a 2.5 cm DDMAU-modified C_{18} monolithic column, with an eluent composed of 1.0 mM phthalic acid (at pH 4) and a wavelength of detection of 279 nm. Flow rate: 2.0 mL/min.

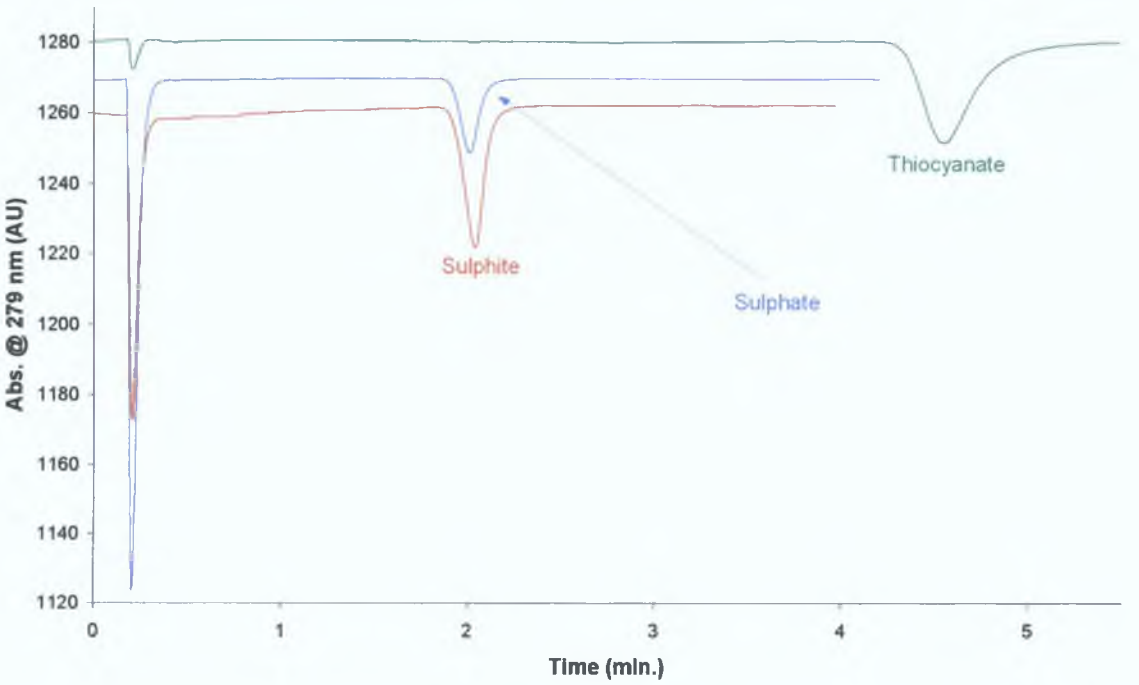

Figure 4.23. Chromatograms of 0.1 mM sulphite, 0.1 mM sulphate and 1.0 mM thiocyanate obtained using a 2.5 cm DDMAU-modified C_{18} monolithic column, with an eluent composed of 1.0 mM phthalic acid (at pH 4) and a wavelength of detection of 279 nm. Flow rate: 2.0 mL/min.

Further reduction of the ionic strength of the eluent employed was also undertaken, in order to investigate the possibility of fully resolving both the chloride and phosphate peaks, and the peaks representing sulphate and sulphite. Using eluents of 0.50 mM and 0.25 mM phthalic acid (both at pH 4.0) resulted in a further lengthening of retention times, but did not result in an improvement in the resolution of chloride, fluoride and phosphate, or of sulphite and sulphate. Sample chromatograms showing the separation of analyte anions achieved using an eluent comprised of 0.25 mM phthalic acid (at pH 4.0) are displayed in Figs. 4.24 and 4.25. Taking thiocyanate for example, retention time was seen to increase from approx. 1.8 min, using 2.0 mM phthalic acid as eluent, to approx. 14.0 min, when using an eluent of 0.25 mM phthalic acid. Some of the peak shapes in Figs. 4.24 and 4.25 are poor, particularly in the case of the nitrate peak in Fig. 4.25, due to the low concentration of the eluent used (i.e. 0.25 mM phthalic acid at pH 4).

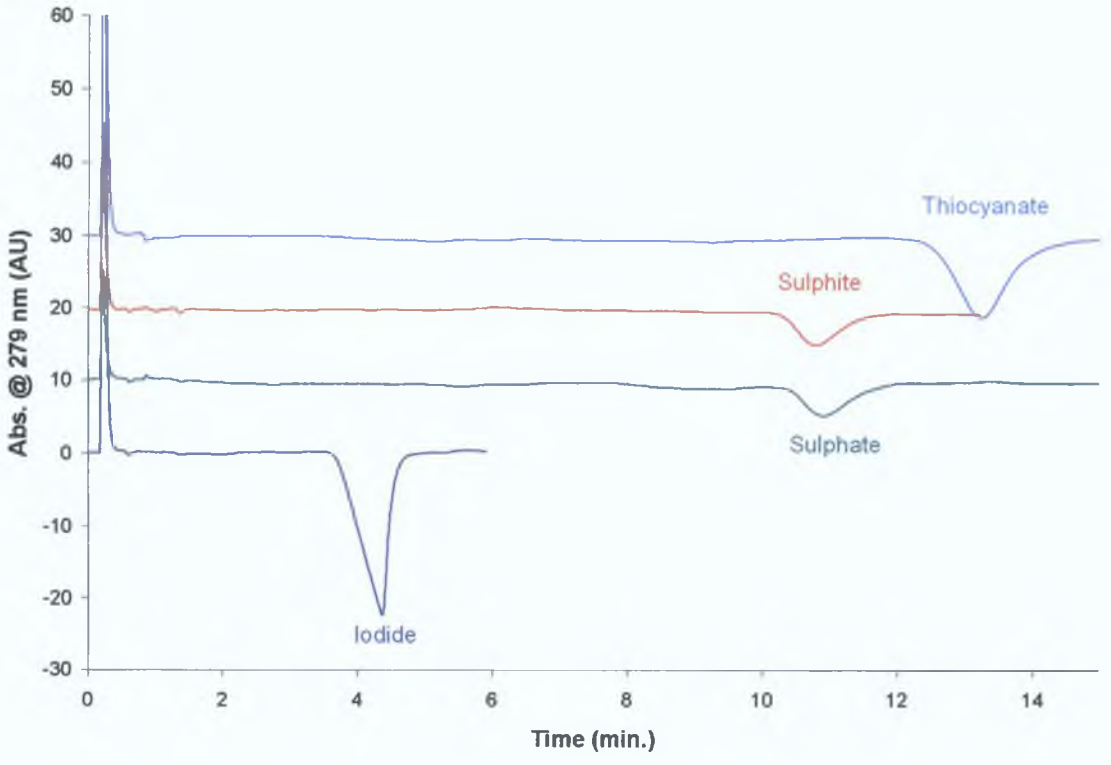

Figure 4.24. Chromatograms of 1.0 mM iodide, 0.1 mM sulphite, 0.1 mM sulphate and 1.0 mM thiocyanate obtained using a 2.5 cm DDMAU-modified C_{18} monolithic column, with an eluent composed of 0.25 mM phthalic acid (at pH 4) and a wavelength of detection of 279 nm. Flow rate: 2.0 mL/min.

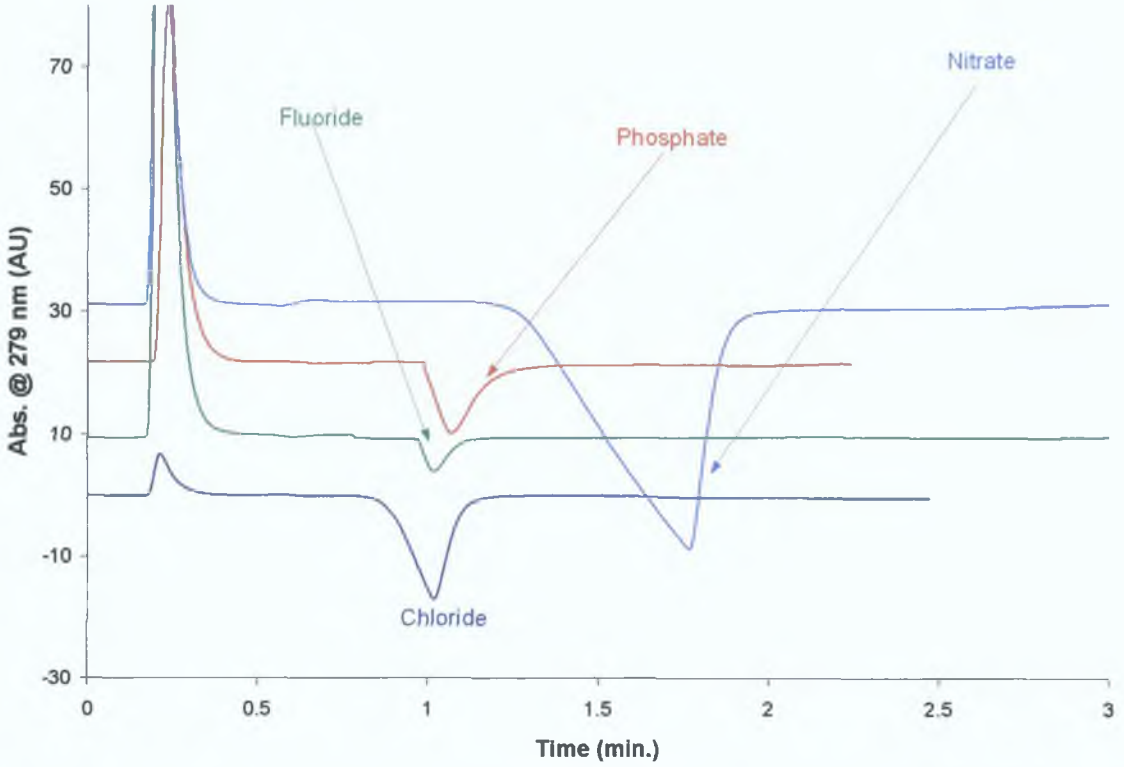

Figure 4.25. Chromatograms of 0.6 mM chloride, 1.0 mM fluoride, 0.2 mM phosphate and 1.0 mM nitrate obtained using a 2.5 cm DDMAU-modified C_{18} monolithic column, with an eluent composed of 0.25 mM phthalic acid (at pH 4) and a wavelength of detection of 279 nm. Flow rate: 2.0 mL/min.

The effect of phthalate eluent ionic strength on retention is summarised in Fig. 4.26, where log k is plotted against the log of phthalic acid concentration. The resulting plots were calculated to have R^2 values ranging from a minimum of 0.9331 (for fluoride) to a maximum of 0.9999 (for chloride).

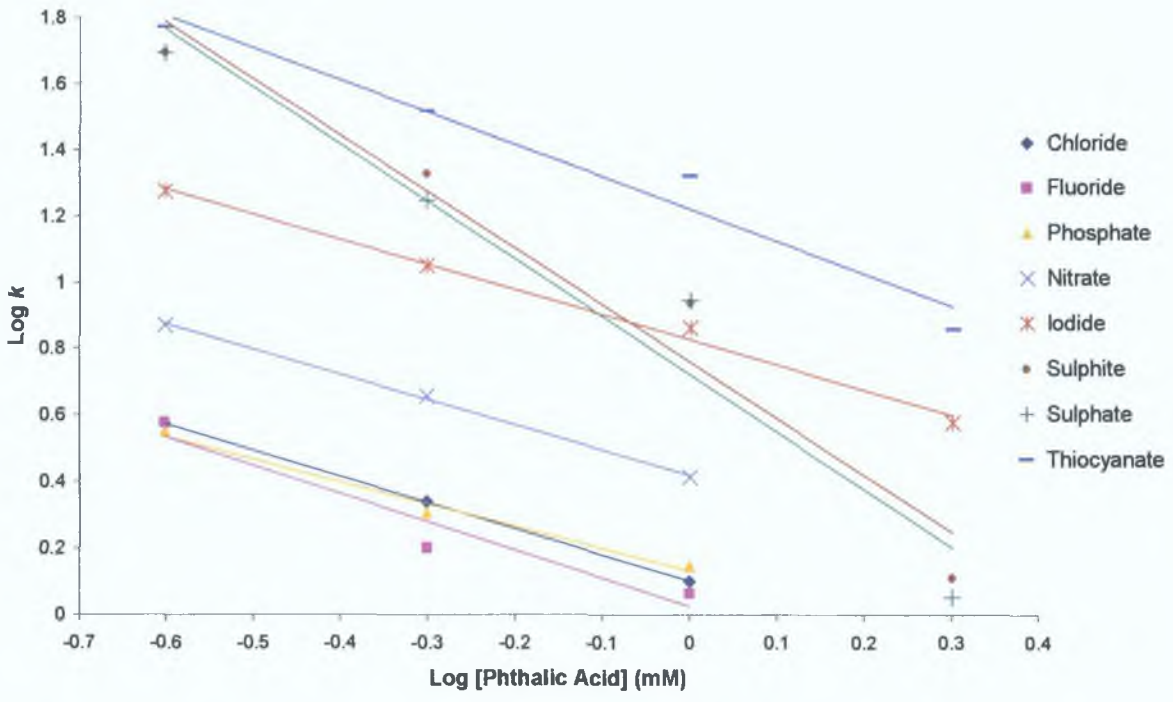

Figure 4.26. Plots of log *k* vs. [phthalic acid] for all analyte anions investigated, showing the relationship between retention and eluent concentration.

4.3.7. Analysis of Nucleoside Bases

To investigate the retention of polar organic compounds using DDMAU-modified C_{18} monoliths, the analysis of nucleoside bases (i.e. adenine (A), guanine (G), cytosine (C), thymine (T) and uracil (U)), as attempted in Chapter 3, was examined. 20 μM standards of all 5 bases were injected using 10 mM phosphate buffer at pH 7.0 as the eluent, and detected at 210 nm. The resulting chromatograms can be seen in Fig. 4.27, where it can be seen that all 5 analytes eluted before 1.5 min. It was observed that baseline resolution of all 5 nucleoside bases could not be achieved, as uracil would have overlapped with the peak for cytosine, while guanine would have interfered with the signal for both thymine and adenine. The order of retention (C < U < T < G < A) demonstrated how the pyrimidine bases (i.e. cytosine, uracil and thymine) eluted before the purine bases (guanine and adenine), as the purine bases are more hydrophobic than the pyrimidine bases. However, for reasons unknown, this order of elution was slightly different to that observed using a monolith modified with dodecyldimethylaminoacetic acid (i.e. C < U < G < A < T), see Section 3.3.8. The slightly longer retention of adenine, relative to guanine, may be attributed to the presence of the carbonyl group within the guanine molecule, not present in the adenine molecule.

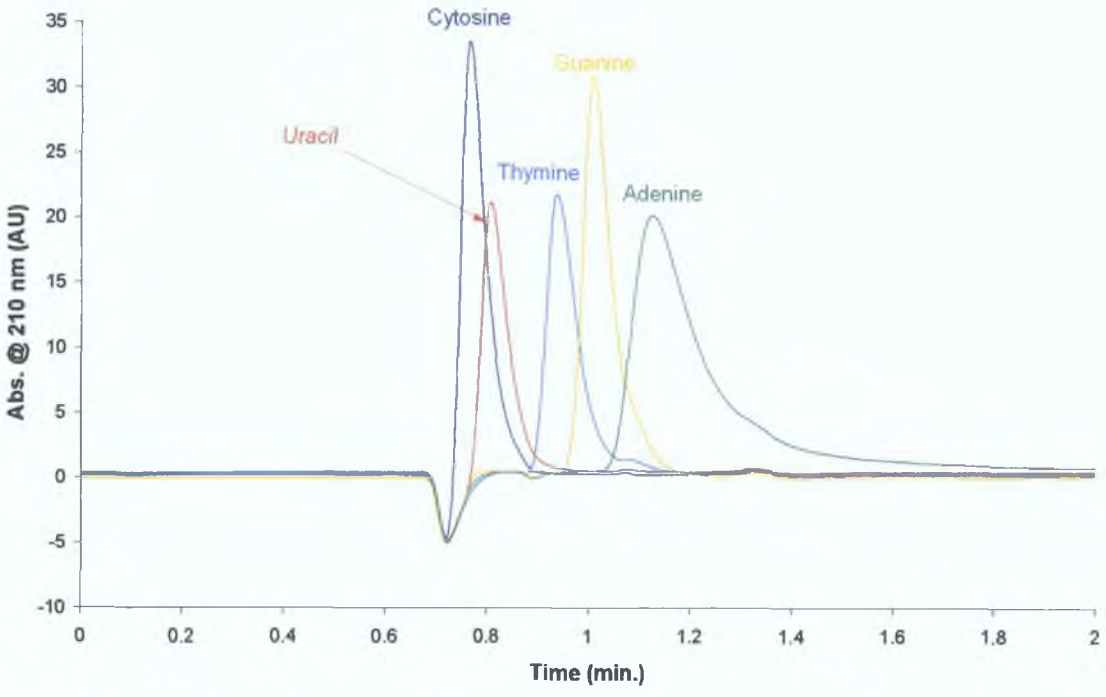

Figure 4.27. Chromatograms of 20 μM standards of cytosine (dark blue trace), uracil (red trace), thymine (light blue trace), guanine (yellow trace) and adenine (green trace), obtained using a 10 cm DDMAU-modified C_{18} monolithic column, and an eluent composed of 10 mM phosphate buffer (at pH 7.0), with a flow rate of 2.0 mL/min. Wavelength of detection: 210 nm.

The pH of the eluent employed was decreased from pH 7.0 to pH 3.0, and the same 20 μM nucleoside base standards re-analysed. The chromatograms obtained for each analyte can be seen in Fig. 4.28. Once again, resolution of all 5 bases was not possible, with retention times decreasing slightly, resulting in an overall runtime of approx 1.0 min (with cytosine and adenine appearing to co-elute with the injection peak, at approx. 0.65 min), less than 0.3 min than that observed with an eluent pH of 7.0. Retention was found to decrease with corresponding decrease in eluent pH. The order of elution was also found to have changed slightly, from C < U < T < G < A, to C < A < G < U < T. The reason for the shift in elution order is due to pH 3 being lower than the pK_a for both adenine (pK_a = 3.88) and guanine (pK_a = 3.6), causing them to become protonated, thereby decreasing their effective charge, thus leading to a decrease in retention. The observed order of elution for the nucleoside bases at pH 3.0 was identical to that seen under similar chromatographic conditions using a C_{18} monolithic column modified with dodecyldimethylaminoacetic acid, as in Section 3.3.8.

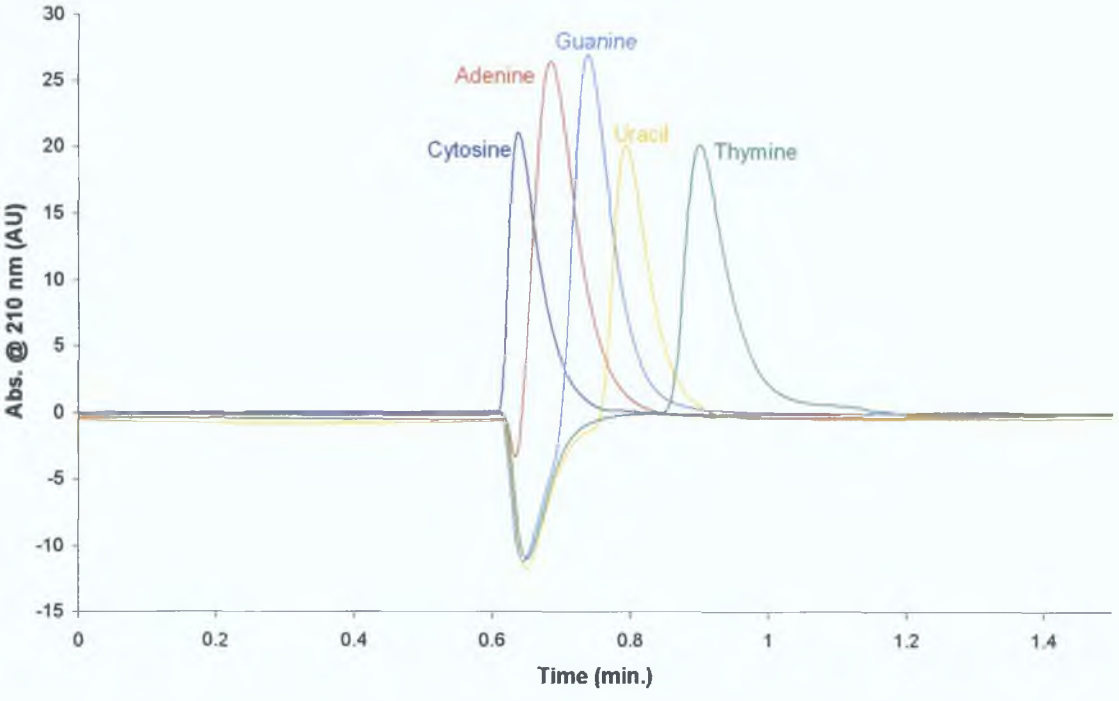

Figure 4.28. Chromatograms of 20 μM standards of cytosine (dark blue trace), adenine (red trace), guanine (light blue trace), uracil (yellow trace) and thymine (green trace), obtained using a 10 cm DDMAU-modified C_{18} monolithic column, and an eluent composed of 10 mM phosphate buffer (at pH 3.0), with a flow rate of 2.0 mL/min. Wavelength of detection: 210 nm.

4.4 Conclusions

It has been demonstrated that DDMAU can be used to dynamically modify C_{18} monolithic columns to produce a stable stationary phase for the efficient separation of anions. The DDMAU stationary phase exhibited a pH dependent effective column ion-exchange capacity, due to the presence of a terminal weak acid group, which enabled the use of an eluent pH gradient for the rapid elution of otherwise strongly retained anions, such as iodide and thiocyanate. The monolithic structure of the columns utilised, meant that the application of a combined eluent pH and flow gradient could be employed to reduce retention times even further, without sacrificing the baseline resolution of other, early eluting anions, and even improve the peak shape significantly for the thiocyanate peak. Effective column ion-exchange capacity could be determined through monitoring of the eluent pH, and subsequent comparison to column eluate pH profiles obtained with a union replacing the DDMAU-modified C_{18} monolithic column.

References

1 Y. Chevalier, Y. Storet, S. Pouchet, P. Le Perchec, Langmuir 7 (1991) 848-853.

2 C. Brenner, G. Jan, Y. Chevalier, H. Wróblewski, Anal. Biochem. 224 (1995) 515-523.

3 G. Jan, C. Brenner, H. Wróblewski, Protein Expression and Purification 7 (1996) 160-166.

4 S. Welling-Wester, M. Feijlbrief, D.G.A.M. Koedijk, G.W. Welling, J. Chrom. A 816 (1998) 29-37.

5 E. Twohill, B. Paull, J. Chrom. A 973 (2002) 103-113.

6 www.sensorex.com/products/ph_electrodes/lab/low_volume_flow_pH_ detector.html, Sensorex, Garden Grove, CA 92841, U.S.A., viewed 21/02/06.

7 G. Hendriks, J.P. Franke, D.R.A. Uges, J. Chrom. A 1089 (2005) 193-202.

8 Ion Chromatography: Principles and Applications (J. Chrom. Library Vol. 46), P.R. Haddad and P.E. Jackson, 1st edition 1990, published by Elsevier Science Publishers B.V., Amsterdam.

Chapter 5

Capillary Zwitterionic Ion Chromatography Using DDMAU-Modified Stationary Phases With Direct Contactless Conductivity Detection

5.1 Introduction

One of the clear trends in modern science and technology is miniaturisation [1]. This is also the case within the field of analytical chemistry, where one of the driving forces for the rapid development of miniaturised techniques is the growing interest in analysing small sample volumes of high matrix complexity [2]. The use of capillary columns is one such approach in the downscaling of liquid chromatographic (LC) techniques.

A chromatographic column is usually considered to be a capillary column if the inner diameter is less than 1 mm [3], and they can be (i) packed, (ii) open tubular (OT), and (iii) monolithic. Chervet *et al.* [2] suggested defining chromatographic techniques according to the range of the flow rate used, with the use of flow rates of 10 to 100 μL/min referring to micro-LC, 1 to 10 μL/min referring to capillary LC, and 10 to 1000 nL/min referring to nano-LC. Capillary LC has not yet seen widespread use in commercial and industrial laboratories. The principal reason for this is that, up until relatively recently, there was a lack of reliable instrumentation for use in conjunction with capillary systems. In the past, there was also limited availability of high quality capillary columns, which may have prevented this technique from gaining more widespread acceptance.

The 5 major advantages of capillary LC are:

(a) Better resolving power within a shorter time frame [4, 5].

(b) The reduced sample requirements of miniaturised LC eliminates the need to prepare large amounts of sample [6], which is of great benefit when there is a limited amount of sample available, as is often the case in various fields, such as clinical, forensic, pharmaceutical chemistry, and biotechnology.

(c) On-line coupling to a mass spectrometer is easily accomplished [7].

(d) Expenses connected to the consumption and disposal of chemicals and materials are greatly reduced. This is becoming increasingly significant, as the costs of solvent disposal are increasing steadily [8].

(e) As the volume of eluent pumped through a capillary column is significantly smaller than through a standard chromatographic column, the analytes of

interest are dissolved in much less eluent, which results in higher mass sensitivity [8].

There are, of course, some inherent disadvantages of capillary LC:

(a) Due to the small column volume, any local irregularities of the stationary phase packing can result in dramatic reductions in column efficiency [8].

(b) Capillary LC instrumentation must be configured with low injection volumes, be able to deliver reproducible gradients at low flow rates, and requires a sensitive, low-volume detector [8].

(c) The use of filters is very important, as all particulate matter must be removed from the eluent prior to reaching the column, lest flow through the column become obstructed [9].

(d) In the case of on-column detection, the stationary phase within the column will bring about a reduction in sensitivity, thus leading to an increase in the baseline noise observed [10].

5.1.1 History of Capillary Ion Chromatography

The concept of capillary LC is generally regarded to have been introduced by Horvath *et al.* in the late sixties [11,12]. However, the first publication on capillary ion chromatography (capillary IC) was by Rokushika *et al.* in 1983 [13]. They used a surface agglomerated anion-exchange capillary column of 0.19 mm internal diameter (I.D.), packed with 10 μm particles, and coupled this to a 0.2 x 10 mm Nafion perfluorosulfonate hollow fibre suppressor, immersed in a low-bleed, large counterion acid regenenerant, dodecylbenzenesulfonic acid. Using an eluent comprised of sodium carbonate-bicarbonate, Rokushika *et al.* demonstrated the separation and detection of various inorganic anions and organic acids at low ppm levels. The developed methodology was also applied to real samples, namely river water samples and several types of fruit juices. Later in the same year, Rokushika *et al.* [14] used the same column again for the separation of several anions, in conjunction with UV detection, rather than conductivity detection, as before. Employing a carbonate- or hydroxide-based eluent (both with and without added methanol), it was shown that the system could be applied to the detection of several UV-absorbing anions, as well as some organic acids (including aminobenzoic acids, nucleotides and nucleobases).

5.1.2 Use of Monolithic Columns in Capillary IC

The utilisation of both polymer and silica-based monolithic phases is well established within the field of capillary electrochromatography. However, there has only been a limited amount of work presented using pressure-driven flow together with capillary columns containing ion-exchange, monolithic stationary phases, i.e. capillary IC [3]. The benefit of switching from a traditional monolithic column to a capillary monolithic column is that most problems with conventional non-capillary monoliths arise from radial non-uniformity associated with their fabrication, and from axial non-uniformity, i.e. gaps in the stationary phase due to the instability of the column packing material. The wider the dimensions of the column, the greater the extent of this non-uniformity, and its detrimental effect on column efficiency [15]. Therefore, capillary monolithic columns have a significant advantage over traditional monolithic columns.

Zakaria *et al.* [16] established the use of latex-modified monolithic polymeric stationary phases for the "micro-ion chromatography" of inorganic anions. The column used was a 250 μm I.D. fused silica capillary, with a length of 30 cm, and containing a monolithic stationary phase prepared through the polymerisation of butylmethacrylate and ethylenedimethacrylate with 2-acrylamido-2-methyl-1-propanesulfonic acid, followed by modification with quaternary ammonium latex particles. Separation efficiencies achieved were relatively poor (e.g. 13,000 plates/m for iodate), but as retention was observed at relatively high eluent flow rates (up to 42 μL/min, owing to the high porosity of the monolith employed), rapid separations could be achieved, with 7 analytes resolved in less than 2 minutes. Motokawa *et al.* [17] prepared porous silica monoliths in 50 to 200 μm I.D. fused silica capillaries with various skeleton and throughpore sizes, and found that the monolithic silica columns prepared within the capillaries yielded theoretical plate heights in the region of 8-12 μm. More recently, Suzuki *et al.* [18] used a 0.1 mm I.D. monolithic capillary column, using a silica-based, rather than a polymeric, stationary phase (column lengths: 20 cm and 40 cm), modified with cetyltrimethylammonium ions for the rapid determination of bromide in seawater samples, with a runtime of less than 1.5 min, with a flow rate of 5.6 μL/min. Suzuki *et al.* [18] also demonstrated the separation of a 0.5 mM

mixture of iodate, bromate, nitrite, bromide and nitrate was achieved in less than 1 min, using elevated flow rates of 11.1 μL/min.

5.1.3 Application of Capillary Columns to ZIC

Zwitterionic ion chromatography (ZIC) utilising capillary columns was demonstrated briefly by Hu *et al.* in their seminal work using CHAPSO micelles as a zwitterionic stationary phase in 1993 [19]. The C_{18} column used as support for the zwitterionic stationary phase had an internal diameter of 0.35 mm and a total length of 150 mm. Employing UV detection at 230 nm, and a pure water eluent (at a flow rate of 2.8 μL/min), the separation of iodate, nitrite, nitrate, iodide and thiocyanate was accomplished within approximately 12 minutes, as displayed in Fig. 5.1 below. This capillary LC system was only briefly introduced, while no specific mention was made of parameters such as efficiency values etc.

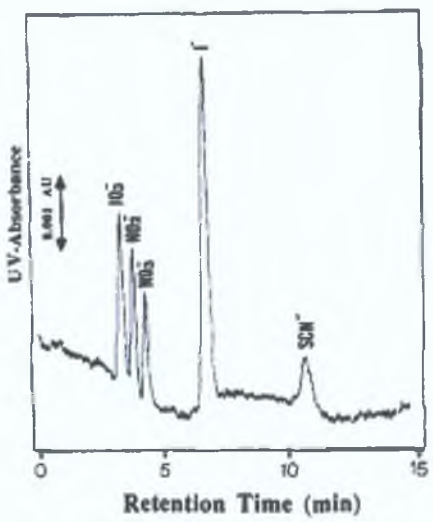

Figure 5.1. Chromatogram of a 0.1 mM inorganic anion mixture (containing iodate, nitrite, nitrate, iodide and thiocyanate) obtained using a Develosil ODS-5 column modified with CHAPSO micelles, using pure water as eluent, and UV detection at 230 nm [Reproduced from ref. 19]. Flow rate: 2.8 μL/min.

Capillary ZIC, using phosphate buffer as eluent, was also briefly mentioned the following year by Hu and Haraguchi [20], when CHAPS micelles were used to modify a capillary column, for the separation and determination of various inorganic anions. The micro-LC setup (including the chromatographic column) was identical to that mentioned in the previous paragraph, and again separation of a mixture of inorganic anions was possible within a 12 minute time frame (see Fig. 5.2). The

capillary column modified with CHAPS was also utilised in the investigation of the effect of increasing the ionic strength of the eluent on analyte retention times. However, since then, no further research focusing on capillary ZIC has been shown.

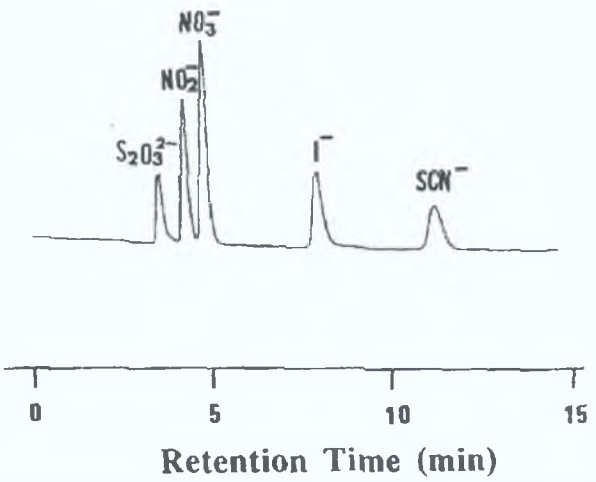

Figure 5.2. Chromatogram of a 1.0 mM mixture of thiosulphate, nitrite, nitrate, iodide and thiocyanate, obtained using a Develosil ODS-5 column modified with CHAPS micelles, using phosphate buffer as eluent, and UV detection at 230 nm [Reproduced from ref. 20]. Flow rate: 2.8 μL/min.

The aim of this Chapter was to further investigate capillary ZIC, using monolithic columns modified with the zwitterionic surfactant DDMAU. It was also intended to evaluate the use of capacitively coupled contactless conductometric detection (C^4D) with such a capillary ZIC system. C^4D was employed as the method of detection, because of several advantages offered by this technique [3]: (1) The detector cell can be positioned at any location along the length of the capillary column; (2) The dependence of detection sensitivity and/or signal-to-noise ratio on the capillary I.D. is not nearly as great as for optical detection; and (3) C^4D electronics are so compact that they can be easily used with portable instrumentation. C^4D detection has yet to be widely used as a detection method for capillary IC, with the majority of the papers on this topic focusing on coupling of C^4D with capillary electrophoresis (CE) separations [21], with a small minority of the work published concerned with capillary electrochromatographic separations (CEC, which combines features of both CE and LC, using an electric field as the driving force to transport the eluent and analytes through a capillary column containing the stationary phase [22]), such as the work carried out by Hilder *et al.* [23], who employed across column detection on a packed

bed ion-exchange capillary column. The use of C^4D detection across a modified silica-based C_{18} monolithic capillary column has never before been investigated.

5.2 Experimental

5.2.1 Instrumentation

Part of the experimental setup employed (i.e. the capillary column, the nano-injector unit, and the detector unit) is shown in Fig. 5.3. The pump used for eluent delivery was an Applied Biosystems 400 Solvent Delivery System (Foster City, CA, U.S.A.). Eluent flow through the capillary column was controlled by custom built adjustable flow splitter based upon a T-piece connector with variable backpressure applied to the waste line (with eluent flow being directed to both a waste container and to the column itself). Samples were injected using a Rheodyne MX Module Nano Injector (purchased from Alltech Associates, Applied Science Ltd., Lancashire, U.K.), with a fixed injection volume of 10 nL, into which the capillary column itself was connected directly. Sample was delivered to the appropriate position of the MX module using a Knauer K-120 HPLC Pump (obtained from Presearch Limited, Hitchin, Hertfordshire, U.K.). The detector used was a TraceDec Contactless Conductivity Detector (Innovative Sensor Technologies GmbH, Innsbruck, Austria), through which the capillary column was placed.

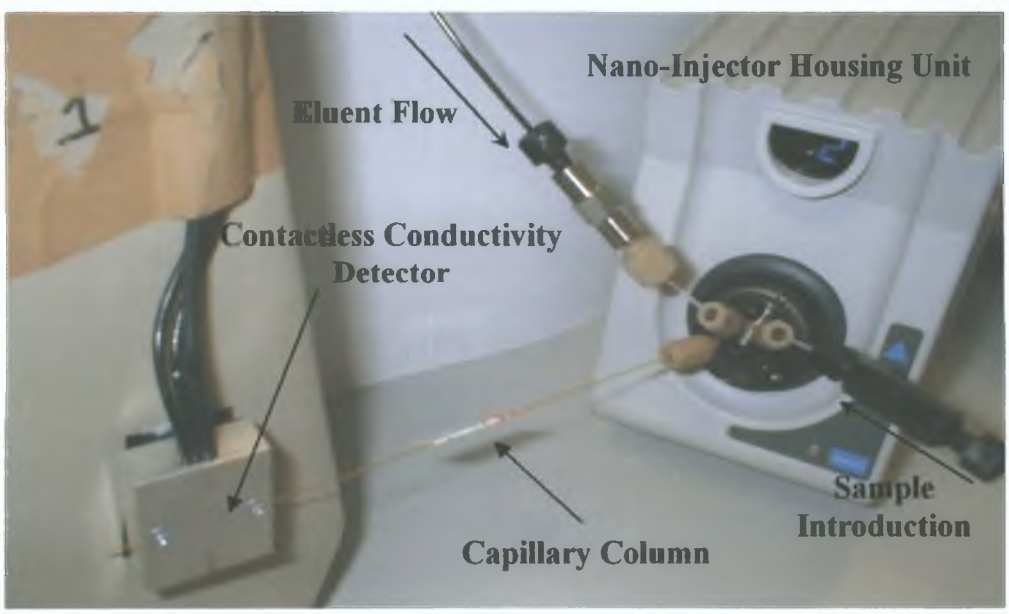

Figure 5.3. Photograph illustrating part of the experimental setup of the capillary LC system used.

Eluent pH was measured using an Orion Model 420 pH meter (Thermo Orion, Beverly, MA, U.S.A.) with a glass electrode. Processing of chromatograms was carried out using a PeakNet 6.30 chromatography workstation (Dionex, Sunnyvale, CA, U.S.A.).

Microscopy was used to verify the structural uniformity of the capillary columns. The column used initially for this experimental work was observed under X 2 magnification using a microscope with live camera feed. Microscopy was undertaken using a Nikon Eclipse E800 microscope (obtained from the Micron Optical Co., Enniscorthy, Co. Wexford, Ireland), interfaced with a high resolution PARISS VHR-HIS system (Lightform Inc., Belle Mead, New Jersey, U.S.A.) for spectral imaging purposes. The resulting micrographs (examples of which can be seen in Fig. 5.4, where the lighter shaded areas within the column represent a break in the stationary phase material, which is visualised as the darker shaded area) displayed numerous gaps in the stationary phase material. This was corroborated by data generated by placing the contactless conductivity detector on the beginning of the column and dragging it across the entire length of the column at a uniform rate, when conductivity was seen to drop sharply at locations corresponding to interruptions in the C_{18} stationary phase. Therefore, a second, identical capillary column was purchased, which upon examination by microscopy, as before, was found to have a more uniform stationary phase within the capillary (see the comparison of the micrographs in Fig. 5.4 (a) and (b)). Therefore, microscopy can be used as a tool to check column integrity, or to investigate the exact location of blockages etc.

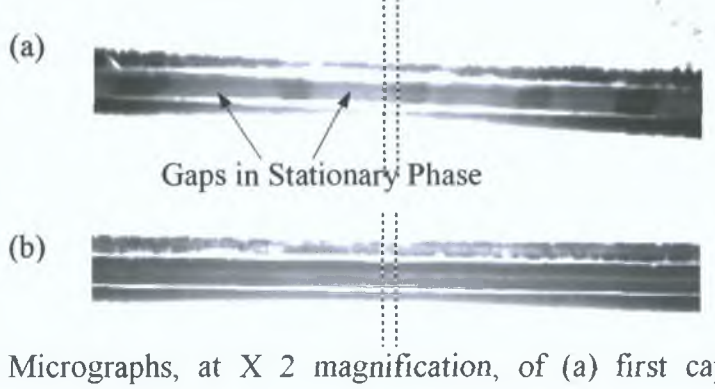

Figure 5.4. Micrographs, at X 2 magnification, of (a) first capillary monolithic column, from 1.0 to 1.5 cm of total column length (showing non-continuity of stationary phase within capillary walls), and (b) second capillary column utilised from 1.0 to 1.5 cm of total column length (displaying a uniform internal structure).

5.2.2 Reagents

The zwitterionic surfactant used to dynamically modify the capillary column was N-dodecyl-N, N-(dimethylammonio)undecanoate (DDMAU) (Calbiochem, La Jolla, CA, U.S.A.). All other chemicals used were of analytical reagent grade, and were supplied by Sigma-Aldrich (Tallaght, Dublin, Ireland). All eluents and standard solutions were prepared using deionised water from a Millipore Milli-Q water purification system (Bedford, MA, U.S.A.), and were filtered through a 0.45 μm filter twice, and degassed by sonication. The cation-exchange cartridges used were Supelco Supelclean LC-SCX 1 ml tubes (supplied by Sigma-Aldrich, Tallaght, Dublin, Ireland). The reversed-phase-exchange cartridges used were Strata C18-E 200 mg/3 ml cartridges (Phenomenex, Macclesfield, U.K.).

5.2.3 Column Preparation

The capillary column used for this section of work was an Onyx Monolithic reversed-phase C_{18} column (150 x 0.1 mm I.D., obtained from Phenomenex, Cheshire, U.K.). In a manner analogous to that described in previous experimental subsections, the capillary column was dynamically modified with DDMAU by passing a 2.0 mM DDMAU solution through the column at a flow rate of approx. 1 μL/min for approximately 3 hours, before washing thoroughly with Milli-Q water for approx. 1.5 hours at the same flow rate.

5.3 Results and Discussion

5.3.1 Investigation Into Eluent Choice for the Separation of Anions

At first, it was decided to use a phosphate buffer as eluent for the separation of a mixed standard of anions, as these types of eluents had been employed in previous experiments using standard monolithic columns modified with DDMAU. An eluent comprised of 10 mM phosphate buffer at pH 6.0 was prepared, and individual standards of nitrate, thiocyanate and sulphate injected. Upon investigation of the subsequent chromatograms, it was found that nitrate and thiocyanate were unretained, and so they eluted within the eluent dip. Sulphate gave rise to a very minor positive peak at approx. 1.6 minutes, but as the concentrations of sulphate that had been injected were relatively high (ranging from 1 to 10 mM), it had been expected that the resulting peaks would have been significantly larger.

In an attempt to lengthen retention times of analyte anions, the eluent pH was reduced from pH 6.0 to 3.0. Nitrate and thiocyanate remained undetected, while sulphate was seen to produce a negative peak at approx. 3.9 minutes. As some of the analytes were not detected, and sensitivity for sulphate remained very poor, it was concluded that this eluent composition (i.e. 10 mM phosphate buffer at pH 3.0), which had been utilised for UV detection in previous chapters, was unsuitable for use in conjunction with conductivity detection, as the background conductivity (approx. 1050 μS) was so high that it dwarfed the analyte responses.

Phthalic acid was used as an eluent, as it has seen widespread use in IC coupled with direct conductivity detection [24]. Upon converting to an eluent composed of 5 mM phthalic acid at pH 3.61, background conductivity was observed to decrease by almost half (i.e. approx. 450-500 μS), with sulphate eluting as a large, sharp peak at approx. 2.4 minutes. Comparison of the peak area values for a 5 mM sulphate standard show that the peak area for sulphate increased threefold compared to the value obtained using the sodium phosphate buffer-based eluent (1.36 mV min vs. 0.45 mV min).

In order to obtain a significantly longer retention time for sulphate, the ionic strength of the phthalic acid eluent was decreased to 0.5 mM, with the pH of the eluent adjusted to 4.05. This resulted in lengthier analyte retention times, with sulphate, for example, eluting at 7.5 – 8.0 minutes, compared to 2.4 minutes for the higher ionic strength phthalic acid eluent. The higher concentration standards that had been injected before now exhibited significant peak fronting, possibly due to column overload. This increased sensitivity enabled the detection of considerably lower analyte concentrations, e.g. for sulphate there was a similar analyte response (in terms of peak height and peak area) for a 0.5 mM standard using the 0.5 mM phthalic acid eluent, as there was for a 10.0 mM standard using the 10 mM phosphate buffer eluent. Taking nitrate as an example, distortion of the ideal Gaussian peak shape occurred at sample concentrations in excess of 1.0 mM, as the peak asymmetry factor, A_s, for nitrate fell below 0.9 at higher concentrations than this, where, for acceptable symmetry, the A_s should range between 0.9 and 1.2. The broadness and asymmetry of the higher concentration standards indicate that for future work, the capacity of the monolithic column should ideally be increased, or smaller sample volumes injected.

A sample separation of a 0.5 mM 6 anion mixture can be seen in Fig. 5.5. As is evident from this chromatogram, each of the 6 peaks corresponding to each of the analyte anions were satisfactorily efficient, with values for N/m (no. of theoretical plates per metre) ranging from 13,700 for iodate to 50,000 for sulphate.

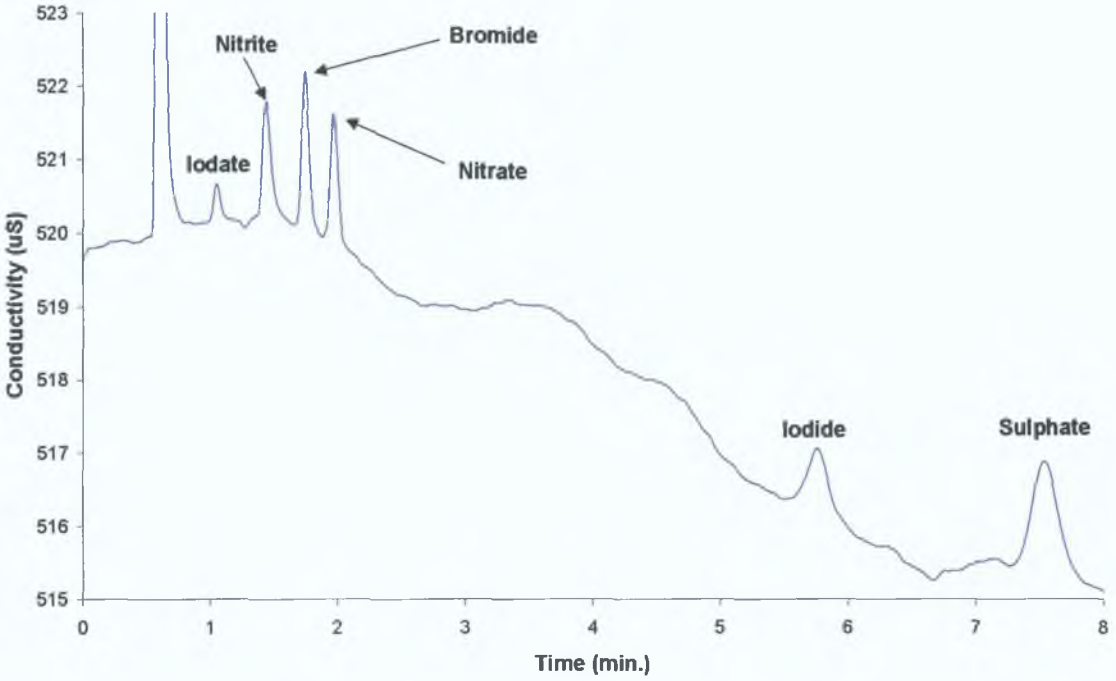

Figure 5.5. Separation of a 0.5 mM mixture of iodate, nitrite, bromide, nitrate, iodide and sulphate achieved on a DDMAU-modified capillary C_{18} monolithic column, using contactless conductivity detection, and a flow rate of 1.0 μL/min. Eluent: 0.5 mM phthalic acid at pH 4.05. Effective column length: 13.0 cm.

5.3.2 Adjustment of Effective Column Length

As the mode of detection employed was across-column detection, by placing the contactless conductivity detector at various positions along the length of the capillary column, the effective column length could be altered, i.e. placing the detector near the beginning of the column inlet, and placing it at the very end of the column length would essentially produce 2 columns with an identical stationary phase but of different lengths, resulting in sizeable differences in observed retention times. This concept is visualised in Fig. 5.6.

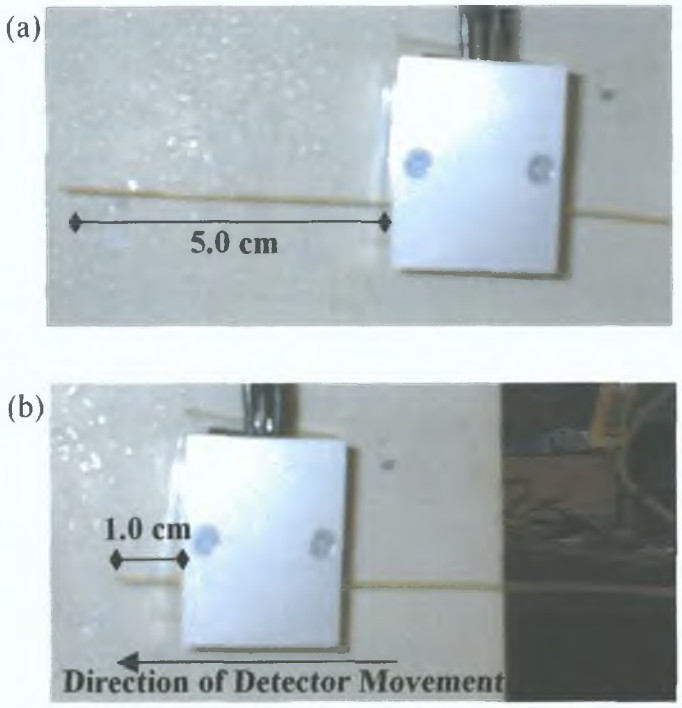

Figure 5.6. Photographs illustrating how placing the contactless conductivity detector further down the length of the capillary column would result in a longer effective column length, with (a) representing an effective column length of approx. 8.5 cm, and (b) representing an effective column length of approx 12.5 cm.

Therefore, in order to investigate the exact effect of varying the detector position on analyte retention and efficiency, the position of the detector was changed in 1.0 cm increments, and the subsequent chromatograms examined. Initially the detector was placed as close as possible to the top of the column, which resulted in an effective column length of 4.5 cm, when the length of capillary within the nano-injector module and the dimensions of the detector unit were taken into account. The farthest the detector was placed down the length of the capillary gave an effective column length of 12.5 cm, as the detector housing unit could not be placed at the very end of the capillary column, as eluent flowing out of the capillary would build up in droplets and flow back into the detector on the outside surface of the capillary, thereby causing detector overload. Fig. 5.7 (a) shows overlays of some of the chromatograms obtained as the detector advanced down the length of the capillary in 1.0 cm increments. Fig. 5.7 (b) represents a blow up of the first 4 min of the chromatograms seen in Fig. 5.7 (a).

(a)

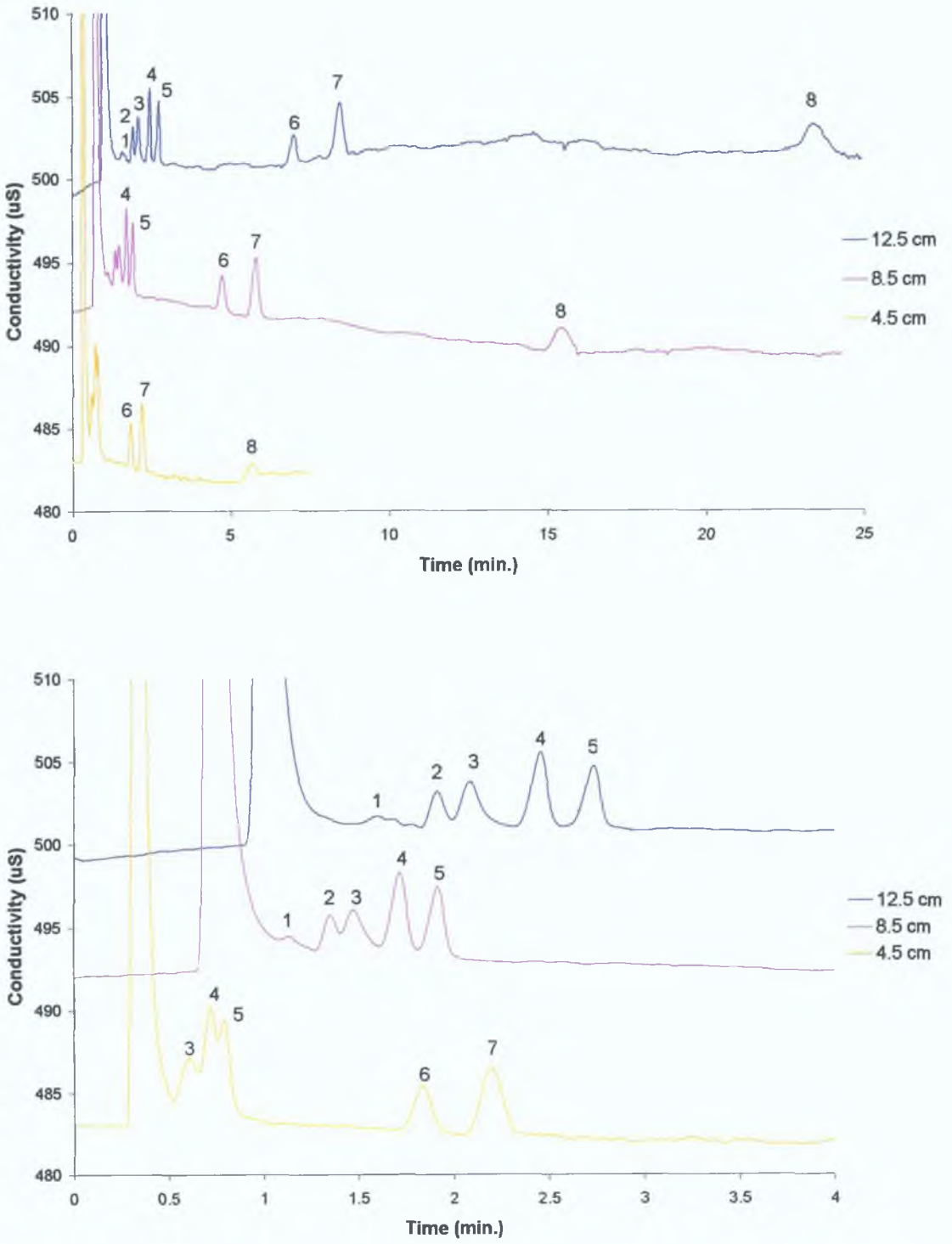

Figure 5.7 (a). Overlays of chromatograms of a 0.5 mM 8 anion mixture (where 1 represents iodate, 2 - bromate, 3 - nitrite, 4 - bromide, 5 - nitrate, 6 - iodide, 7 – sulphate, and 8 - thiocyanate) obtained using a DDMAU-modified capillary column, with an eluent composed of 0.5 mM phthalic acid at pH 4.05 and a flow rate of 1.0 μL/min., at effective column lengths of 4.5 cm (yellow trace), 8.5 cm (pink trace) and 12.5 cm (blue trace). Fig. 5.7 (b) is a blow up of the first 4 min of Fig. 5.7 (a).

(a)

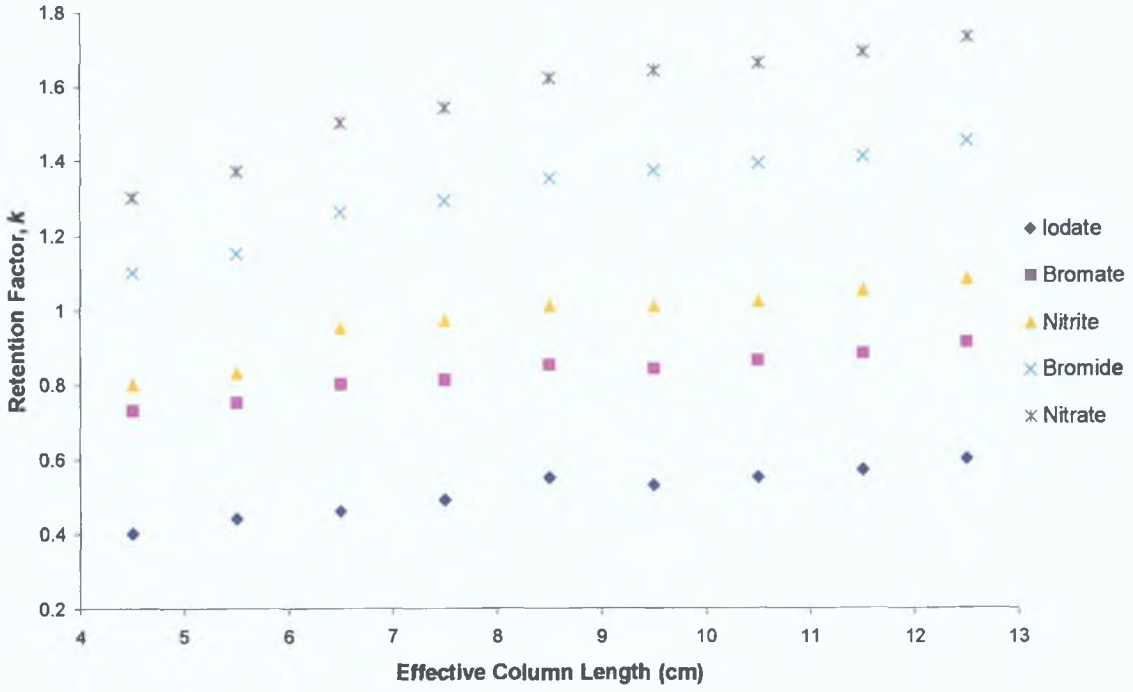

(b)

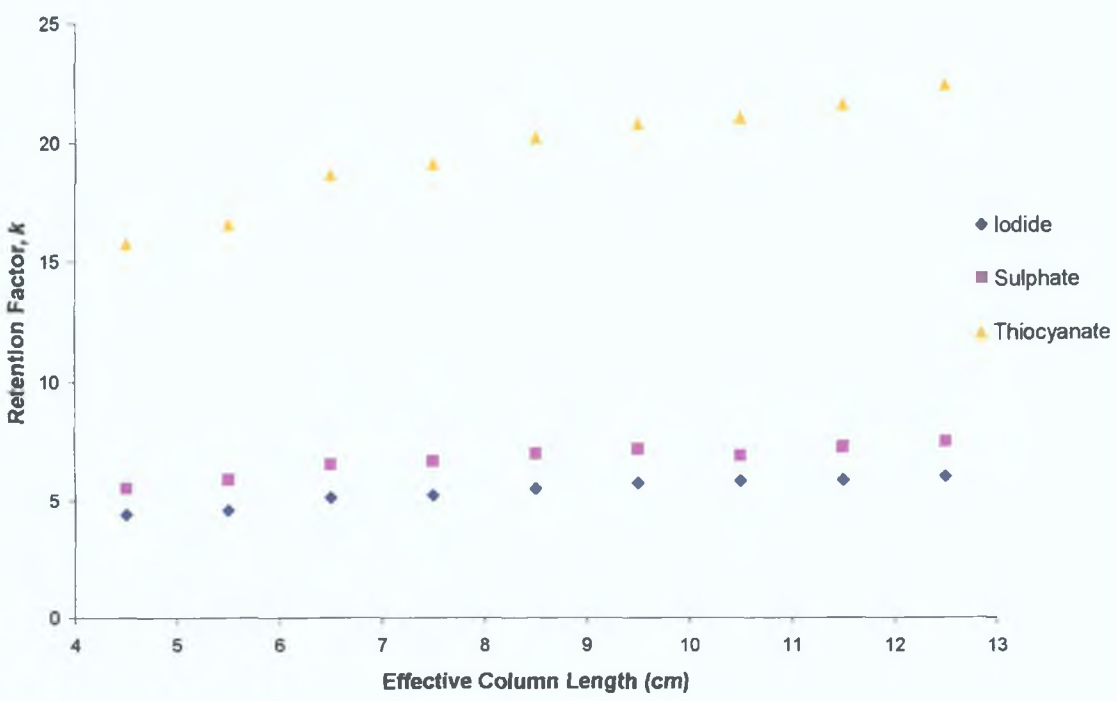

Figure 5.8 (a) and (b). Graphs showing the change in retention factor, *k*, as effective column length was increased, for (a) iodate, bromate, nitrite, bromide and nitrate, and for (b) iodide, sulphate and thiosulphate. Eluent: 0.5 mM phthalic acid at pH 4.05. Flow rate: 1.0 µL/min.

Fig. 5.7 shows that the use of an effective column length of 12.5 enabled the baseline separation of all 8 analyte anions, although thiocyanate was retained for approx. 24 min. Shortening the column length, lead to a decrease in the total runtime to aprox. 16 min. Further shortening of the effective column length (to 4.5 cm) resulted in thiocyanate eluting in less than 6 min, although the resolution of the earlier eluting analyte anions (namely iodate, bromate, nitrite, bromide and nitrate) was compromised, with iodate and bromate eluting as part of the injection peak, while nitrite, bromide and nitrate were no longer baseline resolved, as was seen at the higher effective column lengths. Therefore, the use of extremely short effective column lengths would be beneficial if the later eluting peaks are the only peaks of interest. Fig. 5.8 demonstrates how the values for k for each of the eight test analytes increased slightly as the effective column length became longer. This was not anticipated, as k should have remained the same, regardless of column length, as, although the retention times of analyte anions obviously increases with increased column length, the void time, t_0, also increases when using columns of longer length, which should lead to the same values for k (as $k = t_r - t_0 / t_0$, where t_r is the retention time of a particular sample component) being observed for a single analyte anion. Therefore, the plots displayed in Fig. 5.8 should have been flat, and not sloped, as was the case, particularly for the later eluting anions, such as thiocyanate. This suggests that the DDMAU coating is not consistently distributed along the entire length of the capillary column. If, for example, a greater amount of DDMAU molecules were adsorbed onto the stationary phase towards the end of the column, compared to earlier sections of the column, this would result in increased values for k, as either more, or less, DDMAU molecules would be present to interact with analyte anions at different points along the length of the capillary.

As is evident from Table 5.1, the calculated values for N/m at each effective column length did not display any clear trend, although in general peak efficiency was higher for all analyte anions (bar bromate and sulphate) with an effective column length of 12.5 cm. This indicates, again, that the column coating is non-uniform across the length of the capillary, as peak efficiencies expressed as N/m should have been the same at any point along the length of the column, if the DDMAU molecules were uniformly distributed. The average peak efficiency across all 3 column lengths in Table 5.1 was found to be approx. 35,150 N/m, which is almost 3 times more efficient

than has been reported (8,500-13,000 N/m) for polymeric monolithic capillary columns for IC separations [16].

Table 5.1. No. of theoretical plates/m for 8 sample anions at various effective column lengths.

Column Length (cm)	**Iodate N/m**	**Bromate N/m**	**Nitrite N/m**	**Bromide N/m**	**Nitrate N/m**	**Iodide N/m**	**Sulphate N/m**	**Thiocyanate N/m**
4.5	19,213	30,586	19,227	28,066	36,778	39,467	37,933	53,978
8.5	24,729	29,835	18,976	27,423	35,329	43,353	44,317	43,871
12.5	26,280	29,352	21,600	33,032	42,648	47,072	44,312	67,456

5.3.3 Use of Capillary Connectors

As peak dimensions (i.e. peak areas and heights) appeared to be relatively small using the capillary monolith, the limits of detection associated with the capillary chromatographic system (with contactless conductivity detection) were quite high, with limits of detection for nitrate and sulphate being in the region of 0.019 mM and 0.049 mM respectively. A possible reason for this is that the internal diameter of the column was too large for sensitive on-column detection, and/or that the stationary phase itself impeded detection in some way. Therefore, as a means of addressing this issue, it was thought that connecting the outlet of the modified capillary column with an additional piece of empty open tubular fused silica capillary (across which detection would occur) would lead to an increase in the signal detected for analyte anions, which would, in turn, yield lower limits of detection.

A zero dead-volume capillary-to-capillary union (from Upchurch Scientific, supplied by Presearch Limited, Hitchin, Hertfordshire, U.K.) was used to connect the eluent outlet of the capillary column with a 5.0 cm piece of open tubular fused silica capillary, with an internal diameter (I.D.) of 100 μm, and this extraneous piece of capillary, which was not modified with DDMAU, was pushed through the contactless conductivity detector. Therefore, the conductivity of the eluent was monitored post-column, using the connected piece of open tubular capillary as a "detector cell". A visual representation of such a detection setup can be seen in Fig. 5.9.

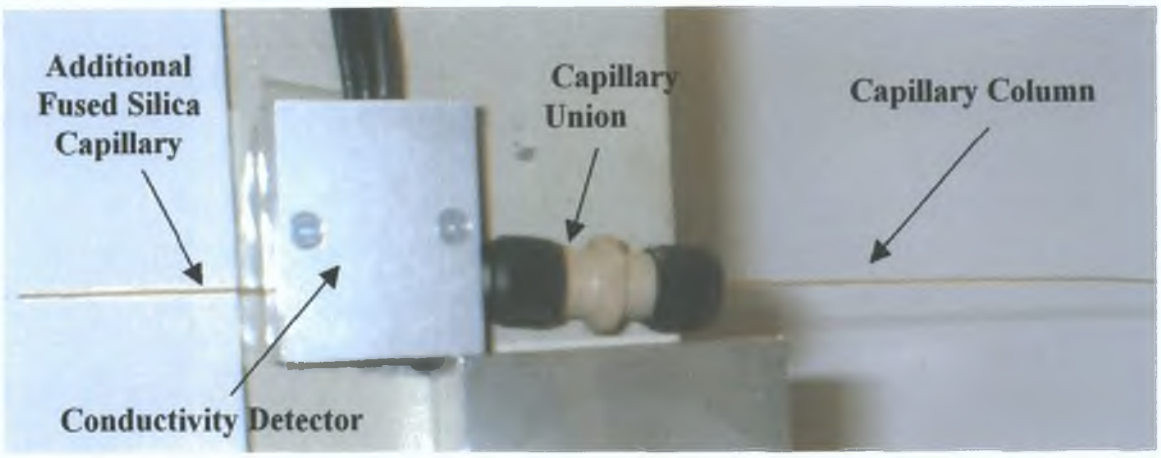

Figure 5.9. Photograph of the experimental setup employed to connect the capillary column to an additional piece of open tubular fused silica capillary, across which the conductivity of the eluent would be measured after leaving the column.

Unfortunately, this technique did not bring about an improvement in detector sensitivity, as can be seen by comparing the magnitude of the peaks observed both with and without connection to the piece of 100 μm I.D. capillary, as in Fig. 5.10 (a). Retention times were slightly longer for the chromatogram obtained using detection across the connected open tubular capillary, as this caused the effective column length to increase slightly. As would be expected, the addition of the open tubular capillary detector cell resulted in a clear peak broadening effect, as is clear from the comparison of the injection peaks for both configurations, as seen in Fig. 5.10 (b). It is obvious from the chromatograms overlaid in Fig. 5.10 that detector response using the additional piece of open tubular capillary was only a fraction of that observed when detection occurred across-column. This was confirmed by calculation of the signal-to-noise ratios for all of test anions both with and without the use of the connector system, and comparing the calculated values in Table 5.2. The determined values for the signal-to-noise ratios decreased by factors of approx. 3 (for iodate, nitrite, nitrate, sulphate and thiosulphate) to 5 (for bromate and iodide).

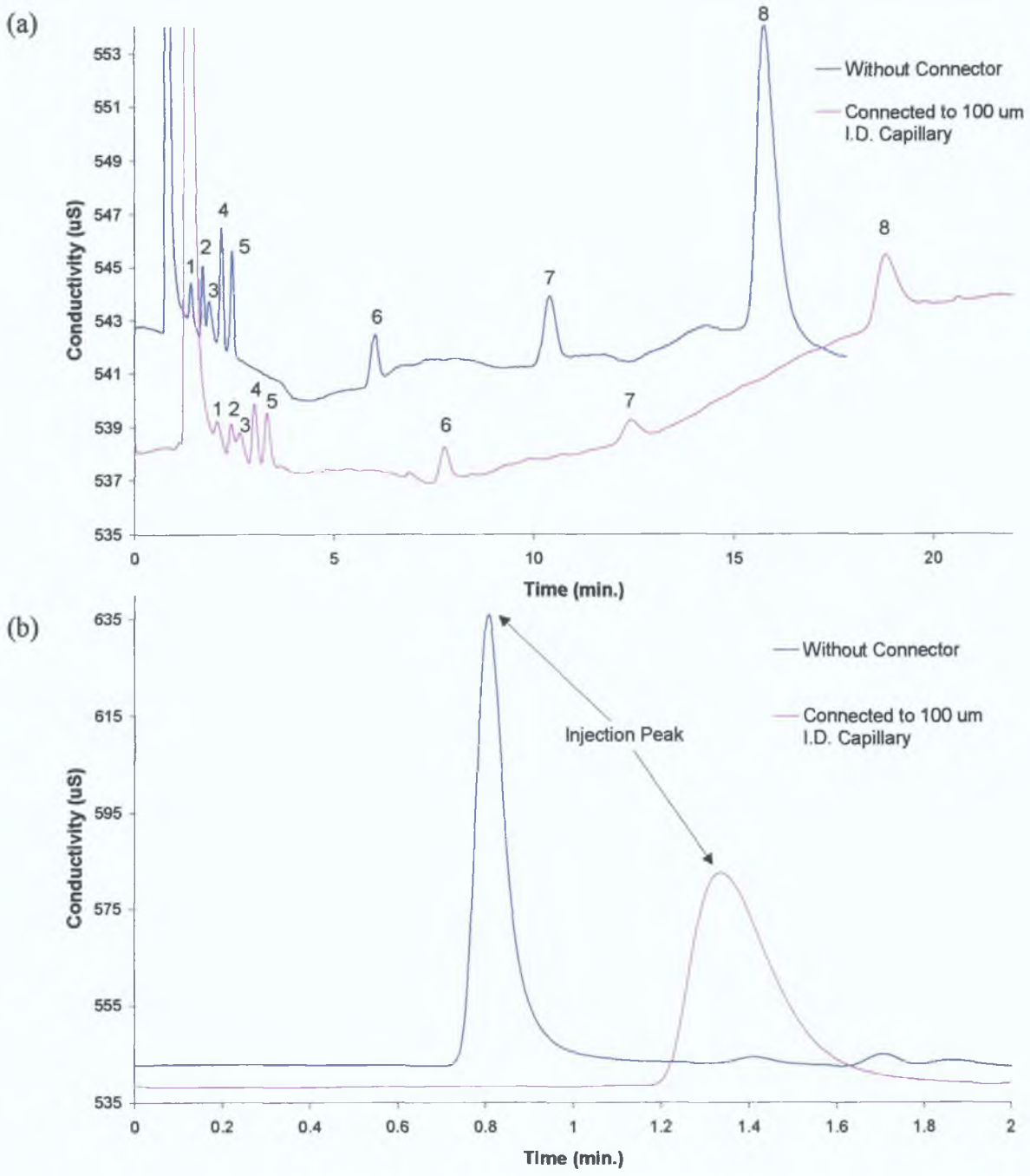

Figure 5.10 (a) and (b). Chromatograms of a 0.5 mM 7 anion mixture (plus 2.0 mM thiosulphate) obtained using a DDMAU-modified capillary C_{18} monolithic column, with contactless conductivity detection applied directly across the capillary monolithic column (blue trace), and also across a 100 μm I.D. open tubular capillary connected to the capillary monolith (pink trace). Eluent: 0.5 mM phthalic acid at pH 4.05. Flow rate: 1.0 μL/min. Effective column length: 13 cm. Peak identification: 1 – iodate, 2 – bromate, 3 – nitrite, 4 – bromide, 5 – nitrate, 6 – iodide, 7 – sulphate, and 8 – thiosulphate.

Table 5.2. Comparison of signal-to-noise ratios for 0.5 mM anion standards (except for 2.0 mM thiosulphate) using across-column detection, and detection across an open tubular capillary of 100 μm I.D.

Analyte Anion	**Signal-to-Noise Ratio (Across-Column Detection)**	**Signal-to-Noise Ratio (Connected to 100 μm I.D. Capillary)**
Iodate	38.25	10.99
Bromate	67.61	13.97
Nitrite	29.53	9.44
Bromide	123.36	36.59
Nitrate	106.75	31.55
Iodide	48.39	9.33
Sulphate	24.19	8.39
Thiosulphate	81.69	27.30

It was postulated that the reason for the apparent decrease in sensitivity associated with this new mode of detection might have been that the I.D. of the piece of open tubular capillary was too large (i.e. the open tubular capillary had a large internal volume, compared to the internal volume of the capillary monolithic column), leading to a subsequent dilution effect, ultimately resulting in a reduction in peak size. It was thought that the use of another piece of open tubular capillary, of smaller I.D., might bring about an improvement in sensitivity, as the volume of eluent within the length of capillary within the detector would be smaller. Therefore, a length of open tubular capillary of 75 μm I.D. was used in place of the 100 μm I.D. capillary. (Use of a 10 μm capillary resulted in leakages from the capillary union.) However, this proved equally unsatisfactory, as it resulted in even smaller peaks than before, as is demonstrated by the data tabulated in Table 5.3, with peak area values decreasing by a further 80 – 90%. In keeping with these experimental findings, it was decided that the most suitable option for detection was direct detection across the monolithic column itself.

Table 5.3. Peak areas for 0.5 mM anion standards (except for 2.0 mM thiosulphate) using across-column detection, and detection across open tubular fused silica capillaries of 2 different internal diameters (100 μm and 75 μm).

Capillary Connector I.D. (μm)	**Analyte Peak Areas (mV min)**							
	Iodate	**Bromate**	**Nitrite**	**Bromide**	**Nitrate**	**Iodide**	**Sulphate**	**Thiosulphate**
No Connector	0.06	0.14	0.24	0.41	0.33	0.37	0.91	0.97
100 μm	0.11	0.09	0.10	0.31	0.30	0.30	0.29	0.34
75 μm	Undet.	Undet.	0.01	0.01	0.02	0.04	0.03	0.08

5.3.4 Effect of Flow Rate on Peak Efficiency

In order to determine the optimum flow rate for peak efficiency, it was decided to prepare a van Deemter curve for the capillary IC system, by investigating the dependence of theoretical plate height (HETP) on the linear flow velocity (u) of the eluent for two test anions, namely nitrate and iodide (both at 0.5 mM). The eluent flow rate was varied between 0.04 μL/min and 1.0 μL/min ($n = 15$), and the values for HETP calculated for nitrate and iodide peaks, with an effective column length of 8.0 cm. The resulting plot of HETP vs. u can be seen in Fig. 5.11. Flow rates in excess of 1.0 μL/min. could not be facilitated by the split-flow system used, as increasing the flow setting on the pump used beyond this point merely lead to increase in the amount of eluent being vented, while the rate of eluent delivery to the column itself remained constant.

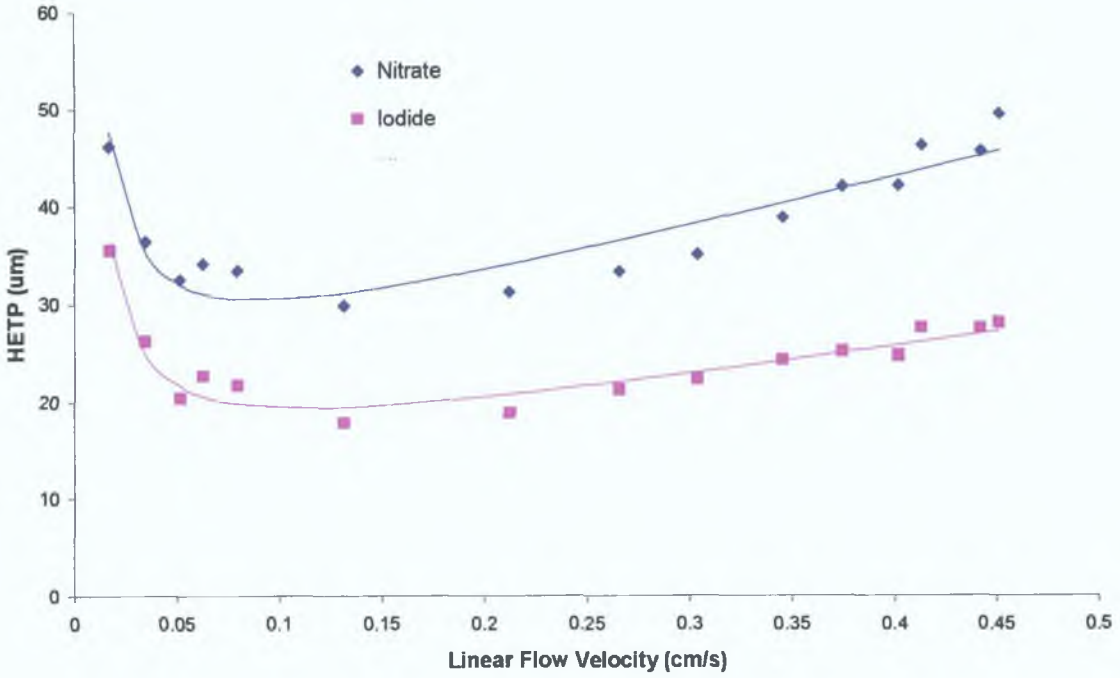

Figure 5.11. Plots of the effect of flow velocity (u) of eluent on the height equal to a theoretical plate (HETP) for nitrate and iodide. Eluent: 0.5 mM phthalic acid at pH 4.05. Effective column length: 8.0 cm. Concentration of standards injected: 0.5 mM.

The graphical trend observed in Fig. 5.11 was identical for both nitrate and iodide. As can be seen from Fig. 5.11, peak efficiency increased (i.e. lower values for HETP) at flow velocities less than 0.45 cm/s (corresponding to a 1.0 μL/min flow rate) until reaching a flow velocity of approx. 0.13 cm/s (approx. 0.29 μL/min), with peak efficiency at its highest between 0.29 and 0.45 μL/min. However, as is usually seen with other types of monolithic columns, the relatively flat C-term meant that higher flow rates could be used without significantly affecting peak efficiencies. Using the Solver tool function in Microsoft Excel, values for the A, B and C terms of the van Deemter equation (i.e. HETP = A + B/u + Cu, where A represents the contribution from eddy diffusion, B, the contribution from longitudinal diffusion, and C, the contribution from mass transfer effects) for both nitrate and iodide were calculated. The C-term was found to be equal to approx. 52 for nitrate, and approx. 31 for iodide. These are relatively low C-terms, which illustrate how superior efficiency can be maintained across a wide range of flow rates, and compare quite well to values for C determined by Pyo *et al.* for a 50 μm I.D. open tubular capillary column modified with latex particles [25], with the C-term for nitrate (at 75^0C) for such a chromatographic system being approx. 56. Under optimal flow conditions, peak

efficiency for nitrate and iodide was approx. 33,500 N/m and 56,100 N/m respectively, which compare favourably to a reported optimal analyte anion efficiency of approx. 8,500 N/m, for an alternative polymeric monolithic capillary IC system [16].

5.3.5 Analysis of Tap Water Samples

The suitability of the DDMAU-modified capillary column for the analysis of real samples was examined, and the separation and determination of chloride, nitrate and sulphate in tap water samples investigated. The monitoring of levels of these anions within drinking water systems is highly important for a number of reasons. The significance of nitrate determination in drinking water samples is because of the human body's reduction of nitrate to the more toxic nitrite form [26,27]. This reaction can cause methemoglobulinemia (or "blue-baby disease"), which can be fatal to infants, and so the determination of nitrate in drinking waters is regulated. Chloride and sulphate are considered to be secondary contaminants, and while the determination of these two anions is not generally regulated, elevated concentrations of both analytes have many detrimental effects, and therefore the observation of their presence in tap waters etc. is highly recommended. The level of chloride, for example, above which the taste of water may become objectionable is 250 mg/L, while higher chloride levels also contribute to the deterioration of domestic plumbing, water heaters etc. [28]. High levels of sulphate in drinking waters can also be problematic, as high concentrations of sulphate impart objectionable taste to water, while also causing laxative effects upon excessive intake [28]. Water containing appreciable amounts of sulphate also tends to form hard scales in boilers and heat exchangers [28].

The effective column length was set as short as possible, in order to give the shortest runtimes possible. A tap water sample taken from a source tap within the research laboratory was filtered using a 0.45 μm filter, and injected onto the capillary column without subjecting the water sample to any further sample pretreatment. The resulting chromatogram, as well as a chromatogram of a 0.5 mM standard of chloride, nitrate and sulphate, for comparative purposes, can be seen in Fig. 5.12. The overall runtime was less than 3 min, but the excessive tailing of the injection peak partially masked

the peaks for chloride and nitrate. This tailing may have been caused by excessive quantities of divalent cations present in the tap water sample, which were only slightly retained by the zwitterionic stationary phase.

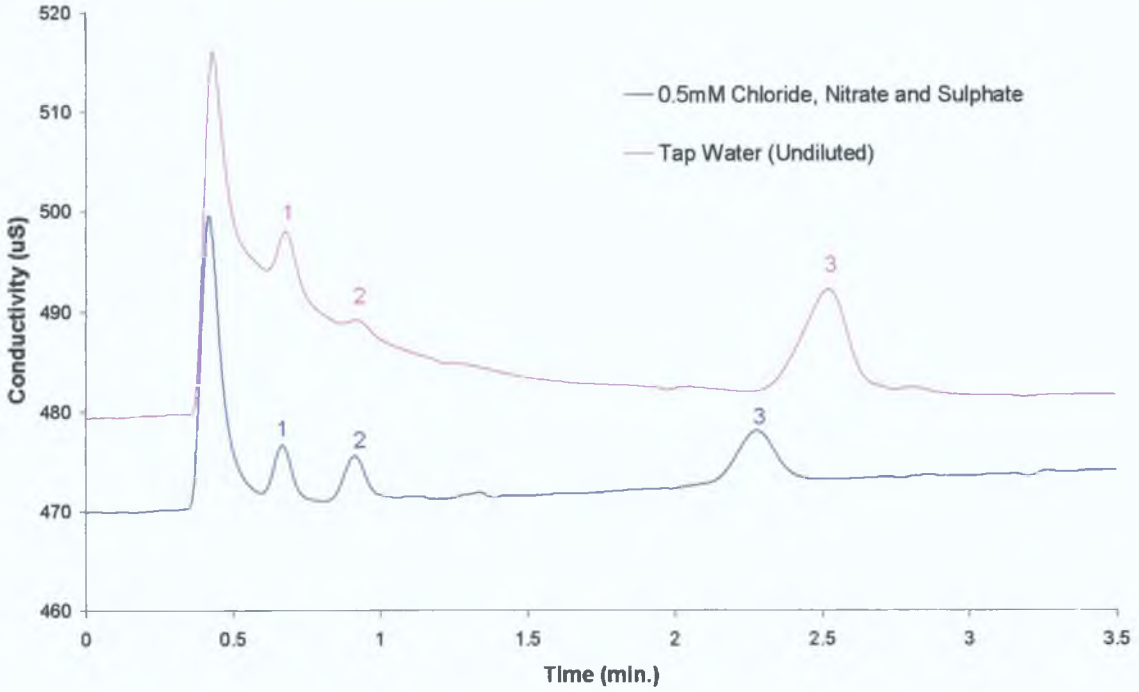

Figure 5.12. Overlays of chromatograms of a 0.5 mM standard solution of chloride, nitrate and sulphate (blue trace) and an undiluted tap water sample (pink trace) obtained using a DDMAU-modified capillary C_{18} monolithic column, with an eluent composed of 0.5 mM phthalic acid at pH 4.05, and contactless conductivity detection. Flow rate: 1.0 μL/min. Peak identification: 1 – chloride, 2 – nitrate, and 3 – sulphate.

In an attempt to minimise the effects of the severe tailing of the injection peak, as seen in Fig. 5.12, the tap water sample was diluted 1/5 with Milli-Q water, but this did not bring about the desired improvement in the shape and dimensions of the injection peak, as shown in Fig. 5.13. Movement of the detector position 4.0 cm further down the length of the capillary column (giving an effective column length of 8.5 cm) did not improve resolution of the chloride and nitrate peaks from the injection peak, see Fig. 5.13, but merely resulted in a longer total runtime of approx. 5.8 minutes. A further dilution of the tap water sample, giving a total dilution factor of 1/10, resulted in chloride and nitrate being barely detectable above the background conductivity of the eluent.

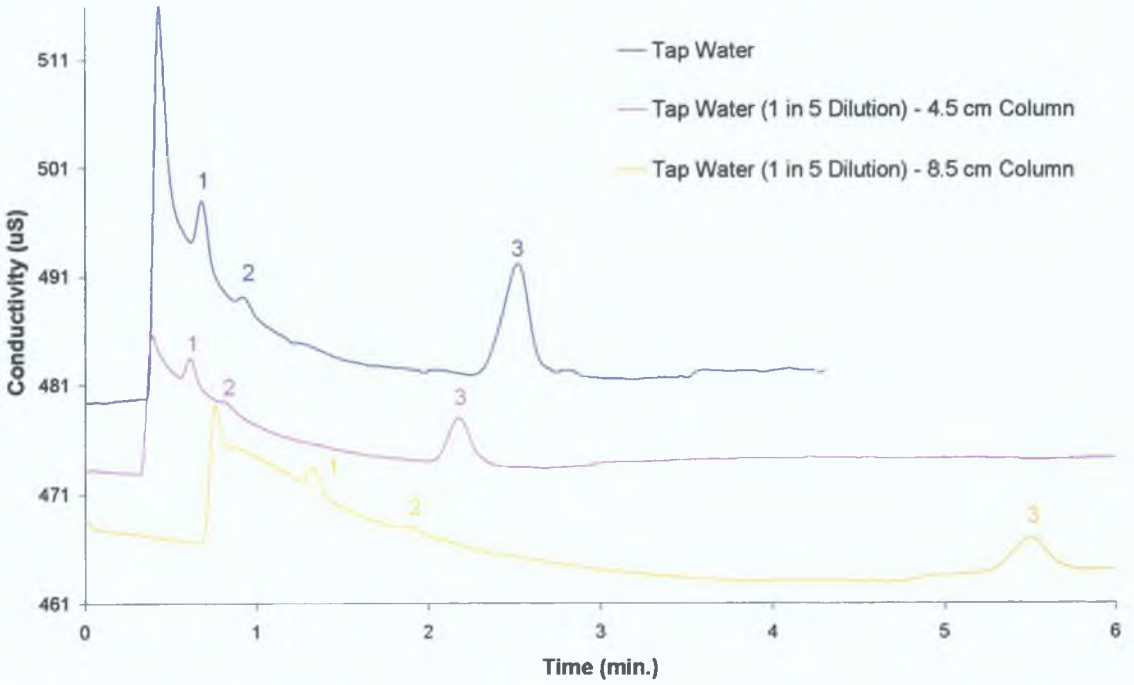

Figure 5.13. Overlays of chromatograms of a tap water sample injected neat (blue trace) and diluted by a factor of 5 (pink and yellow traces) obtained on the DDMAU-modified capillary C_{18} monolithic column with an effective column length of 4.5 cm (blue and pink traces) and 8.5 cm (yellow trace), in conjunction with contactless conductivity detection. Eluent: 0.5 mM phthalic acid at pH 4.05. Flow rate: 1.0 μL/min. Peak identification: 1 – chloride, 2 – nitrate, and 3 – sulphate.

As the tailing of the injection peak remained a hindrance to the analysis of chloride and nitrate, the tap water sample was pretreated by passing it through a cation-exchange cartridge in the acid form prior to injection. This replaced the various cationic species within the tap water sample with hydronium ions. The subsequent chromatogram can be seen as the pink trace in Fig. 5.14. While a certain degree of injection peak tailing was still evident, comparison of the chromatograms seen in Fig. 5.14 demonstrated that the signal-to-noise ratios for chloride, nitrate and sulphate obtained after performing cation-exchange on the tap water sample were 2.6, 1.9 and 1.5 times the respective values of the signal-to-noise ratios calculated for the tap water sample that had not been subject to any sample pretreatment. This indicates that the employment of the cation-exchange cartridges resulted in a greater sensitivity for the analyte anions, particularly for chloride and nitrate, making the system more suitable for quantification of the 2 aforementioned anions.

The total time of analysis in Fig. 5.14 was less than 1.5 minutes. The retention times were lower than those shown in Figs. 5.12 and 5.13, as the column had become blocked in the meantime, and was therefore cut to remove the section of the capillary which contained the observed blockage, which resulted in a shorter total capillary length, although the effective column length was the same as before, i.e. 4.5 cm. This would again suggest that the DDMAU stationary phase was not entirely uniform along the complete length of the capillary.

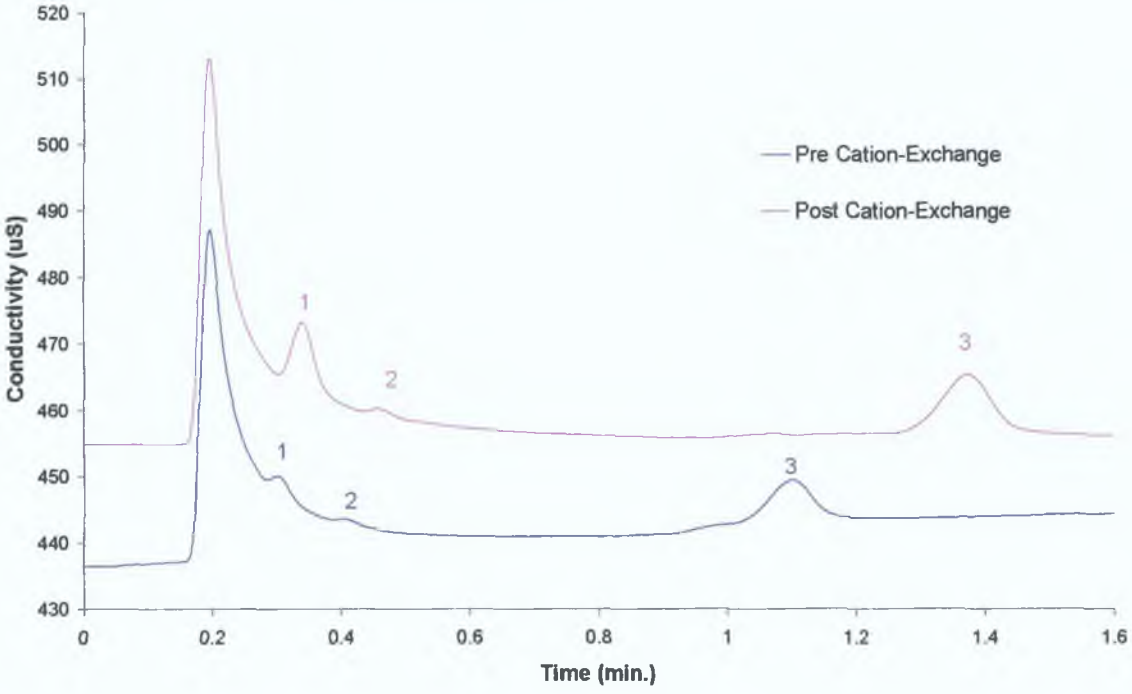

Figure 5.14. An overlay of the chromatograms of a tap water sample obtained pre and post cation-exchange (blue and pink traces respectively) using a DDMAU-modified capillary C_{18} monolithic column with an effective column length of 4.5 cm, with an eluent comprised of 0.5 mM phthalic acid at pH 4.05, and contactless conductivity detection. Flow rate: 1.0 µL/min. Peak identification: 1 – chloride, 2 – nitrate, and 3 – sulphate.

In a bid to further minimise interference from the injection peak, the effective column length was increased from 4.5 cm to 8.5 cm, as illustrated in Fig. 5.15. This resulted in greater resolution between the injection peak and the peaks corresponding to chloride and nitrate, i.e. from 2.31 to 4.21, and from 4.23 to 7.71 respectively, but this did not bring about another increase in sensitivity, as the values for the signal-to-noise ratio for the chloride peak remained unchanged, while the signal-to-noise ratio for the nitrate peak was only approx. 1.1 times greater than before. Both reversed-phase and

cation-exchange cartridges were utilised to pretreat the tap water samples prior to analysis, in order to remove any organic matter/contaminants that may be present, which would elute as part of the injection peak and so would contribute to overloading of this peak. The resulting chromatogram is displayed as the yellow trace in Fig. 5.15. However, the use of both pretreatment cartridges did not produce the desired improvement in injection peak shape, or, consequently, a further improvement in analyte sensitivity, with the signal-to-noise ratio for chloride being 43% of the signal-to-noise ratio for the peak obtained after pretreatment with the cation-exchange cartridge alone. However, this was not the case for the signal-to-noise ratios for nitrate and sulphate, which were seen to decrease by less significant amounts, of 5% and 2% respectively. The reason for this decrease in the signal-to-noise ratio for chloride is not entirely clear.

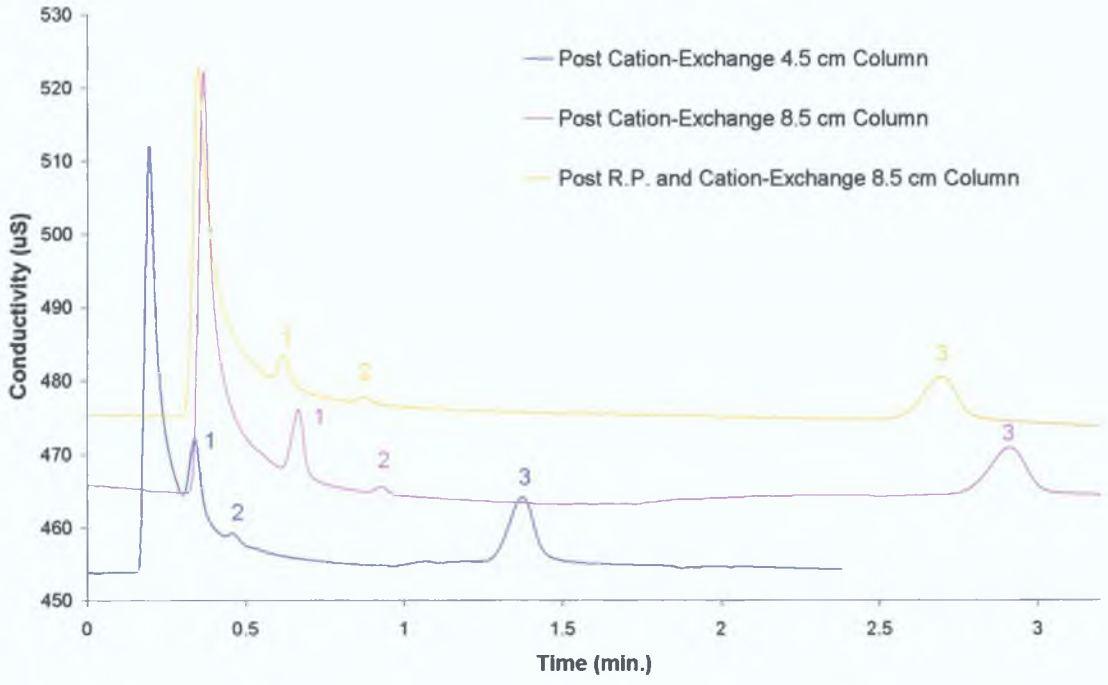

Figure 5.15. Overlays of chromatograms of a tap water sample obtained using a DDMAU-modified capillary C_{18} monolithic column, with an eluent comprised of 0.5 mM phthalic acid at pH 4.05, and contactless conductivity detection, after passing through a cation-exchange cartridge (blue and pink traces) and both a cation-exchange cartridge and a reversed-phase cartridge (yellow trace). Effective column lengths: 4.5 cm (blue trace) and 8.5 cm (pink and yellow traces). Flow rate: 1.0 μL/min. Peak identification: 1 – chloride, 2 – nitrate, and 3 – sulphate.

In order to investigate the robustness of the developed method, the analysis of the tap water sample after pretreatment with both types of solid phase exchange cartridges was carried out 8 times, and was found to exhibit a high degree of reproducibility, with % RSD values for *k* of 3.18%, 2.72% and 2.81% for chloride, nitrate and sulphate, respectively.

5.3.6 Anion Selectivity

Finally, the selectivity of the DDMAU-modified capillary monolith for a range of anionic analytes was assessed. Solutions of 35 anion standards were prepared and analysed using an eluent composed of 0.5 mM phthalic acid at pH 4.05, and the results summarised in Table 5.4 below:

Table 5.4. Retention factors for each anion analysed, using 0.5 mM phthalic acid (pH 4.05) as eluent, with contactless conductivity detection and a flow rate of 0.30 μL/min. Effective column length: 8.0 cm.

Anion	**Retention Factor, *k***
Bicarbonate	0.30
Selenite	0.49
Iodate	0.71
Formate	0.77
Arsenate	0.85
Bromate	1.00
Chloride	1.03
Nitrite	1.17
Chloroacetate	1.23
Chlorite	1.32
Bromide	1.39
Nitrate	1.52
Chlorate	2.25
Iodide	5.35
Sulphite	7.09
Sulphate	7.18
Thiosulphate	13.12
Thiocyanate	20.88
Perchlorate	23.40

The sensitivity of the capillary IC system with C^4D detection would appear to be providing a significant challenge for the detection of many of the analyte anions injected, as no peaks were detected for fifteen injected anion standards, namely acetate, borohydride, carbonate, citrate, chromate, fluoride, hydrogen phosphate, 4-

hydroxybenzoate, molybdate, oxalate, periodate, persulphate, phosphate, tetraborate, and tungstate. The limits of detection for these anions were evidently too high, as even elevated sample concentrations of 2.0 to 5.0 mM did not yield any peaks within the 70 minute runtime allowed, meaning they could be either unretained on the DDMAU-modified column (thereby eluting as part of the injection peak), or fully retained. Also, in the case of several analyte anions which were detected, the peak dimensions were relatively slight compared to other analytes such as bromide, sulphate etc. For example, selenite and bicarbonate were seen to elute as small shoulders on the tail of the injection peak.

A sample separation of a 10 anion mixture (containing 0.5 mM iodate, bromate, nitrite, bromide, nitrate, iodide, sulphate and thiosulphate, and 2.0 mM thiocyanate and perchlorate) can be seen in Fig. 5.16. The addition of any other sample anions to this mixture would have resulted in co-elution of several analytes.

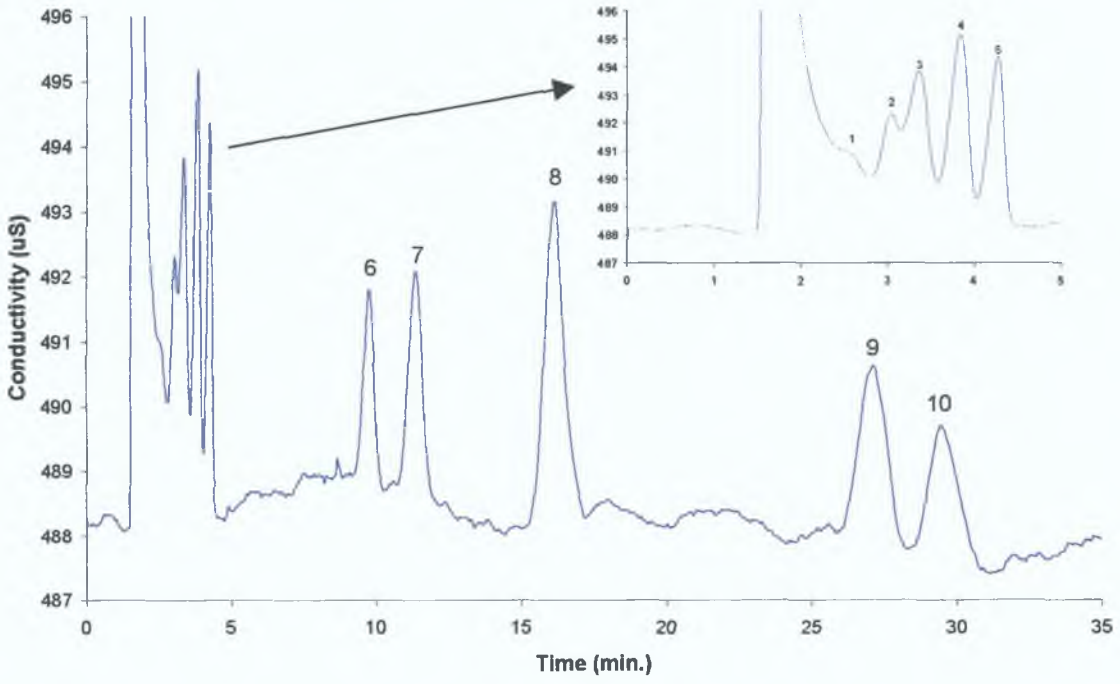

Figure 5.16. Chromatogram of a 0.5 mM mixture of iodate, bromate, nitrite, bromide, nitrate, iodide, sulphate and thiosulphate (with 2.0 mM thiocyanate and perchlorate) obtained using a DDMAU-modified capillary C_{18} monolithic column, with an eluent composed of 0.5 mM phthalic acid at pH 4.05, and contactless conductivity detection. Flow rate: 0.30 μL/min. Effective column length: 8.0 cm. Peak identification: 1 – iodate, 2 – bromate, 3 – nitrite, 4 – bromide, 5 – nitrate, 6 – iodide, 7 – sulphate, 8 – thiosulphate, 9 – thiocyanate, and 10 – perchlorate.

Sulphate and sulphite could not be resolved from each other, but the separation of chloride, chlorite and chlorate was achieved in less than 4 minutes, as can be seen in Fig. 5.17, while the separation of formate, chloride and chloroacetate within the same time frame can be seen in Fig. 5.18.

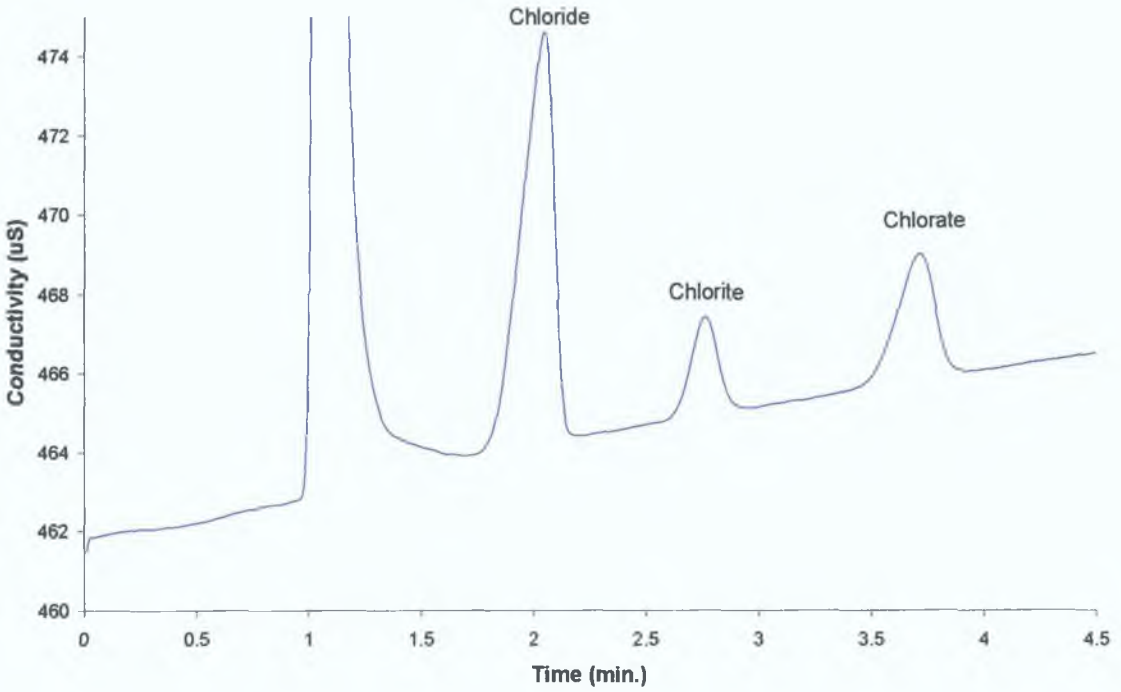

Figure 5.17. Chromatogram of a mixture of chloride (0.5 mM), chlorite (2.0 mM) and chlorate (0.5mM) obtained using a DDMAU-modified capillary C_{18} monolithic column, with 0.5 mM phthalic acid as eluent, and contactless conductivity detection. Flow rate: 0.30 μL/min. Effective column length: 8.0 cm.

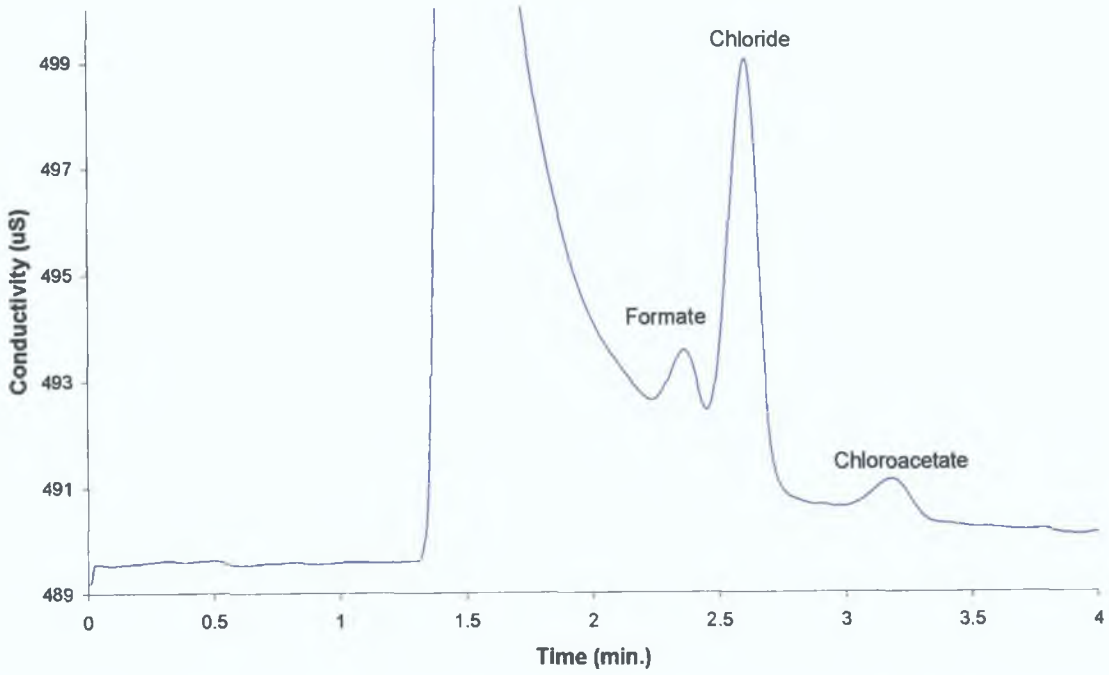

Figure 5.18. Chromatogram of a 0.5 mM mixture of formate, chloride and chloroacetate obtained using a DDMAU-modified capillary C_{18} monolithic column, with 0.5 mM phthalic acid as eluent, and contactless conductivity detection. Flow rate: 0.30 μL/min. Effective column length: 8.0 cm.

The behaviour of dithionite was slightly anomalous, as the resulting chromatogram (as in Fig. 5.19) had 3 peaks present. The assignation of dithionite peak identity was problematic, but it was thought that the middle peak at approx. 9.5 minutes could be attributed to the presence of either sulphate or sulphite, while the larger peak at approx. 14 minutes corresponded to the retention factor of thiosulphate. This was not entirely unexpected, as commercial sources of dithionite are usually contaminated with other sulphur species, which are present unavoidably as by-products or decomposition products [29].

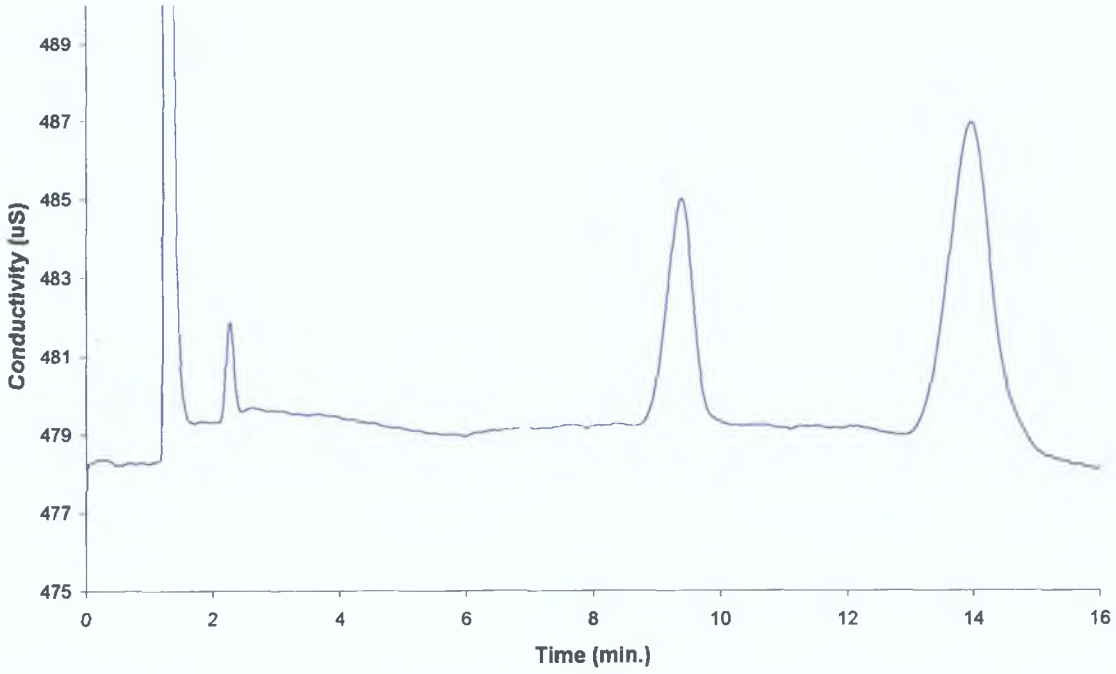

Figure 5.19. Chromatogram of a 0.5 mM standard of dithionite obtained using 0.5 mM phthalic acid as eluent, with contactless conductivity detection. Flow rate: 0.30 μL/min. Effective column length: 8.0 cm.

5.4 Conclusions

Across-column C^4D detection in capillary IC using modified C_{18} monolithic capillary columns has not previously been demonstrated, and therefore, the significance of the work outlined in this Chapter is that is has been shown that this mode of detection is indeed a simple and viable option with such columns. Using a low-conducting organic acid-based eluent, it was possible to separate iodate, bromate, nitrite, bromide, nitrate, iodide and sulphate, with peak efficiencies of 14,000-70,000 N/m. The ability to move the detector cell along the length of the capillary column meant effective column length, and therefore retention and resolution of analyte anions, could be altered through the adjustment of the position of the contactless conductivity detector. The application of the DDMAU-modified capillary to the analysis of real tap water samples was also shown, with the determination of chloride, nitrate and sulphate in a drinking water sample possible within 1.5 to 4.0 minutes, depending on the opted course of sample pre-treatment. Microscopy was also proven to be a useful tool in the determination of the quality and structural integrity of the capillary column.

References:

1 M.D. Luque de Castro, C. Gamriz-Gracia, Anal. Chim. Acta 351 (1997) 23-40.

2 J.P. Chervet, M. Ursem, J.P. Salzmann, Anal. Chem. 68 (1996) 1507-1512.

3 P. Kuban, P.K. Dasgupta, J. Sep. Sci. 27 (2004) 1441-1457.

4 K. Karlsson, M. Novotny, Anal. Chem. 60 (1988) 1662-1665.

5 R.T. Kennedy, J.W. Jorgenson, Anal. Chem. 61 (1989) 1128-1135.

6 M. Novotny, J. Chrom. B 689 (1997) 55-70.

7 M.T. Davis, D.C. Stahl, T.D. Lee, J. Am. Soc. Mass Spectrom. 6 (1995) 571-577.

8 H. Oberacher, A. Krajete, W. Parson, C.G. Huber, J. Chrom. A 893 (2000) 23-35.

9 M.T. Davis, D.C. Stahl, K.M. Swiderek, T.D. Lee, Methods: A Companion to Methods in Enzymology 6 (1994) 304-314.

10 T. Takeuchi, S. Tatsumi, S. Masuoka, K. Hirose, H. Uzu, J. Jin, C. Fujimoto, K. Ohta, K. Lee, J. Ryoo, S. Choi, J. Chrom. A 1021 (2003) 55-59.

11 C.G. Horvath, B.A. Preiss, S.R. Lipsky, Anal. Chem. 39 (1967) 1422-1428.

12 C. Horvath, S.R. Lipsky, Anal. Chem. 41 (1969) 1227-1234.

13 S. Rokushika, Z.Y. Qiu, H. Hatano, J. Chrom. 260 (1983) 81-87.

14 S. Rokushika, Z.Y. Qiu, Z.L. Sun, H. Hatano, J. Chrom 280 (1983) 69-76.

15 I. Gusev, X. Huang, C. Horvath, J. Chrom. A 855 (1999) 273-290.

16 P. Zakaria, J.P. Hutchinson, N. Avdalovic, Y. Liu, P.R. Haddad, Anal. Chem. 77 (2005) 417-423.

17 M. Motokawa, H. Kobayashi, N. Ishizuka, H. Minakuchi, K. Nakanishi, J. Jinnai, K. Hosoya, T. Ikegami, N. Tanaka, J. Chrom. A 961 (2002) 53-63.

18 A. Suzuki, L.W. Lim, T. Hiroi, T. Takeuchi, Talanta *In Press* (2006).

19 W. Hu, T. Takeuchi, H. Haraguchi, Anal. Chem. 65 (1993) 2204-2208.

20 W. Hu and H. Haraguchi, Anal. Chem. 66 (1994) 765-767.

21 A.J. Zeeman, Electrophoresis 24 (2003) 2125-2137.

22 M. Lämmerhofer, F. Svec, J.M.J. Fréchet, W. Lindner, J. Chrom. A 925 (2001) 265-277.

23 E.F. Hilder, A.J. Zeeman, M. Macka, P.R. Haddad, Electrophoresis 22 (2001) 1273-1281.

24 Ion Chromatography, J.S. Fritz and D.T. Gjerde, 3rd edition 2000, published by Wiley-VCH, Weinheim, Germany.

25 D. Pyo, H. Kim, P.K. Dasgupta, Bull. Korean Chem. Soc. 20 (1999) 223-225.

26 P.E. Jackson, TRAC 20 (2001) 320-329.

27 Encyclopedia of Analytical Chemistry, R.A. Meyers, 2000 Edition, published by John Wiley & Sons Ltd., Chichester, U.K.

28 www.walrus.com/~gatherer/interpret.html, "Interpreting Drinking Water Analysis: What Do the Numbers Mean?", T.B. Shelton, Cook College – Rutgers University, New Brunswick, NJ, U.S.A., viewed 03/02/06.

29 L.M. Carvalho, G. Schwedt, J. Chrom. A 1099 (2005) 185 – 190.

Overall Summary and Future Work

The aim of this project was to modify various reversed-phase materials with carboxybetaine-type zwitterionic surfactants (namely dodecyldimethylaminoacetic acid and N-dodecyl-N,N-(dimethylammonio)undecanoate (DDMAU)), and to fully investigate and characterise the selectivity of the resultant modified columns for inorganic and cationic species.

The results presented in Chapters 2-5 have shown that carboxybetaine-modified C_{18} columns exhibit unique anion-exchange selectivity, which differs to that seen previously with alternative zwitterionic surfactant-modified stationary phases, such as sulfobetaine-modified columns etc. Ion-exchange capacity and efficiency have been demonstrated to be dependent upon eluent pH and eluent electrolyte concentration, both of which provided new options for the manipulation of analyte retention.

Particle-packed C_{18} columns modified with dodecyldimethylaminoacetic acid (Chapter 2) displayed variable retention of analyte anions (nitrite, bromide, nitrate and iodide) across a range of eluent electrolyte concentrations, with increased concentrations of KCl in the eluent resulting in decreased retention times for the aforementioned anions, although the effect was less significant than that normally observed with conventional ion-exchange, due to the eradication of intra- and inter-molecular salt structures of the carboxybetaine surfactant molecules upon addition of increased amounts of electrolyte molecules to the eluent composition. The effect of eluent pH was also investigated, with increased eluent pH values causing retention of analyte anions to decrease, due to a decrease in the number of dissociated carboxylate groups of the carboxybetaine molecules. The optimal eluent conditions, in terms of resolution, total runtime and peak efficiency, were found to be a KCl concentration of 150 mM, and an eluent pH of 6. The applicability of the dodecyldimethylaminoacetic acid-modified stationary phase to the analysis of saline samples, without any need for pretreatment or dilution of the saltwater matrix, was also illustrated.

The use of monolithic C_{18} columns in ZIC with carboxybetaine-type stationary phases (Chapter 3) has been shown to be of great potential in the truncation of analyte anion

retention times, without significantly affecting resolution or peak efficiency. Employing elevated flow rates (up to 4.5 mL/min), which are easily facilitated by the porous structure of monolithic columns, allowed the separation of the 4-anion test mixture in less than 4 min, compared to almost 16 min at 0.5 mL/min. Further decreases in overall runtimes were accomplished using flow gradients, and combined eluent pH and flow gradients, which enabled the stationary phase to act as an adjustable-capacity anion-exchanger, with increased eluent pH values causing capacity to decrease. The runtime for the separation of nitrite, bromide, nitrate, iodide and thiocyanate was shortened from 110 min under isocratic conditions (eluent pH 3, and a flow rate of 0.5 mL/min) to approx. 7.5 min upon application of a combined pH and flow gradient (up to pH 8, and a flow rate of 5.0 mL/min). The use of these dual gradient programs also resulted in improved peak efficiencies for later eluting anions (such as iodide and thiocyanate). Polar organic compounds (as represented by nucleoside bases) were only weakly retained on the dodecyldimethylaminoacetic acid-modified column, with unsatisfactory resolution of all 5 nucleoside bases. It was also demonstrated that high efficiency, rapid IC separations could be achieved using ultra-short (1.0 cm) monolithic columns modified with dodecyldimethylaminoacetic acid, which were compatible with flow gradient and dual gradient separations, with the separation of nitrite, nitrate, iodide and thiocyanate possible in approx. 3 min.

It was shown that DDMAU can be used to dynamically modify C_{18} monolithic columns (Chapter 4) to produce a stable stationary phase for the efficient separation of anions. Because of the larger number of inter-charge methylene groups in the DDMAU molecule, in comparison to the dodecyldimethylaminoacetic acid molecule, the hydrophobic character of the surfactant used was increased, meaning there was no need for the addition of any amount of the zwitterionic surfactant to the eluent. It was found that eluent buffering was necessary, as the modified column itself exhibited significant column buffering. Again, the DDMAU stationary phase displayed a pH dependent effective column ion-exchange capacity, due to the presence of a terminal weak acid group. The effect of pH on analyte anion retention was even more pronounced than for the previously employed dodecyldimethylaminoacetic acid, e.g. with nitrate, for example, eluting at approx. 38 min at pH 3, but eluting within 3 min at pH 6. Even faster separations were possible upon switching to a DDMAU-modified monolithic column of smaller length (i.e. 2.5 cm vs. 10 cm), with average

peak efficiencies of 41,721 N/m and 28,771 N/m for the modified 10 cm and 2.5 cm columns respectively. Again, application of a combined eluent pH and flow gradient meant that runtimes were shortened significantly, with the separation of iodate, bromate, nitrite, bromide, nitrate, iodide and thiocyanate possible within 4.5-6.0 min, depending on the start and end conditions of the applied gradient, leading to visible improvements in the peak shapes for thiocyanate. The presence of a system peak upon application of the dual gradient program was found to be due to the release of retained eluent phosphate ions from the stationary phase as the anion-exchange capacity of the column decreased with increased eluent pH. Effective column ion-exchange capacity could be determined through monitoring of the pH of the column eluate, and was found to be equal to 112 μmol of DDMAU. As with the previously employed dodecyldimethylaminoacetic acid-modified column, negligible retention of nucleoside bases was observed using the DDMAU-modified stationary phase.

DDMAU was also successfully used to modify a monolithic C_{18} capillary column (15.0 cm in length with a 0.1 cm I.D.), for the subsequent separation of common inorganic anions (Chapter 5). The mode of detection utilised was across-column C^4D detection, which had never previously been used for capillary IC separations using modified C_{18} monoliths, and therefore, the significance of the work outlined in Chapter 5 is that is has been shown that this mode of detection is indeed a simple and viable option with such columns. Using a low-conducting organic acid-based eluent (i.e. phthalic acid), it was possible to separate iodate, bromate, nitrite, bromide, nitrate, iodide and sulphate in less than 8 min using a flow rate of 1.0 μL/min, with peak efficiencies calculated to be in the region of 14,000-70,000 N/m. Effective column length could be adjusted simply by moving the detector cell to a different point along the length of the capillary column. The effect of flow rate on peak efficiency was studied, with optimal values for HETP observed using flow rates of between 0.29 and 0.45 μL/min, although the relatively flat C-term of the van Deemter curves plotted meant that higher flow rates could also be used without causing peak efficiency to decrease significantly. The application of the DDMAU-modified capillary column to the analysis of real tap water samples was also shown, with the determination of chloride, nitrate and sulphate in a drinking water sample possible within 1.5 to 4.0 minutes, depending on the opted course of sample pre-treatment.

Future work following on from the experiments outlined here may include further development and refinement of the capillary IC system described in Chapter 5. Evidently, the across-column C^4D detection method employed using the DDMAU-modified capillary column in Chapter 5 was not as sensitive as was hoped, as peak dimensions were relatively small, considering the concentration of the injected anion solutions. Connection of a length of open tubular capillary (to be used as a detector cell) to the end of the capillary column did not result in an improvement in the observed limits of detection. Therefore, future work should include further development of the detection method used. Detector response to the passing of various electrolytic eluent solutions (at various concentrations) through the capillary column (both pre- and post-modification with zwitterionic surfactant) could be compared to the response across a piece of unmodified open tubular capillary, replacing the column in the chromatographic setup. Another possible avenue of investigation may include electrochemical detection with a wall jet electrode, possibly after removing a small part of the column packing, in order to carry out detection across this void.

The use of a dedicated nano LC/capillary LC eluent delivery system, capable of delivering eluent at flow rates of 50 nL/min to 50 μL/min and above (as long as backpressure values were maintained below 300 bar for the 150 x 0.1 mm Onyx monolithic C_{18} column), without the need for the use of a custom built flow splitter to regulate eluent flow rates, would make possible the application of flow gradients to capillary IC separations, such as those seen in Fig. 5.7. As can be seen from Fig. 5.7, depending on the effective column length, the run time for the separation of an 8 anion mixture (i.e. iodate, bromate, nitrite, bromide, nitrate, iodide, sulphate and thiocyanate) varied from less than 6 min (at an effective column length of 4.5 cm) to approx. 25 min (at an effective column length of 12.5 cm). However, at the smaller effective column lengths the resolution of the early eluting anions (i.e. iodate, bromate, nitrite, bromide and nitrate) was severely compromised, leading to coelution of analyte anion peaks). Therefore, if a pump capable of being programmed to carry out gradient runs was employed, the optimal resolution of early eluting anions would be maintained, while later eluting anions (especially thiocyanate) would be retained for a significantly smaller length of time.

Section 5.3.5 described a practical application for the DDMAU-modified monolithic column for the analysis of tap water samples for chloride, nitrate and sulphate. Another possible environmental application might be the analysis of seawater and estuarine samples for nutrient anions, as undertaken before in Chapters 2 and 3. However, care must be taken to filter the seawater samples effectively, as particulate matter within the seawater samples may cause blockages within the capillary column, and/or voids in the stationary phase material contained within.

Additional future work could incorporate the use of additional zwitterionic surfactants, as well as non-zwitterionic surfactants possessing only a single fixed charged site, as possible stationary phases for capillary IC using monolithic capillary columns, and the results obtained compared with those described in Chapter 5 for DDMAU-modified capillary monoliths. A mixed-bed stationary phase could also be investigated, whereby a mixture of a anionic surfactant (e.g. sodium dioctyl sulfosuccinate (DOSS)) and a zwitterionic surfactant (e.g. DDMAU) could be used to modify the capillary monolith, thus conferring cation-exchange characteristics on the modified column, supplementing the anion-exchange characteristics of the sorbed DDMAU molecules. Adjusting the relative ratios of both types of surfactant in the column modification solution would alter the relative amounts of each surfactant molecule available to undergo ion-exchange, and therefore, retention of either analyte anions or cations could be increased or decreased as desired. The possibility of using such a mixed-bed stationary phase for the simultaneous analysis of anions and cations could then be studied thoroughly.

The contactless conductivity detector (in conjunction with a microscope equipped with camera imaging) could also be further developed as a commercial method for the verification of column quality and integrity. Solutions of high conductivity could be passed through the capillary column, thus making the dips in conductivity corresponding to possible gaps in the stationary phase more pronounced in response, while microscopy could then be employed to confirm the existence and location of these possible gaps in the stationary phase material.